2-2009

Molecular Designs Toward Improving Organic Photovoltaics

Arpornrat Nantalaksakul
University of Massachusetts - Amherst

MOLECULAR DESIGNS TOWARD IMPROVING ORGANIC PHOTOVOLTAICS

A Dissertation Presented

by

ARPORNRAT NANTALAKSAKUL

Submitted to the Graduate School of the
University of Massachusetts Amherst in partial fulfillment
of the requirements for the degree of

DOCTOR OF PHILOSOPHY

February 2009

Chemistry

MOLECULAR DESIGNS TOWARD IMPROVING ORGANIC PHOTOVOLTAICS

A Dissertation Presented

by

ARPORNRAT NANTALAKSAKUL

Approved as to style and content by:

_____
Sankaran Thayumanavan, Chair

_____
Dhandapani Venkataraman, Member

_____
Michael D. Barnes**,** Member

_____
E. Bryan Coughlin, Outside Member

_____
Bret Jackson, Department Head
Chemistry

ACKNOWLEDGEMENTS

This dissertation is simply impossible without assistance from many individuals who deserve special mention. I would like to use this opportunity to convey my gratitude to all of them in my humble acknowledgement.

Above all, I am grateful to my research advisor, Professor Sankaran (Thai) Thayumanavan for his supervision, guidance and advice since an early state of this work as well as giving me an extraordinary experience throughout the work. More importantly, I am very thankful for the freedom he allows to conduct research quite independently. He also supports me in the best possible ways that a teacher could provide to his student. His true dedication, enthusiasm and scientific integrity are always inspiring and it is certainly my good fortune to get an opportunity to interact with a person with a full spirit in science like him during my Ph.D. career.

I am also thankful to Professor Dhandapani Venkataraman, Professor Michael Barnes and Professor Bryan Coughlin for serving on my dissertation committee. Their constructive critisms and useful advice helped me in understanding and completing this work. I also would like to thank Professor Christopher Bardeen at University of California, Riverside for the photophysical measurements performed in his lab. I have learned a lot from him through discussions and his suggestions.

Besides, I am grateful to the former and present Thai group members for always being friendly and helpful in many ways. You all make my life in the lab more enjoyable. My special thanks to all my collaborators, Dr. Raghunath Reddy Dasari, Dr. Kothandam Krishnamoorthy and Akamol Klaikherd. I always enjoyed the scientific discussions we have had and you guys have taught me how important teamwork is.

Encouragement, support and help that we all shared helped me pass all hardships and frustrations when things seem to be failing. I really value and appreciate them.

I also would like to thank all my past and current Thai sisters and brothers here at UMass for your care, support and encouragement. Thank you very much for always being there with me through my good and bad times. As a sister of a big family here, I promise that I will never be too far away when any of you need me.

My deepest gratitude goes to my family. I really appreciate unconditional love and constant support that my mom and dad provide throughout my life. Being thousands of miles apart for such a long period of time, I know for sure how hard it could be for you both. You, however, never even once mention it and always let me fully concentrate on my work to achieve my goal. I have also enjoyed scientific talks that I have had with you for over almost 10 years since I have got myself involved in chemistry. Even though you do not understand the meaning of a single word I say, you never get bored of listening to my research progress and always tried to help me figure out why things did not work the way they should be. Thank you very much for being there for me every step of the way. I find it impossible to reach this stage without you both in my life and I just hope that my success will at least make you proud. I also would like to thank my brother for always being a good listener and a good company. My life could have been tough without constant support and encouragement from you. You are the only life-long best friend I have in the whole world. Thanks a lot.

ABSTRACT

MOLECULAR DESIGNS TOWARD IMPROVING ORGANIC PHOTOVOLTAICS

FEBRUARY 2009

ARPORNRAT NANTALAKSAKUL, B.S., CHULALONGKORN UNIVERSITY

M.S., CHULALONGKORN UNIVERSITY

Ph.D., UNIVERSITY OF MASSACHUSETTS AMHERST

Directed by: Professor Sankaran Thayumanavan

Organic photovoltaics (OPVs) that have been studied to date have poor power conversion efficiencies. This dissertation focuses on various molecular designs that could lead to both a fundamental understanding of photoinduced charge separation at a molecular level and also provide a solution to improve bulk properties of organic materials to overcome the poor efficiencies of OPV devices.

The effect of molecular architectures on the efficiency of electron transfer, a primary step in OPVs functioning, is evaluated in this work. We have shown that even though dendrimer provides an interesting architecture for efficient electron transfer due to the presence of multiple peripheries around a single core, this architecture leads to trapping of charge at the dendritic core. This results in a decrease in the electron transfer efficiency in solution and also limits the possibility of charge transport to the electron in a photovoltaic device.

Non-conjugated polymers containing conductive EDOT units at side chains were also designed and synthesized. The frontier energy levels of these polymers can be easily tuned by changing the conjugation lengths of side chain EDOT oligomers. Moreover, by

incorporating crosslinkable units as co-side chains, the absorption bandwidth of these polymers can be manipulated as well.

CONTENTS

Page

LIST OF TABLES

LIST OF FIGURES

LIST OF SCHEMES

LIST OF CHARTS

Chart Page

CHAPTER 1

INTRODUCTION

1.1 Dendrimers

In natural photosynthetic systems, a large array of chlorophyll molecules surrounds a single reaction center. The intricate chlorophyll assembly acts as an efficient light harvesting antenna that captures photons from the sun and transfers its energy to the reaction center, where conversion of solar energy into chemical potential energy via the formation of a charge-separated state takes place. Interestingly, the energy of any photon absorbed anywhere in this relatively large assembly of chromophores is passed rapidly to the reaction center with energy transfer quantum yield that approaches unity over nanometer distances.[1-5]

In the past decade, much attention has been devoted to the design and synthesis of supramolecular systems that can function as artificial light harvesting systems for the photochemical conversion of solar energy.[6-10] Five features of these complexes play key roles in the efficient collection of incident light for conversion into chemical energy: (1) large absorption cross-section of the complex due to a large number of chromophores with high extinction coefficients; (2) relative spatial orientation of these chromophores; (3) energy hopping of the exciton along the chromophores at the rim of the complex; (4) efficient and uni-directional energy transfer (ET) of the exciton from a chromophore at the rim to the chromophore in the center of the complex; (5) the generation of efficient photoinduced charge separation from excited state of peripheral chromophores and neutral state of the core.

Dendrimers are perfectly branched synthetic macromolecules having numerous chain ends all emanating from core (Figure 1.1). The number of peripheral functionalities in dendrimers can be controlled systematically with generations. Dendrimers are interesting scaffolds for light harvesting applications. Light harvesting is the trapping of energy where the peripheral chromophores absorb light and funnel it to a central point, where it can be utilized as photon energy or converted into chemical energy. Dendrimers possess the architecture to facilitate such a conversion. These properties include its tree-like structure that could potentially act as an energy gradient for the funneling process. The periphery of dendrimers can be functionalized with multiple light absorbing chromophore units that gives a high probability to capture light. The relatively short through-space distance from the periphery to the core, due to back folding, allows for high efficiency energy transfer.

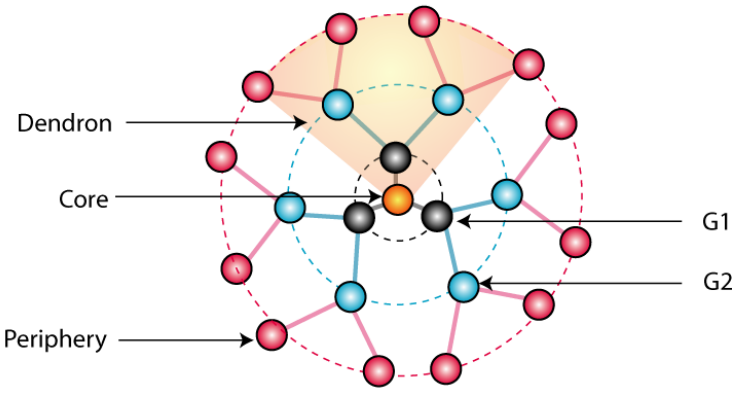

Figure 1.1. A dendritic architecture.

1.1.1 Dendrimers for energy transfer

1.1.1.1 Dendron as a scaffold

Non-conjugated dendrons such as the widely used poly(aryl ether) dendron function as just a scaffold linking together light-harvesting chromophores at the rim and the energy acceptor chromophore at the core. Owing to the lack of the electronic communication between donor and acceptor chromophores through dendritic backbone, these dendrimers provide the ability to independently tune the energy level of each chromophore. Moreover, the flexibility of the backbone also helps increase the solubility and processability of dendrimers.

Fréchet and coworkers synthesized non-conjugated poly (aryl ether) dendrimers containing amino-functionalized Coumarin-2 as the donor and acid-functionalized Coumarin-343 as the acceptor (Figure 1.2(a)).[11] The excitation of Coumarin-2 at 343 nm resulted in the fluorescence mainly at ~480 nm, which represented the characteristics of Coumarin-343 acceptor emission. This result implied an efficient energy transfer within these molecules. Steady-state and time-resolved studies revealed that the energy transfer efficiency in these dendrimers approached unity even at higher generations. Also, an interesting study on the relative rate between the energy transfer and nonradiative relaxation was carried out in this work. The model compounds of these dendrimers containing chromophores at the periphery, but not at the core, were also designed and used for this study (Figure 1.2(b)**)**. The fluorescence spectra of G1 and G2 model dendrons showed the quenching of the Coumarin-2 emission in methanol upon the excitation of donors resulting from the nonradiative relaxation due to the hydrogen bonding of the solvent with the tertiary amine lone pair. In contrast, corresponding

dendrimers with the acceptor at the core showed strong emission exclusively from Coumarin-343 core. This study revealed that the fast energy transfer can overcome the rate of the nonradiative pathways.

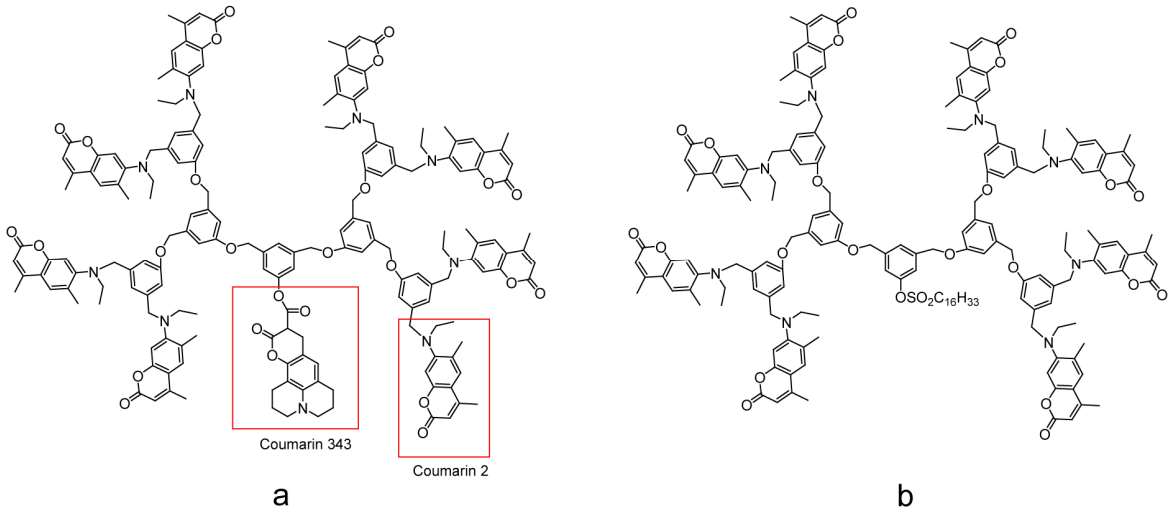

Figure 1.2. G2 dendrimers containing Coumarin-2 as an energy donor and Coumarin-343 as an energy acceptor (left) and dendrimers without Coumarin-343 chromophore (right) for relative rate study.

1.1.1.2 Dendrimer backbone as the chromophore

Dendrimer backbone themselves can also be concurrently used as the energy donor. Conjugated dendrimers such as phenylacetylene chains were mainly used for this purpose. By controlling over the conjugation length of dendritic branches in these dendrimers, rapid and directional energy transport could be obtained resulting in efficient energy transfer.

Efficient, unidirectional energy transfer from a dendritic framework to a single core chromophore was reported by Xu and Moore (Figure 1.3).[12] Conjugated phenylacetylene dendrimers functionalized with a low band gap perylene chromophore at the core were synthesized. Here, the phenylacetylene monomer units act as the energy donors, and perylene acts as the central energy acceptor. Excitation of the dendrimer backbone at 312

nm resulted in emission emanating solely from the perylene dye (450–600 nm), with nearly complete quenching of the dendrimer emission.

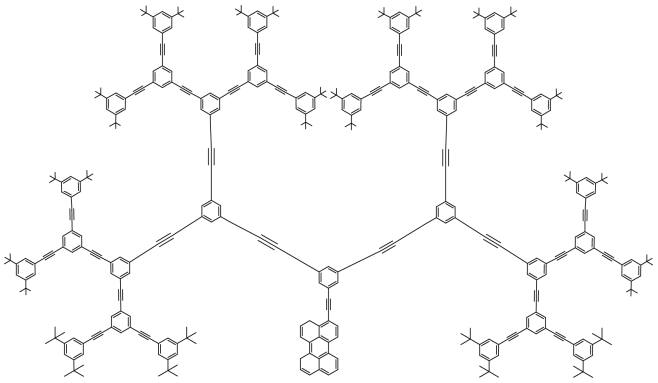

Figure 1.3. Chemical structure of perylene-functionalized phenylacetylene dendrimer**.**

Another conjugated dendrimer containing polyphenylene backbone and a perylene diimide core was synthesized by Mullen and co-workers. (Figure 1.4)[13] In this system, polyphenylene dendrimer scaffold exhibits strong fluorescence, with quantum yields ranging from 0.2 to 0.5 depending on the dendrimer generation. The authors noted that, high extinction coefficients of polyphenylene dendritic arms at shorter wavelength and their strong fluorescence intensity, together with the efficient intramolecular energy transfer, result in a strong emission from the core by indirectly exciting the polyphenylene dendritic arms.

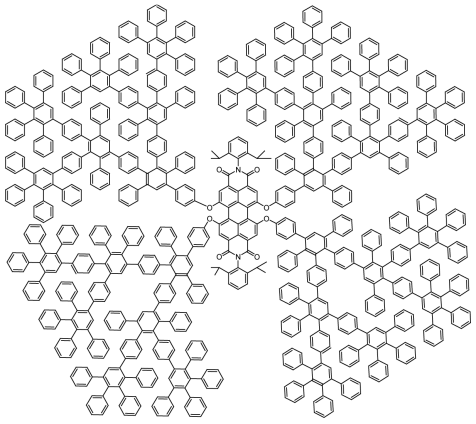

Figure 1.4. Molecular structure of polyphenylene dendrimer.

1.1.1.3 Energy migration

In dendrimers fully decorated with peripheral chromophores, after one of the peripheral chromophores were excited by incident light, it was shown by several groups that the migration of the excitation energy could be initiated before energy transfer to the core and that this energy migration can enhance the efficiency of energy transfer. Jiang and Aida demonstrated porphyrin dendrimers ($(L5)_nP$, n = 1-4) having different number (n) of five-layered aryl ether dendron subunits (L5) (Figure 1.5).[14] The excitation of dendron subunits in $(L5)_4P$ at 280 nm in CH_2Cl_2 resulted in strong emission at 656 and 718 nm which is characteristic of the porphyrin core. In contrast to this result, the excitation of partially substituted dendrimers resulted in a strong emission in the dendron region with only a weak emission from the porphyrin core. The energy transfer quantum yield dropped dramatically with the decreasing number of substituents on the porphyrin core. (n = 4, ϕ_{EET} = 80.3%; n = 3, ϕ_{EET} = 31.6%; n = 2, ϕ_{EET} = 19.7%; n = 1, ϕ_{EET} = 10.1%) For this observation, the authors suggested that before energy transfer happens, the excitation energy first migrates among neighboring dialkyoxybenzyl units until it can find the chromophore that has a suitable orientation for energy transfer. Then, the excitation energy is efficiently transferred to the core. As a result, this energy migration process would be able to enhance the energy transfer efficiency. The evidence for the presence of this energy shuttling was confirmed by fluorescence anisotropic measurements. The excitation of $(L5)_4P$ at 280 nm with polarized light resulted in the depolarized emission whereas emission of partially substituted $(L5)_nP$ (n = 1-3) still exhibited polarization character. We have recently shown that such energy shuttling is an important parameter in obtaining high ET efficiency in dendrimers.[15]

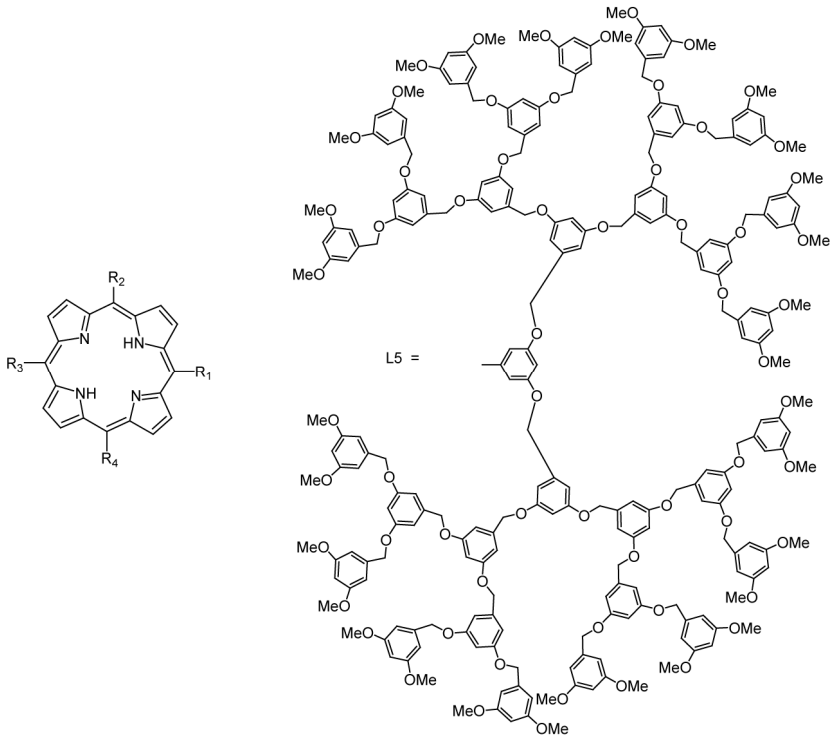

a $(L5)_1P$: R_1 = L5, $R_2 = R_3 = R_4$ = tolyl
b $(L5)_2P$: $R_1 = R_2$ = L5, $R_3 = R_4$ = tolyl or $R_1 = R_3$ = L5, $R_2 = R_4$ = tolyl
c $(L5)_3P$: $R_1 = R_2 = R_3$ = L5, R_4 = tolyl, **d** $(L5)_4P$: $R_1 = R_2 = R_3 = R_4$ = L5

Figure 1.5. Structure of porphyrin dendrimers containing different numbers of dendron subunits.

1.1.1.4 Energy Cascade

A versatile synthetic scheme allowed for the synthesis of dendrimers having a directional energy gradient. Moore and coworkers have reported dendrimers based on phenylacetylene chains that are specially arranged to form an energy gradient (Figure 1.6). Interestingly, it was found that this energy gradient dramatically increases (by two orders of magnitude) the energy transfer rate constant within the dendrimer.[16] Hence, the directional energy transfer from periphery to core must be greatly facilitated by the built-in energy gradient. Indeed, theoretical work by Klafter and coworkers afforded the same conclusion, suggesting that 'random walk' energy transfer from periphery to core, as in the former structures, is much less productive than the directed process in funnel

structures.[17, 18] However, the mechanism of energy transfer in these systems was difficult to ascertain. Owing to the cross-conjugated dendrimer backbone, orbital overlap contributions to the energy transfer cannot be ruled out.[19] In addition, spectral overlap between donor emission and acceptor absorption is not very large in this case, and would preclude the Förster mechanism alone from producing the high energy transfer efficiencies that were observed.[20]

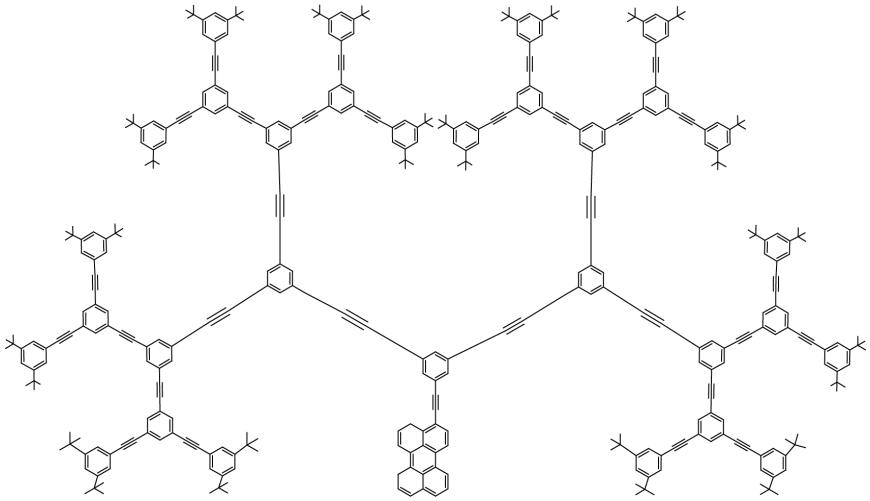

Figure 1.6. Chemical structure of perylene-functionalized phenylacetylene dendrimer with an energy gradient.

Dendrimers containing multichromophoric units that can absorb light in a wide visible range and efficiently transfer it to the core would be ideal for light harvesting systems. Fréchet and co-workers designed and synthesized poly (aryl ether) dendrimer containing coumarin-2 and fluorol-7GA at the third and second branch point, respectively as energy donors and a perylenebis(dicarboximide) derivative at the core as the energy acceptor (Figure 1.7).[21] The cascade energy transfer in this dendrimer was designed in such a way that energy would be harvested by coumarin-2 units and transferred to fluorol-7GA chromophores and then to perylene core. The direct energy transfer from coumarin-2 to the perylene core was expected to be less favorable owing to the smaller

spectral overlap between the emission spectra of coumarin-2 and the absorption spectra of perylene core and the longer interchromophore distance between these two dyes. The authors showed spectroscopic evidence for a cascade energy transfer from coumarin-2 to fluorol-7GA and finally to perylene core from the steady-state measurements. The energy transfer efficiency from coumarin-2 to fluorol-7GA was 99% and from fluorol-7GA to perylene core was 96%. Therefore, this would be a more favorable pathway compared to a direct transfer from coumarin-2 to perylene core that was calculated to be at the most 79%.

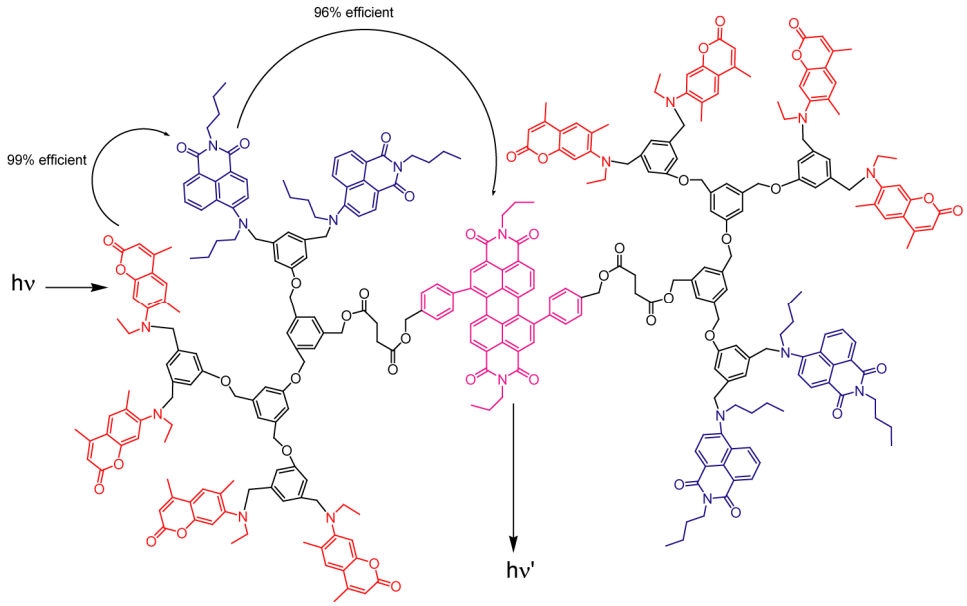

Figure 1.7. The structure of multichromophoric dendrimers containing coumarin-2 and fluorol-7GA as energy donors and perylenebis(dicarboximide) as the energy acceptor.

While all these energy cascade schemes increase the efficiency of energy transfer to the core, they do so at an energetic cost. The exciton loses energy at every step down the cascade, so the energy available when it reaches the core is less than what it had when it started at the periphery. Thus while the efficiency of an excitation reaching the core may be 100%, that excitation may only have 75% of the original photon energy. It is worth

noting that in nature, the light-harvesting complex consists of isoenergetic chlorophylls, and that the cascade motif is not the dominant one (although there is some energy gradient which directs the excitation to the reaction center). Thus it is not immediately clear that the cascade or energy funnel types of structures are necessarily the best for solar light harvesting. High ET efficiency to the core does not directly translate to high overall energy efficiency of the structure.

1.1.2 Dendrimers for electron transfer

After energy transfer, electron transfer (ET) is the next key step in photosynthetic systems and it involves a pair of electron-donor and acceptor entities, and its efficiency reduces exponentially with donor-acceptor distance. However, while a highly efficient FRET results in fluorescence emitted mainly from the acceptor chromophore, a highly efficient ET usually leads to a strong quenching of the fluorescence of the emitting chromophore. Recently, Müllen and coworkers have reported perylenetetracarboxidimides (PDI) with peripheral triphenylamine (TPA) dendrimers (Figure 1.8).[22] Steady state and time-resolved data revealed that this dendrimer is capable of intramolecular electron transfer from periphery to core and this occurs more efficiently in polar solvents.

Guldi and co-workers have reported fullerene based dendrimers to mimic the natural photosynthetic assemblies (Figure 1.9).[23] These dendrimers function as rigid molecular scaffolds where dendritic spacers are end capped with dibutylaniline or dodecyloxynaphthalene as donors, while the electron accepting fullerene is placed at the focal point of the dendron. Photophysical investigations showed that upon

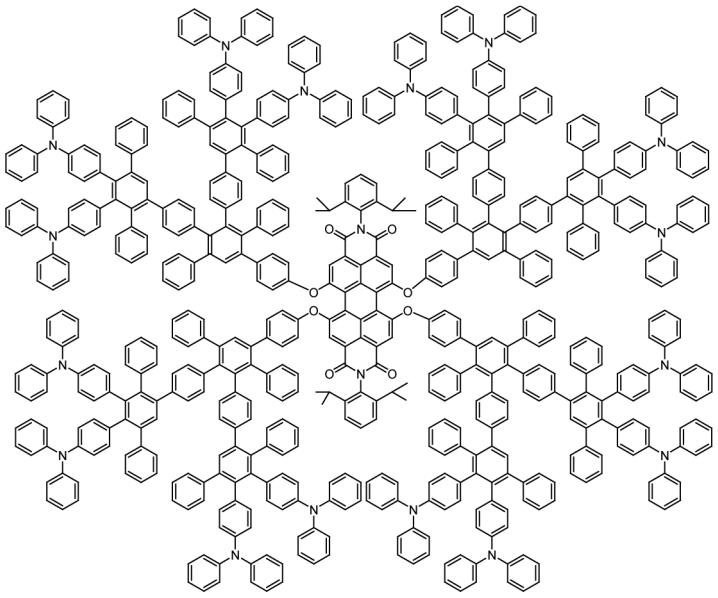

Figure 1.8. Polyphenylene dendrimer with peripheral triarylamines and a central perylenetetracarboxidiimide chromophore.

photoexcitation there was an efficient and rapid transfer of singlet excited state energy that controls the reactivity of the initially excited antenna portion. Spectroscopic and kinetic evidence suggests that photoinduced electron transfer from periphery to core resulted in $C_{60}^{\cdot -}$ -dendron$^{\cdot +}$ charge transfer state with quantum yields as high as 0.76 with lifetimes in the order of hundreds of nanoseconds (220-725 ns). They also found that this

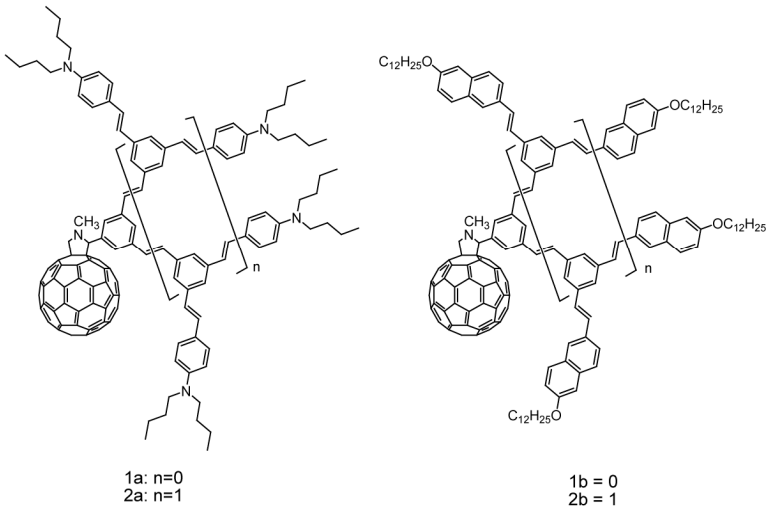

Figure 1.9. First (1a, 1b) and second (2a, 2b) generations of new C_{60}-dendron dyads.

charge transfer state can be modulated by varying the energy gap and that higher generations stabilize this charge transfer state efficiently.

The example of non-conjugated dendrimers that are capable of photoinduced electron transfer was demonstrated by Aida and co-workers.[24] Electron donor metalloporphyrin having benzyl ether dendritic shell was synthesized (Figure 1.10). In this work, methyl viologen (MV^{2+}) noncovalently-attached on the exterior surface of dendritic shell was used as an electron acceptor. The titration of dendrimer with methyl viologen showed no change on absorption spectra of metalloporphyrin region implying that dendritic shells protect metalloporphyrin core by steric shielding and that methyl viologen has no interaction with the metalloporphyrin core. However, upon irradiation of this dendrimer in the presence of MV^{2+}, fluorescence from the core was quenched and fluorescence lifetime was shortened. This phenomenon implied the long range photoinduced electron transfer from metalloporphyrin core to methyl viologen through the dendrimer framework. Similar dendrimer-viologen binding, where a conjugated polymer is used as the chromophore, was also used for a demonstration of solar hydrogen production.

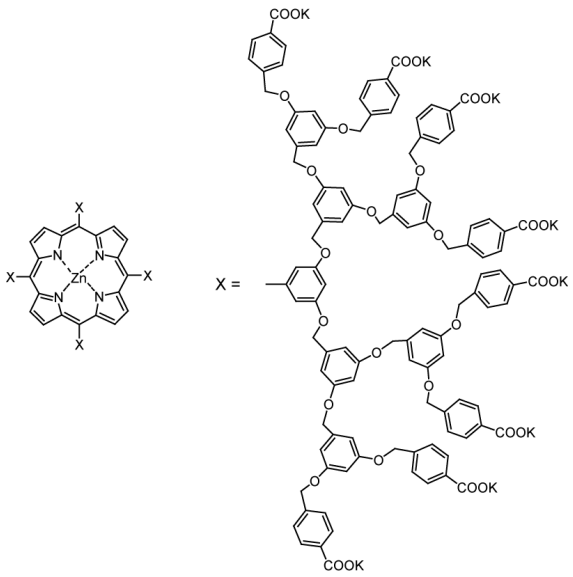

Figure 1.10. Benzyl ether dendrimers having metalloporphyrin core.

1.1.3 Bifunctional dendrimers

In order to mimic the complete photosynthetic event, recently, our group had designed dendrimers that are capable of undergoing both energy transfer and electron transfer properties. These dendrimers contained benzthiadiazole derivatives as the energy and electron acceptor at the core and diarylaminopyrene units as the energy and electron donors at the periphery.[25] The emission of diarylaminopyrene units overlapped with the absorption of benzthiadiazole moiety implying that Förster energy transfer can happen in these dendrimers. Moreover, the oxidation potential of benzthiadiazole units obtained from cyclic voltammogram was 595 mV, which is above that of diarylaminopyrene units which exhibited at about 444 mV (with respect to ferrocene/ferrocenium couple). This electrochemical data suggested that it is possible for the excited state of the chromophore at the core to be reduced by peripheral chromophores.

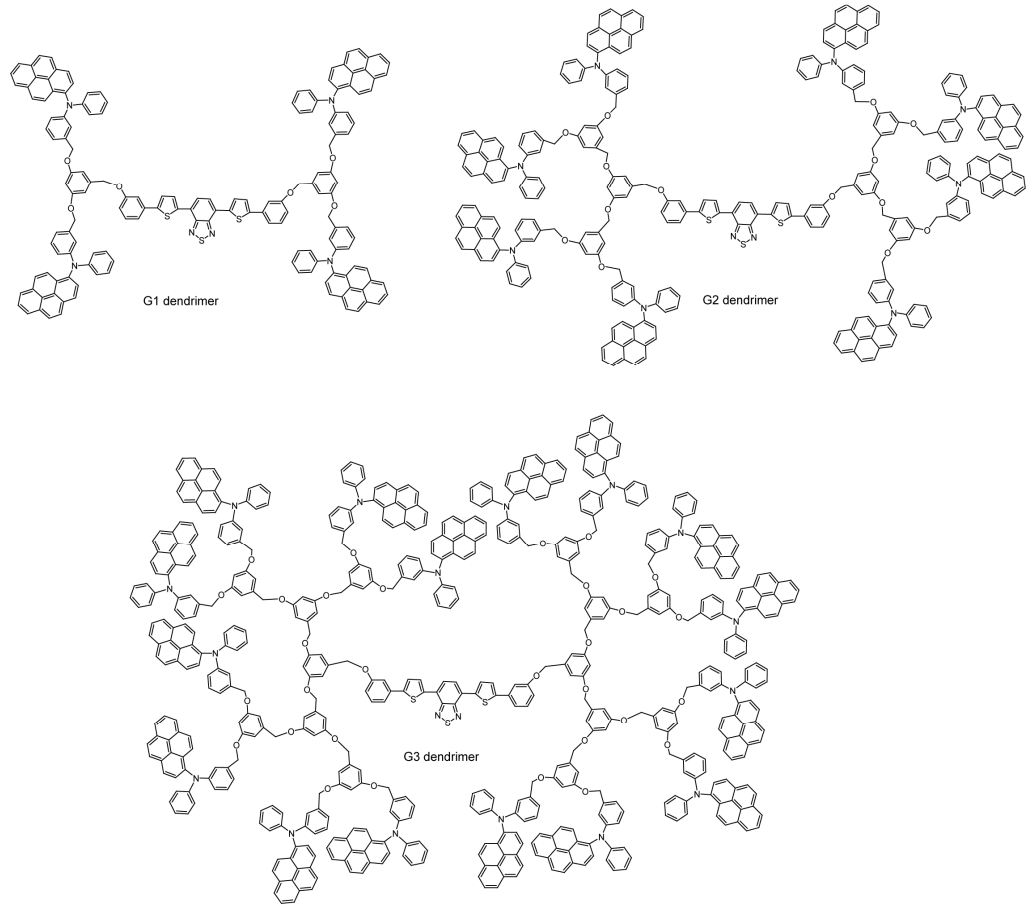

Figure 1.11. Light-harvesting dendrimers containing benzthiadiazole derivatives at the core and diarylaminopyrene at the periphery.

The excitation of peripheral chromophores at 395 nm resulted in the fast rise of the fluorescence from the acceptor at 605 nm implying rapid Förster energy transfer in these molecules. Also, the energy transfer efficiency in these molecules was high even at high generations (η_{EET} ~ 0.89-0.97). This efficiency was found to be solvent-independent, which is common for energy transfer processes. However, we found that the fluorescence lifetimes of the core altered with the change in the dielectric constant of solvents. The different degree of the fluorescence quenching from the core upon changing the solvent polarity implied the presence of a charge transfer event. In fact, this fluorescence quenching was found to be faster in high polar solvents. This would be due

to the fact that more polar solvent can better stabilize the charged-intermediate species and thereby increase the charge transfer rate. In addition, it was found that the long-lived (microseconds) transient absorption spectrum closely resembled that of the radical cation spectra obtained from both chemical and electrochemical oxidation of the peripheral diarylaminopyrene units. This provided additional evidence to confirm the presence of charge separated state in these dendrimers. The charge transfer efficiency in these dendrimers was calculated to be as high as 70% in the polar solvent DMF, and the overall efficiency of the photon to charge-separated state process was calculated to be approximately 50%.

1.2 Organic Photovoltaic Devices

1.2.1 Basic principle

A typical organic photovoltaic (OPV) device consists of an active layer sandwiched between two dissimilar metal/ semiconductor electrodes. The relatively higher work function electrode serves as the anode while the lower work function electrode serves as the cathode. Indium-tin-oxide (ITO) coated glass is the most commonly used transparent anode. The cathode can be a metal such as Au, Ag, Al, Ca, and Mg.

The active layer consists of a chromophore, a hole transporting (HT) and an electron transporting (ET) material. A single material can function as a chromophore and hole transporter or electron transporter, though most commonly a chromophore also functions as a hole transporter. Commonly used HT materials are based on conjugated polymers as shown in Figure 1.12[26] while ET materials are often based on fullerene derivatives.

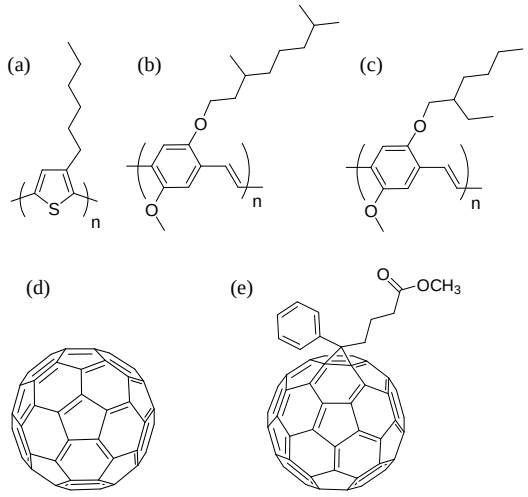

Figure 1.12. Structures of (a) RR-P3HT, (b) MDMO-PPV, (c) MEH-PPV, (d) C60 and (e) PCBM.

The working of an OPV device in terms of relative energy levels of constituent materials is depicted in Figure 1.13. When the incident light hits an organic chromophore, excitation of the molecules can occur if the light is of equal or higher energy than the

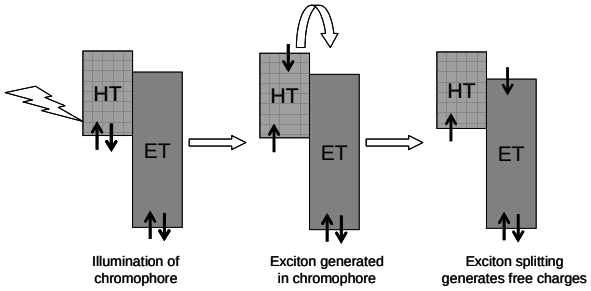

Figure 1.13. Working of an OPV device in terms of energy levels.

band gap of the chromophore. The highest flux of photons occurs around 700 nm (1.8 eV) in the solar spectrum.[27] Therefore the most preferred chromophore for OPVs is that which has a band gap of 1.8 eV. Once the exciton is generated, a potential difference greater than its binding energy (approximately 0.3 eV) is required to split it into electrons and holes. This potential difference can be created at an interface with a material with a relatively larger electron affinity. Such an interface however, must be encountered within the diffusion length in order to obtain high exciton splitting efficiency. Upon separation of charges, these must be carried to electrodes which can accept them to be subsequently run through an external circuit. Thus, the challenge in designing organic semiconductor based photovoltaics is to generate large number of excitons, harvest a majority of these, if not all, and ensure efficient charge transport to electrodes. This has been the focus of research for the past few decades.

1.2.2. Device performance

Each of the stages mentioned above, from exciton generation to charge collection, impacts the overall efficiency, η, of the device which is determined using measurable parameters, viz. the open circuit voltage (V_{oc}), short circuit current (I_{sc}), fill factor (FF), incident radiation intensity (P_{in}), voltage at peak power (V_{pp}) and current at peak power (I_{pp}). The mathematical expression relating these parameters is as follows.

$$\eta = \frac{FF * Voc * Isc}{Pin} \tag{1.1}$$

$$FF = \frac{Vpp * Ipp}{Voc * Isc} \tag{1.2}$$

The performance is experimentally measured under standard illumination conditions (AM 1.5 spectrum) and represented in an I-V curve. A typical I-V curve is shown in Figure 1.14. The non-ohmic nature of the curve is on account of photo-generation of charges. The further the deviation from ohmic behavior, the better will be performance of the device. The voltage at which no current flows through the device is called the open circuit voltage (V_{oc}) while the current flowing in absence of applied voltage is called the short circuit current (I_{sc}). Optimal output occurs at the point where the power generated is the maximum, the theoretical maximum being the product of V_{oc} and I_{sc}. The closer the V_{pp} and I_{pp} are to the V_{oc} and I_{sc} respectively, the higher will be the fill factor, a parameter indicating the fraction of the theoretical output being harnessed from the device. Let us now discuss the factors affecting each of these parameters.

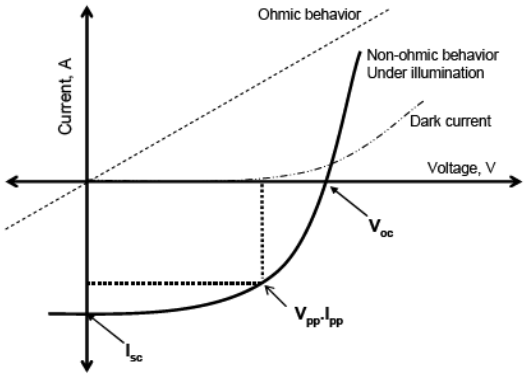

Figure 1.14. I-V curve.

1.2.1.1 Open circuit Voltage (V_{oc})

In a single layer device, wherein the organic layer functions as both the HT and ET, there is no inherent chemical potential difference in the active layer. Therefore, exciton splitting occurs only due to the potential difference arising from the difference in

work functions of the two electrodes. This is present only at the interface of the organic layer and metal electrode, leading to exciton splitting happening at this interface. Thus, the difference in the work functions of the two electrodes dictates the V_{oc}. The metal-insulator-metal (MIM) model is used to explain this. However, this model could not explain the origin of V_{oc} in devices where two different materials function as HT and ET individually.[28-30] For instance, bilayer devices consist of a layer of HT and ET mounted on each other, sandwiched between two electrodes, while the bulk heterojunction based OPV devices consist of an active layer constituted by a blend of the HT and ET materials sandwiched between two electrodes.

The fact that the donor and acceptor are separate provides a chemical potential difference at the interface of the HT and ET materials which can drive exciton splitting. In such cases, the V_{oc} can exceed the electrical potential difference due to the difference in work functions of the electrodes.[31] It was reported that the V_{oc} in bilayer and bulk heterojunction devices is a function of the difference between the LUMO energy level of the ET and the HOMO energy level of the HT.[29, 32-36]

Morphology of the active layer also has an impact on the V_{oc}. A theoretical model developed for understanding the origin of V_{oc} in bulk heterojunction OPV devices predicts that the degree of phase separation of HT and ET materials has a significant impact on the V_{oc} of the device.[28, 37] According to this model, an increase in the degree of mixing increases the I_{sc} but leads to a decrease in the V_{oc}. They find that layered morphology yields the highest V_{oc} while homogenous blends show low values on account of higher internal energy losses arising from multiple charge separation events. Hence, partially blended morphology of the active layer should serve best to provide optimal V_{oc}

in the device. Other approaches towards improving the V_{oc} of the device include changing the ratio of HT and ET present in the blend[38], modification of electrodes[39, 40], modification of interface between HT and ET material[41] and using a cascade energy band structure.[42]

1.2.1.2 Short circuit current (I_{sc})

The short circuit current can be calculated from equations 1.3 and 1.4. From these relationships, the photocurrent generated in the device can be enhanced by improving the amount of light absorbed (η_λ), the efficiency of exciton separation (η_{ED}) and charge transport (η_{CC}).

$$Isc = EQE(\lambda) * S_{AM1.5}\, d\lambda \tag{1.3}$$

$$EQE(\lambda) = \eta_\lambda * \eta_{ED} * \eta_{CC} \tag{1.4}$$

Below, we would like to discuss material design strategies used in literatures to improve the efficiency of each of these parameters.

1.2.1.2.1 Light absorption

As photovoltaic devices convert one photon into one electron, it is essential that the chromophoric materials absorb light in the high photon flux region in the solar spectrum to reduce the photon loss. As mentioned earlier, the highest intensity of solar spectrum occurs at 700 nm (1.8 eV), therefore, the desirable band gap for light absorbing organic materials should be at least 1.8 eV or lower. The band gap of a material is represented by the following equation which considers all its significant contributors.[43, 44]

$$E_g = E_{BLA} + E_{RES} + E_\theta + E_{int} + E_{sub} \tag{1.5}$$

1. Bond length alteration (E_{BLA}): This is defined as the difference in ground state, aromatic form, and the excited state, quinoid form, energy results in which dictates the confinement of electron in the aromatic structure. For instance, increasing the contribution of the quinoid form in conjugated polymers can extend the conjugation length and, thus, reduce the band gap.

2. Aromaticity (E_{RES}): Aromaticity results in the confinement of the π-electron on to aromatic rings. Reducing steric hindrance between adjacent aromatic rings will enable the electrons to delocalize throughout the conjugated system, therefore, decreasing the band gap.

3. Planarity (E_{θ}): Increasing of planarity in conjugated systems by either reducing the steric interaction or applying the rigidification into conjugated systems will result in the high degree of electron delocalization of the π electrons and thus reducing the band gap.

4. Intermolecular Effects (E_{int}): The band gap reduction due to an intermolecular effect can be obviously seen from the difference in optical properties of solid and solution phase. Mesoscopically ordered phases is a reason for the decrease in band gap in solid state compared to the disordered solution phases.

5. Substituent effects (E_{sub}): Inductive effect of electron withdrawing and electron donating groups can result in the reduction of the band gap.

Examples of low band gap materials are showed in Figure 1.15.[45-48] A synergistic combination of several effects mentioned above is attributed to the low band gap in these materials. It should be noted, however, that reducing band gap alone might not necessarily help obtaining high power conversion efficiency in OPV devices. All low band gap materials shown below provide very low efficiency when intermixed with

PCBM. This may be the consequence of increasing HOMO level of these donors upon reducing the band gap resulting in the decline of the V_{oc}.[49]

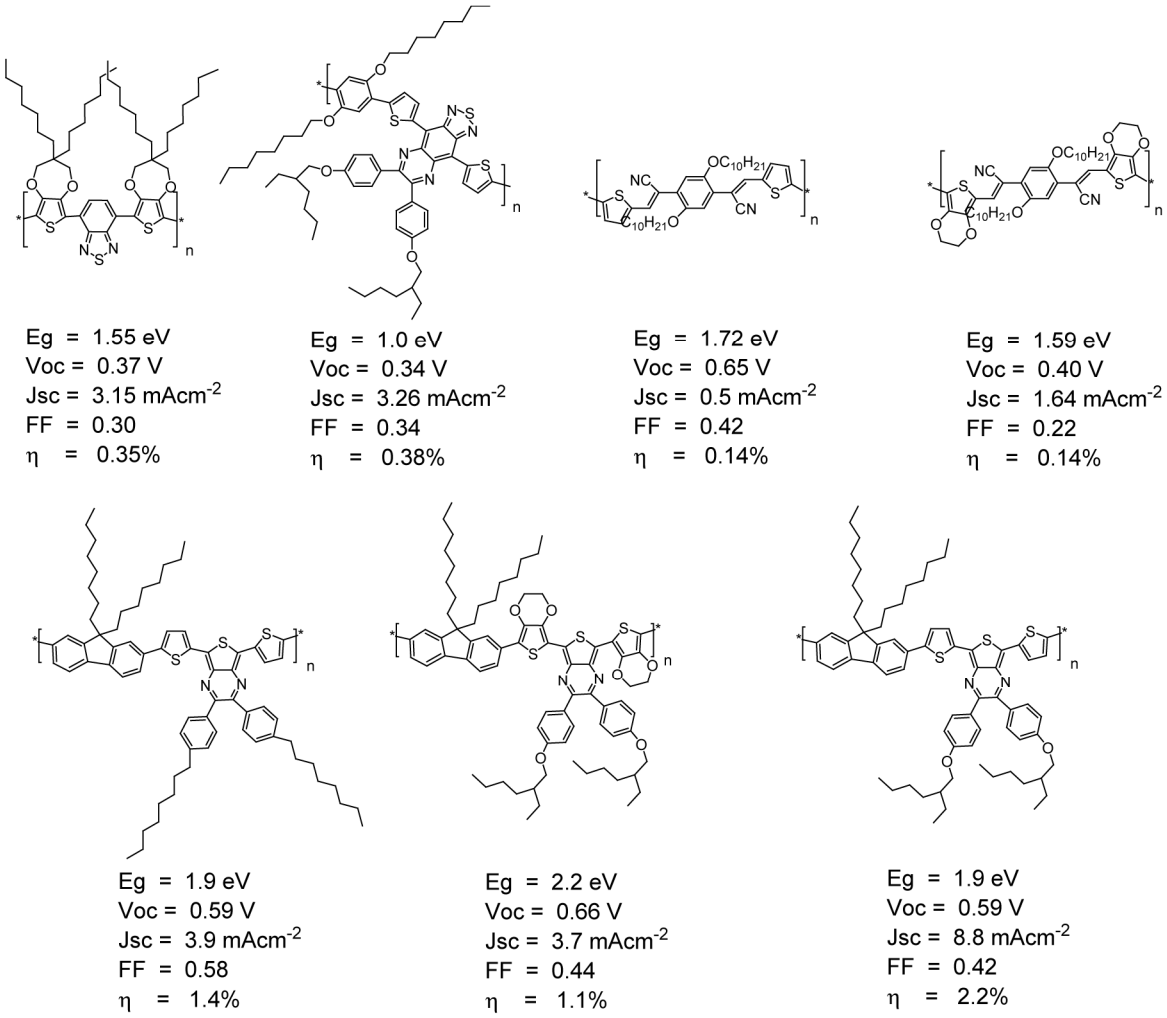

Figure 1.15. Examples of low band gap materials and their power conversion efficiency.

1.2.1.2.2 Charge separation

The morphology of the active layer plays a significant role, as it affects the charge separation and mobility to an appreciable extent. A large interface between the HT and ET materials is desirable in order to have the maximum opportunity for charge separation. Blending the two kinds of materials meets this requirement satisfactorily, but without providing a control over the morphology of the blend. Isolated phases of the ET

material dispersed in the HT material, which are unavoidably formed in blends, hamper the flow of charges through the combined phase. This is an important drawback of the bulk heterojunction devices, the state-of-the-art OPV devices.

In order to address this issue in bulk heterojunction OPVs, the concept of "double cable" polymers has been introduced. These materials consist of a conjugated polymer as the donor (p cable) whose pendent side chains function as acceptors (n cable). This design ensures large donor/acceptor interface enforced at the molecular level and also prevents aggregation of either donor or acceptor materials.[50, 51] The advantages of this design are quite intuitive. The intramolecularly-linked D/A can accelerate the electron transfer kinetics appreciably as the donor and acceptor interface is tremendously increased in a molecular level.

While designing double cable polymers, it is important to ensure that there is no ground state electronic communication between donor and acceptor units. In order to achieve this, photo-inactive alkyl chains are generally employed as linkers between the acceptor side chains and the donor main chain The most widely used polymers for constructing these molecules are poly(thiophene) and poly(phenylenevinylene), while the acceptor is most commonly fullerene.[52-56] The main drawback of double cable type materials is their insolubility.[57] As a result, these polymers often have very short chain lengths, which may impede their charge transport property. The methodology adopted to increase the solubility of the double cables is incorporating flexible units as co-side chains. However, increasing the amount of solubilizing groups decreases the acceptor content of the polymers. As a result, the electron hopping from one acceptor unit to its neighboring unit becomes more difficult resulting in low power conversion efficiency.

An example of double cable with photodiode behavior is illustrated in Figure 1.16. This double cable was synthesized by the copolymerization of poly(p-phenylene vinylene) having solubilizing side chains and poly(p-phenylene ethylene) containing fullerene side chains.[58] The photoinduced charge transfer in this double cable was confirmed by fluorescence quenching of the PPV donor in double cable and the presence of methanofullerene anion band at 1.2 eV in the photoinduced absorption spectra. It is noteworthy that even though the I_{sc} (0.42 mA/cm^2) of this double cable polymer is low compared to that of the blended system[59], the percentage of fullerene leading in the double cable is much lower (31.5%wt in the double cable polymer vs. 75 %wt in the blend).

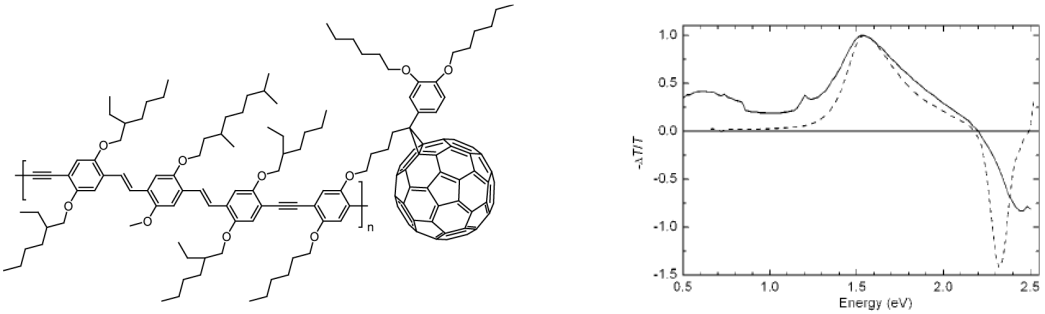

Figure 1.16. Structure of copolymers of poly (p-phenylene vinylene) having solubilizing side chains and poly(p-phyneylene ethylene) containing fullerene side chains. The PIA spectra revealed the presence of electron transfer in this copolymer.

One of the reasons that cause the poor power conversion efficiency of devices made of double cables is the low percent loading of the acceptor which in turn limits the transportation of electrons. Soluble double cable copolymers of polythiophene containing 7% and 14% of fullerene side groups have been reported. (Figure 1.17)[60] The photodiode performance of these double cables was low compared to the blended system due to the low percentage of fullerene incorporated onto the molecules. This assumption

was proved by mixing double cable containing 7% of fullerene with PCBM in 1:3 ratio**.** The efficiency of the device was improved and became comparable to the bulk heterojunction one. [61]

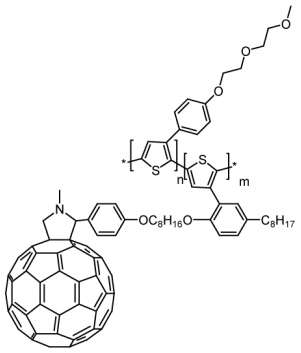

Figure 1.17. The structure of polythiophene containing fullerene double cables.

Even though power conversion efficiency in double cables is not comparable with that in the blended system, there still is room for optimization. It has to be borne in mind that increasing the charge dissociation alone by maximizing D/A interfaces in double cables may not lead to improved efficiency. The power efficiency is also dictated by other parameters including the carrier transport. To improve the carrier transport, the self organization of double cable polymers needs to be considered. If π-stacking of donor conjugated polymers can be achieved, hole transport may be further facilitated, thus enhancing the efficiency of charge transport to the electrode. Moreover, the drift carriers in organic materials result not only from the potential built-in by different electrodes, but also from the photoinduced chemical potential gradient generated by A-D moieties.[62] Therefore, a perfect double cable polymer need not necessarily have a perfect distribution of A moieties in each and every repeating unit of D donor as this is too homogeneous and could erase the photoinduced chemical potential gradient in the materials, the driving force for carrier separation and collection. Therefore, tuning D-A ratio, morphology and

separation could be promising ways to improve the efficiency of OPV devices made of this type of materials.

1.2.1.2.3 Charge collection

The above molecular architecture was designed to enhance the charge separation efficiency in an OPV. The other significant parameter directly influencing I_{sc} is the charge collection. The process of charge generation occurs at femtosecond time scale, while the recombination of these charges is a microsecond time scale process.[63] The recombination step is also assisted by the favorable Coulombic interaction of opposite charges. Therefore, the generated charges have to be transported fast enough to their respective electrodes to obtain high charge collection efficiency lest the carrier loss will lower the power conversion efficiency. Materials with high electron and hole mobilities have been designed and used for this purpose. In an ideal scenario, both the HT and ET should form two continuous phases, where each phase has a size on the order of the average exciton diffusion length, generally less than 10 nm.[64] Considering this, small molecules and block copolymers containing donors and acceptors functionalities are particularly of interest. Block copolymers provide an advantage over the small molecules in terms of tunability of the block length and donor/acceptor units in each block.[65] Systematic control of these factors should lead to improved photovoltaic efficiency.

1.2.1.2.3.1 Small molecules

The self assembly of small molecules into segregated donor and acceptor domains can generate the transport pathway for carriers to the respective electrodes resulting in improved photovoltaic efficiency. However, the problem with this kind of assembly is that electronically rich donor chromophores preferentially interact with electron-poor

acceptor chromophores. This interaction is not favorable for photovoltaic cells. In order to acquire a desirable self organization, Venkataraman *et al.* incorporated hydrocarbon chain onto donor chromophores and fluorocarbon chain onto acceptor chromophores (Figure 1.18).[66] It was confirmed by X-ray that the incompatibility of hydrocarbon and fluorocarbon drives the molecular assembly in such a way that segregated domains of electron rich and electron poor units can be obtained. However, photocurrent of this D/A assembly was not investigated.

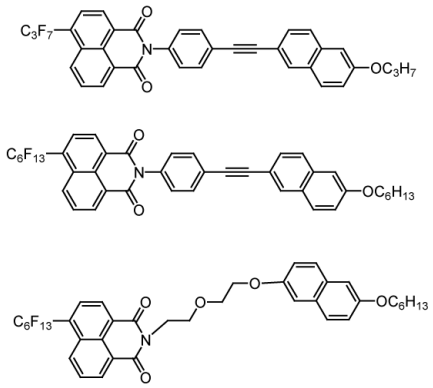

Figure 1.18. Structures of electron rich and electron poor chromophores having incompatible side chains.

Another example of the self-assembly of donor-acceptor diads has been illustrated by Aida *et al.*[67] In this case, self assembly was controlled by the incompatibility of hydrocarbon and glycolic moiety and the π-π interaction of hexabenzocoronene (HBC) donor units. Well-defined self-assembled coaxial nanowires of trinitrofluorenone (TNF)-appended hexabenzocoronene (HBC) (Figure 1.19) showed photoconductivity enhancement by the factor of $>10^4$ upon irradiation. This improved photoconducting efficiency could have resulted from an efficient hole and electron transport through a layer of HBC and TNF, respectively. They also found that increasing the ratio of the acceptor:donor upto a certain limit increases the photoconductivity beyond which distortion of the nanoassembly reduces it.[68]

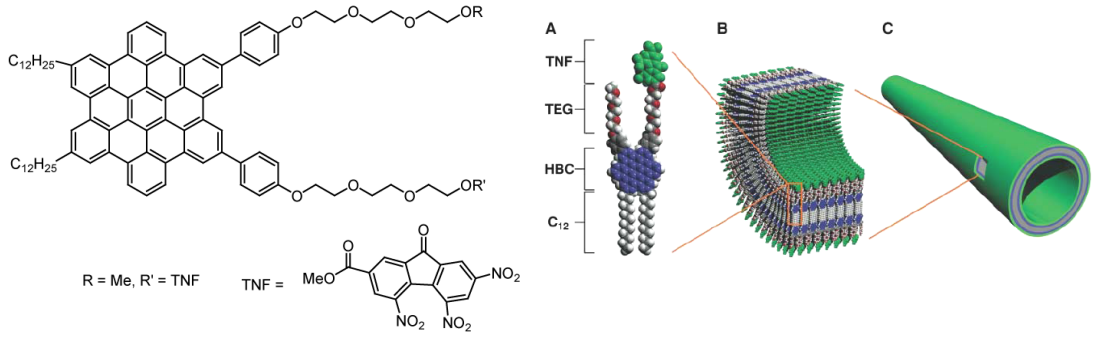

Figure 1.19. The structure of HBC-TNF and its assembly into a nanotube.

In another instance, amphiphilicity of the molecules was used to trigger self assembly. The self assembly of amphiphilic oligothiophene-C60 dyads was studied and compared with their nonamphiphilic analogs (Figure 1.20).[69] It was observed by synchrotron radiation small angle X-ray scattering (SAXS) analysis that each repeating layer in amphiphilic A-D dyads formed tail-to-tail pairs and such layers are connected at the fullerene-appended hydrophilic head part to form 2D lamellar strucuture. Unlike in amphiphilic A-D dyads, nonuniform assembly was observed in the nonamphiphilic analogs. The assembly of amphiphilic dyads led to 10 fold enhancement in photocurrent as compared to nonamphiphilic molecules.

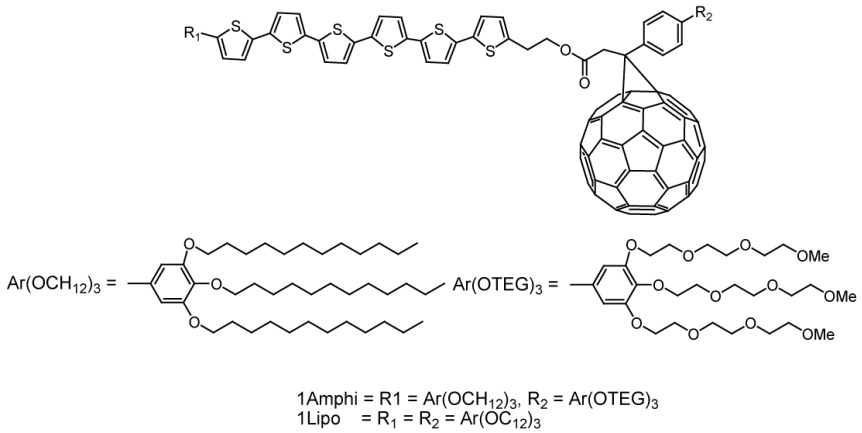

Figure 1.20. Amphiphilic and lipophilic oligothiophene donor containing fullerene acceptor.

1.2.1.2.3.2 Block Copolymers

Block copolymers are well known to self assemble into several discrete morphologies such as spheres, cylindrical, gyroidal and lamellar structures depending on the volume fraction of each block. Amongst these, cylindrical and lamellar morphologies can generate clear pathways for charge transport significantly reducing carrier losses.[70] Moreover, it is possible to adjust the block length of each block to obtain the assembly that is within the excition diffusion length, thus minimizing the exciton losses. Finally, by carefully selecting the donor and acceptor functionalities in each block, we should be able to maximize the amount of light captured by the chromophoric constituent. As a result, the photon losses can be minimized. Therefore, a block copolymer approach seems to be promising to acquire efficient OPV cells.

To investigate the performance of block polymers in photovoltaic devices, Hadziioannou and co-workers synthesized PPV-*b*-P(S-*stat*-C_{60}MS) based diblock copolymer (Figure 1.21).[71] The morphologies of block copolymers in CS2 observed from SEM images exhibit a highly ordered honeycomb structure with spherical cavities of diameter of 3-5 μm. This highly ordered structure was not seen in chloroform or *o*-dichlorbenzene where, instead a disordered morphology was observed.

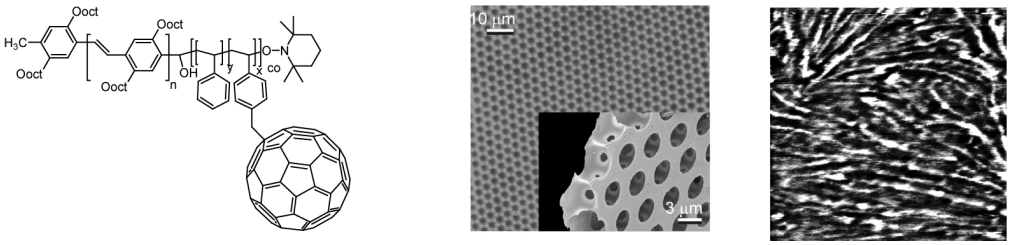

Figure 1.21. structure of PPV-b-P(S-stat-CMS) block copolymer and its morphology.

OPV devices were fabricated from the PPV-*b*-(S-*stat*-C_{60}MS) copolymers and from the blend of PPV and C60 containing the same amount of donor and acceptor components and their performance was compared. (Figure 1.22)[72] The D-A block copolymer showed superior response over the blend system. However, it was observed that the collection efficiency was still low in this device. This low efficiency may have been a result of inefficient exciton dissociation owing to competing energy transfer process. Moreover, the non-conjugated nature of C_{60} acceptor might result in the poor electron mobility and thus charge carrier losses in this device.

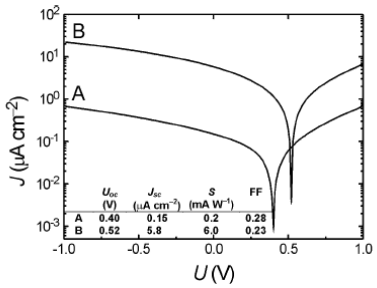

Figure 1.22. Photovoltaic parameters obtained in the D-A copolymers (B) and PPV/C_{60} blend (A) linker (B).

In order to address these issues, A and D conjugated block polymers with non-conjugated bridge (BDBA system) were designed (Figure 1.23(a)). Photo inactive linkers are aimed to separate the electronic state of the donor from the acceptor and to reduce the charge recombination rate. The flexibility of the linkers also assists in the phase separation and self assembly of block copolymers.[73] Figure 1.23(b) shows the structures of this type of block polymers. Alkyloxy derivative of polyphenylenevinylene or "RO-PPV" was synthesized as the D block, a sulfone derivatized polyphenylenevinylene or "SF-PPV" was incorporated as the A block and a long alkyl chain was used as a flexible bridge. STEM image of the block copolymer showed a regular pattern implying the

phase separation between donor and acceptor blocks. This characteristic was not observed in the D/A blend film. Moreover, the columnar morphological pattern was observed in AFM image of the block copolymer on a silicon substrate (Figure 1.23(c)). The current density of devices made of this BDBA film was 2-3 orders of magnitude higher than that of the D/A blend film prepared under the same condition. The mobilities in the blend film and the block copolymer were found to be 3.21 x 10^{-10} and 5.66 x 10^{-8} cm^2/Vs, respectively. This implied that the enhanced photoconductivity observed in self assembled film originated from the bi-continuous phase separated morphology in BDBA system.

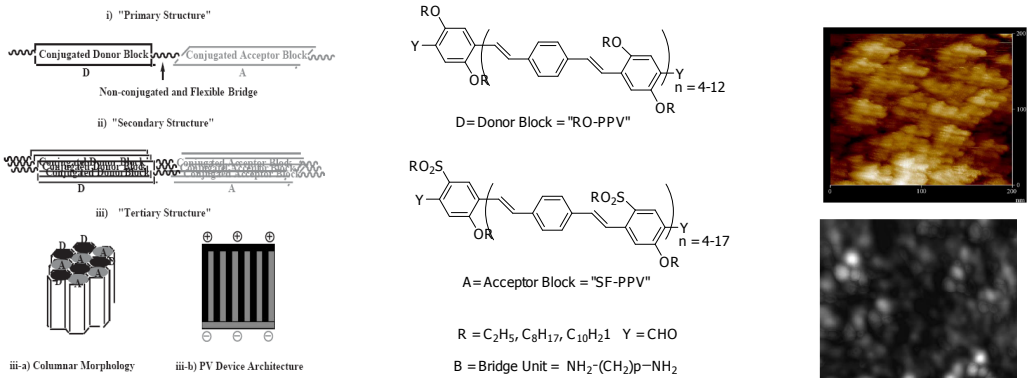

Figure 1.23. (a) A schematic representation of a conjugated donor/acceptor copolymer linked with flexible and non-conjugated linker and its self assembly. (b) The structure of the copolymer used in this study. (c) STEM and AFM images of block copolymer film.

Another BDBA type block copolymer was illustrated by Bonner et al. (Figure 1.24)[74-77] I-V characteristics of PPV based block copolymers exhibited improved photovoltaic performance compared to their corresponding blends. (1.10 vs 0.14 V, and 0.058 vs 0.017 mA/cm^2) It was observed by XRD that the D/A phase separation in the blend was on the order of several hundred nanometers, while this was on the order of around 20 nm (D phase) an 10 nm (A) phase in the block copolymer system. This

reduction in the phase segregation explains the reduction of exciton loss in the block copolymers. Moreover, the more ordered D/A crystalline phases in block copolymers resulted in the improved charge carrier transport in turn improving the V_{oc} and I_{sc} of block copolymer based device. The cell performance can be further improved by several factors such as optimization of energy levels, organic-metal interface treatment and morphology of materials.

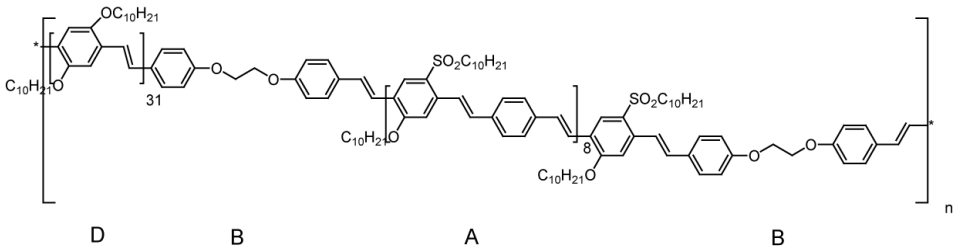

Figure 1.24. Structure of BDBA block copolymers in this study.

1.3 References

1. McDermott, G.; Prince, S. M.; Freer, A. A.; Hawthornthwaitelawless, A. M.; Papiz, M. Z.; Cogdell, R. J.; Isaacs, N. W., "Crystal-structure of an Integral Membrane Light-Harvesting Complex from Photosynthetic Bacteria" *Nature* **1995,** 374, (6522), 517-521.

2. Barber, J.; Andersson, B., "Reveling the Blueprint of Photosynthesis" *Nature* **1994,** 370, (6484), 31-34.

3. Deisenhofer, J.; Epp, O.; Miki, K.; Huber, R.; Michel, H., "Structure of the Protein Subunits in the Photosynthetic Reaction Center of Rhodopseudomonas-viridis at 3A Resolution" *Nature* **1985,** 318, (6047), 618-624.

4. Deisenhofer, J.; Michel, H., "The Photosynthetic Reaction Center from the Bacterium Rhodopseudomonas-Viridis" *Science* **1989,** 245, (4925), 1463-1473.

5. Hu, X. C.; Damjanovic, A.; Ritz, T.; Schulten, K., "Architecture and Mechanism of the Light-harvesting Apparatus of Purple Bacteria" *Proc. Natl. Acad. Sci. U.S.A.* **1998,** 95, (11), 5935-5941.

6. Fox, M. A., "Polymeric and Supramolecular Arrays for Directional Energy and Electron Transport over Macroscopic Distances" *Acc. Chem. Res.* **1992,** 25, (12), 569-574.

7. Gust, D.; Moore, T. A.; Moore, A. L., "Molecular Mimicry of Photosynthetic Energy and Electron Transfer" *Acc. Chem. Res.* **1993,** 26, (4), 198-205.

8. Gust, D.; Moore, T. A.; Moore, A. L., "Mimicking Photosynthetic Solar Energy Transduction" *Acc. Chem. Res.* **2001,** 34, (1), 40-48.

9. Wasielewski, M. R., "Photoinduced Electron-transfer in Supramolecular for Artificial Photosynthesis" *Chem. Rev.* **1992,** 92, (3), 435-461.

10. Webber, S. E., "Photon-harvesting Polymers" *Chem. Rev.* **1990,** 90, (8), 1469-1482.

11. Adronov, A.; Gilat, S. L.; Frechet, J. M. J.; Ohta, K.; Neuwahl, F. V. R.; Fleming, G. R., "Light Harvesting and Energy Transfer in Laser-dye-labeled Poly(aryl ether) Dendrimers" *J. Am. Chem. Soc.* **2000,** 122, (6), 1175-1185.

12. Xu, Z. F.; Moore, J. S., "Design and Synthesis of a Convergent and Directional Molecular Antenna" *Acta Polym* **1994,** 45, (2), 83-87.

13. Liu, D. J.; De Feyter, S.; Cotlet, M.; Stefan, A.; Wiesler, U. M.; Herrmann, A.; Grebel-Koehler, D.; Qu, J. Q.; Mullen, K.; De Schryver, F. C., "Fluorescence and Intramolecular Energy Transfer in Polyphenylene Dendrimers" *Macromolecules* **2003,** 36, (16), 5918-5925.

14. Jiang, D. L.; Aida, T., "Morphology-dependent Photochemical Events in Aryl Ether Dendrimer Porphyrins: Cooperation of Dendron Subunits for Singlet Energy Transduction" *J. Am. Chem. Soc.* **1998,** 120, (42), 10895-10901.

15. unpublished result in our laboratory.

16. Devadoss, C.; Bharathi, P.; Moore, J. S., "Energy Transfer in Dendritic Macromolecules: Molecular Size Effects and the Role of an Energy Gradient" *J. Am. Chem. Soc.* **1996,** 118, (40), 9635-9644.

17. Bar-Haim, A.; Klafter, J., "Geometric versus Energetic Competition in Light Harvesting by Dendrimers" *J. Chem. Phys. B* **1998,** 102, (10), 1662-1664.

18. BarHaim, A.; Klafter, J.; Kopelman, R., "Dendrimers as Controlled Artificial Energy Antennae" *J. Am. Chem. Soc.* **1997,** 119, (26), 6197-6198.

19. Gaab, K. M.; Thompson, A. L.; Xu, J. J.; Martinez, T. J.; Bardeen, C. J., "Meta-conjugation and Excited-state Coupling in Phenylacetylene Dendrimers" *J. Am. Chem. Soc.* **2003,** 125, (31), 9288-9289.

20. Thompson, A. L.; Gaab, K. M.; Xu, J. J.; Bardeen, C. J.; Martinez, T. J., "Variable Electronic Coupling in Phenylacetylene Dendrimers: The Role of Forster, Dexter, and Charge-transfer Interactions" *J. Phys. Chem. A* **2004,** 108, (4), 671-682.

21. Serin, J. M.; Brousmiche, D. W.; Frechet, J. M. J., "Cascade Energy Transfer in a Conformationally Mobile Multichromophoric Dendrimer" *Chem. Commun.* **2002**, (22), 2605-2607.

22. Qu, J. Q.; Pschirer, N. G.; Liu, D. J.; Stefan, A.; De Schryver, F. C.; Mullen, K., "Dendronized Perylenetetracarboxdiimides with Peripheral Triphenylamines for Intramolecular Energy and Electron Transfer" *Chem. Eur. J.* **2004,** 10, (2), 528-537.

23. Guldi, D. M.; Swartz, A.; Luo, C. P.; Gomez, R.; Segura, J. L.; Martin, N., "Rigid Dendritic Donor-acceptor Ensembles: Control over Energy and Electron Transduction" *J. Am. Chem. Soc.* **2002,** 124, (36), 10875-10886.

24. Sadamoto, R.; Tomioka, N.; Aida, T., "Photoinduced Electron Transfer Reactions through Dendrimer Architecture" *J. Am. Chem. Soc.* **1996,** 118, (16), 3978-3979.

25. Thomas, K. R. J.; Thompson, A. L.; Sivakumar, A. V.; Bardeen, C. J.; Thayumanavan, S., "Energy and Electron Transfer in Bifunctional Non-conjugated Dendrimers" *J. Am. Chem. Soc.* **2005,** 127, (1), 373-383.

26. Coakley, K. M.; McGehee, M. D., "Conjugated Polymer Photovoltaic Cells" *Chem. Mater.* **2004,** 16, (23), 4533-4542.

27. Bundgaard, E.; Krebs, F. C., "Low Band Gap Polymers for Organic Photovoltaics" *Sol. Energy Mater. Sol. Cells* **2007,** 91, (11), 954-985.

28. Gregg, B. A., "Excitonic Solar Cells" *J. Phys. Chem. B* **2003,** 107, (20), 4688-4698.

29. Scharber, M. C.; Wuhlbacher, D.; Koppe, M.; Denk, P.; Waldauf, C.; Heeger, A. J.; Brabec, C. L., "Design Rules for Donors in Bulk-heterojunction Solar Cells - Towards 10 % Energy-conversion Efficiency" *Adv. Mater.* **2006,** 18, (6), 789-794.

30. Waldauff, C.; Schilinsky, P.; Hauch, J.; Brabec, C. J., "Material and Device Concepts for Organic Photovoltaics: Towards Competitive Efficiencies" *Thin Solid Films* **2004,** 451-52, 503-507.

31. Cravino, A., "Origin of The Open Circuit Voltage of Donor-acceptor Solar Cells: Do Polaronic Energy Levels Play a Role?" *Appl. Phys. Lett.* **2007,** 91, (24), 243502-243502.

32. Cremer, J.; Bauerle, P.; Wienk, M. M.; Janssen, R. A. J., "High Open-circuit Voltage Poly(ethynylene bithienylene): Fullerene Solar Cells" *Chem. Mater.* **2006,** 18, (25), 5832-5834.

33. Gadisa, A.; Svensson, M.; Andersson, M. R.; Inganas, O., "Correlation between Oxidation Potential and Open-circuit Voltage of Composite Solar Cells Based on Blends of Polythiophenes/fullerene Derivative" *Appl. Phys. Lett.* **2004,** 84, (9), 1609-1611.

34. Ishwara, T.; Bradley, D. D. C.; Nelson, J.; Ravirajan, P.; Vanseveren, I.; Cleij, T.; Vanderzande, D.; Lutsen, L.; Tierney, S.; Heeney, M.; McCulloch, I., "Influence of Polymer Ionization Potential on the Open-circuit Voltage of Hybrid Polymer/TiO2 Solar Cells" *Appl. Phys. Lett.* **2008,** 92, (5), 053308-3.

35. Mutolo, K. L.; Mayo, E. I.; Rand, B. P.; Forrest, S. R.; Thompson, M. E., "Enhanced Open-circuit Voltage in Subphthalocyanine/C-60 Organic Photovoltaic Cells" *J. Am. Chem. Soc.* **2006,** 128, (25), 8108-8109.

36. Roquet, S.; Cravino, A.; Leriche, P.; Aleveque, O.; Frere, P.; Roncali, J., "Triphenylamine-thienylenevinylene Hybrid Systems with Internal Charge Transfer as Donor Materials for Heterojunction Solar Cells" *J. Am. Chem. Soc.* **2006,** 128, (10), 3459-3466.

37. Haerter, J. O.; Chasteen, S. V.; Carter, S. A.; Scott, J. C., "Numerical Simulations of Layered and Blended Organic Photovoltaic Cells" *Appl. Phys. Lett.* **2005,** 86, (16), 164101-3.

38. Peng, Q.; Park, K.; Lin, T.; Durstock, M.; Dai, L. M., "Donor-pi-acceptor Conjugated Copolymers for Photovoltaic Applications: Tuning the Open-circuit Voltage by Adjusting the Donor/acceptor Ratio" *J. Phys. Chem. B* **2008,** 112, (10), 2801-2808.

39. Irwin, M. D.; Buchholz, B.; Hains, A. W.; Chang, R. P. H.; Marks, T. J., "p-Type Semiconducting Nickel Oxide as an Efficiency-enhancing Anode Interfacial Layer in Polymer Bulk-heterojunction Solar Cells" *Proc. Natl. Acad. Sci. U. S. A.* **2008,** 105, (8), 2783-2787.

40. Zhang, T.; Ceder, M.; Inganas, O., "Enhancing the Photovoltage of Polymer Solar Cells by using a Modified Cathode" *Adv. Mater.* **2007,** 19, (14), 1835-1838.

41. Goh, C.; Scully, S. R.; McGehee, M. D., "Effects of Molecular Interface Modification in Hybrid Organic-inorganic Photovoltaic Cells" *J. Appl. Phys.* **2007,** 101, (11), 114503-12.

42. Sista, S.; Yao, Y.; Yang, Y.; Tang, M. L.; Bao, Z. A., "Enhancement in Open Circuit Voltage through a Cascade-type Energy Band Structure" *Appl. Phys. Lett.* **2007,** 91, (22), 225308-3.

43. Roncali, J., "Molecular Engineering of the Band Gap of Pi-conjugated Systems: Facing Technological Applications" *Macromol. Rapid Commun.* **2007,** 28, (17), 1761-1775.

44. Winder, C.; Sariciftci, N. S., "Low Bandgap Polymers for Photon Harvesting in Bulk Heterojunction Solar Cells" *J. Mater. Chem.* **2004,** 14, (7), 1077-1086.

45. Colladet, K.; Fourier, S.; Cleij, T. J.; Lutsen, L.; Gelan, J.; Vanderzande, D.; Nguyen, L. H.; Neugebauer, H.; Sariciftci, S.; Aguirre, A.; Janssen, G.; Goovaerts, E., "Low Band Gap Donor-acceptor Conjugated Polymers toward Organic Solar Cells Applications" *Macromolecules* **2007,** 40, (1), 65-72.

46. Mammo, W.; Admassie, S.; Gadisa, A.; Zhang, F. L.; Inganas, O.; Andersson, M. R., "New Low Band Gap Alternating Polyfluorene Copolymer-based Photovoltaic Cells" *Sol. Energy Mater. Sol. Cells* **2007,** 91, (11), 1010-1018.

47. Perzon, E.; Zhang, F. L.; Andersson, M.; Mammo, W.; Inganas, O.; Andersson, M. R., "A Conjugated Polymer for near Infrared Optoelectronic Applications" *Adv. Mater.* **2007,** 19, (20), 3308-3311.

48. Shin, W. S.; Kim, S. C.; Lee, S. J.; Jeon, H. S.; Kim, M. K.; Naidu, B. V. K.; Jin, S. H.; Lee, J. K.; Lee, J. W.; Gal, Y. S., "Synthesis and Photovoltaic Properties of a Low-band-gap Polymer Consisting of Alternating Thiophene and Benzothiadiazole Derivatives for Bulk-heterojunction and Dye-sensitized Solar Cells" *J. Polym. Sci. Pol. Chem.* **2007,** 45, (8), 1394-1402.

49. Soci, C.; Hwang, I. W.; Moses, D.; Zhu, Z.; Waller, D.; Gaudiana, R.; Brabec, C. J.; Heeger, A. J., "Photoconductivity of a Low-bandgap Conjugated Polymer" *Adv. Funct. Mater.* **2007,** 17, (4), 632-636.

50. Cravino, A.; Sariciftci, N. S., "Double-cable Polymers for Fullerene Based Organic Optoelectronic Applications" *J. Mater. Chem.* **2002,** 12, (7), 1931-1943.

51. Roncali, J., "Linear Pi-conjugated Systems Derivatized with C-60-fullerene as Molecular Heterojunctions for Organic Photovoltaics" *Chem. Soc. Rev.* **2005,** 34, (6), 483-495.

52. Cravino, A.; Zerza, G.; Neugebauer, H.; Maggini, M.; Bucella, S.; Menna, E.; Svensson, M.; Andersson, M. R.; Brabec, C. J.; Sariciftci, N. S., "Electrochemical and Photophysical Properties of a Novel Polythiophene with Pendant Fulleropyrrolidine Moieties: Toward "Double Cable" Polymers for Optoelectronic Devices" *J. Phys. Chem. B* **2002,** 106, (1), 70-76.

53. Ferraris, J. P.; Yassar, A.; Loveday, D. C.; Hmyene, M., "Grafting of Buckminsterfullerene onto Polythiophene: Novel Intramolecular Donor-acceptor Polymers" *Opt. Mater.* **1998,** 9, (1-4), 34-42.

54. Murata, Y.; Suzuki, M.; Komatsu, K., ""Synthesis and Electropolymerization of Fullerene-terthiophene Dyads"" *Org. Biomol. Chem.* **2003,** 1, (15), 2624-2625.

55. Xiao, S. X.; Wang, S.; Fang, H. J.; Li, Y. L.; Shi, Z. Q.; Du, C. M.; Zhu, D. B., "Synthesis and Characterization of a Novel Class of PPV Derivatives Covalently Linked to C-60" *Macromol. Rapid Commun.* **2001,** 22, (16), 1313-1318.

56. Yassar, A.; Hmyene, M.; Loveday, D. C.; Ferraris, J. P., "Synthesis and Characterization of Polythiophenes Functionalized by Buckminsterfullerene" *Synth. Met.* **1997,** 84, (1-3), 231-232.

57. Giacalone, F.; Martin, N., "Fullerene Polymers: Synthesis and Properties" *Chem. Rev.* **2006,** 106, (12), 5136-5190.

58. Ramos, A. M.; Rispens, M. T.; van Duren, J. K. J.; Hummelen, J. C.; Janssen, R. A. J., "Photoinduced Electron Transfer and Photovoltaic Devices of a Conjugated Polymer with Pendant Fullerenes" *J. Am. Chem. Soc.* **2001,** 123, (27), 6714-6715.

59. Shaheen, S. E.; Brabec, C. J.; Sariciftci, N. S.; Padinger, F.; Fromherz, T.; Hummelen, J. C., "2.5% Efficient Organic Plastic Solar Cells" *Appl. Phys. Lett.* **2001,** 78, (6), 841-843.

60. Zhang, F. L.; Svensson, M.; Andersson, M. R.; Maggini, M.; Bucella, S.; Menna, E.; Inganas, O., "Soluble Polythiophenes with Pendant Fullerene Groups as Double Cable Materials for Photodiodes" *Adv. Mater.* **2001,** 13, (24), 1871-1874.

61. Cravino, A.; Zerza, G.; Maggini, M.; Bucella, S.; Svensson, M.; Andersson, M. R.; Neugebauer, H.; Brabec, C. J.; Sariciftci, N. S., "A Soluble Donor-acceptor Double-cable Polymer: Polythiophene with Pendant Fullerenes" *Mon. Fur. Chem.* **2003,** 134, (4), 519-527.

62. Cravino, A., "Conjugated Polymers Electron-accepting with Tethered Moieties as Ambipolar Materials for Photovoltaics" *Polym. Int.* **2007,** 56, (8), 943-956.

63. Sun, S.; Fan, Z.; Wang, Y.; Haliburton, J., "Organic Solar Cell Optimizations" *J. Mater. Sci.* **2005,** 40, (6), 1429-1443.

64. Scerf, U.; Gutacker, A.; Koenen, N., "All-Conjugated Block Copolymers" *Acc. Chem.. Res.* **2008,** ASAP article.

65. Sun, S. S., "Polymer Photovoltaic Optimizations from Exciton Level" *J. Mater. Sci.-Mater. Electron.* **2007,** 18, (11), 1143-1146.

66. Benanti, T. L.; Saejueng, P.; Venkataraman, D., "Segregated Assemblies in Bridged Electron-rich and Electron-poor Pi-conjugated Moieties" *Chem. Commun.* **2007**, (7), 692-694.

67. Yamamoto, Y.; Fukushima, T.; Suna, Y.; Ishii, N.; Saeki, A.; Seki, S.; Tagawa, S.; Taniguchi, M.; Kawai, T.; Aida, T., "Photoconductive Coaxial Nanotubes of Molecularly Connected Electron Donor and Acceptor Layers" *Science* **2006,** 314, (5806), 1761-1764.

68. Yamamoto, Y.; Fukushima, T.; Saeki, A.; Seki, S.; Tagawa, S.; Ishii, N.; Aida, T., "Molecular Engineering of Coaxial Donor-acceptor Heterojunction by Coassembly of Two Different Hexabenzocoronenes: Graphitic Nanotubes with Enhanced Photoconducting Properties" *J. Am. Chem. Soc.* **2007,** 129, (30), 9276-9277.

69. Li, W.-S.; Yamamoto, Y.; Fukushima, T.; Saeki, A.; Seki, S.; Tagawa, S.; Masunaga, H.; Sasaki, S.; Takata, M.; Aida, T., "Amphiphilic Molecular Design as a Rational Strategy for Tailoring Bicontinuous Electron Donor and Acceptor Arrays: Photoconductive Liquid Crystalline Oligothiophene-C60 Dyads" *J. Am. Chem. Soc.* **2008,** 130, (28), 8886-8887.

70. Heiser, T.; Adamopoulos, G.; Brinkmann, M.; Giovanella, U.; Ould-Saad, S.; Brochon, C.; van de Wetering, K.; Hadziioannou, G., "Nanostructure of Self-assembled Rod-coil Block Copolymer Films for Photovoltaic Applications" *Thin Solid Films* **2006,** 511, 219-223.

71. Stalmach, U.; de Boer, B.; Videlot, C.; van Hutten, P. F.; Hadziioannou, G., "Semiconducting Diblock Copolymers Synthesized by Means of Controlled Radical Polymerization Techniques" *J. Am. Chem. Soc.* **2000,** 122, (23), 5464-5472.

72. de Boer, B.; Stalmach, U.; van Hutten, P. F.; Melzer, C.; Krasnikov, V. V.; Hadziioannou, G., "Supramolecular Self-assembly and Opto-electronic Properties of Semiconducting Block Copolymers" *Polymer* **2001,** 42, (21), 9097-9109.

73. Sun, S. S., "Design of a Block Copolymer Solar Cell" *Sol. Energy Mater. Sol. Cells* **2003,** 79, (2), 257-264.

74. Sun, S.; Fan, Z.; Wang, Y.; Haliburton, J.; Taft, C.; Maaref, S.; Seo, K.; Bonner, C. E., "Conjugated Block Copolymers for Opto-electronic Functions" *Synth. Met.* **2003,** 137, (1-3), 883-884.

75. Sun, S. S.; Fan, Z.; Wang, Y. Q.; Winston, K.; Bonner, C. E., "Morphological Effects to Carrier Mobility in a RO-PPV/SF-PPV Donor/acceptor Binary Thin Film Opto-electronic Device" *Mater. Sci. Eng. B-Solid State Mater. Adv. Technol.* **2005,** 116, (3), 279-282.

76. Sun, S. S.; Zhang, C.; Ledbetter, A.; Choi, S.; Seo, K.; Bonner, C. E.; Drees, M.; Sariciftci, N. S., "Photovoltaic Enhancement of Organic Solar Cells by a Bridged Donor-acceptor Block Copolymer Approach" *Appl. Phys. Lett.* **2007,** 90, (4), 279-282.

77. Zhang, C.; Choi, S.; Haliburton, J.; Cleveland, T.; Li, R.; Sun, S. S.; Ledbetter, A.; Bonner, C. E., "Design, Synthesis, and Characterization of a Donor-Bridge-Acceptor-Bridge-Type Block Copolymer Via Alkoxy- and Sulfone-Derivatized Poly(phenylenevinylenes)" *Macromolecules* **2006,** 39, (13), 4317-4326.

CHAPTER 2

EVALUATION OF NON-CONJUGATED DENDRITIC ARCHITECTURES FOR ENERGY AND CHARGE TRANSFER BY COMPARISON WITH LINEAR ANALOGS

2.1 Introduction

Increasing energy needs and the rapid depletion of fossil fuels highlight the need for developing methods for harvesting energies from renewable sources.[1-3] Solar energy is one of the widely available, yet largely untapped, sources of energy. The photosynthetic apparatus in nature is an example of converting solar energy in to chemical potential energy with high efficiency.[4-6] Two key steps in this energy conversion process involve energy transfer from the chromophores absorbing the light to the one that collects the absorbed energy at the reaction center and uses it to drive a charge separation event.[7] Factors such as the extinction coefficient of the chromophores, relative orientation of the chromophores and the charge transport units, and exciton hopping among the chromophore units could all influence the efficiency of the electronic energy transfer (EET) and/or the charge transfer (CT) events. Therefore, while designing artificial scaffolds for this purpose, it is necessary that a certain control over the functional group placements exist. Although a number of small molecules have been studied,[8-29] it is interesting to consider the possibility of using macromolecules for this purpose because of the potential to achieve charge separation over longer distances.

While polymers have been studied for this purpose,[30-33] dendrimers provide a unique opportunity to carry out systematic structure-property relationship studies in a macromolecular system due to the excellent control that one could achieve over the

molecular weight and polydispertsity.[34, 35] More importantly, the possibility of having a functionally dense periphery along with a single core unit makes dendrimers potentially useful for light harvesting applications. Both conjugated[36-40] and non-conjugated dendrimers[41-47] have been studied for this purpose. While conjugated dendrimers provide the advantage of through-bond communication between the periphery and the core for electronic energy transfer (EET), non-conjugated dendrimers provide the opportunity to dissect the electronic and architectural advantage of dendrimers. This is mainly because the role of dendrimers in a non-conjugated system is only structural and not functional. Moreover, the lack of electronic communication through conjugation allows for the independent tuning of the donor and the acceptor. Considering these advantages, several reports exist on the light harvesting properties of non-conjugated dendrimers. There have been a relatively few reports on charge transfer within dendritic architectures as well in both conjugated[48, 49] and non-conjugated systems.[50-53] We have recently reported a system that combines both EET and CT events sequentially in the same dendrimer.[54] While all these studies highlight the impressive possibilities with dendrimers, a systematic study to understand whether dendrimers provide architectural advantages in light harvesting applications has been lacking. We address this here for both energy transfer and charge transfer using non-conjugated dendrimers.

The obvious advantage of dendrimers in light-harvesting applications is their ability to pack multiple chromophores around a central acceptor. The ability of those absorbers to transfer energy to the core acceptor results in a large effective cross section for the acceptor, which in turn can use the transferred photon energy to do useful work, *e.g.* charge separation. But it is certainly possible that the covalent attachment of the

multiple donor chromophores carries some penalty in terms of the photophysical properties. For example, the branched architecture may sterically hinder the average through-space proximity of the donor and acceptor and force the donor-acceptor distance *R* to be larger than it would normally be for an unbranched (*i.e.* linear) analog. Since the Förster mechanism predicts an EET rate that scales as $1/R^6$, even small changes in distance can drastically alter the EET efficiency. After the energy is transferred to the core, in our bifunctional dendrimers, an electron transfer can then take place from one of the CT donors to the excited core. Since electron transfer reactions generally require orbital overlap, the possible lack of conformational freedom in dendrimers, relative to linear molecules, could be expected to present an obstacle to efficient charge separation as well. On the other hand, it is also possible that steric crowding at the dendrimer periphery actually increases backfolding and charge separation relative to linear molecules. In this work, we test the influence of these two competing structural possibilities upon charge transfer. In the flexible benzyl-ether systems studied here, we find that any deleterious effects of steric congestion on the EET or CT efficiencies is more than compensated for by the advantages of having greater donor densities around the core. In these conformationally disordered systems, the existence of multiple transfer pathways overcomes the slight increase in the average donor-acceptor distance in the branched molecules.

To demonstrate this experimentally, we have synthesized the set of molecules shown in Chart 2.1. The EET and CT donor moiety involves a diarylaminopyrene functionality at the periphery of the dendrimer and the acceptor unit involves a benzthiadiazole based dendritic core. We use these functionalities to achieve the fully

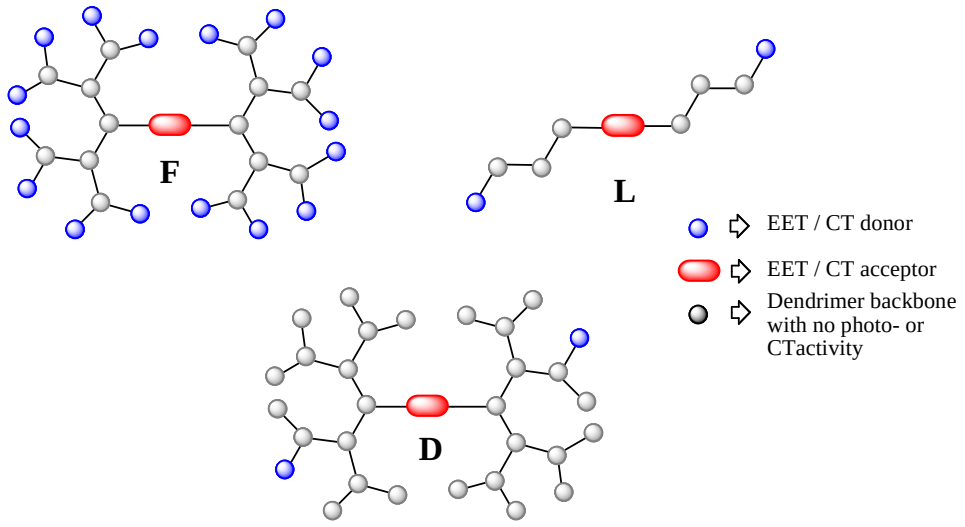

Figure 2.1. Schematic of a fully-decorated dendrimer (**F**), linear analog **(L),** and dendrimer with difunctionalized periphery (**D**).

decorated dendrimers, difunctionalized dendrimers and the linear analogs. Comparison of dendrimers with linear analogs has been previously done in the context of their physical properties.[55, 56] However, similar comparison in light harvesting dendrimers is more complicated. The complications are schematically illustrated in Figure 2.1. Classical dendrimers with the periphery fully decorated with energy or electron donor moieties and a single acceptor unit at the core are represented by **F** in Figure 2.1. Comparison of **F** with the linear analog **L** accounts for the distance between the donor and the acceptor that dendrimers and the linear oligomers provide, but fails to provide the equivalent chromophore densities (*i.e.* number of donors *vs*. acceptor). The only way to avoid this complication is to synthesize a difunctionalized dendrimer **D**, in which the number of and the distance between donors and acceptor moieties are identical to those in **L**. This work demonstrates the synthesis and photophysical characterization of all three types of molecules. We analyze the structural advantages of dendrimers both in the context of EET and CT properties.

2.2 Result and Discussion

2.2.1 Synthesis and Characterization

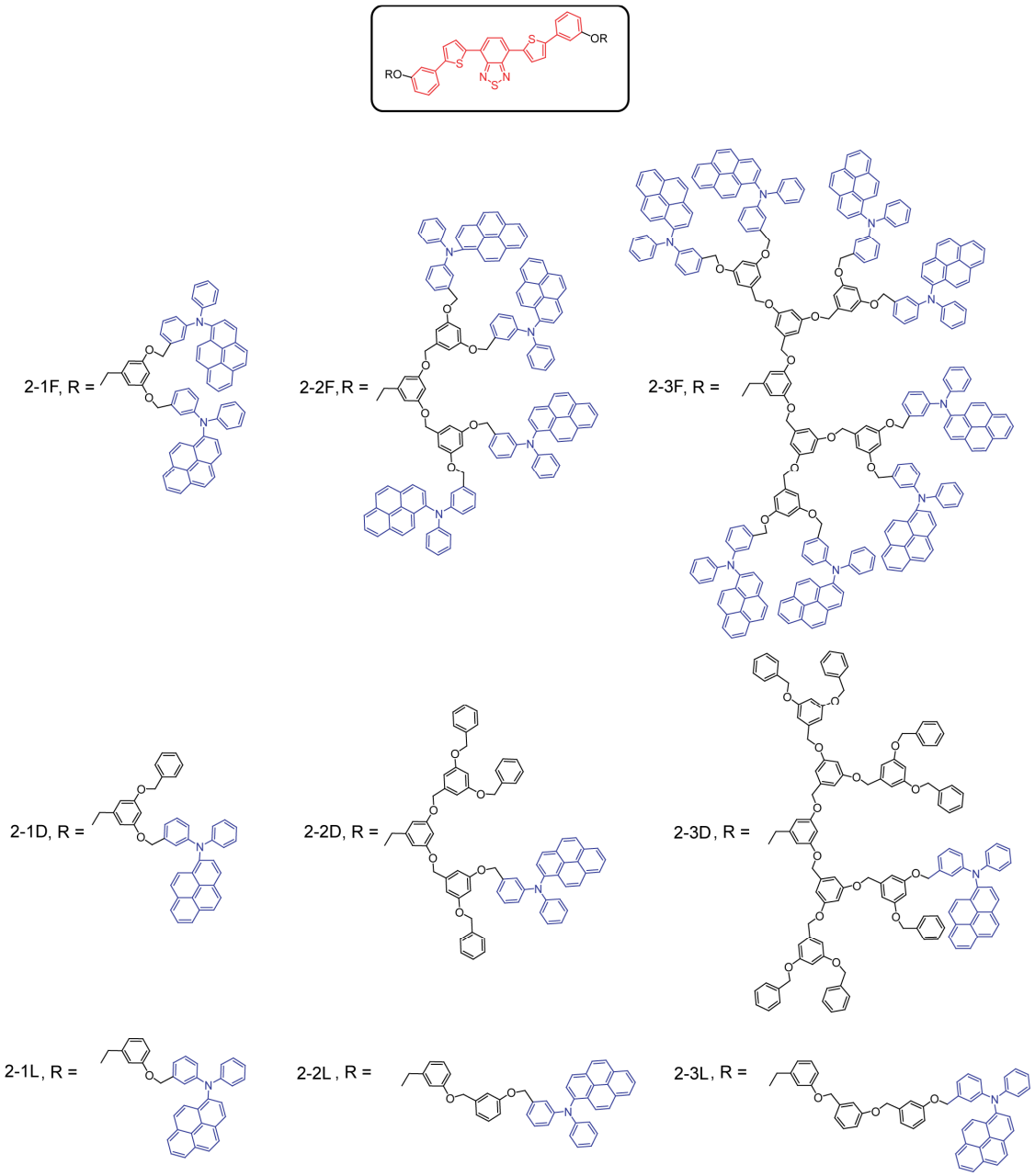

Chart 2.1. Structures of the fully functionalized dendrimers **2-1F**, **2-2F**, and **2-3F**, difunctionalized dendrimers **2-1D, 2-2D, and 2-3D** and the corresponding linear analogs (**2-1L**, **2-2L**, and **2-3L**).

We have synthesized dendrimers that contain diarylaminopyrene-based units as the energy and electron donor and a benzthiadiazole-based core as the energy and electron acceptor. Structures of the fully functionalized dendrimers **2-1F**, **2-2F**, and **2-3F**, difunctionalized dendrimers **2-1D, 2-2D, and 2-3D**, and the corresponding linear analogs **2-1L**, **2-2L**, and **2-3L** are shown in Chart 2.1.

Synthesis of these dendrimers was approached in a modular fashion. The synthesis of dihydroxy benzthiadiazole core (**2-3**) and hydroxymethyl diarylaminopyrene periphery (**2-23**) were followed the methodologies published previously by our group.[54] Synthesis of chromophore core was achieved by using bromination and Stille coupling as two main steps (Scheme 2.1). Benzothiadiazole (**2-1**) was first brominated using HBr/Br_2 as a reagent. Dibrominated product was obtained with 47% yield and was then coupled with 2-tributyl tin thiophene to get dithiophene benzothiadiazole (**2-2**) with 53% yield. The bromination of this compound using NBS gave 4,7-bis(5-bromothiophene-2-yl)benz[c][1,2,5]thiadiazole as a product with 64% yield. The Stille coupling of this

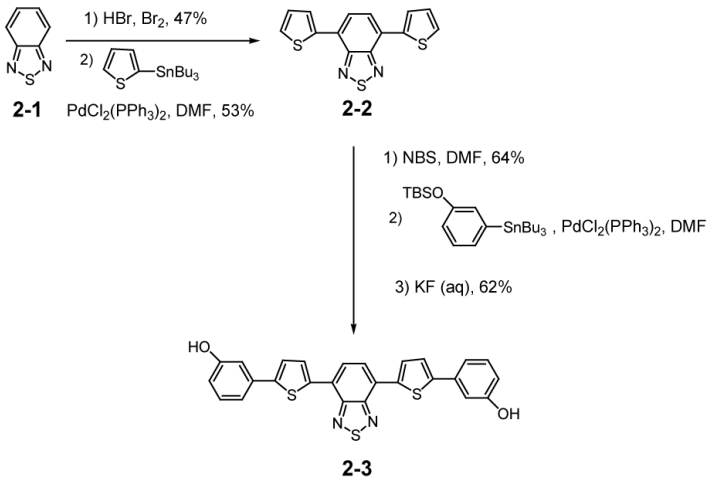

Scheme 2.1. The synthetic pathway of the benzthiadiazole core.

dibromo compound with aryl stannane followed by the deprotection of TBS protecting group using KF gave the desire benzthiadiazole core (**2-3**) in 62% yield.

Synthesis of the peripheral unit was accomplished by using the palladium catalyzed C-N coupling reaction as the key step (Scheme 2.2). Bromopyrene (**2-4**) obtained by reacting pyrene with NBS was coupled with aniline under Hartwig's conditions[57, 58] to get secondary amine as a product with 70% yield. The product was further reacted with 2-(3-bromophenyl)-1,3-dioxolane to obtain the protected tertiary amine as a product with quantitative yield. The protecting group was removed under acidic condition to get aldehyde functionalized diarylaminopyrene derivative (**2-5**) with 78% yield. The aldehyde moiety (**2-5**) was then reduced to get corresponding hydroxymethyl group in which it was converted into bromomethyl functionality upon treatment with $MsCl/NEt_3$ followed by LiBr reagent. The desired bromomethyl diarylaminopyrene unit (**2-6**) was used for further elaboration into the dendrons.

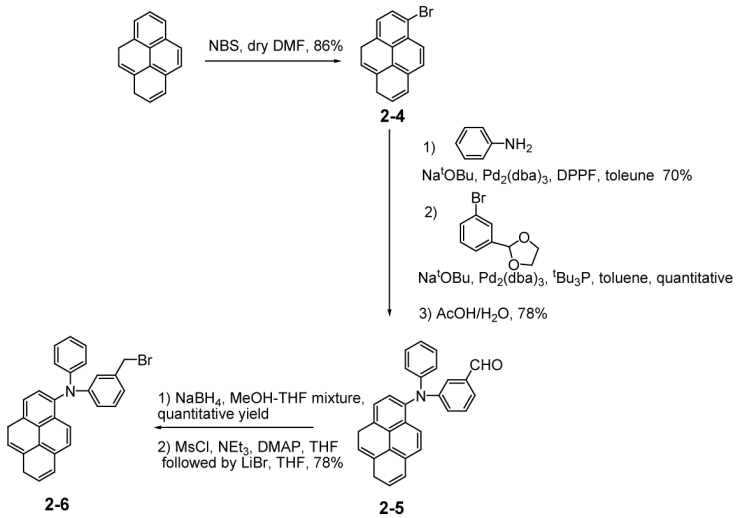

Scheme 2.2. The synthesis of the diarylaminopyrene peripheral unit.

The dendrimers and the linear analogs were assembled by the reaction of a bromomethyl functionalized dendron or a hydroxyl functionalized linear molecule with the benzthiadiazole core chromophore (**2-3**), which contains two phenolic functionalities, as shown in Scheme 2.3.

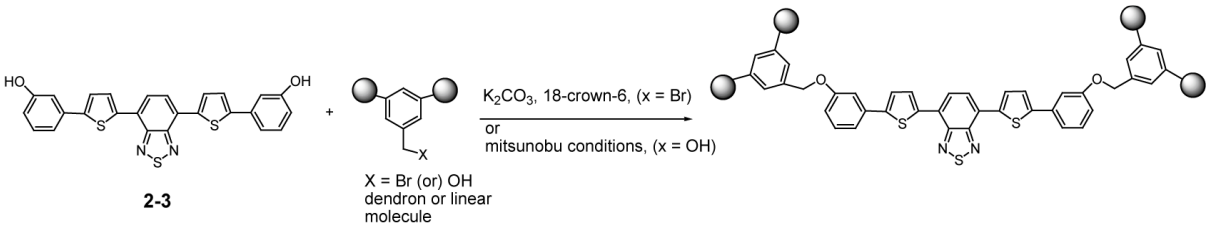

Scheme 2.3. Assembly of dendrimers and linear analogs.

The key steps in the synthesis of fully decorated **2-1F**, **2-2F**, and **2-3F** and difunctionalized **2-1D**, **2-2D**, and **2-3D** dendrons are alkylation and bromination. It is noteworthy that the brominating reagents were carefully selected to avoid the possibility of extra ring bromination as the presence of bromine atoms could affect our photophysical results, due to heavy atom effect.[59, 60] This conversion was performed using a combination of methanesulfonyl chloride/ triethylamine, and lithium bromide. The reaction here is thought to proceed through the formation of the mesylate initially, which then gets converted to the bromoalkyl functionality by nucleophilic displacement. The lack of the opportunity to form an electrophilic Br^+ functionality obviates the possibility of ring bromination.

In the convergent assembly of fully decorated dendrons, the diarylaminopyrene units having bromomethyl functionality **2-6** was treated with 3,5-dihydroxybenzyl alcohol under Williamson alkylation conditions to afford G1-OH dendrons with 56% yield. Conversion of the hydroxymethyl compound to the bromomethyl version to obtain G1-Br (**2-7**) using MsCl/LiBr regents was achieved with quantitative yield. G1-Br (**2-7**)

was then taken through the above two synthetic steps iteratively to obtain the G2 and G3 monodendron with a bromomethyl functionality at the focal point (**2-8** and **2-9**). Treatment of the bromomethyl functionalized dendrons **2-7**, **2-8** and **2-9** with the chromophore core (**2-3**) in the presence of potassium carbonate afforded the fully decorated dendrimers **2-1F**, **2-2F**, and **2-3F** respectively (Scheme 2.4).

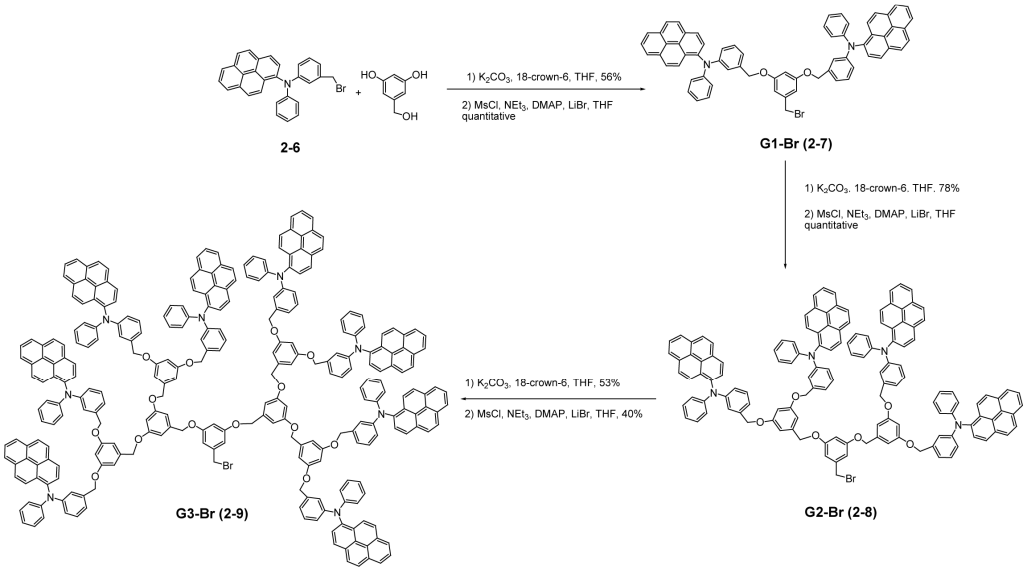

Scheme 2.4. The convergent synthesis of fully decorated dendrons.

To obtain the partially functionalized G-1 dendron **2-12**, the diarylaminopyrene compound **2-6** was first treated with monophenolic G1-OH **(2-10)** under the potassium carbonate alkylation conditions to obtain the hydroxymethyl functionalized dendron **2-11** in 80% yield (Scheme 2.5). Conversion of this compound to the corresponding bromomethyl version afforded the targeted G-1 dendron **2-12**. The compound **2-10** was obtained by the reaction of 3,5-dihydroxybenzyl alcohol with benzyl bromide in a 1:1 ratio. This reaction afforded a mixture of the **2-10** along with the corresponding disubstituted G1-OH **(2-13)** (Scheme 2.5). The dendron **2-11** was converted to the corresponding bromomethyl compound **2-12** and was used for the next generation of dendrons.

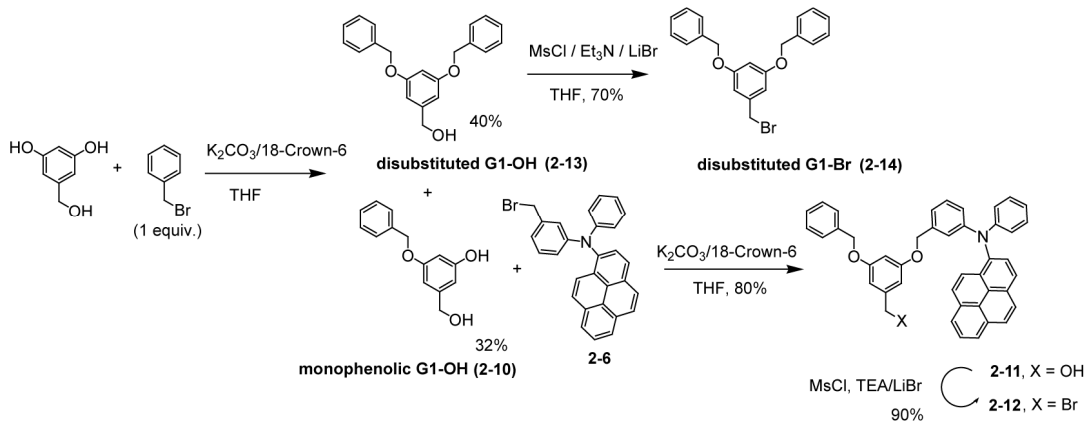

Scheme 2.5. Synthetic pathways for diarylaminopyrene incorporated difunctionalized dendrons.

The disubstituted G1-Br **(2-14)** obtained from bromination reaction of compound **2-13** using MsCl/LiBr reagents was treated with one equivalent of 3,5-dihydroxybenzyl alcohol to afford a mixture of dendron **2-15** and dendron **2-16**. Separation of these compounds followed by the reaction of dendron **2-15** with the bromomethyl G-1 dendron **2-12** afforded the hydroxymethyl functionalized G2-OH dendron **2-17**, which was then converted to the bromomethyl G2 dendron **2-18**. Similarly the Dendron **2-16** was converted to the disubstituted G2-Br **2-19** followed by treatment with 3,5-dihydroxybenzyl alcohol afforded the monosubstituted G3-OH **2-20**. A reaction between this dendron **2-20** and compound **2-18** in the presence of potassium carbonate and 18-crown-6 afforded the G3-OH dendron **2-21** followed by conversion to the bromomethyl dendron **2-22** (Scheme 2.6). Treatment of the bromomethyl functionalized dendrons **2-12**, **2-18**, and **2-22** with compound **2-3** in the presence of potassium carbonate afforded the difunctionalized dendrimers **2-1D**, **2-2D**, and **2-3D** respectively.

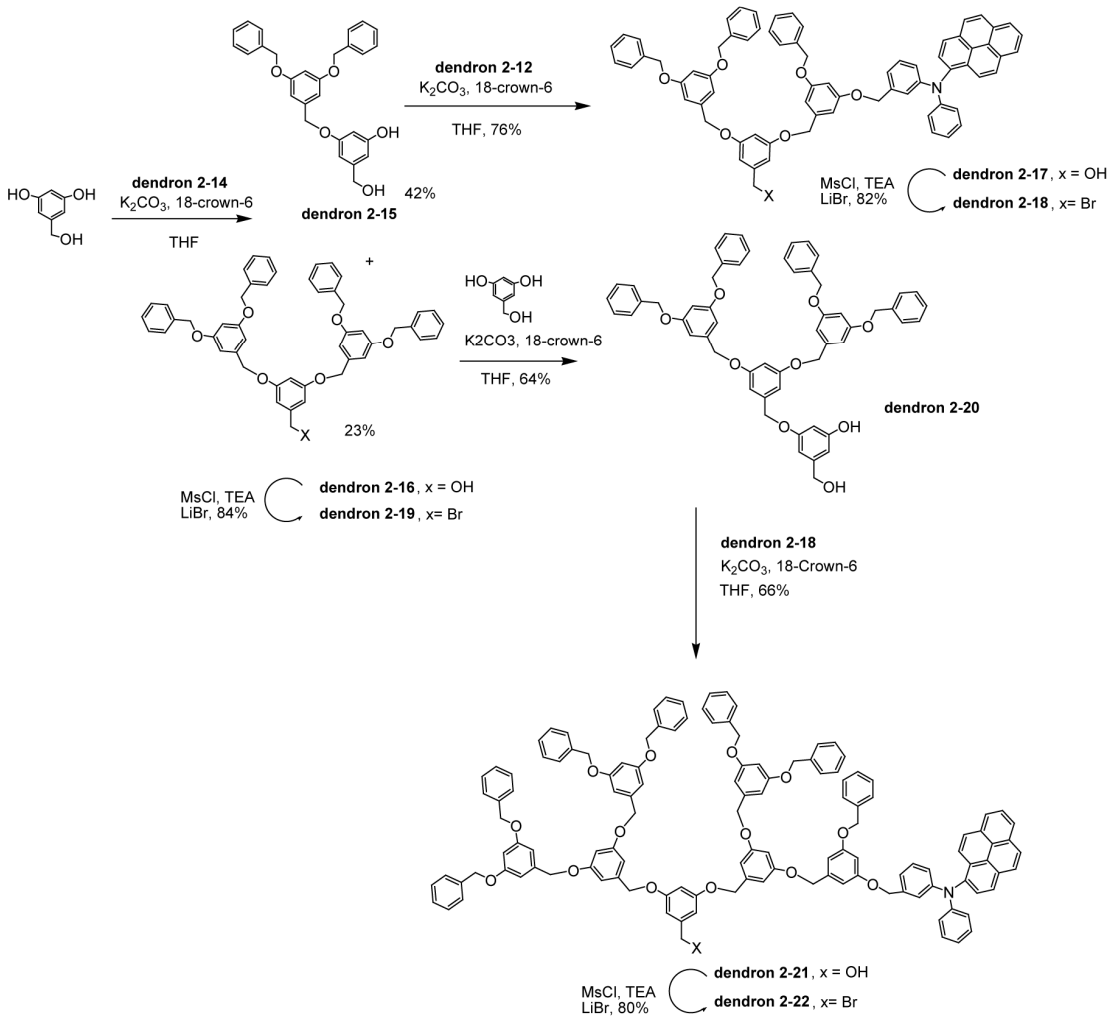

Scheme 2.6. Synthetic pathway for G2 and G2 difunctionalized dendrons.

The linear analogs **2-1L**, **2-2L**, and **2-3L** were synthesized with Mitsunobu reaction as the key step in the synthesis. The hydroxymethyl functionalized diarylaminopyrene **(2-23)** was treated with 3-hydroxybenzaldehyde under Mitsunobu reaction conditions followed by the reduction of carboxaldehyde to the alcohol provided **2-24**, linear analog for the G-1 dendron (Scheme 2.7). Reaction of compound **2-23** with the aldehyde **2-25**, followed by reduction afforded the G-2 analog **2-26**, whereas a similar reaction sequence with the compound **2-24** afforded the G-3 analog **2-27**. Reaction of the

hydroxymethyl compounds **2-24**, **2-26**, and **2-27** with compound **2-3** under the Mitsunobu reaction conditions afforded the linear **2-1L**, **2-2L**, and **2-3L**, as illustrated in Scheme 2.3. Note that these reactions also do not involve the possibility of any heavy atom incorporation into the dendrimers. When we attempted the Mitsunobu based reaction for the syntheses of the dendrimers **2-1D**, **2-2D**, and **2-3D** and **2-1F**, **2-2F**, and **2-3F**, the yields of reactions were poor especially at higher generations.

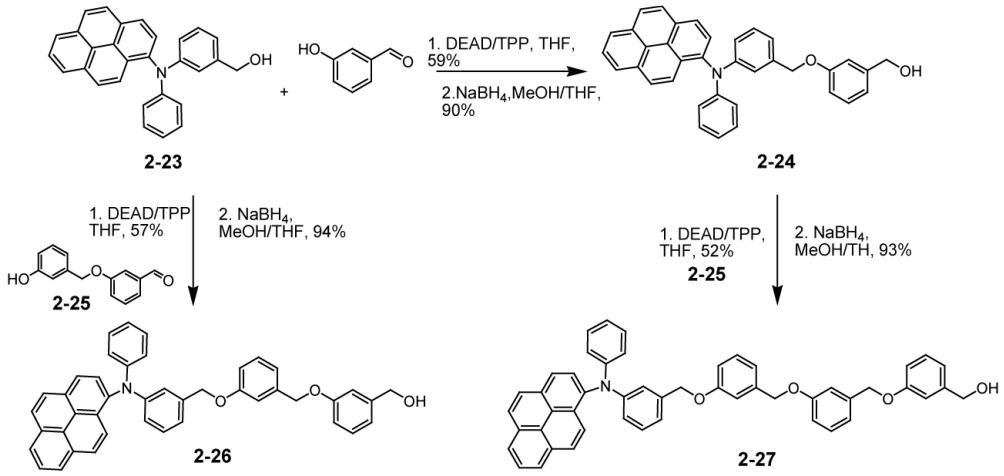

Scheme 2.7. Synthesis of linear analogs.

The dendrons, dendrimers, linear analogs, and the key compounds that lead to these molecules were characterized by ^{1}H, ^{13}C NMR, mass spectrometry, and elemental analysis. The key feature of each generation of the dendrimer is that the number of pyrene units remains the same in **2-1D**, **2-2D**, and **2-3D**, but relative ratio of the pyrene units *vs.* the number of phenyl rings in the periphery or the dihydroxybenzyl ether rings in the inner layers of the dendrimers vary. The ^{1}H NMR peaks for pyrene appeared between 8.2 and 7.8 ppm, whereas those of the peripheral phenyl rings and the inner layer dihydroxylbenzyl ether rings appeared between 7.4 and 6.8 ppm and between 6.7 and 6.4 ppm respectively. The relative integration of these three areas was useful in confirming

the identity of the dendrons and the dendrimers assembled. Similar ratios were also found to be useful in characterization of the linear analogs **2-1L**, **2-2L**, and **2-3L**, although assignment of ^{1}H NMR spectra of these linear molecules were inherently less complicated. In fully decorated dendrimers, the difference in a number of benzylic protons in each generation of dendrimers can be used to confirm the success in obtaining the desired dendrimers. For example, there appear four different benzylic signals in the ratio of 8:4:2:1 in **2-3F**.

Moreover, all the dendrimers exhibited the parent ion peak with calculated isotopic distribution pattern in the MALDI-ToF spectra. Particular attention was paid to the presence of even a small peak containing bromine atoms (M+80 or M+160 and so on) which might imply the presence of extra bromine in final compounds. No such peaks were observed even in small amounts. Additionally, the purity of the samples was also determined using GPC. All dendrimers exhibited a single sharp peak in the size exclusion chromatogram indicating the presence of a single large species. We also characterized the dendrimers **2-1F**, **2-2F**, **2-3F**,and **2-1D**, **2-2D**, **2-3D** and the linear analogs **2-1L**, **2-2L**, and **2-3L** using absorption spectra. While the relative number of the diarylaminopyrene periphery units and the benzthiadiazole core increases with increasing generation in **2-1F**, **2-2F**, and **2-3F**, this number remains constant in the other two series of compounds. While a linear increase in the relative absorbance with generation was observed in the fully decorated dendrimers, the relative absorbance was essentially unchanged in the difunctionalized dendrimers and the linear analogs as elaborated below.

Initial photophysical characterization of the difunctionalized dendrimers **2-1D**, **2-2D**, and **2-3D** and the linear analogs **2-1L**, **2-2L**, and **2-3L** were done using steady-state

linear absorption spectroscopy and emission spectroscopy. Absorption spectra of the difunctionalized dendrimers **2-1D**, **2-2D**, and **2-3D** and the linear analogs **2-1L**, **2-2L**, and **2-3L** are shown in Figure 2.2a, while the spectra of the fully functionalized dendrimers **2-1F**, **2-2F**, and **2-3F** are shown in Figure 2.2b. As expected and mentioned above, the relative area of absorption of the donor versus the acceptor increases with generation in the case of the fully functionalized dendrimers. However, there is no significant difference among generations for both the difuncitonalized dendrimers and the linear analogs series, relative to what is observed in the **F** series. This provides the evidence of the lack of the ground state electronic communication between the donor and the acceptor in all these molecules and also that all these molecules behave similarly electronically, but differ in the chromophore densities and molecular architecture.

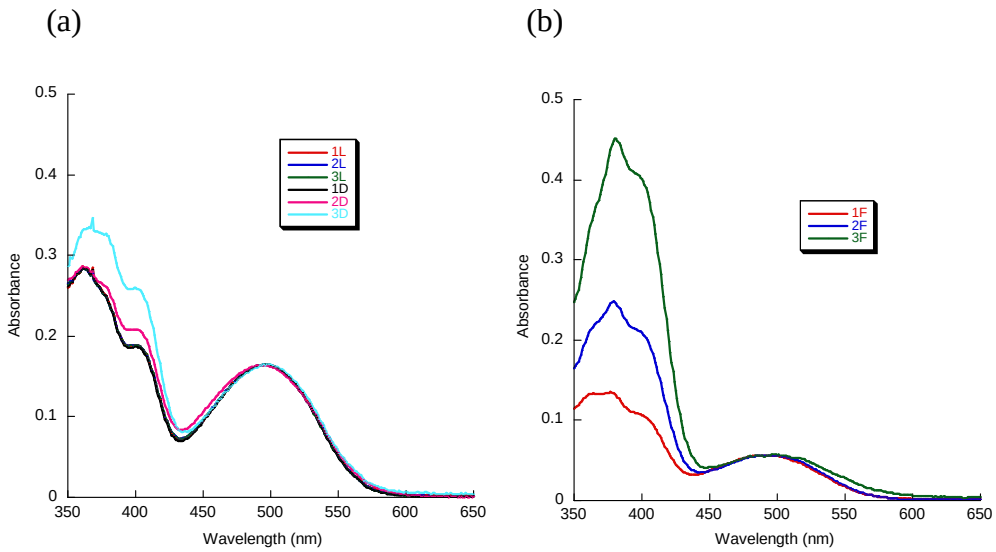

Figure 2.2. (a) Absorption spectra of the compounds **1L-3L** and **1D-3D**, normalized at the absorption maximum of the acceptor. (b) Absorption spectra of the compounds **1F-3F**, normalized at the absorption maximum of the acceptor.

The emission spectra of the both dendrimer series and the linear analogs are shown in Figure 2.3a-2.3c. In all these cases, when the donor component of the molecules is excited at about 395 nm, the emission arises mainly from the acceptor. This indicates a high degree of EET from the periphery to the core of both difunctionalized and fully functionalized dendrimers, as wells as from the linear analogs. We have quantified the EET and CT efficiencies in all three classes of dendrimers using time-resolved spectroscopy measurements (*vide infra*).

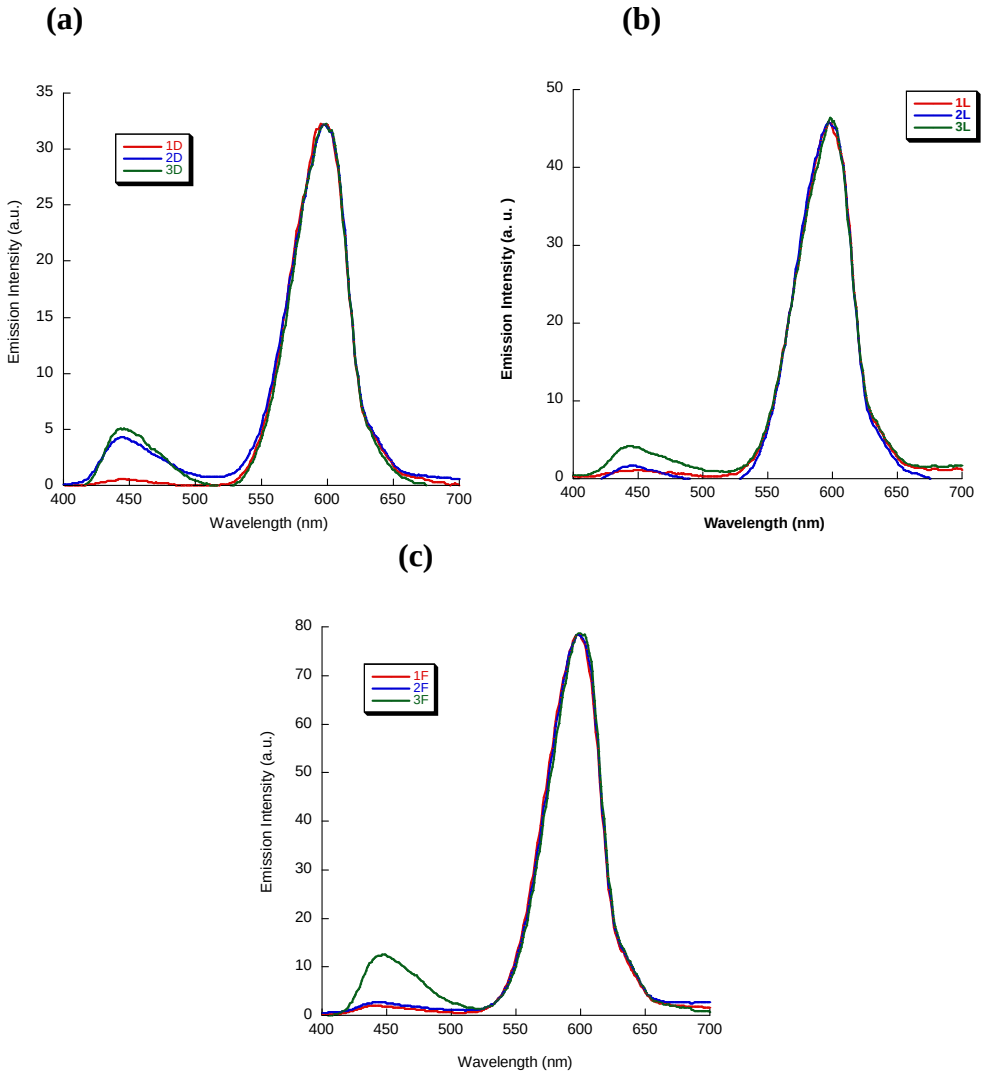

Figure 2.3. Emission spectra when excited at the donor at 395 nm in toluene (a) **2-1D**, **2-2D**, and **2-3D**; (b) **2-1L**, **2-2L**, and **2-3L**; (c) **2-1F**, **2-2F**, and **2-3F**.

2.2.2 Time-Resolved Electronic Energy Transfer Studies

We have previously shown that the diarylamino pyrene unit is energetically suitable for energy transfer to the benzthiadiazole based chromophore core.[61] The redox potential of this amine is also such that an electron transfer from this unit to the excited state of the chromophore core is thermodynamically feasible. If the energy transfer occurs incoherently between well-separated molecules as in the case of the molecules reported here, we can apply the Förster formula

$$\frac{1}{\tau_{EET}} = \frac{1}{\tau_{fl}} \frac{R_0^6}{R^6} \tag{2.1}$$

$$R_0^6 = \frac{9000 \ln(10) \phi_{fl} \kappa^2}{128 \pi^5 N_A n^4} \int_0^\infty \varepsilon(\nu) f(\nu) \frac{d\nu}{\nu^4} = \frac{9000 \ln(10) \phi_{fl} \kappa^2}{128 \pi^5 N_A n^4} J \tag{2.2}$$

where R is the separation between chromophores, n is the index of refraction, τ_{fl} is the fluorescence lifetime of the donor (which in this case is identical to the acceptor), ϕ_{fl} is the quantum yield, κ is an orientation factor, N_A is Avagadro's number, ε(ν) is the absorption spectrum and $f(\nu)$ is the fluorescence spectrum whose integral has been normalized to 1. R_0 combines these factors into a single length called the critical Förster radius. For the diarylaminopyrene/benzthiadiazole pair, we have calculated a Förster radius R_0 of 48 Å.[61] This large value results from the very good overlap of the diarylaminopyrene's fluorescence with the benzthiadiazole's absorption. In all the molecules studied here, the donor-acceptor distance is less than R_0 due to the constraints of the molecular structure. Thus in all cases, we expect rapid energy transfer and accelerated fluorescence decays for the diarylaminopyrene donors. This is exactly what is observed for all three classes of molecules, as shown in Figure 2.4. In toluene at room

temperature, for the linear, difuntionalized, and fully decorated dendritic molecules, the decay of the donor fluorescence ranges from ~40 ps for the first generation molecules to 100-146 ps for the third generation molecules. The decays are generally biexponential, with a small (~10%) long-lived component whose decay is close to that of the isolated donor in solution (4.9 ns). In fitting the data in Figure 2.4, we set the long component to be 4.9 ns in all cases. The origin of this long-lived component is not clear. This has been attributed to a very small fraction of impurities not detectable by classical

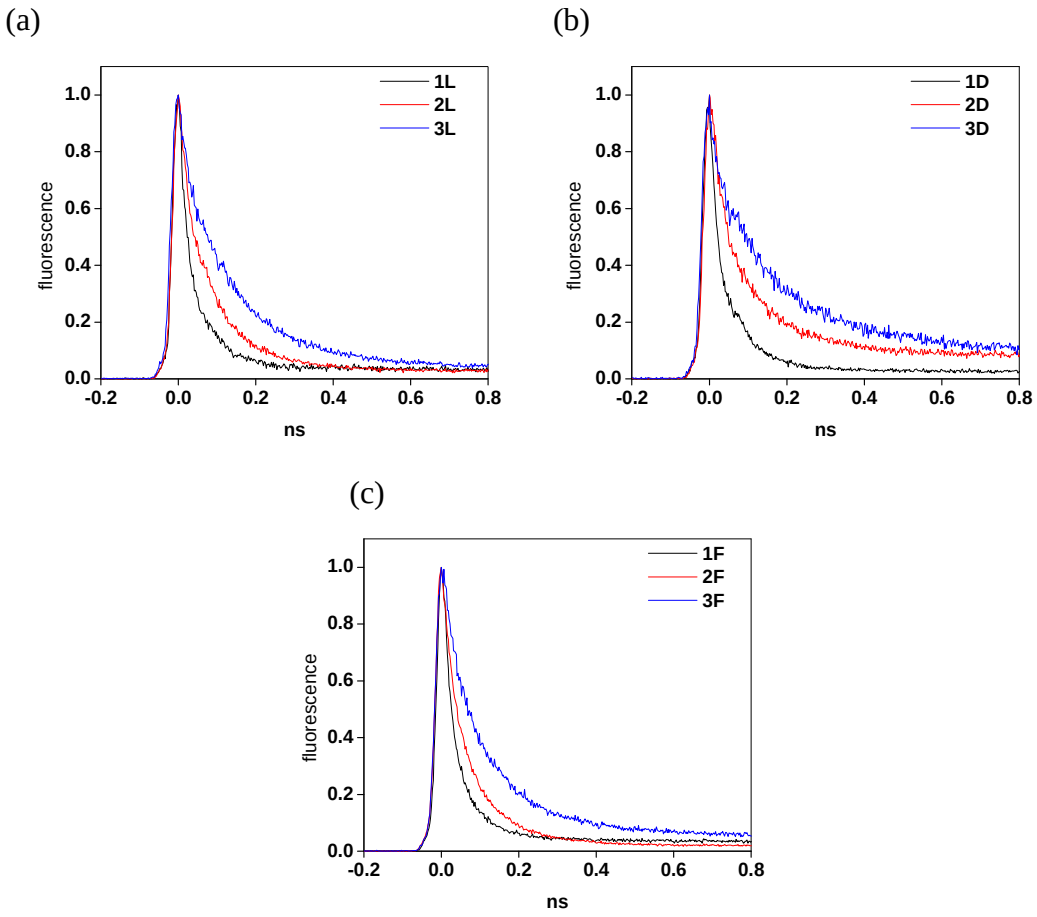

Figure 2.4. Donor fluorescence decays for a) **2-1L**, **2-2L**, and **2-3L** linear analogs, **b) 2-1D**, **2-2D**, and **2-3D** dendritic analogs, and **c) 2-1F**, **2-2F**, and **2-3F** fully decorated dendrimers. Dendrimers are excited at 400 nm and donor fluorescence measurement is made from 430 nm to 510 nm in toluene.

characterization techniques.[54, 62] The results of the fitting of the data are given in Table 2.1.

Table 2.1. Donor Fluorescence Decays and estimated EET Efficiencies. Excitation wavelength = 400 nm, and emission detected in 50 nm window centered at 440 nm. Decays with two time scales are fit with a biexponential fit of the form $A\exp(t/\tau_A)+B\exp(t/\tau_B)$. All times are in ns. Donor fluorescence lifetime in toluene is 4.94 ns.

	A_1	τ_1	A_2	τ_2	$\langle\tau\rangle$	EET efficiency
2-1L	0.95	0.040	0.05	4.94	0.29	0.94
2-2L	0.96	0.075	0.04	4.94	0.27	0.95
2-3L	0.93	0.124	0.07	4.94	0.46	0.91
2-1D	0.95	0.044	0.05	4.94	0.29	0.94
2-2D	0.88	0.079	0.12	4.94	0.66	0.87
2-3D	0.85	0.146	0.15	4.94	0.87	0.82
2-1F	0.95	0.038	0.05	4.94	0.28	0.94
2-2F	0.96	0.065	0.04	4.94	0.26	0.95
2-3F	0.92	0.099	0.08	4.94	0.49	0.90

For the biexponential decays, we have defined $\langle\tau_{don}\rangle$, the weighted average of the donor fluorescence decay times, as

$$\langle\tau_{don}\rangle = A_1\tau_1 + A_2\tau_2 \tag{2.3}$$

where A_1 and A_2 are the amplitudes of the two components for the normalized decay data. It is straightforward to show that this single parameter can be related to the EET quantum yield ϕ using the following equation:

$$\phi_{EET} = 1 - \frac{\langle\tau_{don}\rangle}{\tau'_{don}} \tag{2.4}$$

where τ'_{don} is the lifetime of the donor in the absence of EET. Note that the EET times for the fully decorated dendrimers in toluene are faster than those tabulated in our previous observation,[54] where the lifetimes were measured in DMF. The Förster energy transfer rate is proportional to $1/n^4$, and if we plug in the refractive indices of toluene (n = 1.494)

and DMF (n = 1.427), Eq. (2.1) predicts that τ_{EET} in toluene should be 20% longer, the opposite of what is observed. An alternative explanation for the more rapid EET in toluene is that the conformational structure, or degree of folding, is slightly different in these two solvents. It is reasonable that toluene could lead to a more compact structure given the polar nature of the BE framework used here.[18]

There are two trends in Table 2.1 which are of interest for this work. The first is the increase of relative EET times with increase in the length of the BE arms, which is observed within all three families of molecules. The second is the trend in τ_{EET} values in the three families. Below we address each of these two issues in detail. The dependence of τ_{EET} on dendrimer size was observed previously for the fully decorated dendrimers.[54] In that work, it was found that if R, the donor-acceptor separation distance, scaled linearly with N, the number of intervening chemical bonds, then τ_{EET} was predicted to scale as N^6, much more rapidly than observed experimentally. If, on the other hand, we assumed that the actual interchromophore distance through space scaled as $\sqrt{N}$, we have

$$\tau_{EET} \propto R^6 \propto (\sqrt{N})^6 = N^3 \qquad (2.5)$$

This scaling reproduced the observed dependence of τ_{EET} on molecular size. Figure 2.5 shows that this analysis is valid for all three families of dendrimers studied in this work. While there are slight divergences between the different families, none of them comes close to the N^6 dependence expected for a rigid dendrimer. The $R \propto \sqrt{N}$ dependence can be deduced from simple theoretical considerations for a flexible, multi-segment system. The benzyl ether linkages employed in the set of compounds under consideration are known to be quite flexible,[35] and it would appear from our results that this flexibility is

not significantly degraded by the steric crowding present in the multiple branched **D** and **F** families.

A second observation is that although families **L, D,** and **F** exhibit the same general behavior of τ_{EET} with generation, their absolute values of τ_{EET} differ. This difference is most pronounced at the third generation, where τ_{EET} of **2-3D** (146 ps) is almost 50% longer than that of **3F** (99 ps). The slight slowdown in EET in going from the **L** to **D** families can be rationalized in terms of increased donor-acceptor separations in the **D** molecules. Such increased separations would be expected in the **D** family due to increased steric hindrance to the conformational motions that would bring the donor and acceptor closer. The only surprising thing is that this effect is so small – it only slows down EET by about 15% in the third generation, where the effect is most pronounced. Considering that $\tau_{EET} \propto R^6$, this would translate to only a 2% change in the average donor-acceptor distance.

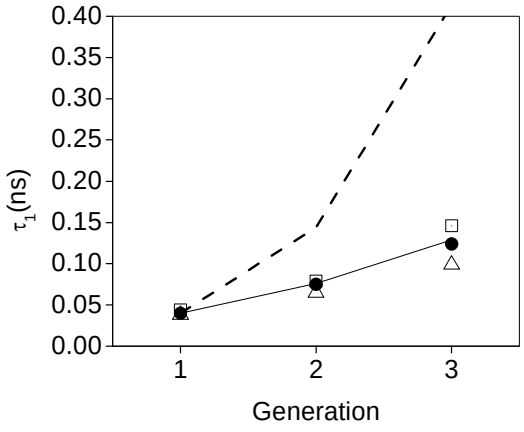

Figure 2.5. Measured fast decay times (τ_1) for the donor fluorescence versus generation for linear analogs **L** (filled circles), disubstituted dendrimers **D** (open squares), and fully decorated dendrimers **F** (open triangles). The predicted variation for $R \propto N^6$ (dashed line) and $R \propto N^3$ (solid line), where N is the number of bonds between the acceptor and donor, are also shown.

If anything, steric congestion should be even more pronounced due to the addition of the bulky amino-pyrene chromphores in the **F** compounds, where *R* would be expected to increase even further. But instead of decreasing, the EET rate increases in the **2-1F**, **2-2F**, and **2-3F** family. Again, this trend is most pronounced in the third generation, where a comparison of the τ_{EET}'s shows an almost 30% drop in going from **2-3D** to **2-3F**. One explanation for this effect is that the average value for *R* is lower in the **F** dendrimer than in the **D** dendrimer due to increased backfolding driven by steric crowding by the amino-pyrene chromophores at the periphery. A second possibility is that there is difference in the orientational structure of the **D** and **F** families. Examination of Eq. (2.2) shows that the orientation factor κ^2, which can range between 0 and 4, plays an important role in determining τ_{EET}. If the initially excited chromophore is randomly oriented with respect to the acceptor, it may have a low κ^2 value and thus a long τ_{EET}, even if R is small. Of course, if the donor and acceptor are reorienting rapidly with respect to each other, we can use the rotationally averaged value for $\kappa^2 = 0.667$, while for an isotropic static distribution, $\kappa^2 = 0$.[63]

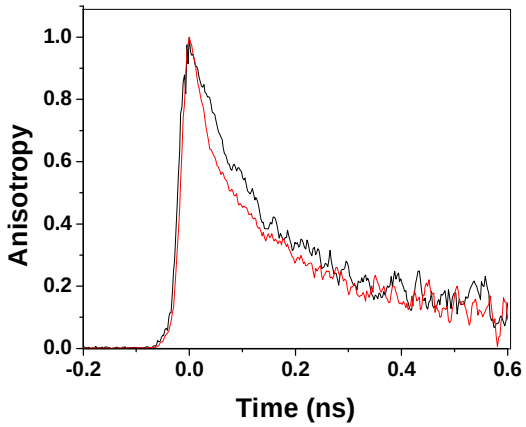

Figure 2.6. Normalized donor fluorescence anisotropy decay of **2-3D** (black) and **2-3F** (red) dendrimers.

To analyze the role of chromophore orientations, we need to look at the evolution of the donor fluorescence anisotropy. Two examples are shown in Figure 2.6, where the normalized anisotropy decays of **2-3D** and **2-3F** are compared. The values for the decays of all the compounds are given in Table 2.2. Note that a slight constant offset, usually about 10% of the initial amplitude, was required to fit the entire decay, and that the values for the initial anisotropies varied between 0.3 and 0.4, as expected for a dipole-allowed transition. We are most concerned, however, with how τ_r, the exponential decay time, changes between families. From Table 2.2, several things are clear. First, attaching the diarylaminopyrene to the benzylether chain slows down its rotational diffusion by only about 50%. Even in the smallest dendrimer, the effective molecular radius is expected to change by at least a factor of 3, assuming a rigid molecule. The lack of a corresponding increase in τ_r indicates that the flexible benzylether linker probably constrains the motion of the diarylaminopyrene to some extent, but that it can still rotate more or less freely. Second, the EET is so rapid that in all molecules the anisotropy decay occurs on the same time scale as the energy transfer. The assumption of rapid rotational averaging that leads to $\kappa^2 = 0.667$ is thus not valid for these molecules, and static conformations probably play an important role in determining the overall EET efficiency. Such an effect has been observed in DNA-dye molecular complexes have been used to demonstrate how different donor orientations can effectively 'gate" Förster energy transfer to a fixed acceptor.[64] Understanding how these conformations change among the **L**, **D** and **F** families will probably require detailed molecular dynamics simulations. The last point is that the data in Table 2.2 does suggest that dynamic reorientation of the excited state may play a role in accelerating the EET in the **F**

dendrimers. Unlike the **L** and **D** molecules, there is a systematic decrease in τ_r with increasing size in the **F** dendrimers. It is unlikely that the rapid anisotropy decay in **2-3F** is due to more rapid rotational diffusion, since the diarylaminopyrene units are much bulkier than the phenyl groups. Instead, EET between the donors on the periphery would help explain why both in τ_r and τ_{EET} are enhanced for higher generations in **F**. Such donor-donor energy hopping provides an explanation for the more rapid EET in **2-3F** and has previously been used to explain efficient EET in other light-harvesting dendrimers.[45, 65, 66] In our molecules, the extra donor chromophores in the **2-1F**, **2-2F**, and **2-3F** molecules provide additional pathways which both randomize the polarization and optimize EET to the core acceptor. It is important to point out, however, that even at the level of **2-3F**, the differences in τ_r are only on the order of 30% at most. Whether the decrease in τ_r in **2-3F** is sufficient to explain its shorter τ_{EET} with respect to the other third generation dendrimers is unclear. We simply emphasize that the observed trends in τ_{EET} and τ_r are consistent with what is expected based on considerations of steric congestion and chromophore density.

Table 2.2. Donor fluorescence anisotropy decays. Decays are fit with a single exponential fit of the form $r(t) = r_0 \exp(t/\tau_r) + y_0$. All times are in ns.

	τ_r	r_0	y_0
2-1L	0.126	0.315	0.050
2- 2L	0.119	0.412	0.042
2-3L	0.135	0.290	0.016
2-1D	0.118	0.388	0.032
2-2D	0.178	0.342	0.047
2-3D	0.180	0.268	0.028
2-1F	0.151	0.295	0.056
2-2F	0.134	0.314	0.053
2-3F	0.115	0.249	0.050
2-23	0.082	0.427	0

Although the difference in EET rates between families does not lead to large differences in the overall EET efficiencies, since all the rates are so fast, they do reveal differences between the different architectures which could become more significant in larger structures. Our results do not, however, provide a compelling case for the architectural superiority of the classical, fully decorated dendrimers as opposed to the linear analog in terms of EET to the core. Of course, the fully decorated dendrimer still has the advantage of having a much larger absorption cross-section due to its additional chromophores, which still make it a better light-harvesting molecule overall.

2.2.3 Time-resolved Charge Transfer Studies

The dendrimers studied in this work are bifunctional, demonstrating both EET and subsequent CT from the ground state of the amino-pyrene donor to the excited state of the benzthiadiazole acceptor. Although the dendrimer structure does not provide a significant advantage in terms of EET efficiency, we do find that it does provide a significant advantage in terms of CT efficiency. Figure 2.7 shows the decays of the third generation molecules **2-3L** and **2-3F** in a series of solvents: toluene, CH_2Cl_2, and DMF. As the solvent polarity increases, the benzthiadiazole fluorescence decay becomes more rapid. It has been shown that for **2-1F**, **2-2F**, and **2-3F** compounds this fluorescence quenching is accompanied by the formation of a long-lived, charge separated species.[54] Thus at least part of the rapid fluorescence decay represents CT quenching. Table 2.3 summarizes the acceptor fluorescence decay data for all 9 compounds in the three solvents specified. Biexponential acceptor decays are analyzed in the same way as the donor decays in the previous section, except that the time constant of the second decay component is not fixed. It is clear that all three families of compounds undergo some

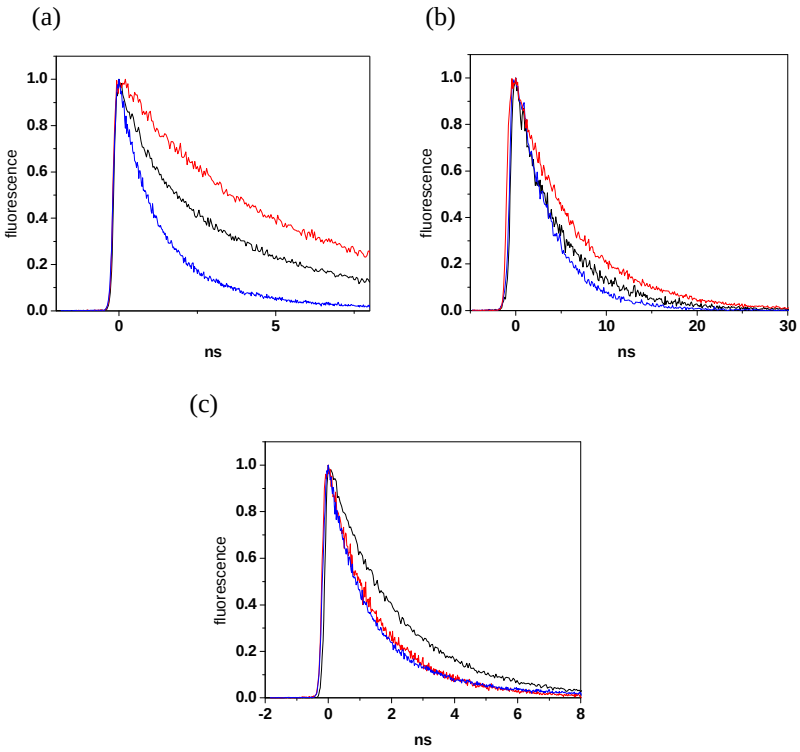

Figure 2.7. Acceptor fluorescence decay of (a) **2-3F** in toluene (red), methylene chloride (black), and DMF (blue), b) **2-3L** in toluene (red), methylene chloride (black), and DMF (blue), and (c) the size dependence of the acceptor fluorescence decay of **2-1F** (black), **2-2F** (red), and **2-3F** (blue) in DMF.

Table 2.3. Acceptor Fluorescence Decays (excitation at 400 nm, detection in 50 nm window centered at 600 nm) and CT Efficiencies calculated. Decays with two time scales are fit with a biexponential fit of the form $A\exp(t/\tau_A)+B\exp(t/\tau_B)$. All times are in ns.

	toluene						methylene chloride						DMF					
	A	τ_A	B	τ_B	$\langle\tau\rangle$	η_{CT}	A	τ_A	B	τ_B	$\langle\tau\rangle$	η_{CT}	A	τ_A	B	τ_B	$\langle\tau\rangle$	η_{CT}
acceptor		6.55						7.99						7.58				
2-1L		6.55				0	0.68	3.91	0.32	7.23	4.97	0.3777		3.29				0.5660
2-2L		6.50				0.0076	0.38	2.92	0.62	6.02	4.84	0.3940		3.51				0.5369
2-3L		6.53				0.0031	0.20	1.77	0.80	5.60	4.83	0.3950		3.86				0.4908
2-1D		6.44				0.0168	0.50	3.36	0.50	6.41	4.89	0.3886		3.35				0.5580
2-2D		6.34				0.0321	0.39	2.62	0.61	6.21	4.81	0.3980	0.52	2.68	0.48	4.95	3.77	0.5027
2-3D		6.53				0.0031	0.74	4.75	0.26	8.25	5.66	0.2916	0.44	2.81	0.56	5.30	4.20	0.4453
2-1F		6.44				0.0168	0.35	1.95	0.65	5.36	4.17	0.4785	0.84	1.93	0.16	3.66	2.21	0.7089
2-2F		6.55				0	0.37	1.33	0.63	5.45	3.93	0.5087	0.36	0.86	0.64	1.93	1.54	0.7962
2-3F	0.28	2.37	0.72	6.83	5.58	0.1479	0.42	1.25	0.58	5.43	3.67	0.5401	0.73	1.00	0.27	2.94	1.52	0.7990

degree of polarity-dependent quenching, and that this is most pronounced for the fully decorated dendrimers. In fact, in DMF the CT efficiency, η_{CT}, as estimated from the fluorescence quenching rate, is 0.80 for **2-3F** as opposed to 0.45 for **2-3D** and 0.49 for **2-3L**. This difference in η_{CT} between families is most pronounced in these larger molecules, but is present for all generations. The evolution of η_{CT} with generation for the three families of compounds in DMF is illustrated in Figure 2.8. The CT efficiency in **2-1L**, **2-2L**, and **2-3L** and **2-1D**, **2-2D**, and **2-3D** decreases as the donor-acceptor separation increases, although not dramatically. For both EET and CT, the decreased transfer rates are likely due to the increased distance between donor and acceptor. The size effect is not as dramatic as it was in the case of EET, and this may have to do with the different timescales of the two processes. The EET event occurs within 50-150 ps, during which the donor moieties barely have time to rotate, much less translate and change *R*, for their separation. CT occurs on the timescale of several ns, allowing these flexible molecules to dynamically sample multiple conformations. This dynamic sampling may blur average distance effects that dominate the EET process. For CT, it would only take a single close encounter during that period to produce a CT event. A better understanding of the role of conformational fluctuations in enabling CT in these compounds probably requires the use of molecular dynamics simulations.

The most interesting trend in η_{CT} is seen in the fully decorated dendrimers, where η_{CT} actually increases with dendrimer size. This unexpected result, which can be discerned both from Table 2.3 and Figure 2.7c and 2.8, cannot easily be explained in terms of backfolding or more rapid conformational fluctuations. But as in the case of EET, here too the presence of additional chromophores can also provide an enhancement

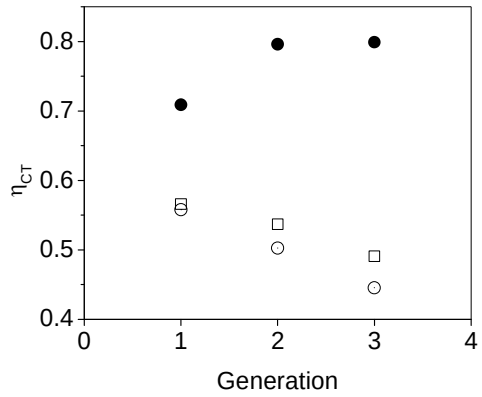

Figure 2.8. Plot of charge transfer efficiency η_{CT} versus generation for the linear analogs **L** (open squares), disubstituted dendrimers **D** (open circles), and fully decorated dendrimers **F** (solid circles).

in the CT rate. In these compounds, the local concentration of chromophores is significantly higher than in the **L** and **D** molecules. If the overall rate is proportional to the concentration, one would expect a 4-fold enhancement in the CT rate for **2-3F** relative to **2-3D**. While we do not see this level of enhancement, it is still almost a factor of 2, which is significant. But while the presence of additional donors explains the enhancement in η_{CT} relative to **2-1L**, **2-2L**, and **2-3L** and **2-1D**, **2-2D**, and **2-3D**, the fact that τ_{CT} decreases with size, while τ_{EET} increases, is surprising. One possible explanation lies in the conformational disorder implied by the $\sqrt{N}$ dependence of the donor-acceptor τ_{EET}. The measured τ_{EET} reflects the average distance of all the donors from the acceptor, since they all have an equal chance of being excited by an incident photon. The measured η_{CT}, on the other hand, is expected to be most sensitive to the position of the donor closest to the acceptor. As the dendrimer size increases, the through-bond distance to each donor increases. But the total number of donors available for CT increases as well, and at least some of those additional donors may end up quite close to the acceptor. These two competing effects tend to cancel each other, and are only present in the **2-1F**,

2-2F, and **2-3F** molecules. In this way, the fully decorated dendrimers appear to provide a clear architectural advantage in terms of CT dynamics. The increase in donor density with generation tends to alleviate the concomitant effect of increasing average donor-acceptor distance. This is not the case when increased molecular size is not accompanied by an increase in the number of transfer pathways, as in the **2-1L**, **2-2L**, and **2-3L** and **2-1D**, **2-2D**, and **2-3D** molecules. In Figure 2.9, we give a very qualitative illustration of how an **F** dendrimer can always have a donor in contact with the core acceptor, while in the **D** dendrimer, given the same set of conformations of the arms, has conformations where the two species are well-separated.

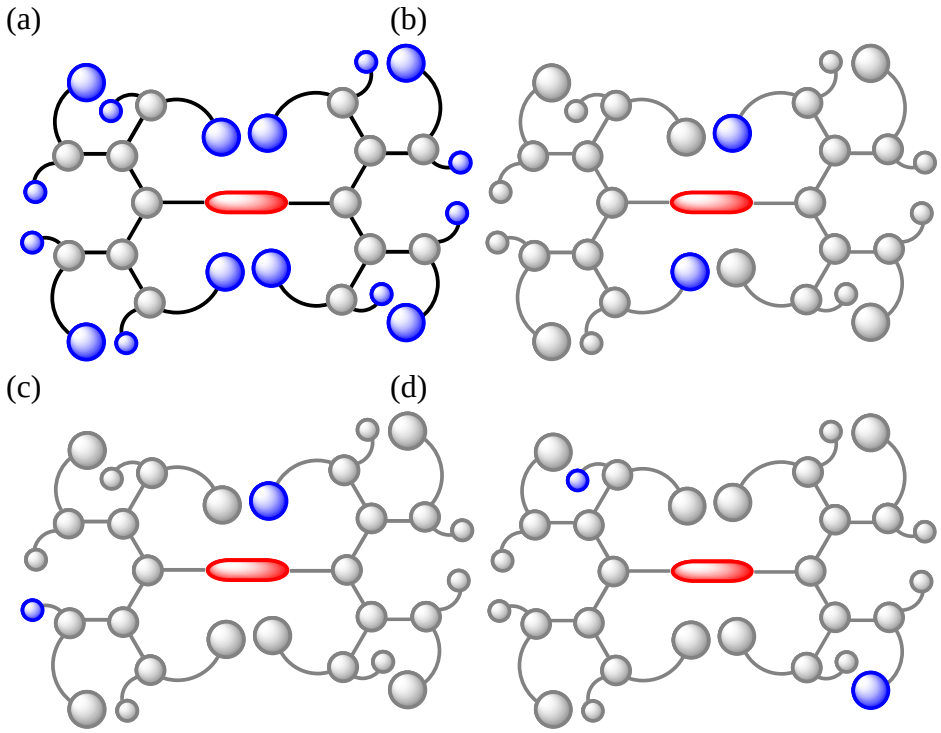

Figure 2.9. (a) Hypothetical conformation of a fully decorated dendrimer. (b-d) Various possible conformations of difunctionalized dendrimers similar to the one in (a). *Note*: Even when one attempts to draw the different conformations with the fully functionalized dendrimers as in (b)-(d), there would be a certain number of diarylamino pyrene units close to the core. This could be sufficient for CT and thus enhances CT efficiency in higher generations, when fully decorated.

2.3 Summary

We have designed and synthesized dendrimers that contain only two donors and one acceptor units in every generation. Such difuntionalized dendrimers allow for a straightforward comparison of dendrimer with the corresponding linear analogs for the purposes of EET and CT in non-conjugated dendrimers. By comparing these two classes of molecules then with the more classical, fully-decorated dendrimers, we carried out a systematic investigation on the architectural advantages that dendrimers provide for energy transfer and charge transfer processes. The study provides insights in to the nature of the advantage that dendrimers could have in light harvesting applications. The deleterious effects of steric crowding can be detected in the **D** family of compounds, but the extra terminal donors in the **F** compounds more than compensate for this loss. As a result of this study, we have shown that: (*i*) The main advantage that dendrimers provide for EET purposes is the opportunity to enhance the density of the donor chromophores around an antenna chromophore. Note that the multiple arms in the periphery allow for the incorporation of a variety of donor chromophore in a single dendrimer, considering the synthetic methods developed.(*ii*) A small and subtle advantage that dendrimers also provide is that a fast energy hopping process among the donor chromophores could allow for an efficient EET, since this process allows for sampling through the relative orientations between the donor and acceptor chromophores until the appropriate one is found. We have shown evidence for this possibility using anisotropy decay experiments. (*iii*) In the case of CT, the key advantage that the dendritic architecture provides involves the functional group density. As the generation increases, the relative number of electron donors *vs.* the excited chromophore increases in the case of fully decorated dendrimers,

and the CT efficiency increases as well. Since this advantage does not exist in the case of difunctional dendrimers, the CT efficiency decreases with generation as in the case of the linear analogs. This effect leads to a significant (factor of 2) enhancement in the CT efficiency in the third generation fully decorated dendrimers relative to the di-substituted dendrimers. Thus, this work demonstrates how multiple conformations in dendrimers can significantly enhance energy and charge transfer pathways relative to structures without branches or multiple peripheral chromophores.

2.4 References

1. Caldeira, K.; Jain, A. K.; Hoffert, M. I., "Climate Sensitivity Uncertainty and the Need for Energy without CO2 Emission" *Science* **2003,** 299, (5615), 2052-2054.

2. Chow, J.; Kopp, R. J.; Portney, P. R., "Energy Resources and Global Development" *Science* **2003,** 302, (5650), 1528-1531.

3. Hoffert, M. I.; Caldeira, K.; Jain, A. K.; Haites, E. F.; Harvey, L. D. D.; Potter, S. D.; Schlesinger, M. E.; Schneider, S. H.; Watts, R. G.; Wigley, T. M. L.; Wuebbles, D. J., "Energy Implications of Future Stabilization of Atmospheric CO2 Content" *Nature* **1998,** 395, (6705), 881-884.

4. Barber, J.; Andersson, B., "Revealing the Blueprint of Photosynthesis" *Nature* **1994,** 370, (6484), 31-34.

5. Deisenhofer, J.; Michel, H., "The Photosynthetic Reaction Center from the Purple Bacterium Rhodopseudomonas-Viridis" *Science* **1989,** 245, (4925), 1463-1473.

6. McDermott, G.; Prince, S. M.; Freer, A. A.; Hawthornthwaitelawless, A. M.; Papiz, M. Z.; Cogdell, R. J.; Isaacs, N. W., "Crystal-structure of an Integral Membrane Light-harvesting Complex from Photosynthetic Bacteria" *Nature* **1995,** 374, (6522), 517-521.

7. Hu, X. C.; Damjanovic, A.; Ritz, T.; Schulten, K., "Architecture and Mechanism of the Light-harvesting Apparatus of Purple Bacteria" *Proc. Natl. Acad. Sci. U. S. A.* **1998,** 95, (11), 5935-5941.

8. Balashov, S. P.; Imasheva, E. S.; Boichenko, V. A.; Anton, J.; Wang, J. M.; Lanyi, J. K., "Xanthorhodopsin: A Proton Pump with a Light-harvesting Carotenoid Antenna" *Science* **2005,** 309, (5743), 2061-2064.

9. Baranoff, E.; Collin, J. P.; Flamigni, L.; Sauvage, J. P., "From Ruthenium(II) to Iridium(III): 15 Years of Triads Based on Bis-terpyridine Complexes" *Chem. Soc. Rev.* **2004,** 33, (3), 147-155.

10. Biemans, H. A. M.; Rowan, A. E.; Verhoeven, A.; Vanoppen, P.; Latterini, L.; Foekema, J.; Schenning, A.; Meijer, E. W.; de Schryver, F. C.; Nolte, R. J. M., "Hexakis Porphyrinato Benzenes. A New Class of Porphyrin Arrays" *J. Am. Chem. Soc.* **1998,** 120, (43), 11054-11060.

11. Browne, W. R.; O'Boyle, N. M.; McGarvey, J. J.; Vos, J. G., "Elucidating Excited State Electronic Structure and Intercomponent Interactions in Multicomponent and Supramolecular Systems" *Chem. Soc. Rev.* **2005,** 34, (8), 641-663.

12. Chiorboli, C.; Indelli, M. T.; Scandola, F., Photoinduced Electron/energy Transfer Across Molecular Bridges in Binuclear Metal Complexes. In *Molecular Wires: From Design to Properties*, 2005; Vol. 257, pp 63-102.

13. Choi, M. S.; Yamazaki, T.; Yamazaki, I.; Aida, T., "Bioinspired Molecular Design of Light-harvesting Multiporphyrin Arrays" *Angew. Chem. Int. Ed.* **2004,** 43, (2), 150-158.

14. Di Valentin, M.; Bisol, A.; Agostini, G.; Liddell, P. A.; Kodis, G.; Moore, A. L.; Moore, T. A.; Gust, D.; Carbonera, D., "Photoinduced Long-lived Charge Separation in a Tetrathiafulvalene-porphyrin-fullerene Triad Detected by Time-resolved Electron Paramagnetic Resonance" *J. Phys. Chem. B* **2005,** 109, (30), 14401-14409.

15. D'Souza, F.; Ito, O., "Photoinduced Electron Transfer in Supramolecular Systems of Fullerenes Functionalized with Ligands Capable of Binding to Zinc Porphyrins and Zinc Phthalocyanines" *Coord. Chem. Rev.* **2005,** 249, (13-14), 1410-1422.

16. Guldi, D. M.; Marcaccio, M.; Paolucci, F.; Paolucci, D.; Ramey, J.; Taylor, R.; Burley, G. A., "Fluorinated Fullerenes: Sources of Donor-acceptor Dyads with [18]Trannulene Acceptors for Energy- and Electron-transfer Reactions" *J. Phys. Chem. A* **2005,** 109, (43), 9723-9730.

17. Gust, D.; Moore, T. A.; Moore, A. L., "Mimicking Photosynthetic Solar Energy Transduction" *Acc. Chem. Res.* **2001,** 34, (1), 40-48.

18. Hagfeldt, A.; Gratzel, M., "Molecular Photovoltaics" *Acc. Chem. Res.* **2000,** 33, (5), 269-277.

19. Hindin, E.; Kirmaier, C.; Diers, J. R.; Tomizaki, K. Y.; Taniguchi, M.; Lindsey, J. S.; Bocian, D. F.; Holten, D., "Photophysical Properties of Phenylethyne-linked Porphyrin and Oxochlorin Dyads" *J. Phys. Chem. B* **2004,** 108, (24), 8190-8200.

20. Kobori, Y.; Yamauchi, S.; Akiyama, K.; Tero-Kubota, S.; Imahori, H.; Fukuzumi, S.; Norris, J. R., "Primary Charge-recombination in an Artificial Photosynthetic Reaction Center" *Proc. Natl. Acad. Sci. U. S. A.* **2005,** 102, (29), 10017-10022.

21. Kurreck, H.; Huber, M., "Model Reactions for Photosynthesis-photoinduced Charge and Energy-transfer between Covalently-linked Porphyrin and Quinone Units" *Angew. Chem. Int. Ed.* **1995,** 34, (8), 849-866.

22. Li, X. Y.; Sinks, L. E.; Rybtchinski, B.; Wasielewski, M. R., "Ultrafast Aggregate-to-aggregate Energy Transfer within Self-assembled Light-harvesting Columns of Zinc Phthalocyanine Tetrakis(perylenediimide)" *J. Am. Chem. Soc.* **2004,** 126, (35), 10810-10811.

23. Martinez-Junza, V.; Rizzi, A.; Jolliffe, K. A.; Head, N. J.; Paddon-Row, M. N.; Braslavsky, S. E., "Conformational and Photophysical Studies on Porphyrin-containing Donor-bridge-acceptor Compounds. Charge Separation in Micellar Nanoreactors" *Phys. Chem. Chem. Phys.* **2005,** 7, (24), 4114-4125.

24. Robel, I.; Bunker, B. A.; Kamat, P. V., "Single-walled Carbon Nanotube-CdS Nanocomposites as Light-harvesting Assemblies: Photoinduced Charge-transfer Interactions" *Adv. Mater.* **2005,** 17, (20), 2458-2463.

25. Rybtchinski, B.; Sinks, L. E.; Wasielewski, M. R., "Combining Light-harvesting and Charge Separation in a Self-assembled Artificial Photosynthetic System Based on Perylenediimide Chromophores" *J. Am. Chem. Soc.* **2004,** 126, (39), 12268-12269.

26. Straight, S. D.; Andreasson, J.; Kodis, G.; Bandyopadhyay, S.; Mitchell, R. H.; Moore, T. A.; Moore, A. L.; Gust, D., "Molecular AND and INHIBIT Gates Based on Control of Porphyrin Fluorescence by Photochromes" *J. Am. Chem. Soc.* **2005,** 127, (26), 9403-9409.

27. Thomas, K. G.; George, M. V.; Kamat, P. V., "Photoinduced Electron-transfer Processes in Fullerene-based Donor - Acceptor Systems" *Helv. Chim. Acta* **2005,** 88, (6), 1291-1308.

28. Wasielewski, M. R., "Photoinduced Electron-transfer in Supramolecular Systems for Artificial Photosynthesis" *Chem. Rev.* **1992,** 92, (3), 435-461.

29. Weiss, E. A.; Chernick, E. T.; Wasielewski, M. R., "Modulation of Radical Ion Pair Lifetimes by the Presence of a Third Spin in Rodlike Donor-acceptor Triads" *J. Am. Chem. Soc.* **2004,** 126, (8), 2326-2327.

30. Fox, H. H.; Fox, M. A., "Fluorescence and Singlet Energy Migration in Conformationally Restrained Acrylate Polymers Bearing Pendant Chromophores" *Macromolecules* **1995,** 28, (13), 4570-4576.

31. Furuta, P. T.; Deng, L.; Garon, S.; Thompson, M. E.; Frechet, J. M. J., "Platinum-functionalized Random Copolymers for Use in Solution-processible, Efficient, Near-white Organic Light-emitting Diodes" *J. Am. Chem. Soc.* **2004,** 126, (47), 15388-15389.

32. Watkins, D. M.; Fox, M. A., "Rigid, Well-defined Block-copolymers for Efficient Light-harvesting" *J. Am. Chem. Soc.* **1994,** 116, (14), 6441-6442.

33. Webber, S. E., "Photon-harvesting Polymers" *Chem. Rev.* **1990,** 90, (8), 1469-1482.

34. Bosman, A. W.; Janssen, H. M.; Meijer, E. W., "About Dendrimers: Structure, Physical Properties, and Applications" *Chem. Rev.* **1999,** 99, (7), 1665-1688.

35. Grayson, S. M.; Frechet, J. M. J., "Convergent Dendrons and Dendrimers: from Synthesis to Applications" *Chem. Rev.* **2001,** 101, (12), 3819-3867.

36. Devadoss, C.; Bharathi, P.; Moore, J. S., "Energy Transfer in Dendritic Macromolecules: Molecular Size Effects and the Role of an Energy Gradient" *J. Am. Chem. Soc.* **1996,** 118, (40), 9635-9644.

37. Gronheid, R.; Hofkens, J.; Kohn, F.; Weil, T.; Reuther, E.; Mullen, K.; De Schryver, F. C., "Intramolecular Forster Energy Transfer in a Dendritic System at the Single Molecule Level" *J. Am. Chem. Soc.* **2002,** 124, (11), 2418-2419.

38. Melinger, J. S.; Pan, Y. C.; Kleiman, V. D.; Peng, Z. H.; Davis, B. L.; McMorrow, D.; Lu, M., "Optical and Photophysical Properties of Light-harvesting Phenylacetylene Monodendrons Based on Unsymmetrical Branching" *J. Am. Chem. Soc.* **2002,** 124, (40), 12002-12012.

39. Shortreed, M. R.; Swallen, S. F.; Shi, Z. Y.; Tan, W. H.; Xu, Z. F.; Devadoss, C.; Moore, J. S.; Kopelman, R., "Directed Energy Transfer Funnels in Dendrimeric Antenna Supermolecules" *J. Phys. Chem. B* **1997,** 101, (33), 6318-6322.

40. Cotlet, M.; Vosch, T.; Habuchi, S.; Weil, T.; Mullen, K.; Hofkens, J.; De Schryver, F., "Probing Intramolecular Forster Resonance Energy Transfer in a Naphthaleneimide-peryleneimide-terrylenediimide-based Dendrimer by Ensemble and Single-molecule Fluorescence Spectroscopy" *J. Am. Chem. Soc.* **2005,** 127, (27), 9760-9768.

41. Adronov, A.; Gilat, S. L.; Frechet, J. M. J.; Ohta, K.; Neuwahl, F. V. R.; Fleming, G. R., "Light Harvesting and Energy Transfer in Laser-dye-labeled Poly(aryl ether) Dendrimers" *J. Am. Chem. Soc.* **2000,** 122, (6), 1175-1185.

42. Balzani, V.; Ceroni, P.; Giansante, C.; Vicinelli, V.; Klarner, F. G.; Verhaelen, C.; Vogtle, F.; Hahn, U., "Tweezering the Core of a Dendrimer: A Photophysical and Electrochemical Study" *Angew. Chem. Int. Ed.* **2005,** 44, (29), 4574-4578.

43. Dichtel, W. R.; Hecht, S.; Frechet, J. M. J., "Functionally Layered Dendrimers: A New Building Block and Its Application to the Synthesis of Multichromophoric Light-harvesting Systems" *Org. Lett.* **2005,** 7, (20), 4451-4454.

44. Hahn, U.; Gorka, M.; Vogtle, F.; Vicinelli, V.; Ceroni, P.; Maestri, M.; Balzani, V., "Light-harvesting Dendrimers: Efficient Intra- and Intermolecular Energy-transfer Processes in a Species Containing 65 Chromophoric Groups of Four Different Types" *Angew. Chem. Int. Ed.* **2002,** 41, (19), 3595-3598.

45. Jiang, D. L.; Aida, T., "Morphology-dependent Photochemical Events in Aryl Ether Dendrimer Porphyrins: Cooperation of Dendron Subunits for Singlet Energy Transduction" *J. Am. Chem. Soc.* **1998,** 120, (42), 10895-10901.

46. Serin, J. M.; Brousmiche, D. W.; Frechet, J. M. J., "Cascade Energy Transfer in a Conformationally Mobile Multichromophoric Dendrimer" *Chem. Commun.* **2002**, (22), 2605-2607.

47. Stewart, G. M.; Fox, M. A., "Chromophore-labeled Dendrons as Light Harvesting Antennae" *J. Am. Chem. Soc.* **1996,** 118, (18), 4354-4360.

48. Lor, M.; Thielemans, J.; Viaene, L.; Cotlet, M.; Hofkens, J.; Weil, T.; Hampel, C.; Mullen, K.; Verhoeven, J. W.; Van der Auweraer, M.; De Schryver, F. C., "Photoinduced Electron Transfer in a Rigid First Generation Triphenylamine Core Dendrimer Substituted with a Peryleneimide Acceptor" *J. Am. Chem. Soc.* **2002,** 124, (33), 9918-9925.

49. Qu, J. Q.; Zhang, J. Y.; Grimsdale, A. C.; Mullen, K.; Jaiser, F.; Yang, X. H.; Neher, D., "Dendronized Perylene Diimide Emitters: Synthesis, Luminescence, and Electron and Energy Transfer Studies" *Macromolecules* **2004,** 37, (22), 8297-8306.

50. Braun, M.; Atalick, S.; Guldi, D. M.; Lanig, H.; Brettreich, M.; Burghardt, S.; Hatzimarinaki, M.; Ravanelli, E.; Prato, M.; van Eldik, R.; Hirsch, A., "Electrostatic Complexation and Photoinduced Electron Transfer between Zn-cytochrome c and Polyanionic Fullerene Dendrimers" *Chem. Eur. J.* **2003,** 9, (16), 3867-3875.

51. Ghaddar, T. H.; Wishart, J. F.; Thompson, D. W.; Whitesell, J. K.; Fox, M. A., "A Dendrimer-based Electron Antenna: Paired Electron-transfer Reactions in Dendrimers with a 4,4 '-Bipyridine Core and Naphthalene Peripheral Groups" *J. Am. Chem. Soc.* **2002,** 124, (28), 8285-8289.

52. Guldi, D. M.; Swartz, A.; Luo, C. P.; Gomez, R.; Segura, J. L.; Martin, N., "Rigid Dendritic Donor-acceptor Ensembles: Control Over Energy and Electron Transduction" *J. Am. Chem. Soc.* **2002,** 124, (36), 10875-10886.

53. Gutierrez-Nava, M.; Accorsi, G.; Masson, P.; Armaroli, N.; Nierengarten, J. F., "Polarity Effects on the Photophysics of Dendrimers with an Oligophenylenevinylene Core and Peripheral Fullerene Units" *Chem. Eur. J.* **2004,** 10, (20), 5076-5086.

54. Thomas, K. R. J.; Thompson, A. L.; Sivakumar, A. V.; Bardeen, C. J.; Thayumanavan, S., "Energy and Electron Transfer in Bifunctional Non-conjugated Dendrimers" *J. Am. Chem. Soc.* **2005,** 127, (1), 373-383.

55. Harth, E. M.; Hecht, S.; Helms, B.; Malmstrom, E. E.; Frechet, J. M. J.; Hawker, C. J., "The Effect of Macromolecular Architecture in Nanomaterials: A Comparison of Site Isolation in Porphyrin Core Dendrimers and Their Isomeric Linear Analogues" *J. Am. Chem. Soc.* **2002,** 124, (15), 3926-3938.

56. Hawker, C. J.; Malmstrom, E. E.; Frank, C. W.; Kampf, J. P., "Exact Linear Analogs of Dendritic Polyether Macromolecules: Design, Synthesis, and Unique Properties" *J. Am. Chem. Soc.* **1997,** 119, (41), 9903-9904.

57. Hartwig, J. F., "Transition metal catalyzed synthesis of arylamines and aryl ethers from aryl halides and triflates: Scope and mechanism" *Angew. Chem. Int. Ed.* **1998,** 37, (15), 2047-2067.

58. Wolfe, J. P.; Wagaw, S.; Marcoux, J. F.; Buchwald, S. L., "Rational development of practical catalysts for aromatic carbon-nitrogen bond formation" *Acc. Chem. Res.* **1998,** 31, (12), 805-818.

59. Khudyakov, I. V.; Serebrennikov, Y. A.; Turro, N. J., "Spin-orbit-coupling in Free-radical Reactions -On the Way to Heavy-elements" *Chem. Rev.* **1993,** 93, (1), 537-570.

60. Plummer, B. F.; Steffen, L. K.; Braley, T. L.; Reese, W. G.; Zych, K.; Vandyke, G.; Tulley, B., "Study of Geometry-effects of Heavy Atom Perturbation of the Electronic-properties of Derivatives of the Nonalternant Polycyclic Aromatic-hydrocarbons Fluoranthene and Acenaphtho[1,2-K]Fluoranthene" *J. Am. Chem. Soc.* **1993,** 115, (24), 11542-11551.

61. Thomas, K. R. J.; Thompson, A. L.; Sivakumar, A. V.; Bardeen, C. J.; Thayumanavan, S., "Energy and Electron Transfer in Bifunctional Non-conjugated Dendrimers" *J. Am. Chem. Soc.* **2005,** 127, (1), 373-383.

62. Neuwahl, F. V. R.; Righini, R.; Adronov, A.; Malenfant, P. R. L.; Frechet, J. M. J., "Femtosecond Transient Absorption Studies of Energy Transfer within Chromophore-labeled Dendrimers" *J. Phys. Chem. B* **2001,** 105, (7), 1307-1312.

63. Baumann, J.; Fayer, M. D., "Excitation Transfer in Disordered Two-dimensional and Anisotropic 3-Dimensional Systems -Effect of Spatial Geometry on Time-resolved Observables" *J. Chem. Phys.* **1986,** 85, (7), 4087-4107.

64. Xu, Q. H.; Wang, S.; Korystov, D.; Mikhailovsky, A.; Bazan, G. C.; Moses, D.; Heeger, A. J., "The Fluorescence Resonance Energy Transfer (FRET) Gate: A Time-resolved Study" *Proc. Natl. Acad. Sci. U. S. A.* **2005,** 102, (3), 530-535.

65. Maus, M.; De, R.; Lor, M.; Weil, T.; Mitra, S.; Wiesler, U. M.; Herrmann, A.; Hofkens, J.; Vosch, T.; Mullen, K.; De Schryver, F. C., "Intramolecular Energy Hopping and Energy Trapping in Polyphenylene Dendrimers with Multiple Peryleneimide Donor Chromophores and a Terryleneimide Acceptor Trap Chromophore" *J. Am. Chem. Soc.* **2001,** 123, (31), 7668-7676.

66. Maus, M.; Mitra, S.; Lor, M.; Hofkens, J.; Weil, T.; Herrmann, A.; Mullen, K.; De Schryver, F. C., "Intramolecular Energy Hopping in Polyphenylene Dendrimers with an Increasing Number of Peryleneimide Chromophores" *J. Phys. Chem. A* **2001,** 105, (16), 3961-3966.

CHAPTER 3

DENDRITIC AND LINEAR MACROMOLECULAR ARCHITECTURES FOR PHOTOVOLTAICS:-A PHOTOINDUCED CHARGE TRANSFER INVESTIGATION

3.1 Introduction

Developing strategies for harnessing energy from renewable sources is a significant challenge facing the scientific community, due to the environmental, economic, and national security implications.[1-4] Photovoltaics is one of the most promising approaches to addressing this issue.[5-7] Nature provides both the source and the inspiration for a solution in the form of the sun and the photosynthetic apparatus respectively. Funneling the sequestered energy from the solar radiation to generate an excited state at a reaction center and utilizing this high energy state to affect a sequence of charge transfer (CT) events are the key preliminary steps in photosynthesis.[8] The resultant charge separated state from these events is ultimately used as a source of chemical energy. Thus, the photosynthetic process involves the conversion of solar energy into chemical energy. Although the ultimate goal of the photovoltaics is to convert the solar energy to electrical energy, the preliminary steps are essentially the same. Considering the high efficiency of the photoinduced charge transfer events in nature, it is desirable to mimic these efficiencies for photovoltaics. While the biomolecular architectures are very efficient and stable in their native conditions, these are neither robust nor cheap enough to be practical materials for photovoltaics. Therefore, several artificial systems based on covalent,[9-19] supramolecular,[20-25] or polymeric[26-32] arrays of photoactive and electroactive units have been approached.

Relative placement of the photoactive and electroactive functionalities plays an important role in the vectorial photoinduced charge transfer process. While it is conceivable that one can precisely control these in a small molecule, achieving similar control in non-biological macromolecular systems is very challenging. Dendrimers provide a unique opportunity, since these molecules can be achieved with excellent control in the relative placement of functional groups while also maintaining a great degree of control over their molecular weight.[33-36] In addition, the decreasing density of functional groups from periphery to the core of the dendrimers is reminiscent of an antenna. Therefore, dendrimers have been extensively investigated as light harvesting antennae, where excited state energy from the peripheral functionalities are funneled to the core of a dendrimer.[26, 37] The dendrimers that have been studies for this purpose can be broadly classified into conjugated and non-conjugated dendrimers.[37-50] Although much more limited, dendrimers have also been investigated as architectures for photoinduced electron transfer processes, the next step in the primary steps of photosynthesis.[51-53] A schematic of the photoinduced electron transfer process in dendrimers is shown in Figure 3.1. Although one could envision utilizing a charge separated species of this type in conversion to chemical energy, such dendritic architectures do not seem ideal for ultimate use in photovoltaics. This is because the charge transfer process causes one of the charges to be at the core of the dendrimer. This location in a dendrimer is significantly encapsulated and therefore the opportunities for ultimately transporting this charge to an electrode is limited, if any at all, as illustrated in Figure 3.1. On the other hand, by carrying out a systematic comparison of linear architectures with the corresponding dendritic structures, we have also demonstrated that the branched architectures indeed provide certain advantages in the photoinduced electron transfer process.[54, 55]

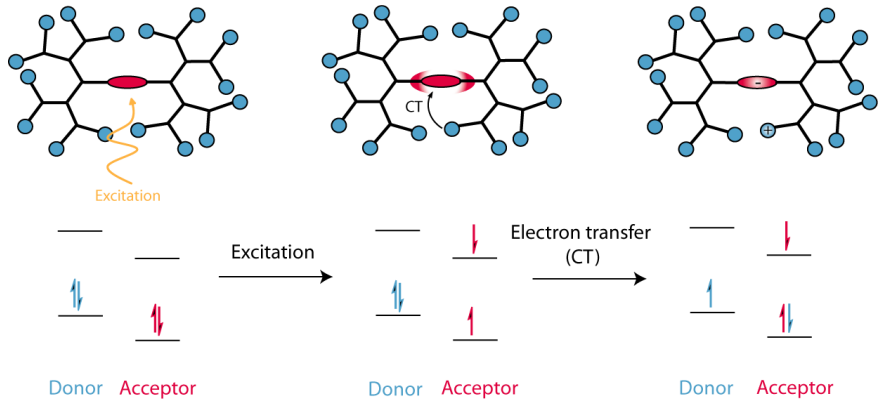

Figure 3.1. Cartoon shows a charge trap at a core by a dendritic backbone.

Considering all these features, we asked whether it is possible to envisage a hybrid architecture where we combine the advantages of dendritic structure in the photoinduced electron transfer process with the relatively open nature of the linear polymers for transporting the separated charges. A structure that would fit all these requirements will involve a dendron-rod-coil based triad, which contains a "rod" chromophore, a "dendron" functionalized with electron-rich moieties, and a polymeric "coil" with electron-poor functionalities (Figure 3.2). An additional advantage of the dendron-rod-coil architecture is that these structures have been investigated as unique architectures for providing microphase separated nanoscale architectures,[56-60] which should provide advantages in our ultimate goal of photovoltaic devices. In this chapter, we describe our molecular design, syntheses, and evaluation of the relative roles of the dendritic and the linear polymer component in the photoinduced electron transfer processes. Our results show that the dendron-rod-coil combination do indeed provide unique advantages in photoinduced charge transfer.

For photoinduced charge transfer in the dendron-rod-coil molecule, it is necessary that the electron-rich functionality in the dendron is capable of reducing the excited state

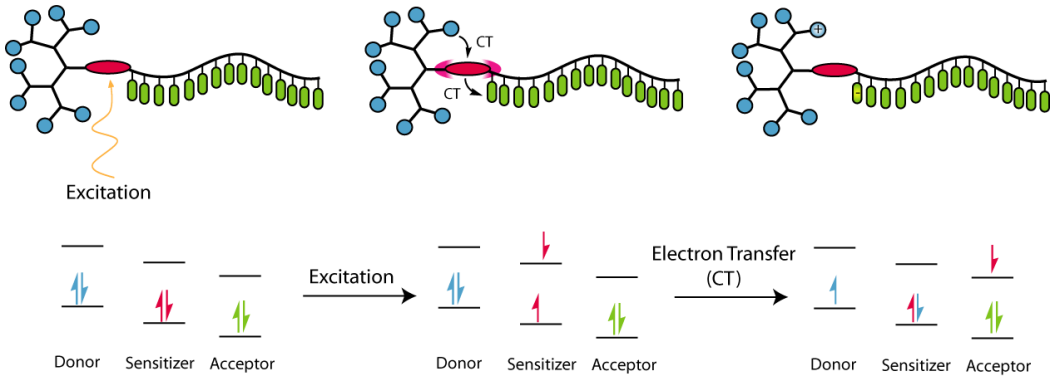

Figure 3.2. Cartoon shows an electron transfer process in dendron-rod-coils.

of the rod chromophore and the electron-poor functionality of the coil is capable of oxidizing the excited state of the rod chromophore as shown in Figure 3.2. From a frontier molecular orbital perspective, this means that the highest occupied molecular orbital (HOMO) of the electron-donating dendron functionality should be higher than that of the chromophore and the lowest unoccupied molecular orbital (LUMO) of the electron-accepting polymer coil functionality should be lower than that of the rod chromophore. Diarylaminopyrene was chosen as the electron-rich functionality (electron donor) on the dendritic periphery, naphthalene diimide as the electron-poor functionality (electron acceptor) in the polymer coil, and benzthiadiazole as the rod chromophore (sensitizer). Target structures are shown in Chart 3.1.

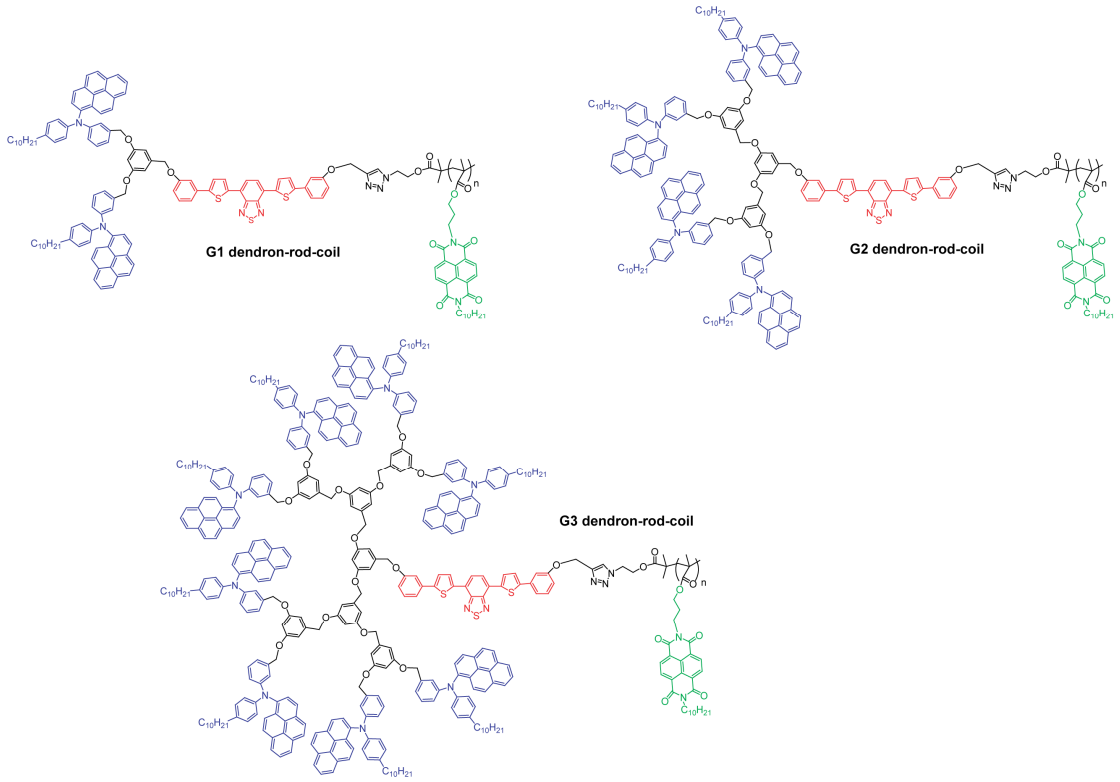

Chart 3.1. Structures of G1-G3 dendron-rod-coils used in these studies.

3.2 Results and Discussion

3.2.1 Synthesis and Characterization

When assembling a macromolecule with different components, such as the ones shown in Chart 3.1, it is advantageous to approach the synthesis in a modular fashion. The modular approach allows for flexibility in varying the functional groups in molecules with relative ease, which allows for any future structure-property relationship study needed. Thus the diarylaminopyrene-based dendron, the benzthiadiazole-based rod, and the naphthalene diimide bearing polymer coil were synthesized separately and then assembled in the final steps of the syntheses to obtain the desired dendron-rod-coils. The key step in our modular approach is to be able to differentially substitute the polymer coil and the dendron on to a symmetrical core chromophore. It is necessary that we use a set

of complementary and versatile reactions to carry out these substitutions. We envisaged the possibility of using a simple alkylation reaction to substitute the dendron on to the chromophore, while utilizing the 1,3-dipolar cycloaddition reaction between an azide and an alkyne (the so-called 'click chemistry') to install the polymer coil.

Considering our targets, it is necessary that the rod chromophore be desymmetrized presenting a phenolic moiety at one terminus, while presenting an alkynyl functionality at the other. To achieve this, we simply utilized the symmetrical dihydroxy functionalized benzthiadiazole chromophore **2-3** reported in the previous chapter. Treatment of this symmetrical dihydroxy chromophore with a deficient amount of propargyl bromide in the presence of K_2CO_3 and 18-crown-6 afforded the targeted unsymmetrical chromophore **3-1**, as shown in Scheme 3.1. The remaining phenolic functionality on the rod chromophore will be subjected to alkylation reaction with bromomethyl functionalized dendrons, while the propargyl group will be utilized to attach the polymer coil *via* 1,3-dipolar cycloaddition or click reaction with azide terminated polymers to obtain the desired dendron-rod-coils as final products.

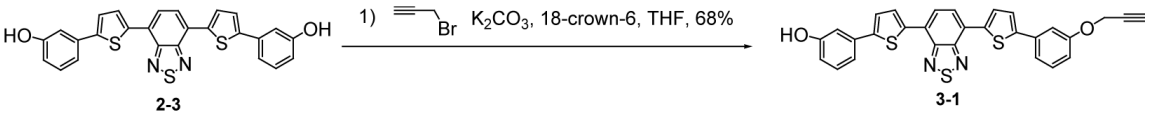

Scheme 3.1. The unsymmetrical substitution of rod species.

The polymer coil contains a naphthalene diimide as the side chain functionality on a polymethacrylate backbone. To attach this polymer to the chromophore through the cycloaddition reaction, it is necessary that the one of the chain ends contains an azide functionality. We utilized atom transfer radical polymerization (ATRP),[61-63] a living radical polymerization technique, that not only allows for selective incorporation of a

single functionality at the initiator end of the polymer but also can be used for the synthesis of methacrylate polymers with very good control over their polydispersities. Thus, we used 2-azidoethyl-bromoisobutyrate (**3-2**) as the initiator for the synthesis of the methacrylate-based naphthalene diimide polymer. To incorporate naphthalene diimide as the side chain to the methacrylate monomer, we first targeted the molecule that contains a single hydroxyalkyl functionality (**3-3**). This functional group will serve as the handle to install the naphthalene diimide functionality onto a polymerizable unit by treatment with mathacryloyl chloride to obtain compound **3-4**. Polymerization of **3-4** using **3-2** as the initiator in the presence of cuprous bromide and PMDETA afforded the polymer **3-5** in 61% yield with a PDI of 1.14 and a Mn of 9326.

While the polymer will be incorporated onto the chromophore core through the cycloaddition reaction, the dendron will be incorporated onto the chromophore using the

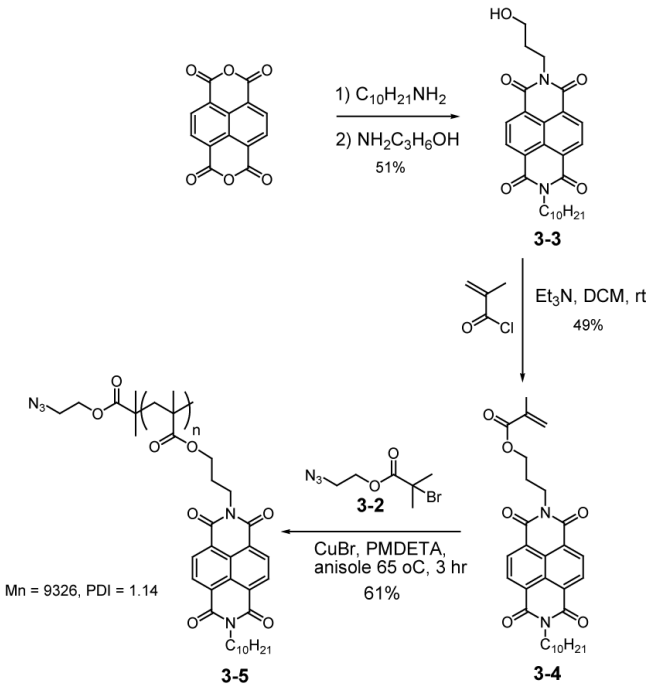

Scheme 3.2. The synthesis of polymer containing NDI units at the side chain.

Williamson ether synthesis. Since the chromophore core contains with a phenolic functionality, the targeted dendrons should have a bromoalkyl functionality at their focal point. We have previously mentioned the syntheses of dendrons **3-6**, **3-7** and **3-8** containing diarylaminopyrene units in the periphery and a bromomethyl functionality at the focal point. These dendrons were treated with the monophenolic chromophore core **3-1** under the Williamson alkylation conditions to obtain the dendron-rod components, which were further reacted with azide-terminated polymers under click chemistry conditions to obtain the G1-G3 dendron-rod-coils (Scheme 3.3). Note that if the polymeric coils were first installed onto the rod moiety to obtain rod-coil precursors, the overall synthetic steps could be reduced since the difference in G1-G3 dendron-rod-coils

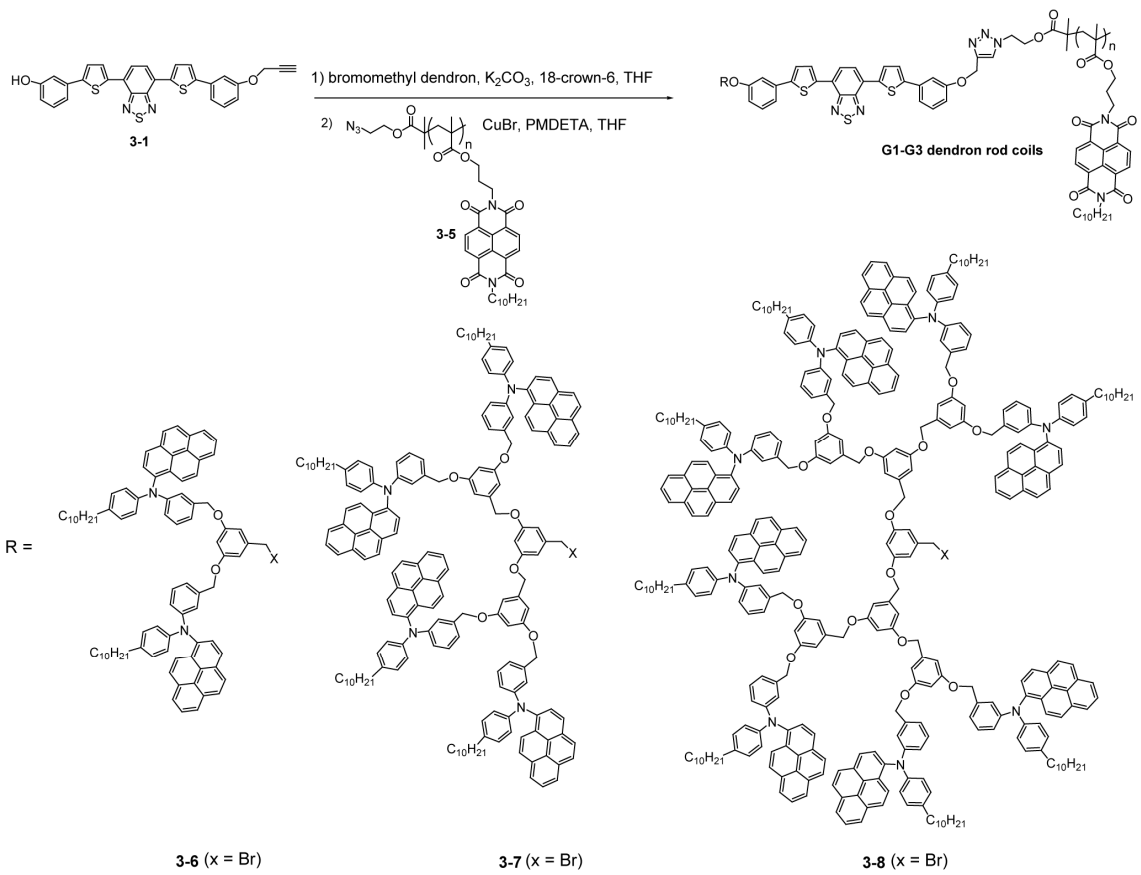

Scheme 3.3. The synthesis of dendron rod-coil species.

arises from the dendron. However, the separation of the rod-coils from the desired dendron-rod-coils in the final step is likely to be problematic from our experience with these molecules. Alternatively, separation of these dendron-rods from the final dendron-rod-coils was possible with a conventional chromatographic method due to the significant difference in polarity between these two species. All newly synthesized compounds were characterized by ^{1}H and ^{13}C NMR. Additionally, the purity of all targeted compounds was elucidated using GPC (Figure 3.3). All dendron-rod-coil species showed a single peak which was shifted towards the higher molecular weight region compared to their polymeric parent species, as shown in Figure 3.3. The molecular weight of dendron-rod-coils was also found to be equivalent to the sum of the molecular weights of their corresponding dendron-rod species and polymeric coil with the similar PDI. These evidences implied that dendron-rod-coils were successfully synthesized. The molecular weights (Mn) of all dendron-rod-coils along with dendron-rod and polymeric-coil species are shown in Table 3.1.

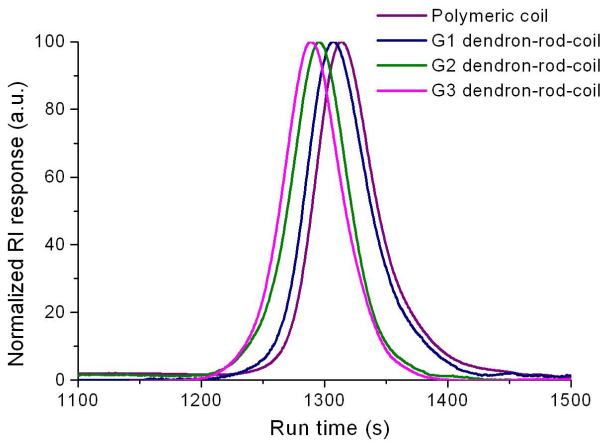

Figure 3.3. GPC (THF) profile of G1-G3 dendron-rod-coil compared to their parent polymeric species.

Table 3.1. Molecular weights (Mn) and PDI of all compounds obtained by GPC (THF).

Molecule	Mn*	PDI
Polymeric coil (**3-5**)	9326	1.14
G1 dendron-rod (**3-9**)	1777	1.03
G2 dendron-rod (**3-10**)	3321	1.03
G3 dendron-rod (**3-11**)	5193	1.02
G1 dendron-rod-coil	10825	1.07
G2 dendron-rod-coil	12940	1.05
G3 dendron-rod-coil	13186	1.09

* Mn is estimated using PMMA standards

Dendron-rod-coils were also characterized using linear absorption spectroscopy. The naphthalenediimide functionality exhibits an absorption maxima around 381 nm; diarylaminopyrene at 380 nm; and the benzthiadiazole chromophore at 490 nm (Figure 3.4). If one physically mixes the three components, *i.e.* the dendron, the chromophore rod, and the polymer coil, the spectrum obtained from these mixtures matches very well with that of the dendron-rod-coil molecule. This not only provides an additional support for characterizing the structure, but also suggests that there is no electronic communication among the diarylaminopyrene, benzthiadiazole, and the naphthalenediimide functionalities in the ground state. This is understandable, because the linkages between these photo- and electroactive functionalities are non-conjugated.

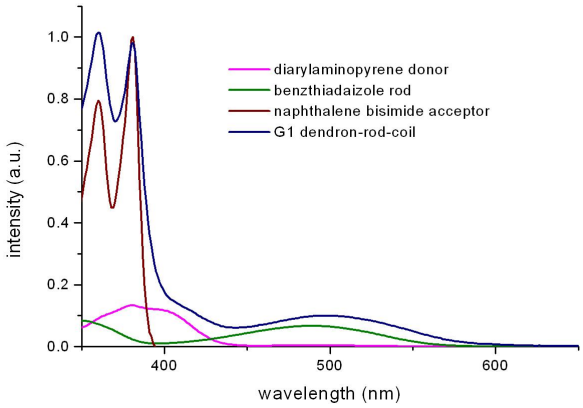

Figure 3.4. UV-Vis absorption spectra of G1 dendron-rod-coil and its chromophore constitutes.

3.2.2 Relative energy levels of the functionalities for photoinduced electron transfer

For photoinduced charge transfer to occur from the excited state of the chromophore rod, the positioning of the frontier orbital energy levels of the diarylaminopyrene and the naphthalenediimide units relative to the benzthiadiazole chromophore core is appropriate, as shown in Figure 3.2. The positioning of the HOMO or the LUMO of a functionality can be estimated by measuring its oxidation or reduction potential respectively. Once one of the frontier orbital energy levels is determined, the energy level of the other orbital can be determined by estimating the HOMO-LUMO gap. This gap can be taken to be equivalent to $\Delta E_{0\text{-}0}$, which is arrived at using the absorption and emission spectra of the photoactive or electroactive molecules. To estimate the energy levels of diarylaminopyrene **3-18**, naphthalenediimide **3-3**, and the benzthiadiazole chromophore **3-13** molecules were used as the control structures (Figure 3.5a). Cyclic voltammograms of these molecules are shown in Figure 3.5b. The onset oxidation potential of molecules **3-18** and **3-13** were 535 and 860 mV respectively, and

the onset reduction potential of molecule **3-3** was -665 mV. The intersection of the absorption and emission spectra of these molecules are taken to be the $\Delta E_{0\text{-}0}$ gap, the values of which are listed in Table 3.2. These values, in combination with the redox potential from cyclic voltammetry, were used to estimate the energy of both HOMO and the LUMO levels of functionalities **3-3, 3-18,** and **3-13**. Using the value of 390 mV as the off-set value between ferrocene/ferrocenium couple and vacuum, the HOMO and the LUMO energy levels relative to vacuum are listed in Table 3.2. These energy levels, graphically shown in Figure 3.5c, clearly indicate that the excited state of the

chromophore **3-13** can be reduced by the diarylaminopyrene **3-18** or oxidized by the naphthalenediimide **3-3**. Therefore, it is thermodynamically feasible that the excitation of

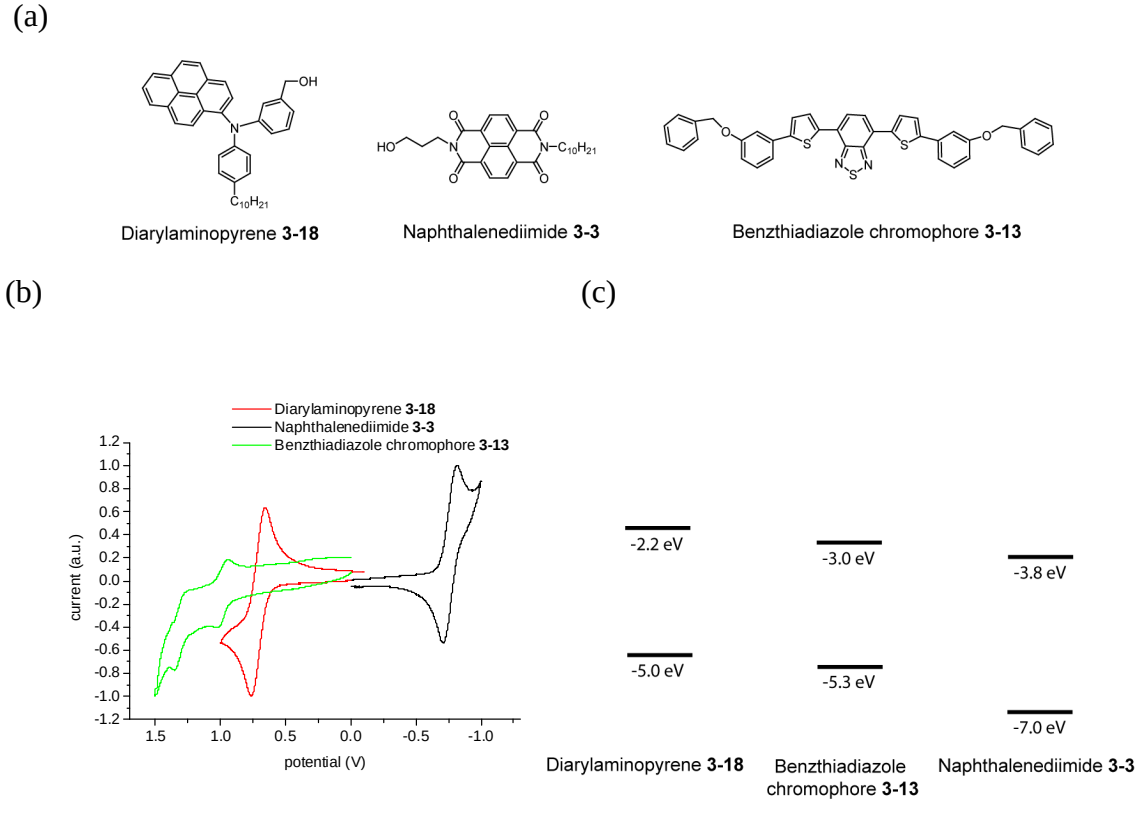

Figure 3.5. (a) Structures of the model molecules investigated (b) cyclic voltammogram in dichloromethane and (c) the relative energy levels of the molecules **3-18, 3-13,** and **3-3**.

the benzthiadiazole chromophore results in a photoinduced charge separated state, where the positive charge is at the diarylaminopyrene functionality in the dendron and the negative charge is at the naphthalenediimide functionality. This also shows that an energy transfer process is not thermodynamically feasible from the chromophore core to the diarylaminopyrene or the naphthalenediimide functionalities.

Table 3.2. Band gap and frontier energy levels of three functionalities.

Functionalities	$\Delta E_{0\text{-}0}$ (eV)	HOMO (eV)	LUMO (eV)
Diarylaminopyrene **3-18**	2.8	-5.0	-2.2
Benzthiadiazole chromophore **3-13**	2.3	-5.3	-3.0
Naphthalenediimide **3-3**	3.2	-7.0	-3.8

3.2.3 Steady State and Time Resolved Spectroscopy

To investigate whether the photoinduced electron transfer process is observed in these molecules, we analyzed the emission spectra of molecules G1-G3 dendron-rod-coils relative to that of the control chromophore rod **3-13**. At identical absorbance with respect to the benzthiadiazole chromophore absorption at 490 nm, the emission centered at 603 nm from the molecules G1-G3 dendron-rod-coils were significantly quenched relative to the control rod molecule **3-13**, as shown in Figure 3.6a. This observation provided the preliminary indication that incorporating an electron-rich dendron and the electron-poor polymeric coil is indeed effective for photoinduced charge separation. The extents of photoinduced electron transfer based quenching were quantified using time-resolved studies (*vide infra*).

` Next, we were interested in identifying whether it is the dendron or the coil that contributes the most to the observed photoinduced charge transfer based quenching. To analyze this, we synthesized dendron-rod and rod-coil counterparts to the dendron-rod coil molecules G1-G3 dendron-rod-coils. Structures of these molecules are shown in Figure 3.6c. The emission spectra of the control rod chromophore, G1 dendron-rod-coils, G1 dendron-rod **3-9** and the rod-coil molecule **3-12** are compared in Figure 3.6b.

(a) (b)

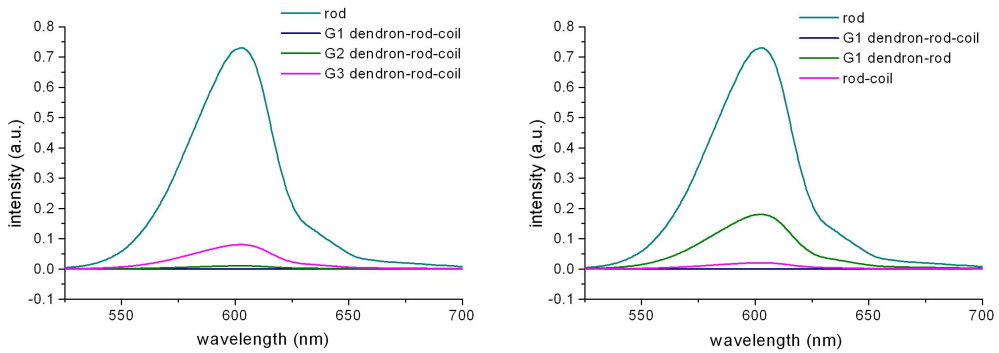

(c)

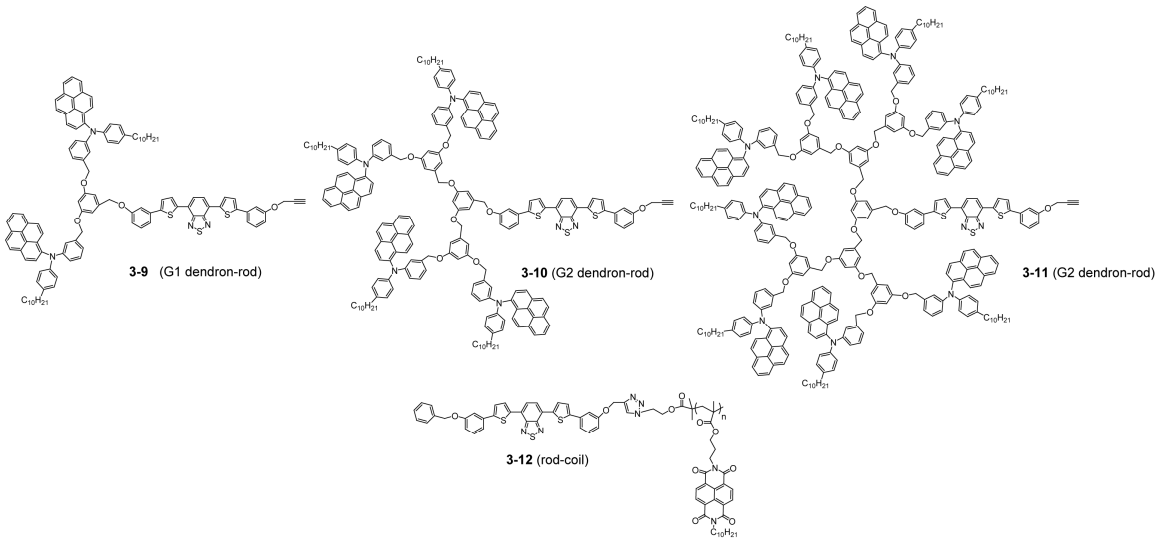

Figure 3.6. (a) Emission spectra of G1-G3 dendron-rod-coils compared to the rod (b) Emission spectra of G1 dendron-rod-coil, G1 dendron-rod and rod-coil compared to the rod. All steady state measurements were carried out in dichloromethane (excitation wavelength = 500 nm). (c) Structures of G1-G3 dendron-rod and rod-coil.

These results qualitatively indicate that the polymeric coil is more efficient in photoinduced charge transfer based quenching compared to the G1 dendron. It is also clear that the combination of the dendron and the polymeric coil is much better in the emission quenching. In order to quantify the efficiency of photoinduced charge transfer, we have carried out time-resolved fluorescence measurements.

As with the steady state measurements shown above, time-resolved fluorescence measurements were also carried out in dichloromethane. As mentioned earlier, the fluorescence decays observed here are due to the charge transfer from diarylamiopyrene and naphthalenediimide to the excited state of the benzthiadiazole rod. All observed fluorescence decays are nonexponential, which implies the distribution of conformations of both benzyl ether dendron and methacrylate polymeric backbone owing to their flexibility. This behavior is consistent with previous observations from our group and others.[64-66] To fit these nonexponential decays, biexponential functions of the form $Ae^{-1/\tau A} + B^{-1/\tau B}$ were used; the results of our fits are given in Table 3.3. As we have done previously, we parametize our biexponential decay dynamics using a single "average" decay rate k_{acc} defined as;

$$k_{acc} = \frac{A + B}{A\tau_A + B\tau_B} \tag{3.1}$$

Once we have the average decay rate k_{acc}, we can also define an effective quenching rate k_Q:

$$k_Q = k_{acc} - k_{acc}^0 \tag{3.2}$$

where k^0_{acc} is the fluorescence decay of the bare benzthiadiazole rod in the absence of both donor and acceptor quenchers. The efficiencies of charge transfer in dendron-rod-coils in all generations were calculated using the relationship:

$$\eta_{CT} = \frac{k_Q}{k_{acc}} \tag{3.3}$$

Table 3.3. Rod fluorescence decay (excited at 500 nm) and CT efficiencies.

Entry	Molecule	A	τ_A (ns)	B	τ_B (ns)	k_Q (ns^{-1})	η_{CT}
1	Rod (**3-13**)		7.66				
2	G1 dendron-rod (**3-9**)	0.32	1.24	0.68	3.56	0.23	0.65
3	G2 dendron-rod (**3-10**)	0.41	0.82	0.59	2.88	0.36	0.74
4	G3 dendron-rod (**3-11**)	0.56	0.73	0.44	3.24	0.42	0.77
5	G1 dendron-rod-coil	0.56	0.74	0.44	2.90	0.47	0.79
6	G2 dendron-rod-coil	0.60	0.64	0.40	2.65	0.57	0.82
7	G3 dendron-rod-coil	0.59	0.62	0.41	2.92	0.51	0.80
8	Rod-coil (**3-12**)	0.49	0.74	0.51	3.95	0.29	0.70
9	G1 dendrimer (**2-1F**)	0.64	5.36	0.36	1.95	0.12	0.48
10	G2 dendrimer (**2-2F**)	0.62	4.76	0.38	0.98	0.18	0.58
11	G3 dendrimer (**2-3F**)	0.60	5.49	0.40	1.00	0.15	0.54

From the data in Table 3.3, several noteworthy trends can be discerned. First, the overall fluorescence quenching rate k_Q is larger in the dendron-rod-coil molecules than in the dendron-rod molecules in all cases. The hypothesis put forward in the introduction, that the addition of the NDI coil would enhance charge transfer, is apparently correct. The total quenching rate, however, is not the sum of the individual contributions from the NDI and TAA moieties. This can be seen from the data in Table 3.3 for the G1

compounds. The sum of the k_Q values for the rod-coil and dendron-rod molecules is 0.23 ns^{-1} + 0.29 ns^{-1} = 0.52 ns^{-1} is greater than 0.47 ns^{-1}, which is the experimental value for the G1-dendron-rod-coil. This discrepancy becomes even more pronounced for later generations, and in the G3 molecules the expected k_Q is 0.71 ns^{-1}, as compared to 0.51 ns^{-1} as measured experimentally. The beneficial effect of larger dendrons on charge transfer appears to be suppressed in the dendron-rod-coil molecules. This can also be seen from the trends in η_{CT} in Table 3.3. Moreover, when comparing the dendritic donor's ability and the acceptor's ability to quench the excited state of the chromophore, it is clear that dendrons are more efficient in photoinduced electron transfer than the acceptor polymer, except in the case of G1 dendron-rod-coil. Therefore, it is intuitively appropriate to assume that the dendron-chromophore-dendron triad should be more efficient than dendron-rod-coil molecules, at least with higher generation dendrimers. We have studied the dendron-chromophore-dendron triad in the previous chapter.[66] Surprisingly, the charge transfer efficiencies of the dendritic triads (**2-1F**, **2-2F**, and **2-3F**) are much worse than the corresponding G1-G3 dendron-rod-coil triads. One could rationalize this observation based on the fact that the dendron-rod-coil is a donor-chromophore-acceptor triad, whereas the dendritic triad is a donor-chromophore-donor triad. However, it is even more interesting that the η_{CT} dendritic triads (**2-1F**, **2-2F**, and **2-3F**) are lesser than those of the donor-chromophore based dendron-rod molecules (**3-9**, **3-10**, and **3-11**). The question then is that why installing large dendron containing TAA groups on one side of the chromophore in dendron-rod-coils does not result in as large an enhancement of electron transfer efficiency as one would expect and installing two of those on the chromophore in dendritic triads leads to even a decrease in the electron transfer efficiency.

One could rationalize the observed results using backfolding and steric interference. We know there exist multiple conformations in both the TAA dendrons and

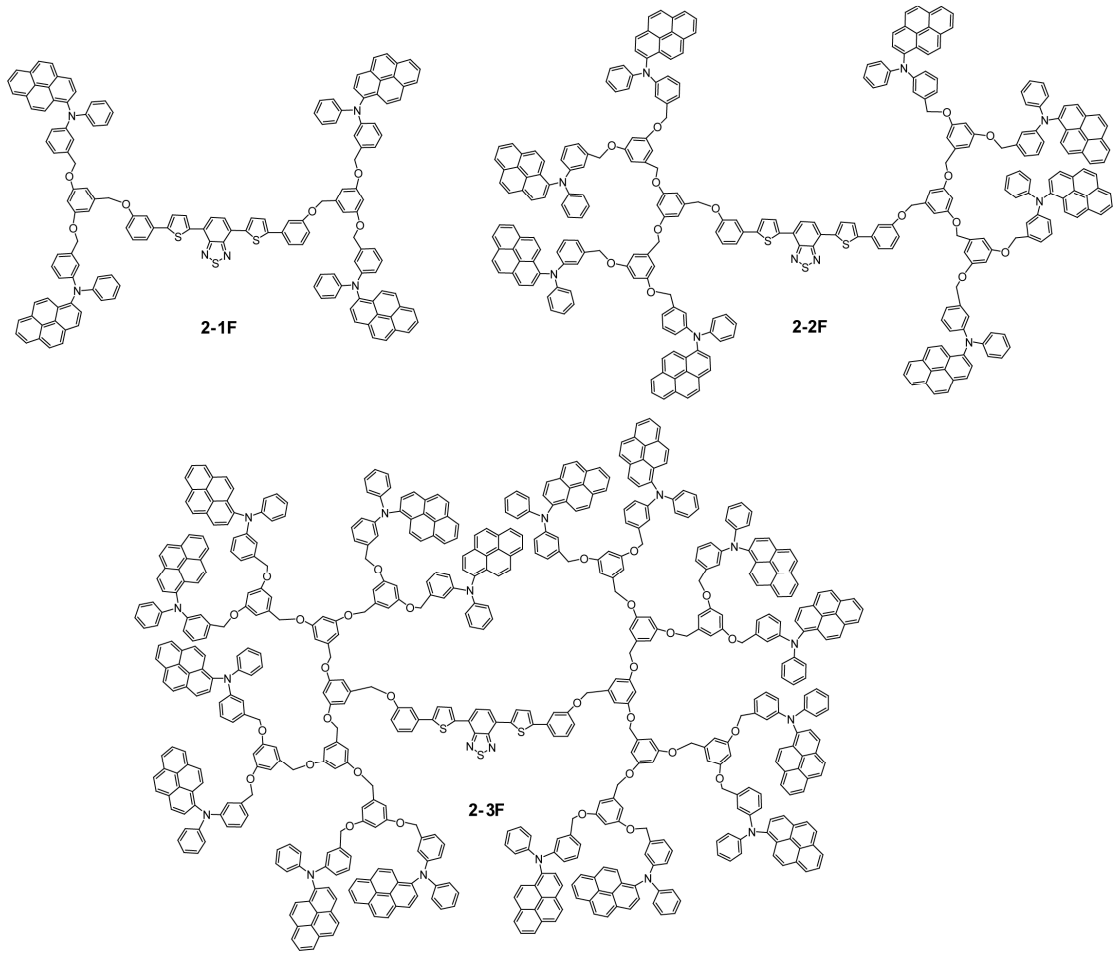

Figure 3.7. Dendrimers used for comparision of photoinduced charge separation efficiency.

the NDI coil, based on their nonexponential fluorescence decays. We have previously shown that as the size of the dendron increases, two competing factors contribute to the overall CT quenching rate. First, the local density of quenchers increases (raising k_Q) but also their average distance increases (lowering k_Q). If we now add a third factor, the presence of a large group on the opposite side of the benzthiadiazole core (either the NDI coil or the TAA dendron), it is reasonable to expect that this large, flexible group would

interfere with the TAA's ability to access the core and thus further suppress the expected increase in k_Q with generation. Thus we believe that conformational congestion, in both the dendron-rod-coil and the dendron-rod-dendron molecules prevents the favorable scaling of k_Q with generation observed in the dendron-rod molecules. Figure 3.8 compares k_Q in different species. The greater difference between k_Q (dendron-rods) + k_Q(rod-coils) and k_Q (dendron-rod-coils) (Figure 3.8a) as well as between k_Q (dendron-rod) and k_Q(dendrimers) (Figure 3.8b) in high generation dendrons where steric congestion plays more significant role to the rate of electron transfer provide support for this hypothesis.

In any case, it is clear from Table 3.3 that the dendron-rod-coils are architecturally better in quenching the excited state of the chromophore rod (Figure 3.9). We were interested in identifying the relative contribution by each of structural components, *i.e.* the dendron and the polymer coil, to the overall photoinduced charge transfer based fluorescence quenching process. We utilized the relative charge transfer rates for the G1-G3 dendron-rod diads (**3-9**, **3-10**, and **3-11**) and the rod-coil (**3-12**) diad to estimate the

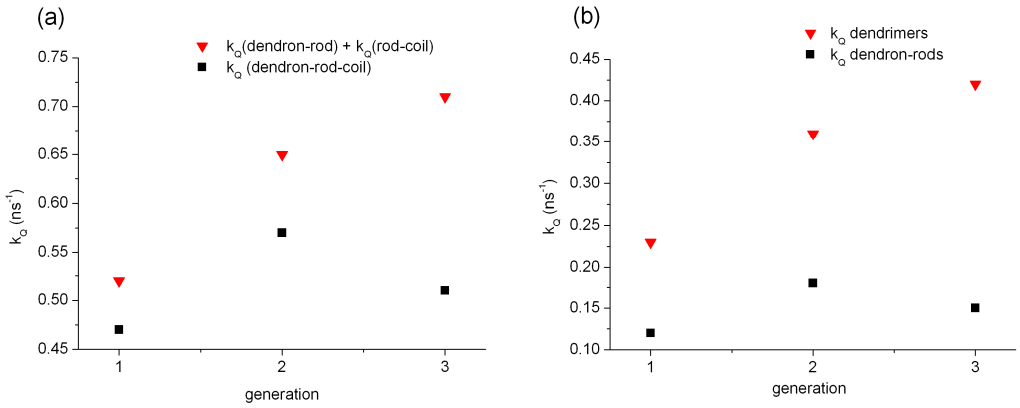

Figure 3.8. Comparison between (a) k_Q(dendron-rods) + k_Q (rod-coils) and k_Q(dendron-rod-coils) (b) k_Q(dendrimers) and k_Q(dendron-rods).

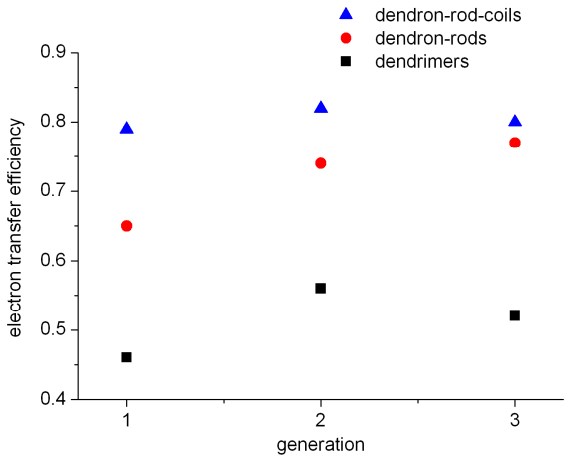

Figure 3.9. A plot of the electron transfer efficiency in different species and different generations.

possible relative contribution. The assumption here is that these diad rates are useful estimates of the effective contribution of the electron donor and the acceptor to the photoinduced charge transfer process in the triads G1-G3 dendron-rod-coils. As we have mentioned above, the contributions by the dendrons are indeed affected by the presence of the coil and therefore note that this assumption is not foolproof. However, we estimated the relative contributions to gain some insight into the architectural contributions by the dendrons and the coils in the photoinduced charge transfer processes. The estimates are shown in Table 3.4.

Table 3.4. Comparison of CT kinetics in dendron and polymer diads with dendron rod coils.

Species	k_Q (dendron-rod) (ns^{-1})	k_Q (rod-coil) (ns^{-1})	% Contribution	
			Dendron	Polymer
dendron-rod-coil	0.23	0.29	44	56
Gdendron-rod-coil	0.36	0.29	55	45
Gdendron-rod-coil	0.42	0.29	59	41

From Table 3.4, one can conclude that the contribution from the dendron and the polymer coil are about the same. However, it should be noted that there is another variation in the triad molecules in addition to the architectural variation (dendron *vs.* polymer). That involves the relative ability of the diarylaminopyrene as the electron donor to quench the excited state of the benzthiadiazole chromophore, compared to that of the naphthalenediimide functionality as the electron acceptor. We carried out Stern-Volmer quenching experiments to identify the relative abilities of these functionalities to quench the excited state of benzthiadiazole through charge transfer. In this experiment, the steady state emission of the benzthiadiazole rod (**3-13**) is measured in the presence of the quencher (diaryalminopyrene (**3-18**) or naphthalenediimide (**3-3**)) at various concentrations. With increasing concentration of the quencher, the emission intensity of the chromophore decreases as one would expect. The fluorescence intensity in the absence (I_0) and presence (I) of either of the quenchers can be related to its concentration ([Q]) using the Stern-Volmer equation: $I_0/I = 1 + K_{SV}[Q]$. A plot of I/I_0 *vs.* [Q] affords K_{SV}, which is a measure of the ability of the diarylaminopyrene or the naphthalenediimide to quench the excited state of the benzthiadiazole chromophore. K_{SV} is also related to the bimolecular quenching rate constant k_q through $K_{SV} = k_q.\tau_0$, where τ_0 is the fluorescence lifetime of dendrimer in the absence of quenchers. The Stern-Volmer plots for the diarylaminopyrene and naphthalenediimide are shown in Figure 3.10. The plots are linear and there are no changes in the absorption and emission spectral shapes of the molecules in the mixture. These suggest that the observed fluorescence quenching is dynamic, *i.e.* based on bimolecular collisions. It is clear from the slopes of these lines that the naphthalenediimide is far more effective than the diarylaminopyrene in quenching the excited state of the chromophore. It is to be noted that the differences between the

photoinduced charge transfer abilities in the dendron-rod *vs*. the rod-coil are relatively minor. Combination of these two observations clearly suggests that the dendritic architecture indeed provides a distinct advantage in the photoinduced electron transfer compared to the polymer coil.

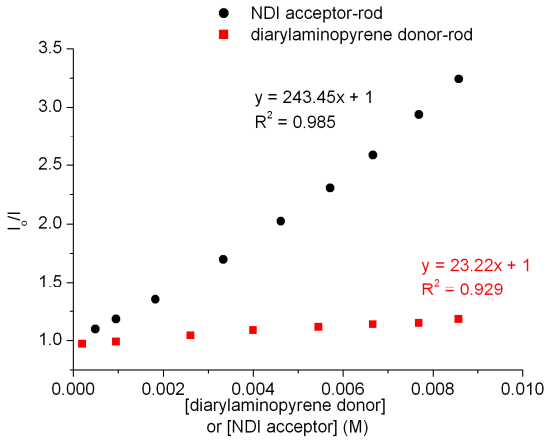

Figure 3.10. The Stern-Volmer plots of NDI acceptor-rod and TAA donor-rod.

What could be the reason for dendrimers providing this architectural advantage in photoinduced charge transfer over linear polymer coils? We have previously suggested that the high density of functionalities and backfolding in higher generations of dendrimers help boosting up the efficiency of the electron transfer in these branched molecules. It is interesting to ask whether such an effect is special for dendrimers or whether this can be observed with polymer coils when a similar number of CT units are incorporated. In our polymer backbone, the average number of repeat units is about 15. Thus the number of naphthalenediimide functionalities in the polymer coil is about twice as much as the number of diarylaminopyrene units in the G3 dendron. Despite this, combined with the fact that the naphthalenediimide is more capable of photoinduced charge transfer, the efficiency from the polymer coil is only comparable with that of the

dendron. It is possible that this is due to the possibility that only the naphthelendiimide functionality closest to the benzthiadiazole chromophore participates in the initial photoinduced charge transfer step, unlike the dendrons. To test this hypothesis, we synthesized a dendron-rod-coil analog where there is a single naphthalenediimide functionality. The distance between the benzthiadiazole chromophore and the naphthalenediimide functionality in this analog **3-15** was kept the same as that with the G1 dendron-rod-coil molecule.

To synthesize **3-15**, 8-bromoctanoic acid was reacted with oxalyl chloride to convert acid functionality into acid chloride, which was then treated with hydroxyl functionalized naphthalenediimide **3-3** in the presence of DMAP as a catalyst to obtain the bromo terminated naphthalenedisimide derivative. Treatment of this compound with sodium azide afforded naphthalenediimide derivative containing azide functionality (**3-14**). This molecule was then clicked with the acetylenic functionality of the dendron-rod

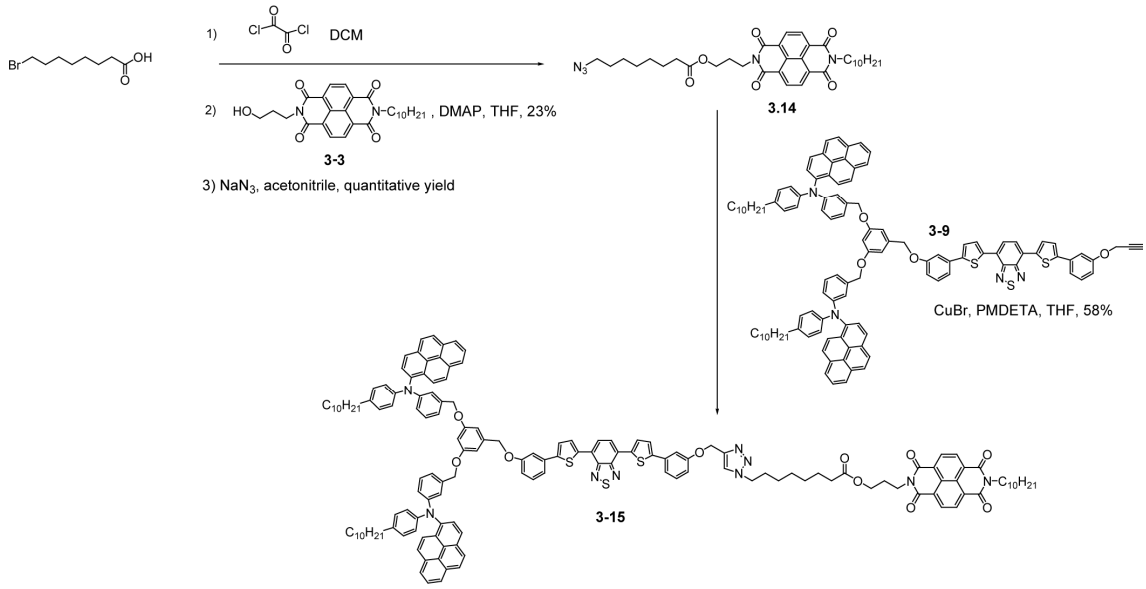

Scheme 3.4. Synthesis of model compounds.

molecule (**3-9**) to obtain the single naphthalenediimide molecule (**3-15**) analog for the G1 dendron-rod-coil, as shown in Scheme 3.4.

The fluorescence decay of the rod in this model compound is shown in Table 3.5. The η_{CT} for the G1 dendron-rod-coil and its analog **3-15** are identical. This indicates that the naphthalenediimide that is closest to the chromophore is the primary participant in the photoinduced charge transfer process in the polymer coil. On the other hand, the population density of functionalities in the dendritic periphery has a positive effect on the charge transfer.[54, 55] Thus, it is reasonable to conclude that the high density packing and the number of peripheral charge transfer functionalities at equidistant from the chromophore are indeed the reasons for the dendritic architectural advantage. Note however that the polymer coil also could play a crucial role in our long-term goals of obtaining microphase separated structures with long lived charge separated state for photovoltaics.

Table 3.5. Rod fluorescence decay (λ_{ex} = 500 nm) and CT efficiency of model compound (**3-15**).

A	τ_A (ns)	B	τ_B (ns)	k_Q (ns^{-1})	η_{CT}
0.21	0.51	0.79	1.95	0.48	0.79

3.3 Summary

Considering the advantages of dendritic architectures in photoinduced electron transfer, but issues in moving the charge away from the core due to encapsulation, we have designed and synthesized dendron-rod-coil based donor-chromophore-acceptor triads for photoinduced charge transfer. We have shown that: (*i*) the combination of the dendron and the polymer coil with a chromophore rod connecting the two is indeed

advantageous for photoinduced charge transfer; (*ii*) dendron-rod-coil based triads exhibit better efficiencies compared to either the dendron-rod or the rod-coil diads; (*iii*) based on the efficiencies of the diads, the dendrons and the polymer coil make similar contribution to the overall charge transfer based quenching process; (*iv*) the polymer coil functionality, naphthalenediimide, is a much better excited state quencher for the benzthiadiazole chromophore than the diarlyaminopyrene based on Stern-Volmer quenching studies. This suggests that the dendrons have an architectural advantage over polymer coils for photoinduced charge transfer; (*v*) although dendrons provide clear advantages in charge transfer quenching, the dendron-rod-dendron triads do not perform better than the donor-chromophore-acceptor triads based on the dendron-rod-coil architecture; (*vi*) while all electron donor functionalities in the dendritic periphery can equally participate in the excited state quenching of the chromophore rod, the naphthalenediimide electron acceptor unit that is closest to the chromophore is the primary participant in the quenching that arises from the polymer coil. The realistic possibility that dendron-rod-coil structures are capable of providing microphase separated architectures based on prior literature, combined with our findings here, suggests that these molecules hold great promise in organic photovoltaics. Polymer processing to achieve morphological control, device fabrication, and charge transfer dynamics in the solid state are part of the current focus in our laboratories.

3.4 References

1. Arunachalam, V. S.; Fleischer, E. L., "Harnessing Materials for Energy - Preface" *Mrs Bulletin* **2008,** 33, (4), 261-263.

2. Chang, M. C. Y., "Harnessing Energy from Plant Biomass" *Curr. Opin. Chem. Biol.* **2007,** 11, (6), 677-684.

3. Walker, T. W., "Harnessing Natural Energy" *Chem. Eng. Prog.* **2008,** 104, (3), S23-S28.

4. Zahedi, A., "Solar photovoltaic (PV) Energy; Latest Developments in the Building Integrated and Hybrid PV Systems" *Renew. Energy* **2006,** 31, (5), 711-718.

5. Hepbasli, A., "A Key Review on Exergetic Analysis and Assessment of Renewable Energy Resources for a Sustainable Future" *Renew. Sust. Energy Rev.* **2008,** 12, (3), 593-661.

6. Jester, T. L., "Crystalline Silicon Manufacturing Progress" *Prog. Photovoltaics* **2002,** 10, (2), 99-106.

7. Senft, D. C., "Progress in Crystalline Multijunction and Thin-Film Photovoltaics" *J. Electron. Mater.* **2005,** 34, (5), 571-574.

8. Wasielewski, M. R., "Photoinduced Electron Transfer in Supramolecular Systems for Artificial Photosynthesis" *Chem. Rev.* **1992,** 92, (3), 435-461.

9. Baffreau, J.; Leroy-Lhez, S.; Van Anh, N.; Williams, R. M.; Hudhomme, P., "Fullerene C-60-Perylene-3,4 : 9,10-bis(dicarboximide) Light-harvesting Dyads: Spacer-length and Bay-substituent Effects on Intramolecular Singlet and Triplet Energy Transfer" *Chem. Eur. J.* **2008,** 14, (16), 4974-4992.

10. D'Souza, F.; Smith, P. M.; Zandler, M. E.; McCarty, A. L.; Itou, M.; Araki, Y.; Ito, O., "Energy Transfer Followed by Electron Transfer in a Supramolecular Triad Composed of Boron Dipyrrin, Zinc Porphyrin, and Fullerene: A Model for the Photosynthetic Antenna-Reaction Center Complex" *J. Am. Chem. Soc.* **2004,** 126, (25), 7898-7907.

11. Elim, H. I.; Jeon, S. H.; Verma, S.; Ji, W.; Tan, L. S.; Urbas, A.; Chiang, L. Y., "Nonlinear Optical Transmission Properties of C-60 Dyads Consisting of a Light-Harvesting Diphenylaminofluorene Antenna" *J. Phys. Chem. B* **2008,** 112, (32), 9561-9564.

12. Haycock, R. A.; Yartsev, A.; Michelsen, U.; Sundstrom, V.; Hunter, C. A., Self-"Assembly of Pentameric Porphyrin Light-harvesting Antennae Complexes" *Angew. Chem. Int. Ed.* **2000,** 39, (20), 3616-3619.

13. Huijser, A.; Suijkerbuijk, B.; Gebbink, R.; Savenije, T. J.; Siebbeles, L. D. A., "Efficient Exciton Transport in Layers of Self-assembled Porphyrin Derivatives" *J. Am. Chem. Soc.* **2008,** 130, (8), 2485-2492.

14. Ishi-i, T.; Murakami, K.; Imai, Y.; Mataka, S., "Light-harvesting and Energy-transfer System Based on Self-assembling Perylene Diimide-appended Hexaazatriphenylene" *Org. Lett.* **2005,** 7, (15), 3175-3178.

15. Kuciauskas, D.; Liddell, P. A.; Lin, S.; Johnson, T. E.; Weghorn, S. J.; Lindsey, J. S.; Moore, A. L.; Moore, T. A.; Gust, D., "An Artificial Photosynthetic Antenna-reaction Center Complex" *J. Am. Chem. Soc.* **1999,** 121, (37), 8604-8614.

16. Kuramochi, Y.; Satake, A.; Itou, M.; Ogawa, K.; Araki, Y.; Ito, O.; Kobuke, Y., "Light-harvesting Supramolecular Porphyrin Macrocycle Accommodating a Fullerene-Tripodal Ligand" *Chem. Eur. J.* **2008,** 14, (9), 2827-2841.

17. Oekermann, T.; Schlettwein, D.; Wohrle, D., "Characterization of N,N'-dimethyl-3,4,9,10-perylenetetracarboxylic Acid Diimide and Phthalocyaninatozinc(II) in Electrochemical Photovoltaic Cells" *J. Appl. Electrochem.* **1997,** 27, (10), 1172-1178.

18. Sugou, K.; Sasaki, K.; Kitajima, K.; Iwaki, T.; Kuroda, Y., "Light-harvesting Heptadecameric Porphyrin Assemblies" *J. Am. Chem. Soc.* **2002,** 124, (7), 1182-1183.

19. Wurthner, F.; Ahmed, S.; Thalacker, C.; Debaerdemaeker, T., "Core-substituted Naphthalene Bisimides: New Fluorophors with Tunable Emission Wavelength for FRET Studies" *Chem. Eur. J.* **2002,** 8, (20), 4742-4750.

20. Adronov, A.; Frechet, J. M. J., "Light-harvesting Dendrimers" *Chem. Commun.* **2000**, (18), 1701-1710.

21. Aida, T.; Jiang, D. L.; Yashima, E.; Okamoto, Y., "A New Approach to Light-Harvesting with Dendritic Antenna" *Thin Solid Films* **1998,** 331, (1-2), 254-258.

22. Gilat, S. L.; Adronov, A.; Frechet, J. M. J., "Light Harvesting and Energy Transfer in Novel Convergently Constructed Dendrimers" *Angew. Chem. Int. Ed.* **1999,** 38, (10), 1422-1427.

23. Hahn, U.; Gorka, M.; Vogtle, F.; Vicinelli, V.; Ceroni, P.; Maestri, M.; Balzani, V., "Light-harvesting Dendrimers: Efficient Intra- and Intermolecular Energy-transfer Processes in a Species Containing 65 Chromophoric Groups of Four Different Types" *Angew. Chem. Int. Ed.* **2002,** 41, (19), 3595-3598.

24. Jiang, D. L.; Aida, T., "Bioinspired Molecular Design of Functional Dendrimers" *Prog. Polym. Sci.* **2005,** 30, (3-4), 403-422.

25. Nantalaksakul, A.; Reddy, D. R.; Bardeen, C. J.; "Thayumanavan, S., Light Harvesting Dendrimers" *Photosynth. Res.* **2006,** 87, (1), 133-150.

26. Balzani, V.; Ceroni, P.; Maestri, M.; Vicinelli, V., "Light-harvesting Dendrimers" *Curr. Opin. Chem. Biol.* **2003,** 7, (6), 657-665.

27. Bundgaard, E.; Krebs, F. C., " Low Band Gap Polymers for Organic Photovoltaics" *Sol. Energy Mater. Sol. Cells* **2007,** 91, (11), 954-985.

28. Colladet, K.; Fourier, S.; Cleij, T. J.; Lutsen, L.; Gelan, J.; Vanderzande, D.; Nguyen, L. H.; Neugebauer, H.; Sariciftci, S.; Aguirre, A.; Janssen, G.; Goovaerts, E., "Low Band Gap Donor-acceptor Conjugated Polymers toward Organic Solar Cells Applications" *Macromolecules* **2007,** 40, (1), 65-72.

29. Gunes, S.; Neugebauer, H.; Sariciftci, N. S., "Conjugated Polymer-based Organic Solar Cells" *Chem. Rev.* **2007,** 107, (4), 1324-1338.

30. Lungenschmied, C.; Dennler, G.; Neugebauer, H.; Sariciftci, S. N.; Glatthaar, M.; Meyer, T.; Meyer, A., "Flexible, Long-lived, Large-area, Organic Solar Cells" *Sol. Energy Mater. Sol. Cells* **2007,** 91, (5), 379-384.

31. Mayer, A. C.; Scully, S. R.; Hardin, B. E.; Rowell, M. W.; McGehee, M. D., "Polymer-based Solar Cells" *Mater. Today* **2007,** 10, (11), 28-33.

32. Peet, J.; Kim, J. Y.; Coates, N. E.; Ma, W. L.; Moses, D.; Heeger, A. J.; Bazan, G. C., "Efficiency Enhancement in Low-bandgap Polymer Solar Cells by Processing with Alkane Dithiols" *Nat. Mater.* **2007,** 6, (7), 497-500.

33. Dykes, G. M., "Dendrimers: A Review of Their Appeal and Applications" *J. Chem. Technol. Biotechnol.* **2001,** 76, (9), 903-918.

34. Gittins, P. J.; Twyman, L. J., "Dendrimers and Supramolecular Chemistry" *Supramol Chem.* **2003,** 15, (1), 5-23.

35. Jang, W. D.; Kataoka, K., "Bioinspired Applications of Functional Dendrimers" *J. Drug Deliv. Sci. Technol.* **2005,** 15, (1), 19-30.

36. Klajnert, B.; Bryszewska, M., "Dendrimers: Properties and Applications" *Acta Biochim. Pol.* **2001,** 48, (1), 199-208.

37. Choi, M. S.; Aida, T.; Yamazaki, T.; Yamazaki, I., "Dendritic Multiporphyrin Arrays as Light-harvesting Antennae: Effects of Generation Number and Morphology on Intramolecular Energy Transfer" *Chem. Eur. J.* **2002,** 8, (12), 2668-2678.

38. Adronov, A.; Gilat, S. L.; Frechet, J. M. J.; Ohta, K.; Neuwahl, F. V. R.; Fleming, G. R., "Light Harvesting and Energy Transfer in Laser-dye-labeled Poly(aryl ether) Dendrimers" *J. Am. Chem. Soc.* **2000,** 122, (6), 1175-1185.

39. Benites, M. D.; Johnson, T. E.; Weghorn, S.; Yu, L. H.; Rao, P. D.; Diers, J. R.; Yang, S. I.; Kirmaier, C.; Bocian, D. F.; Holten, D.; Lindsey, J. S.,"Synthesis and

Properties of Weakly Coupled Dendrimeric Multiporphyrin Light-harvesting Arrays and Hole-storage Reservoirs" *J. Mater. Chem.* **2002,** 12, (1), 65-80.

40. Devadoss, C.; Bharathi, P.; Moore, J. S., "Energy Transfer in Dendritic Macromolecules: Molecular Size Effects and the Role of an Energy Gradient" *J. Am. Chem. Soc.* **1996,** 118, (40), 9635-9644.

41. Gronheid, R.; Hofkens, J.; Kohn, F.; Weil, T.; Reuther, E.; Mullen, K.; De Schryver, F. C., "Intramolecular Forster Energy Transfer in a Dendritic System at the Single Molecule Level" *J. Am. Chem. Soc.* **2002,** 124, (11), 2418-2419.

42. Hahn, U.; Gorka, M.; Vogtle, F.; Vicinelli, V.; Ceroni, P.; Maestri, M.; Balzani, V., "Light-harvesting Dendrimers: Efficient Intra- and Intermolecular Energy-transfer Processes in a Species Containing 65 Chromophoric Groups of Four Different Types" *Angew. Chem. Int. Ed.* **2002,** 41, (19), 3595-3598.

43. Jiang, D. L.; Aida, T., "Morphology-dependent Photochemical Events in Aryl Ether Dendrimer Porphyrins: Cooperation of Dendron Subunits for Singlet Energy Transduction" *J. Am. Chem. Soc.* **1998,** 120, (42), 10895-10901.

44. Kohl, C.; Weil, T.; Qu, J. Q.; Mullen, K., "Towards Highly Fluorescent and Water-soluble Perylene Dyes" *Chem. Eur. J.* **2004,** 10, (21), 5297-5310.

45. Liu, D. J.; De Feyter, S.; Cotlet, M.; Wiesler, U. M.; Weil, T.; Herrmann, A.; Mullen, K.; De Schryver, F. C., "Fluorescent Self-assembled Polyphenylene Dendrimer Nanofibers" *Macromolecules* **2003,** 36, (22), 8489-8498.

46. Melinger, J. S.; Pan, Y. C.; Kleiman, V. D.; Peng, Z. H.; Davis, B. L.; McMorrow, D.; Lu, M., "Optical and Photophysical Properties of Light-harvesting Phenylacetylene Monodendrons Based on Unsymmetrical Branching" *J. Am. Chem. Soc.* **2002,** 124, (40), 12002-12012.

47. Neuwahl, F. V. R.; Righini, R.; Adronov, A.; Malenfant, P. R. L.; Frechet, J. M. J., "Femtosecond Transient Absorption Studies of Energy Transfer within Chromophore-Labeled Dendrimers" *J. Phys. Chem. B* **2001,** 105, (7), 1307-1312.

48. Ranasinghe, M. I.; Varnavski, O. P.; Pawlas, J.; Hauck, S. I.; Louie, J.; Hartwig, J. F.; Goodson, T., "Femtosecond Excitation Energy Transport in Triarylamine Dendrimers" *J. Am. Chem. Soc.* **2002,** 124, (23), 6520-6521.

49. Shortreed, M. R.; Swallen, S. F.; Shi, Z. Y.; Tan, W. H.; Xu, Z. F.; Devadoss, C.; Moore, J. S.; Kopelman, R., "Directed Energy Transfer Funnels in Dendrimeric Antenna Supermolecules" *J. Phys. Chem. B* **1997,** 101, (33), 6318-6322.

50. Stewart, G. M.; Fox, M. A., "Chromophore-labeled Dendrons as Light Harvesting Antennae" *J. Am. Chem. Soc.* **1996,** 118, (18), 4354-4360.

51. Capitosti, G. J.; Cramer, S. J.; Rajesh, C. S.; Modarelli, D. A., "Photoinduced Electron Transfer within Porphyrin-containing Poly(amide) Dendrimers" *Org. Lett.* **2001,** 3, (11), 1645-1648.

52. Lor, M.; Thielemans, J.; Viaene, L.; Cotlet, M.; Hofkens, J.; Weil, T.; Hampel, C.; Mullen, K.; Verhoeven, J. W.; Van der Auweraer, M.; De Schryver, F. C., "Photoinduced Electron Transfer in a Rigid First Generation Triphenylamine Core Dendrimer Substituted with a Peryleneimide Acceptor" *J. Am. Chem .Soc.* **2002,** 124, (33), 9918-9925.

53. Sadamoto, R.; Tomioka, N.; Aida, T., "Photoinduced Electron Transfer Reactions through Dendrimer Architecture" *J. Am. Chem. Soc.* **1996,** 118, (16), 3978-3979.

54. Ahn, T. S.; Nantalaksakul, A.; Dasari, R. R.; Al-Kaysi, R. O.; Muller, A. M.; Thayumanavan, S.; Bardeen, C. J., "Energy and Charge Transfer Dynamics in Fully Decorated Benzyl Ether Dendrimers and Their Disubstituted Analogues" *J. Phys. Chem. B* **2006,** 110, (48), 24331-24339.

55. Nantalaksakul, A.; Dasari, R. R.; Ahn, T. S.; Al-Kaysi, R.; Bardeen, C. J.; Thayumanavan, S., "Dendrimer Analogues of Linear Molecules to Evaluate Energy and Charge-transfer Properties" *Org. Lett.* **2006,** 8, (14), 2981-2984.

56. Cho, B. K.; Jain, A.; Gruner, S. M.; Wiesner, U., "Mesophase Structure-Mechanical and Ionic Transport Correlations in Extended Amphiphilic Dendrons" *Science* **2004,** 305, (5690), 1598-1601.

57. Lecommandoux, S.; Klok, H. A.; Sayar, M.; Stupp, S. I., "Synthesis and Self-organization of Rod-dendron and Dendron-rod-dendron Molecules" *J. Polym. Sci. Pol. Chem.* **2003,** 41, (22), 3501-3518.

58. Messmore, B. W.; Hulvat, J. F.; Sone, E. D.; Stupp, S. I., "Synthesis, Self-assembly, and Characterization of Supramolecular Polymers from Electroactive Dendron Rodcoil Molecules" *J. Am. Chem. Soc.* **2004,** 126, (44), 14452-14458.

59. Tian, L.; Hammond, P. T. "Comb-dendritic Block Copolymers as Tree-shaped Macromolecular Amphiphiles for Nanoparticle Self-assembly" *Chem. Mat.* **2006,** 18, (17), 3976-3984.

60. Zubarev, E. R.; Sone, E. D.; Stupp, S. I., "The Molecular Basis of Self-assembly of Dendron-rod-coils into One-dimensional Nanostructures" *Chem. Eur. J.* **2006,** 12, (28), 7313-7327.

61. Coessens, V.; Pintauer, T.; Matyjaszewski, K., "Functional Polymers by Atom Transfer Radical Polymerization" *Prog. Polym. Sci.* **2001,** 26, (3), 337-377.

62. Pintauer, T.; Matyjaszewski, K., "Atom Transfer Radical Addition and Polymerization Reactions Catalyzed by ppm Amounts of Copper Complexes" *Chem. Soc. Rev.* **2008,** 37, (6), 1087-1097.

63. Yamada, T.; Iida, K.; Yamago, S., "Living Radical Polymerization - Current Status and Future Perspective" *Kobunshi Ronbunshu* **2007,** 64, (6), 329-342.

64. Lee, K. C. B.; Siegel, J.; Webb, S. E. D.; Leveque-Fort, S.; Cole, M. J.; Jones, R.; Dowling, K.; Lever, M. J.; French, P. M. W., "Application of the Stretched Exponential Function to Fluorescence Lifetime Imaging" *Biophys. J.* **2001,** 81, (3), 1265-1274.

65. Phillips, J. C., "Stretched Exponential Relaxation in Molecular and Electronic Glasses" *Rep. Prog. Phys.* **1996,** 59, (9), 1133-1207.

66. Thomas, K. R. J.; Thompson, A. L.; Sivakumar, A. V.; Bardeen, C. J.; Thayumanavan, S., "Energy and Electron Transfer in Bifunctional Non-conjugated Dendrimers" *J. Am. Chem .Soc.* **2005,** 127, (1), 373-383.

CHAPTER 4

NON-CONJUGATED POLYMERS HAVING EDOT OLIGOMERS AS PENDANT GROUPS: DESIGN, SYNTHESIS AND PHOTOPHYSICAL PROPERTIES

4.1 Introduction

Photovoltaic cells are one of the promising approaches in seeking cheap and clean renewable energy sources.[1] Solar cells based on crystalline silicon are too expensive to find widespread use.[2] Therefore, the possibility of devices based on organic materials has generated a lot of interest.[3-5] Although there have been several interesting approaches to organic-based photovoltaics, the efficiencies remain too low to be practical.[6-10] Main reasons causing the low power conversion efficiencies in organic materials include mismatch between the absorption spectrum of chromophores and the solar spectrum, poor exciton dissociation and charge carrier recombination. In chapter 3, the molecular design that contains the donor/acceptor molecular heterojunction was discussed. This design could solve the problem associated with inefficient exciton dissociation in OPVs owing to a considerable increase in donor/acceptor interface. In this chapter, the other two remaining issues, viz., photon and charge carrier loss are addressed. Hypothesis, molecular design, synthesis and characterizations are discussed below.

4.2 Molecular design for charge transport units

In OPV devices, once charges are generated at heterojunctions, there needs to be an efficient charge transport (CT) material to transport these charges to the respective electrodes. Conjugated polymers such as polythiophene[11-12] and polyphenylene vinylene[13-15] are generally employed as charge transporters in OPV devices because of

their appreciable charge diffusion along the π-conjugated main chain. However, charge carrier mobilities are a function of both intrachain charge diffusion and interchain charge hopping. Processibility is a key issue in these conjugated polymers due to their inherently rigid main chain. To solve this problem, flexible alkyl side chains are normally installed onto these stiff conjugated polymers. Even though these side chains alleviate the solubility problem, they create another issue by increasing the interchain distance between conjugated backbones and thereby reducing the mobility in these materials (Figure 4.1a).

In order to obtain both processible and efficient interchain charge hopping materials, we have designed non-conjugated polymers with conductive side chains. We hypothesize that while the flexibility from non-conjugated main chains provides good solubility, the highly dense charge transport functionalities at side chains could facilitate interchain charge hopping and might result in the high mobility in these materials (Figure 4.1b). Moreover, since the overall efficiency of OPV devices is determined both by the charge transporting ability of the molecules used and by the relative frontier orbital energies of the charge transporters, it is also necessary that we have significant control over the band gaps of the CT polymers. The molecular design we propose here also allows the exact control over the energy levels of materials by tuning the conjugation

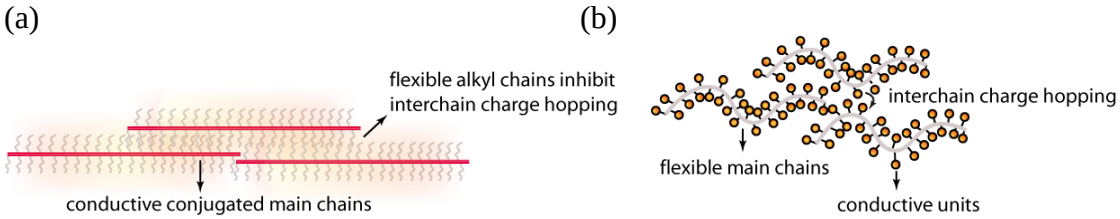

Figure 4.1. (a) Conjugated polymers with flexible side chains (b) Non-conjugated polymers with conductive units.

lengths of conductive side chains. Therefore, systematic tuning of these frontier energy levels to optimize the efficiency of OPV devices would also be possible.

Structures of target polymers are shown in Chart 4.1. Poly(3,4-ethylenedioxythiophene) (PEDOT) is a low band gap polymer that exhibits high charge mobility as well as good thermal and chemical stability.[16, 17] These properties are desirable for OPVs. Therefore, we selected EDOT units as our target for charge transporters. Phenyl groups are caped at the α positions of these EDOT units to eliminate the possibility of air oxidation at these positions, thus increasing the stability of these materials.[18] Polynorbornylene is chosen as a non-conjugated backbone due to the ease in preparation *via* ring-opening polymerization (ROMP).[19] Moreover, this polymerization technique also gives polymers with a great control over MW and PDI.[20, 21]

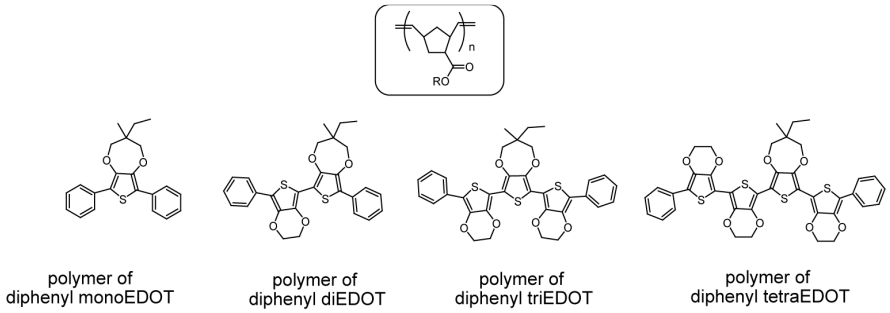

Chart 4.1. Structures of non conjugated polymers with conductive side chains.

4.2.1 Results and discussion

4.2.1.1 Monomer synthesis

The key synthetic methodologies for these EDOT derivatives are bromination using NBS as a reagent and Pd-catalyzed Stille coupling. Hydroxy functionalized ProDOT (**4-1**) were brominated using an excess amount of NBS to obtain dibromo ProDOT (**4-2**) with quantitative yield. Treatment this dibromoProDOT (**4-2**) with phenyl

boronic acid in the presence of $Pd(PPh_3)_4$ as a catalyst gave diphenyl monoEDOT derivative (**4-3**) with 61% yield. Reacting **4-3** with 5-exo norbonene-2-carboxylic acid in the presence of DCC/DMAP gives norbornenyl-based monomer having monoEDOT functionality (**4-4**) with quantitative yield (Scheme 4.1).

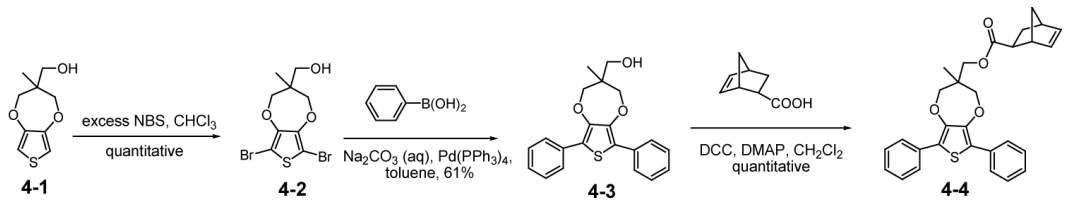

Scheme 4.1. The synthesis of monoEDOT monomer.

To synthesize monomer of diEDOT oligomers, a partial bromination of ProDOT **4-1** with 1 equivalent of NBS was performed. The monobrominated product **4-5** was obtained with 32% yield. Compound **4-5** was then subjected to a Suzuki coupling with phenyl boronic acid to give compound **4-6** with 17% yield. The bromination of **4-6** with NBS gave **4-7** with 39% yield. The Stille coupling of bromo functionlized **4-7** with compound **4-8** containing tributyl tin functionality afforded compound **4-9** with 51% yield. Treatment of this hydroxyl functionalized diEDOT **4-9** with 5-exo norbornene-2-

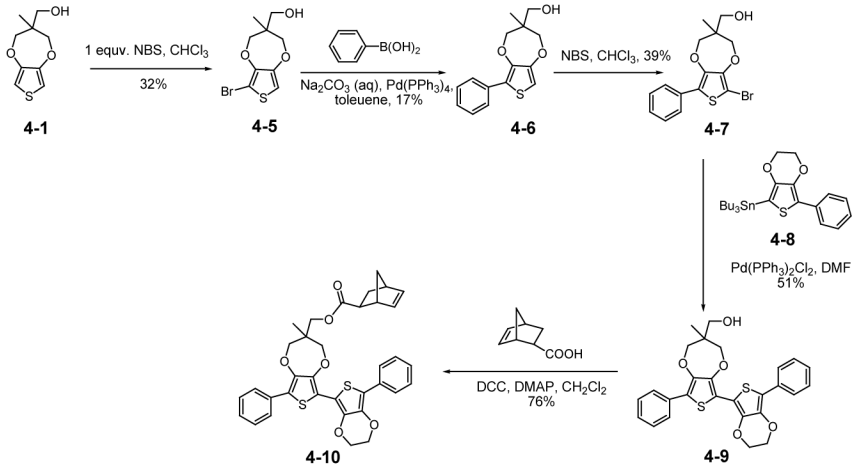

Scheme 4.2. Synthesis of diEDOT monomer.

carboxylic acid in the presence of DCC/DMAP gave a desired monomer of diEDOT unit (**4-10**) with 76% yield (Scheme 4.2).

A triEDOT monomer was synthesized by Stille coupling and bromination. DibromoProDOT **4-2** was treated with 2 equivalents of EDOT functionalized tributyl tin group (**4-8**) in the presence of $Pd(PPh_3)_2Cl_2$ to afford a triEDOT oligomer having hydroxyl functionality (**4-11**) with 17% yield. Treatment of **4-11** with 5-exo norbonene-2-carboxylic acid in the presence of DCC/DMAP as reagents gave a triEDOT monomer with quantitative yield (Scheme 4.3).

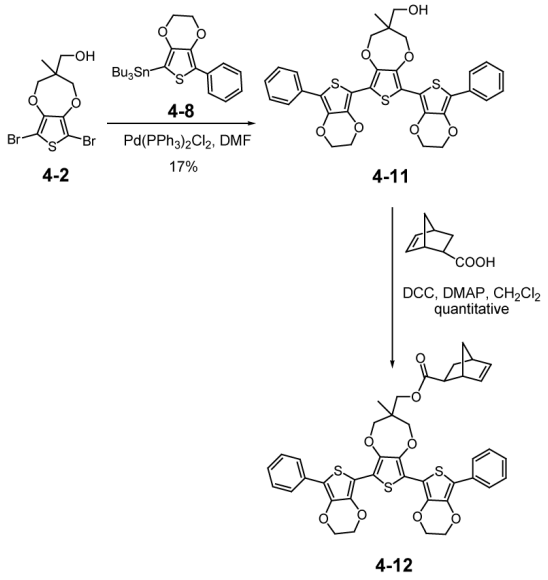

Scheme 4.3. Synthesis of triEDOT monomer.

A tetraEDOT oligomer was synthesized in a similar manner. Monobromo-ProDOT **4-5** was reacted with tributyl tin functionalized EDOT **4-13** under Stille coupling condition to give compound **4-14** with 85% yield. Bromination reaction of compound **4-14** using NBS as a reagent afforded compound **4-15** with 74% yield. Compound **4-15** was then subjected to a Stille coupling reaction with compound **4-8** having tribuyl tin functionality to give tetraEDOT **4-16** with 11% yield. The desired tetraEDOT monomer **4-17** was obtained by reacting compound **4-16** with 5-exo

norbornene-2-carboxylic acid in the presence of DCC/DMAP. The product was obtained with 69% yield (Scheme 4.4).

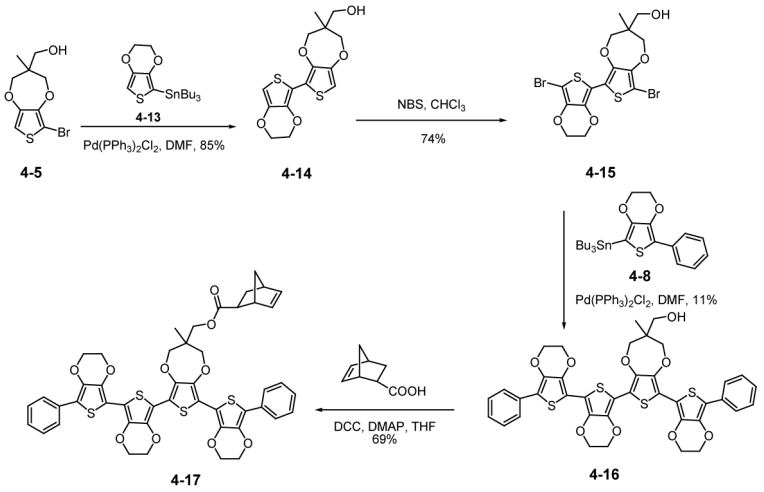

Scheme 4.4. Synthesis of tetraEDOT monomer.

4.2.1.2 Ring Opening Metathesis Polymerization (ROMP)

All monomers were subjected to ROMP by using 3rd generation Grubbs catalyst. Monomer and catalyst were placed in separate vials under inert atmosphere. Dry THF was subjected to three freeze-pump-thaw cycles before adding into monomer and catalyst. A solution of monomer was then added into a solution of catalyst and the polymerization was readily performed in 3 minutes. Then, the polymerization was terminated by the addition of ethyl vinyl ether. The solution was precipitated twice in methanol to obtain the desired polymers. Scheme 4.5 shows structures of the polymers and Table 4.2 shows the molecular weights and PDIs obtained from the polymerization.

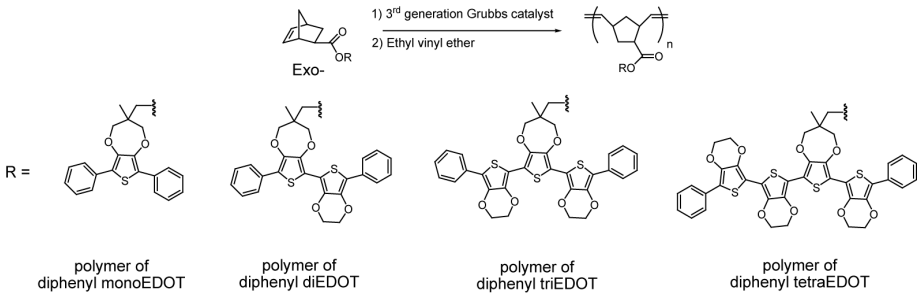

Scheme 4.5. ROMP of monomers investigated.

Table 4.1. Molecular weights (Mn) and PDI of polymers obtained by GPC (THF).

Side Chains	Mn *(g/mol)	PDI
monoEDOT	16862	1.05
diEDOT	17679	1.36
triEDOT	9975	1.09
tetraEDOT	16802	1.12

*Mn is estinated using PMMA standards

4.2.1.3 Optical properties of non-conjugated polymers containing EDOT oligomers

Figure 4.2 shows the absorption spectra of all EDOT monomers and their corresponding polymers in dichloromethane. The absorption maximum of monomers and their polymer counterparts are virtually similar implying that norbornene based main chains do not interrupt the electronic property of EDOT functionalities. Moreover, the λ_{max} shifts toward longer wavelengths with increasing conjugation lengths. This implies that increasing conjugation lengths in these chromophores results in the reduction in the band gaps.

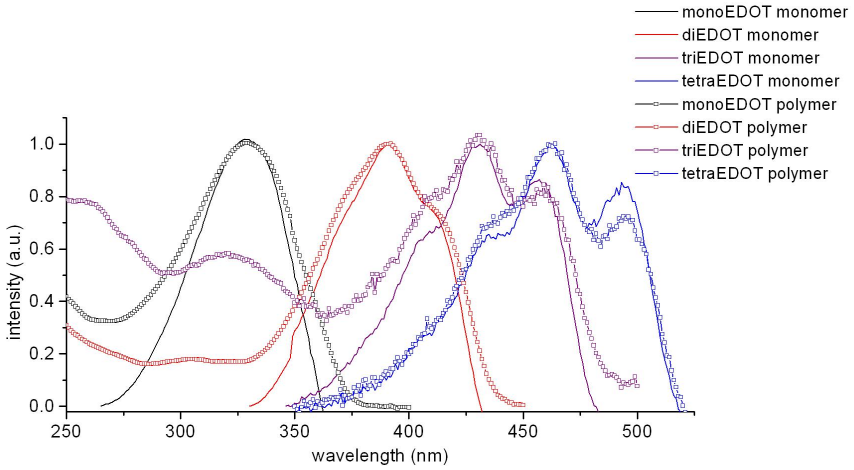

Figure 4.2. The comparison of absorption spectra of monomers and their corresponding polymers.

4.2.1.4 HOMO-LUMO energy levels

Energy levels of all chromophores are calculated by using the combination of information obtained from the absorption spectra and the cyclic voltammetry, as

mentioned in the previous chapter. Relative energy levels calculated by this method are showed in Figure 4.3. It is clearly shown here that the energy levels of oligomers of EDOT derivatives can be systematically tuned by placing these units at side chains of polymers.

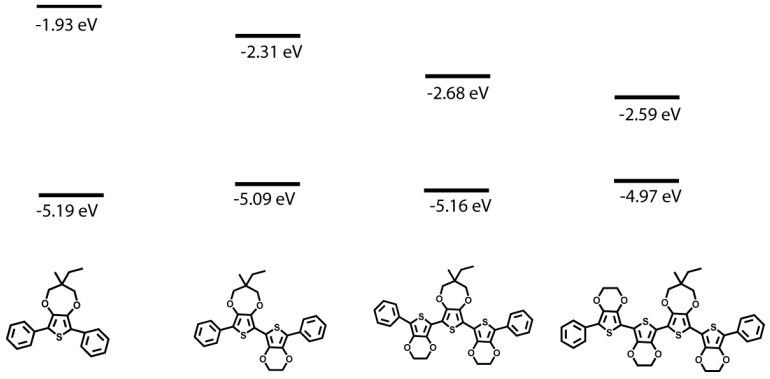

Figure 4.3. Relative energy levels of polymers containing EDOT oligomers with different conjugation lengths.

Note that, in our system, the increasing conjugation lengths seem to affect more on the LUMO energy level than the HOMO energy levels. One of the measure of the efficiency of OPV devices is open circuit voltage (V_{oc}). This parameter can be calculated from the difference between the LUMO of the acceptor and the HOMO of the donor.[22] Since the HOMO of all these polymeric donors remains similar and these molecules are likely to act as hole transporters, the increase in conjugation length should not significantly reduce the V_{oc}. Moreover, the ability to harvest solar energy increases with reducing of band gaps due to the better overlap to the solar spectrum. Therefore, nonconjugated polymers containing oligoEDOT with decent conjugation lengths are promising materials to enhance light absorption efficiency, charge transport efficiency as well as to maintain the high V_{oc}.

4.2.1.5 Aggregation behavior

The emission spectra of monomers and their corresponding polymers are shown in Figure 4.4. It was observed that the emission maxima of polymers are slightly bathochromically shifted compared to their monomers with retained well-defined structures (Figure 4.4). The red-shifting of emission signals in polymers suggests that oligomers of EDOT units at the side chains of polymers slightly aggregate. The degree of aggregation seems to increase with increasing EDOT conjugation lengths. The aggregation of conjugated polymers is well-known and it leads to the higher ability to harvest solar energy in these materials due to the better overlapping with the solar spectrum. In our case, we anticipate that further increase in conjugation lengths of EDOT

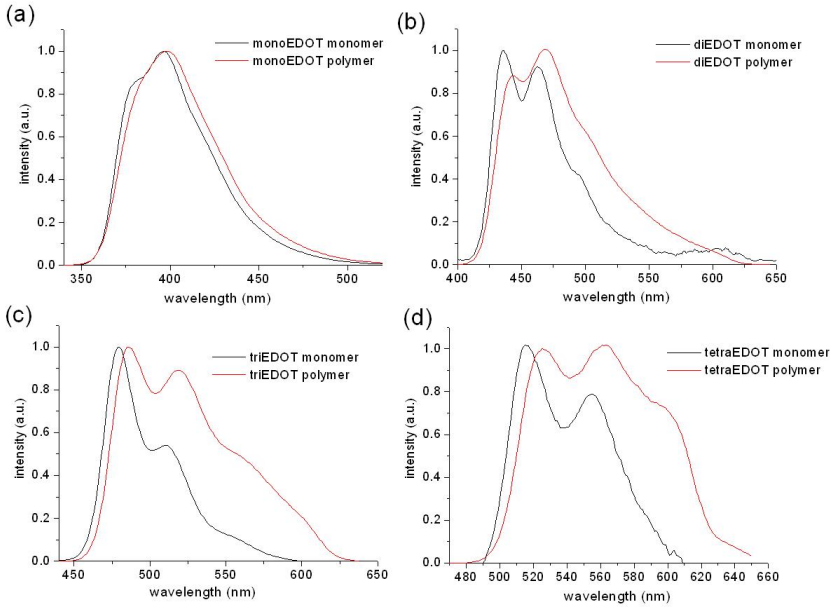

Figure 4.4. Emission spectra of (a) monoEDOT (b) diEDOT (c) triEDOT and (d) tetraEDOT monomers and their polymeric counterparts.

oligomers should lead to the higher degree of side chain aggregation. However, our efforts to extend the conjugation lengths of EDOT oligomers failed due to the instability

of EDOT intermediates. Moreover, we observed that tretraEDOT polymer is soluble in a limited number of solvents. Therefore, it is reasonable to assume that the solubility of polymers will become an issue, if conductive units with longer conjugation lengths are attached onto non-conjugated main chains. In the next section, we propose an alternative method to broaden the absorption spectra of these polymers for more effective utilization of solar light.

4.3 Molecular design for optimizing photon absorption

While EDOT oligomers installed at side chains of polymers might allow rapid interchain charge transport as well as control over the frontier energy levels of these materials, it possesses the short conjugation lengths relative to polymers thus limiting the amount of photon absorbed by these compounds. The problem of poor solar absorption in organic materials is realized even in conjugated polymers. Most of the conjugated polymers absorb in the ultraviolet (UV) and the green part of the visible spectral region. Therefore, photons that are located in low energy part and that are indeed more intense have very little contribution to the photocurrent of OPV devices made from these materials. An effort to obtain materials with better spectral matching with solar radiation has been dedicated through targeting and synthesizing low band gap polymers.[23-25] The absorption spectra of these low band gap polymers show absorption peaks at a longer wavelength suggesting more efficient utilization of photon in these polymers. However, the shorter wavelength sunlight (such as 380-500 nm) is not absorbed by these materials if the bandwidth of their absorption is not sufficiently broad. Obviously, conjugated polymers possessing not only narrow band gap, but also broad bandwidth in the visible region are desirable for application in photovoltaics.

With this in mind, our aim here is to obtain materials with broad spectral bandwidth. The strategy we exploit here is to install crosslinkable and non-crosslinkable conducting units at side chains of polymer. The absorption of polymer before side chain modification should lie in the short wavelength region due to the short conjugation lengths of conducting units. Crosslinking at side chains shifts the absorption of the crosslinkable group into the long wavelength region while non-crosslinkable side groups still remain their absorption in short wavelength region. As a result, the absorption of the polymers after crosslinking should be broad due to a combination of the absorption from non-crosslinkable unit in the short wavelength region and from crosslinked polymer in the long wavelength region. This hypothesis is illustrated in Figure 4.5.

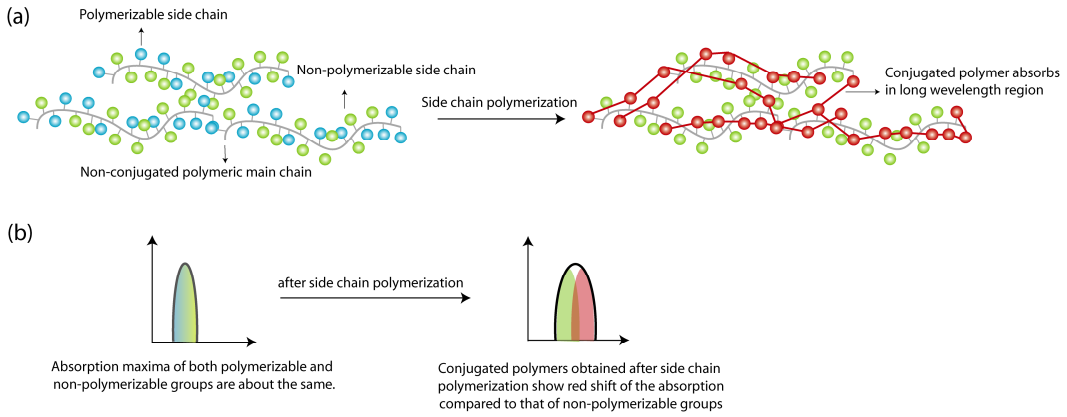

Figure 4.5. (a) Cartoon shows the polymers having polymerizable side chain before and after side chain polymerization. (b) Cartoon illustrated absorption spectral change of polymers before and after side chain polymerization.

Owing to their low oxidation potential, EDOT units can undergo oxidative polymerization at free α-positions.[26] With this, we designed non-conjugated polymers containing crosslinkable and non-crosslinkable EDOT oligomers. Phenyl groups are installed at α-positions of EDOT oligomers to obstruct the polymerization at these positions. These phenyl-capped EDOT oligomers are, therefore, used as non-

polymerizable units. The EDOT oligomers with free α-positions are used as crosslinkable units and are expected to form PEDOT after side chain polymerization. Among all EDOT oligomers we have hands-on experience in synthesizing, mono and triEDOT are relatively easy to make. However, the oxidation potential of triEDOT is lower than that of monoEDOT. Therefore, triEDOT oligomers were chosen as our target for this study. The structure of a target copolymer is shown in Figure 4.6.

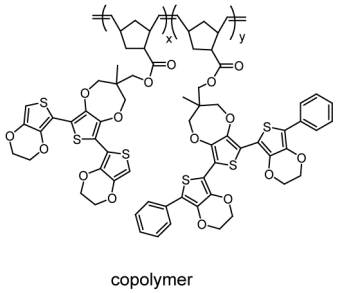

Figure 4.6. A structure of a target polymer.

4.3.1 Results and discussion

4.3.1.1 Monomer Synthesis

Norbornene functionalized triEDOT monomer (**4-19**) was synthesized by using a similar procedure with its phenyl capped monomer counterpart (**4-12**). DibromoProDOT (**4-2**) was reacted with tributyltin functionalized EDOT derivative under Pd-catalyzed Stille coupling condition to obtain triEDOT containing hydroxyl functionality (**4-18**) with 53% yield. This compound was reacted with 5-exo-norbornene-2-carboxylic acid to give

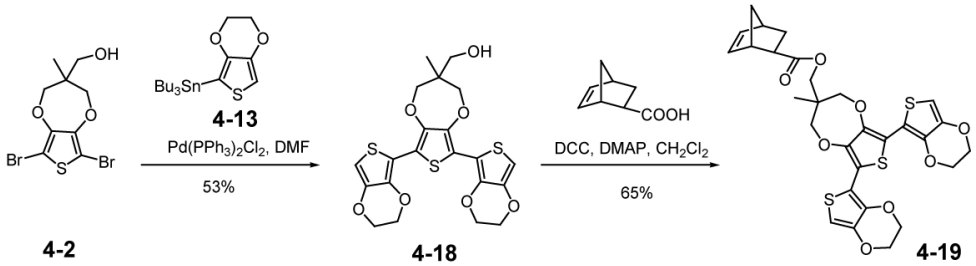

Scheme 4.6. Synthesis of triEDOT monomer with α positions for side chain polymerization.

a desired monomer **4-19** with 65% yield (Scheme 4.6). The synthesis of phenyl-capped triEDOT monomer (**4-12**) has already mentioned in the previous section.

4.3.1.2 Ring Opening Metathesis Polymerization (ROMP) of diphenyl triEDOT and triEDOT homopolymers

Polymerization of non-crosslinkable and crosslinkable EDOT oligomers is shown in Scheme 4.7. To synthesize homopolymers of non crosslinkable triEDOT unit, 40 equivalent monomer **4-12** and one equivalent of 3rd generation Grubbs catalyst were placed into a small vial under inert atmosphere. Dry THF was subjected to three freeze-pump-thaw cycles before adding monomer and catalyst. A solution of monomer was then added into a solution of catalyst and the polymerization was readily performed in 3 minutes. Then, the polymerization was terminated by the addition of ethyl vinyl ether. The solution was precipitated twice in methanol to obtain desired polymers with Mn of 9975 and PDI of 1.10. The synthesis of homopolymer of crosslinkable triEDOT unit using monomer **4-19** was performed under similar condition. The polymer was obtained with Mn of 12775 and PDI of 1.04.

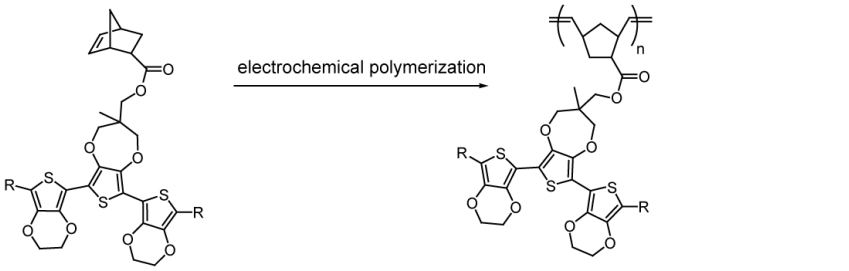

4-12 R = Ph — **homopolymer of diphenyltriEDOT** R = Ph Mn = 9975, PDI = 1.10

4-19 R = H — **homopolymer of triEDOT** R = H Mn = 12775, PDI = 1.04

Scheme 4.7. Polymerization of monomer **4-12** and **4-19**.

4.3.1.3 Spectroelectrochemistry of homopolymer containing triEDOT and diphenyltriEDOT side groups

To test whether free α positions in triEDOT side groups of capped and uncapped norbonylene polymers can undergo oxidative polymerization resulting in crosslinking PEDOT, we performed spectroelectrochemistry of both triEDOT and diphenyl triEDOT homopolymer and the results are compared. We first tested that homopolymer of triEDOT can undergo electrochemical polymerization as shown in Scheme 4.8. In this experiment, the solution of homopolymer of triEDOT in dichlromethane was coated onto an ITO coated glass and spectroelectrochemistry was carriered out. Figure 4.7 shows optoelectrochemistry of crosslinkable homopolymer of triEDOT in 0.1 M TBAP/ACN. Homopolymer of triEDOT showed the absorption signal at 345-430 nm. At oxidation potential of 0.8 V, the absorption signal at 345-430 nm disappears and no other signal could be observed in the region of 300-900 nm. When reduction potential of -0.8 V is applied, the broad signal at 350-680 nm emerges. The disappearance and reappearance of this broad signal can be manipulated by switching the potential between 0.8 and -0.8 V. The original absorption signal at 345-430 nm, however, can not be regained. It can be deduced from this result that upon applying a positive potential, triEDOT side groups are

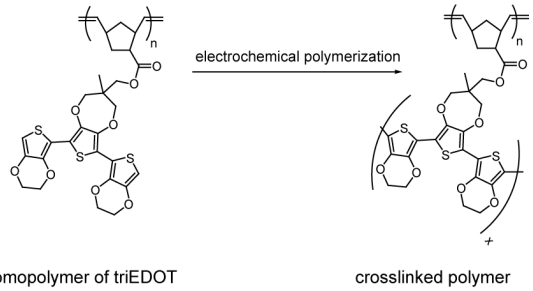

Scheme 4.8. Crosslinking at triEDOT side chains of norbornenyl polymer.

oxidatively polymerized generating polarons and bipolarons. The reduction of these bipolarons generates neutral crosslinked EDOT polymers, which exhibit a red shifted

absorption compared to its original polymer. The reversible generation of bipolarons from this neutral polymer can be obtained by controlling applied potentials.

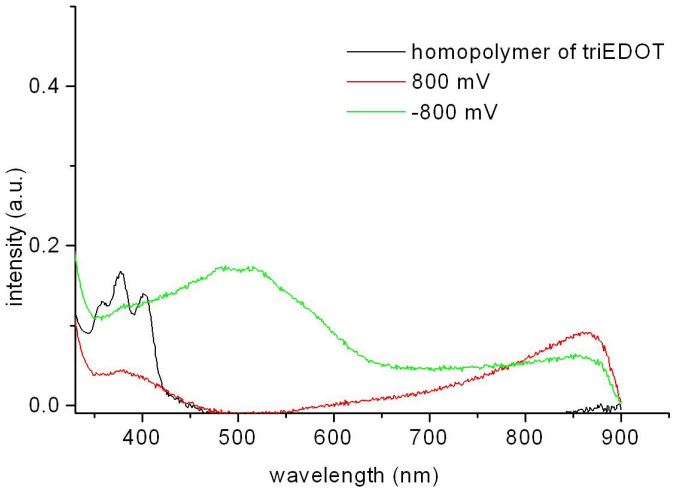

Figure 4.7. Spectroelectrochemistry of homopolymer of triEDOT.

Next, we investigated whether the homopolymer of diphenyl triEDOT, where both α positions of triEDOT units are blocked with a phenyl group exhibits the same behavior. To test this, homopolymer of diphenyl triEDOT was dissolved in dichloromethane and coated onto an ITO-coated glass and spectroelectrochemistry was performed under the same conditions as above. It was observed that homopolymer of diphenyl triEDOT showed the absorption signal at 350-500 nm, slightly red-shifted compared to triEDOT homopolymer owing to the longer conjugation length. Upon appling the potential at 0.8 V, the original absorption signal disappears in accordance with the emergence of the new signal at 500-700 nm. The reductive potential at -0.8 V causes the reappearance of the original signal at 350-500 nm. As expected, phenyl groups of triEDOT units prohibit the oxidative cross-linking at α positions. The signal at 500-700 nm upon oxidation results from the generation of radical cations of diphenyl

triEDOT moieties which can be reduced back to its original state upon applying the negative potential.

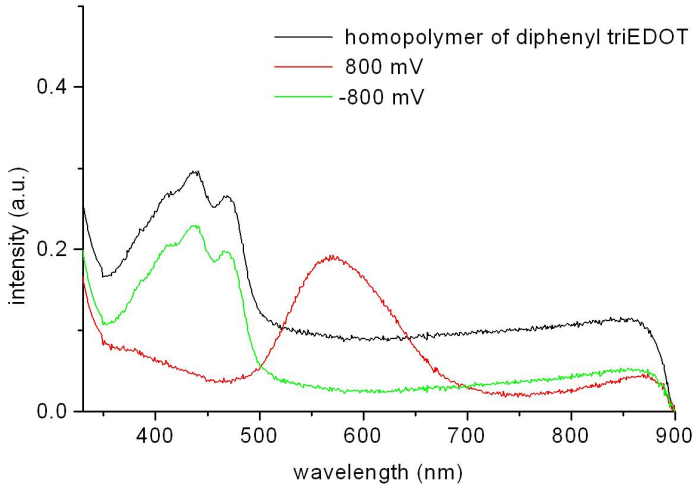

Figure 4.8. Spectroelectrochemistry behavior of polymer diphenyl triEDOT homopolymer**.**

4.3.1.4 Chemically oxidative polymerization of homopolymer of triEDOT

Cross-linking of homopolymer of triEDOT can also be performed chemically. Homopolymer of triEDOT in dichloromethane was spun coat onto the glass substrate. TriEDOT homopolymer shows the absorption signal at 320-430 nm, similar to what is observed earlier. Oxidative polymerization of triEDOT side chain underwent by dipping the thin film into $FeCl_3$ in acetonitrile. Again, the oxidized film shows no absorption signal in the region of 300-900 nm due to the generation of the bipolarons. The reduction of oxidative cross-linking polymer can be obtained by subsequent dipping of the film into the hydrazine solution in acetonitrile. This causes the emergence of the red shift signal relative to the original peak indicative of the generation of crosslinked polymers at side

chains of norbornylene backbone. These behaviors are similar to those observed eariler in the electrochemical cross-linking method (Figure 4.9).

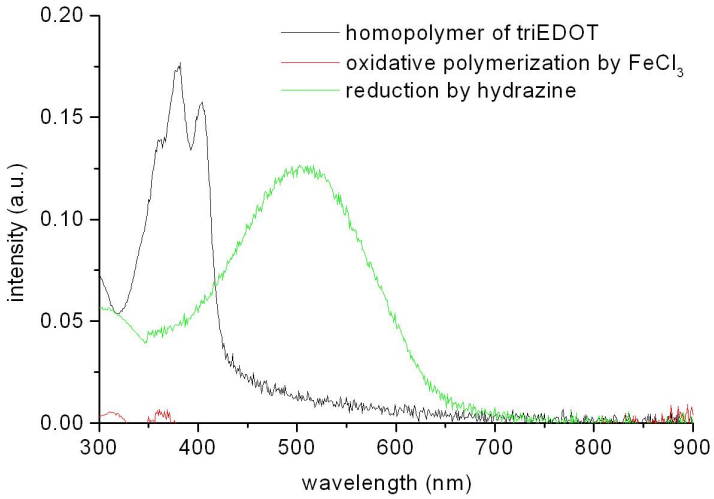

Figure 4.9. Chemical polymerization of triEDOT homopolymer.

4.3.1.5 Broadening the absorption spectra of copolymers by chemical cross-linking of triEDOT units

So far, we have already shown that α positions of triEDOT groups are active for further polymerizations and that blocking these positions inhibits the side chain polymerization. In order to achieve polymers with broad absorption spectra, monomer **4-19** and monomer **4-12** were mixed in 1:3, 1:1 and 3:1 ratio and polymerization was performed under the same conditions as the homopolymers. Scheme 4.9 shows the structure of the copolymer and Table 4.2 shows the Mn along with PDI of random copolymers with various ratio of crosslinker (monomer **4-19**).

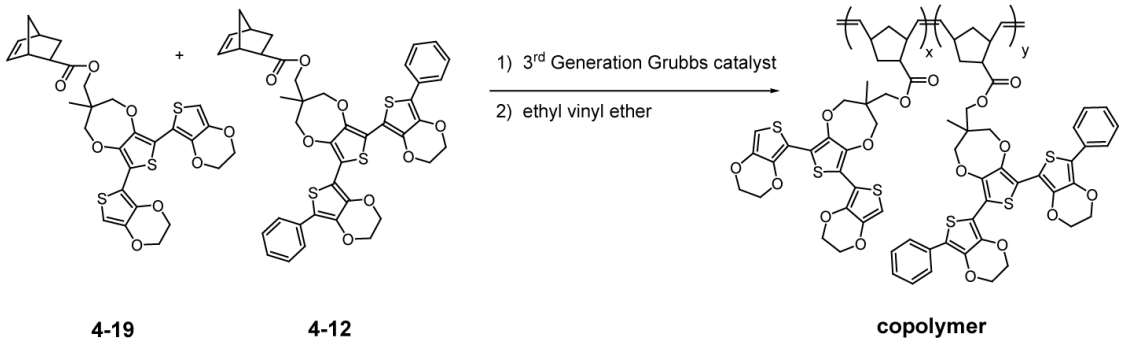

4-19 4-12 copolymer

Scheme 4.9. Copolymerization of monomer **4-20** and **4-12**.

Table 4.2. Molecular weight (Mn) and PDI of copolymer with various ratio of crosslinker

Monomer**4-19**: **4-12**	%crosslinker	Monomer:Catalyst	Mn* (g/mol)	PDI
1:3	25%	100:1	16801	1.10
1:1	50%	100:1	23532	1.08
3:1	75%	100:1	16795	1.06

*PMMA was used as a standard

Copolymers with different ratio of crosslinkers were spun coat on a glass slide. Chemical cross-linking of these copolymers on solid state was carried out using $FeCl_3$ as an oxidant. The color of all thin films changed from their original yellow color to blue color indicating the cross-linking of these copolymers. The film was washed with acetonitrile to remove $FeCl_3$ before it was dipped into hydrazine in acetonitrile to reduce the oxidized crosslinked PEDOT film. The film color changed from blue to brown in accordance with the change in the absorption spectra. The schematic representation of side chain crosslinking of copolymers and the absorption spectra of these crosslinked copolymers are shown in Scheme 4.10 and Figure 4.10, respectively.

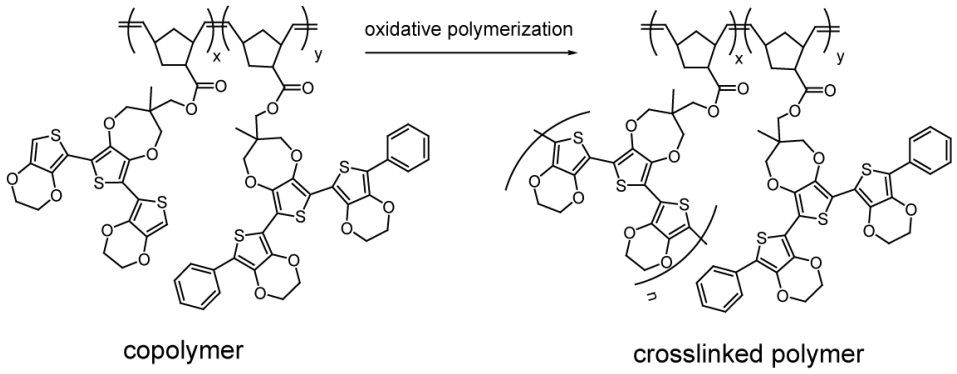

Scheme 4.10. Crosslinking of copolymer at triEDOT side chains.

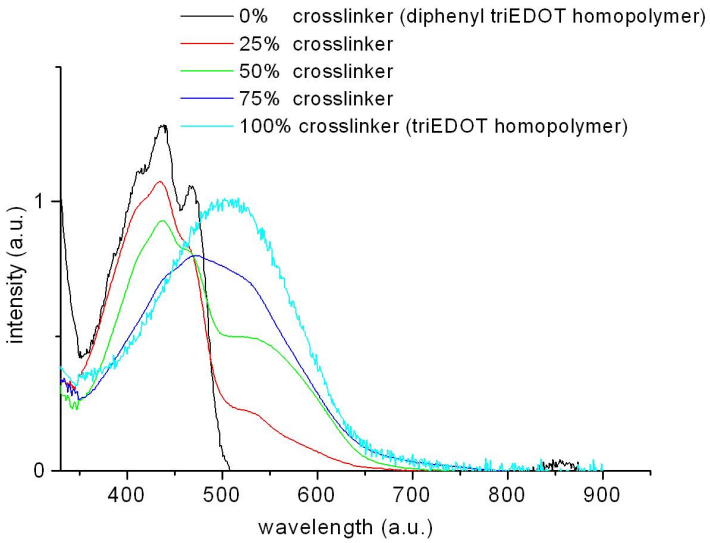

Figure 4.10. Absorption of copolymers with different extent of triEDOT crosslinker.

The homopolymer containing diphenyl triEDOT unit at side chains shows the absorption maxima at 440 nm which is not sensitive to the chemical treatment as explained in the last section. Moreover, crosslinking of triEDOT units at side chains of non-conjugated polymers resulted in the red-shifting of the absorption peak to 513 nm. As expected, the absorption of copolymers with different ratio of crosslinker combined the absorption characteristics of polymer with diphenyl triEDOT group in a short wavelength region and of polymer with crosslinked EDOT group in a long wavelength

region. As a result, the absorption spectra of crosslinked copolymers are very broad and cover a wide range of the visible region. Moreover, the shape of these absorption spectra can be simply tuned by changing the ratio of two monomers.

We also observed that the solubility of the copolymers and their crosslinked polymer counterparts is very different. While copolymers are easily soluble in many common organic solvents, their corresponding crosslinked polymers become insoluble. This may find applications in devices fabricated by layer-by-layer deposition. The solubility of copolymers allows these materials to be easily deposited onto a substrate. Crosslinking at side chains of these polymers completely changes their solubility and thus allows the deposition of another layer by using a simple conventional wet method.

4.4 Summary

In summary, we have demonstrated methodologies that could address the charge carrier loss and photon loss issues in OPVs. By installing conductive units at side chains of non-conjugated polymers, we observed that (*i*) the polymers are soluble in common organic solvents. Processibility of conductive polymers is necessary when these materials are used in the device fabrication. (*ii*) the frontier energy level can be tuned by controlling the conjugation lengths of conductive side chains and (*iii*) the absorption spectra of these polymers can be broadened by incorporating crosslinkable moieties as co-side chains. Mobility measurement and PV performance of these materials are underway.

4.5 References

1. Lewis, N. S.; Nocera, D. G., "Powering the Planet: Chemical Challenges in Solar Energy Utilization" *Proc. Natl. Acad. Sci. U. S. A.* **2006,** 103, (43), 15729-15735.

2. Gregg, B. A., "Excitonic Solar Cells" *J. Phys. Chem. B* **2003,** 107, (20), 4688-4698.

3. Forrest, S. R., "The Path to Ubiquitous and Low-cost Organic Electronic Appliances on Plastic" *Nature* **2004,** 428, (6986), 911-918.

4. Milliron, D. J.; Gur, I.; Alivisatos, A. P., "Hybrid Organic-Nanocrystal Solar Cells" *MRS Bull.* **2005,** 30, (1), 41-44.

5. Spanggaard, H.; Krebs, F. C., "A Brief History of the Development of Organic and Polymeric Photovoltaics" *Sol. Energy Mat. & Sol. Cells* **2004,** 83, (2-3), 125-146.

6. Brabec, C. J.; Durrant, J. R., "Solution-processed Organic Solar Cells" *MRS Bull.* **2008,** 33, (7), 670-675.

7. Currie, M. J.; Mapel, J. K.; Heidel, T. D.; Goffri, S.; Baldo, M. A., "High-Efficiency Organic Solar Concentrators for Photovoltaics" *Science* **2008,** 321, (5886), 226-228.

8. Nelson, J., "Organic Photovoltaic Films" *Curr. Opin. Solid State Mat. Sci.* **2002,** 6, (1), 87-95.

9. Nunzi, J. M., "Organic Photovoltaic Materials and Devices" *C. R. Phys.* **2002,** 3, (4), 523-542.

10. Yourre, T. A.; Rudaya, L. I.; Klimova, N. V.; Shamanin, V. V., "Organic Materials for Photovoltaic and Light-emitting Devices" *Semiconductors* **2003,** 37, (7), 807-815.

11. Berson, S.; De Bettignies, R.; Bailly, S.; Guillerez, S., "Poly (3-hexylthiophene) Fibers for Photovoltaic Applications" *Adv. Funct. Mater.* **2007,** 17, (8), 1377-1384.

12. Mayer, A. C.; Scully, S. R.; Hardin, B. E.; Rowell, M. W.; McGehee, M. D., "Polymer-based Solar Cells" *Mater. Today* **2007,** 10, (11), 28-33.

13. Moet, D. J. D.; Koster, L. J. A.; de Boer, B.; Blom, P. W. M., "Hybrid Polymer Solar Cells from Highly Reactive Diethylzinc: MDMO-PPV versus P3HT" *Chem. Mat.* **2007,** 19, (24), 5856-5861.

14. Offermans, T.; Meskers, S. C. J.; Janssen, R. A. J., "Photoinduced Absorption Spectroscopy on MDMO-PPV:PCBM Solar Cells under Operation" *Org. Electron.* **2007,** 8, (4), 325-335.

15. Shen, P.; Sang, G. Y.; Lu, J. J.; Zhao, B.; Wan, M. X.; Zou, Y. P.; Li, Y. F.; Tan, S. T., "Effect of 3D pi-pi Stacking on Photovoltaic and Electroluminescent Properties in Triphenylamine-containing Poly(p-phenylenevinylene) Derivatives" *Macromolecules* **2008,** 41, (15), 5716-5722.

16. Ha, Y. H.; Nikolov, N.; Pollack, S. K.; Mastrangelo, J.; Martin, B. D.; Shashidhar, R., "Towards a Transparent, Highly Conductive Poly(3,4-ethylenedioxythiophene)" *Adv. Funct. Mater.* **2004,** 14, (6), 615-622.

17. Roncali, J.; Blanchard, P.; Frere, P., "3,4-Ethylenedioxythiophene (EDOT) as a Versatile Building Block for Advanced Functional p-Conjugated Systems" *J. Mater. Chem.* **2005,** 15, (16), 1589-1610.

18. Turbiez, M.; Frere, P.; Roncali, J., "Stable and Soluble Oligo(3,4-Ethylenedioxythiophene)s End-capped with Alkyl chains" *J. Org. Chem.* **2003,** 68, (13), 5357-5360.

19. Jang, S. Y.; Sotzing, G. A.; Marquez, M., "Intrinsically Conducting Polymer Networks of Poly(thiophene) via Solid-state Oxidative Cross-linking of a Poly(norbornylene) Containing Terthiophene Moieties" *Macromolecules* **2002,** 35, (19), 7293-7300.

20. Bielawski, C. W.; Grubbs, R. H., "Living Ring-opening Metathesis Polymerization" *Prog. Polym. Sci.* **2007,** 32, (1), 1-29.

21. Feast, W. J., "Applications of Romp in the Synthesis of New Materials" *Makromolekulare Chemie-Macromolecular Symposia* **1992,** 53, 317-326.

22. Mihailetchi, V. D.; Blom, P. W. M.; Hummelen, J. C.; Rispens, M. T., "Cathode Dependence of the Open-circuit Voltage of Polymer : Fullerene Bulk Heterojunction Solar Cells" *J. Appl. Phys.* **2003,** 94, (10), 6849-6854.

23. Bundgaard, E.; Krebs, F. C., "Low Band Gap Polymers for Organic Photovoltaics" *Sol. Energy Mat. & Sol. Cells* **2007,** 91, (11), 954-985.

24. Perzon, E.; Zhang, F. L.; Andersson, M.; Mammo, W.; Inganas, O.; Andersson, M. R., "A Conjugated Polymer for Near Infrared Optoelectronic Applications" *Adv. Mater.* **2007,** 19, (20), 3308-3311.

25. Winder, C.; Sariciftci, N. S., "Low Bandgap Polymers for Photon Harvesting in Bulk Heterojunction Solar Cells" *J. Mater. Chem.* **2004,** 14, (7), 1077-1086.

26. Bolognesi, A.; DiGianvincenzo, P.; Giovanella, U.; Mendichi, R.; Schieroni, A. G., "Polystyrene Functionalized with EDOT Oligomers" *Eur. Polym. J.* **2008,** 44, (3), 793-800.

CHAPTER 5

SUMMARY AND FUTURE SCOPE

Macromolecules such as dendrimers, dendrimer-linear polymer hybrids and polymers have been designed and synthesized and their photophysical properties have been investigated. While photoinduced charge separation studies of dendrimers in solution provide insights into the structure-property relationship of these materials at a molecular level, bulk property studies of polymers in solid state lead to an understanding of the working principle of PV devices. Our studies are focused on bridging these two areas.

In order to understand the architectural advantages of dendrimers toward energy and electron transfer processes, we designed and synthesized so-called difunctionalized dendrimers; dendrimers that contain two functionalities at their peripheries. Having the same number of chromophores and A-D distance with their corresponding linear analogs, the photophysical property comparison of these two species unveils the role of dendritic structures toward energy and electron transfer processes. Moreover, the comparison of these difunctionalized dendrimers with traditional dendrimers fully decorated with peripheral donors also provides the useful information on the role of the high density of peripheral functionalities toward these two processes. We observed that the dendritic architectures adversely affect the energy transfer due to the sterically hindered dendritic branches, which prohibit the approach of the peripheral donors to the core acceptor. However, the presence of multiple donors in traditional dendrimers enhances the energy transfer efficiency by allowing an alternative energy shuttling pathway. Since the efficiency of the energy transfer is dependent not only on the A/D distance, but also on

the relative orientation of donors and acceptors, the energy shuttling process would allow the energy to sample around the peripheral chromophores until it finds the chromophore that is situated in the right orientation relative to the acceptor resulting in an enhanced energy transfer efficiency. For electron transfer, the presence of multiple donors at the periphery of dendrimers is obviously beneficial to this process. Due to the flexibility of the dendritic arms, the possibility that one of these donors become adjacent to the core enhances the efficiency of electron transfer.

In order to find applications for these materials in practical devices, processibility is a concern. Dendron-rod-coils were designed to address this issue. Dendron-rod-coil structures would provide a phase segregation between the dendritic and polymeric parts which might lead to an interesting nanomorphology. This nanophase segregation might lead to an efficient charge transport to electrodes, which is a key factor in realizing high efficiency solar cells. The morphological studies of this class of compounds are underway. We are also interested in fabricating PV devices using these materials to investigate the effect of nanophase separation on the device efficiency. Moreover, since these molecules contain both donor and acceptor moieties, it might also be interesting to study their bipolar charge transport behaviors.

Apart from the bulk property studies which will be pursued in the near future, we have shown here that, architecturally, these dendron-rod-coils had provided some interesting photoinduced charge separation behaviors. We have observed that the efficiency of the electron transfer in these molecules is higher than that of dendrimers, which were previously investigated in our lab.[1] We hypothesized that the exposed nature of the rod part in these compounds would be responsible for efficient electron transfer

because of the better stabilization of this moiety by the surrounding solvent molecules. We also observed that architecturally, dendrons would assist better in intramolecular electron transfer than the polymers. Furthermore, we have demonstrated a method to solve the photon loss issue encountered in OPV devices. In this regard, polymers with wide range of absorption were introduced. Norbornene-based copolymers containing non-crosslinkable and crosslinkable EDOT units at side chains were synthesized. Oxidative polymerization of crosslinkable EDOT side chains would provide conjugated polymers that absorb in the long wavelength region while non-crosslinkable EDOT side chains retain their absorption in the short wavelength region. These materials are also promising to be employed in a device fabrication. One of the main problems in fabricating devices using organic materials is their solubility in similar solvents. This prohibits a consecutive deposition of donor materials followed by the acceptor, as the deposition of the second layer might end up destroying the previously-coated layer. The strategy to solve this problem is to chemically modify one of the compounds to have different solubility characteristics. This is possible, but chemical modification might sometimes be difficult. Our polymers could provide the answer for this issue. Unlike their parent polymer precursors, the crosslinked polymers become insoluble in any solvent. This allows a convenient coating of the second material by using a conventional wet method. Figure 5.1 illustrates the possible way to fabricate an ordered bulk heterojunction device, an ideal PV device, using these materials. The copolymer having crosslinkable and non-crosslinkable EDOT side chains will be coated onto the porous membrane. Then, the modified membrane will be dipped into an oxidizing agent to polymerize active EDOT side chains. Then, the membrane template will be removed

leaving behind the porous insoluble polymer donors, which will be simply coated with a complementary electron acceptor to get an order-bulk heterojunction device.

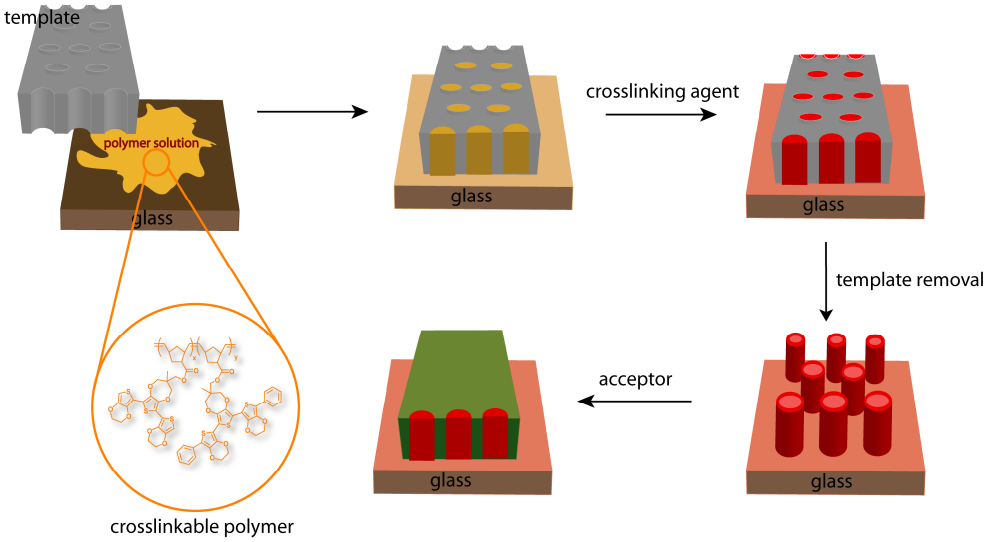

Figure 5.1. An ordered bulk heterojunction device fabricated from polymers containing crosslinkable EDOT side chains.

Horiuchi *et al.* reported that semi-rod-coil block copolymers of styrene and isoprene with oligothiophene modified side chains would self-organize into hexagonally paced micropores.[2] Similar nanostructure was also observed with block copolymers of polystyrene and polystyrene functionalized with EDOT oligomers.[3] In this regard, block copolymers of benzyl ester and EDOT derivatives could be synthesized. Figure 5.2 shows the novel design of promising block copolymers. The two blocks should phase-separate and also provide the porous structures in accordance with the previous literature

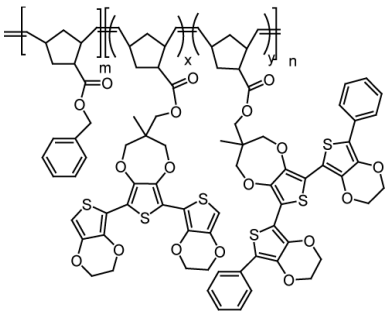

Figure 5.2. Structure of block copolymer.

reports. Oxidizing agent will be used to polymerize EDOT moiety and, therefore, lock the conformation prior to the deposition of the acceptors onto the porous film of polymer donors to obtain an ordered bulk A/D heterojunction device. Since the template is not needed in this case, this method could eliminate the problems that are encountered in the template removal process.

Though the non-conjugated polymers containing EDOT side chains investigated here possess a broad absorption window they do not encompass the whole visible region. An effort to further expand the absorption bandwidth of polymers could be undertaken by incorporating low band gap units as side chains. For example, the combination of electron poor benzothiadiazole unit and electron rich EDOT moiety might lead to a further reduction in the band gap. The free α positions at EDOT units can also be used for side chain polymerization. Figure 5.3 shows an example of the polymer that is anticipated to provide broader absorption spectrum and thus might be of interest for further investigation.

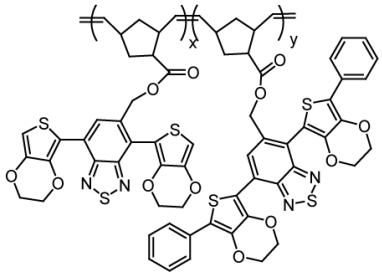

Figure 5.3. Structure of novel low band gap crosslinkable polymer.

Finally, novel non-conjugated polymers with conductive pendant groups were also designed and synthesized for charge mobility studies. By attaching conductive units as side chains of polymers, the band gap of these polymers becomes readily tunable; a property that is not amenable in conductive conjugated polymers. The charge mobility of these materials will be investigated. Moreover, unlike conjugated polymers, self

organization may not be needed for efficient charge mobility in these non-conjugated polymers. Therefore, we hypothesize that the mobility of these polymers on the flat surface and confined spaces such as nanopores should be similar. Therefore, we will also fabricate devices with different architectures and compare the mobility.

5.1 References

1. Thomas, K. R. J.; Thompson, A. L.; Sivakumar, A. V.; Bardeen, C. J.; Thayumanavan, S., "Energy and Electron Transfer in Bifunctional Non-conjugated Dendrimers" *J. Am. Chem. Soc.* **2005,** 127, (1), 373-383.

2. Hayakawa, T.; Horiuchi, S., "From Angstroms to Micrometers: Self-organized Hierarchical Structure within a Polymer Film" *Angew. Chem. Int. Ed.* **2003,** 42, (20), 2285-2289.

3. Bolognesi, A.; DiGianvincenzo, P.; Giovanella, U.; Mendichi, R.; Schieroni, A. G., "Polystyrene Functionalized with EDOT Oligomers" *Eur. Polym. J.* **2008,** 44, (3), 793-800.

CHAPTER 6

EXPERIMENTAL PROCEDURE

^{1}H-NMR spectra were recorded on a 400 MHz NMR spectrometer using the residual proton resonance of the solvent as the internal standard. Chemical shifts are reported in parts per million (ppm). When peak multiplicities are given, the following abbreviations are used: s, singlet; d, doublet; t, triplet; q, quartet; quin, quintet; d of d, doublet of doublet; m, multiplet, br, broad. ^{13}C-NMR spectra were proton decoupled and recorded on a 100 MHz NMR spectrometer using the carbon signal of deuterated solvent as the internal standard. Mass spectrometry was performed on the Bruker Daltonics Reflex III (MALDI-ToF). UV-Visible spectra were obtained using a Cary 100 spectrophotometer and fluorescence data were collected using JASCO FP-6500 spectrofluorimeter. Flash chromatography was performed with 37-75 µm silica gel. Analytical thin layer chromatography was performed on silica plates with F-254 indicator and the visualization was accomplished by a UV lamp. THF and toluene were distilled over Na/Ph_2CO ketyl. Dihydroxy benzthiadiazole derivative, hydroxyl diarylaminopyrene and fully decorated dendrimers containing these 2 moieties have been synthesized and published earlier by our group.[1, 2] Frechet-type dendrons[3-5], benzyl(aryl)ether backbone[6, 7] of linear counterparts, 3rd generation Grubbs catalyst[8], 3,4-propylenedioxythiophene derivative (ProDOT-OH)[9], 2-tributyl tin EDOT[10-12] and 2-phenyl EDOT[13] have been synthesized according to reported procedures. All other chemicals were obtained from commercial sources and used without any purification unless otherwise stated.

Synthesis of compound 2-6

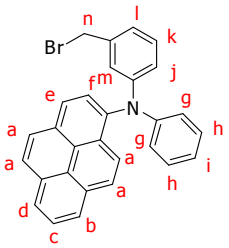

2-6

4.00 g (10.0 mmol) of hydroxyfunctionalized diarylaminopyrene and catalytic amount of DMAP were dissolved in THF and the solution was cooled to 0 ^{o}C under argon atmosphere. 3.50 mL (2.51 mmol) of triethylamine and 1.5 mL (20.7 mmol) of mesyl chloride were added dropwise, and allowed to stir at room temperature for 3 h. Upon completion of the reaction, water was added and the compound was extracted with dichloromethane. The organic layer was concentrated under reduced pressure to afford crude mixture which was taken for further step without any purification.

To the above crude mixture in THF, 4.30 g (50.0 mmol) of LiBr was added and the contents were allowed to reflux overnight. After completion of the reaction, the reaction mixture was partitioned between water and dichloromethane. The aqueous layer was extracted twice with dichloromethane, dried over Na_2SO_4 and evaporated under reduced pressure. The crude product was purified by column chromatography using 30% dichloromethane in hexanes to afford the product (4.17 g, 90% yield). ^{1}H NMR ($CDCl_3$, ppm): δ 8.32-8.03 (m, 8H, a-e), 7.86-7.83 (m, 1H, f), 7.22-6.99 (m, 6H,g, j-m), 6.89-6.86 (m, 3H, h, i), 4.48 (s, 2 H, n), ^{13}C NMR ($CDCl_3$, ppm): δ 148.9, 148.0, 139.9, 138.8, 131.2, 131.0, 129.7, 129.5, 129.3, 128.2, 128.1, 127.2, 127.3, 127.2, 126.3, 126.2, 126.1, 125.3, 125.2, 124.8, 123.1, 122.5, 122.3, 122.1, 121.5, 121.4, 33.3.

Synthesis of compound 2-11

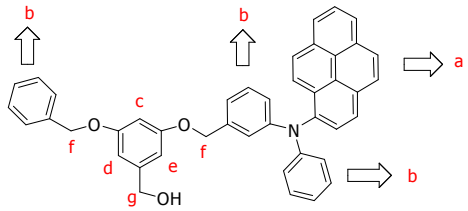

2-11

A mixture of 3.00 g (13.0 mmol) of monosubstituted G1-OH (**2-10**), 6.60 g (14.3 mmol) of compound **2-6**, 5.30 g (39.1 mmol) of K_2CO_3 and 0.6 g (2.60 mmol) of 18-crown-6 was heated at reflux and stirred vigorously under argon for 12 h. The reaction mixture was allowed to cool to room temperature and solvent was evaporated to dryness. The residue was partitioned between water and dichloromethane. The organic layer was separated and aqueous layer was extracted with dichloromethane. The combined organic layer was dried over Na_2SO_4 and evaporated to dryness. The crude product was purified by column chromatography using 2% ethyl acetate in dichloromethane to afford the product (6.99 g, 80% yield). ^{1}H NMR ($CDCl_3$, ppm): δ 8.08-7.84 (m, 9H, a), 7.43-6.98 (m, 14H, b), 6.55 (s, 1H, c), 6.49 (s, 1H, d), 6.45 (s, 1H, e), 4.99 (s, 4H, f), 4.54 (s, 2H, g). ^{13}C NMR ($CDCl_3$, ppm): δ 160.2, 160.2, 160.1, 149.1, 148.7, 143.6, 140.9, 138.3, 137.1, 131.4, 131.3, 129.9, 129.7, 129.5, 128.8, 128.8, 128.4, 128.3, 128.2, 127.9, 127.8, 127.4, 126.6, 126.5, 126.3, 125.5, 125.4, 125.0, 123.5, 122.6, 122.3, 121.5, 121.0, 120.9, 70.1, 65.3, 65.2. MALDI-ToF MS: Found 615.14 (MH^+ calcd. 611.73).

Synthesis of compound 2-12

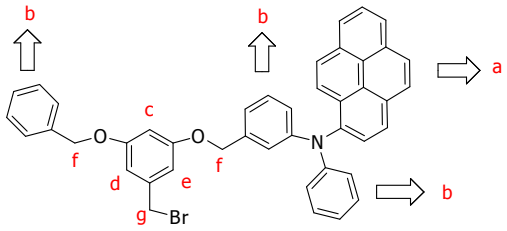

2-12

2.17 g (3.54 mmol) of compound **2-11** and 0.13 g (1.06 mmol) of DMAP were dissolved in THF and the solution was cooled to 0 ^{o}C under argon atmosphere. 1.23 mL (8.85 mmol) of triethylamine and 0.56 mL (7.09 mmol) of mesyl chloride were added dropwise, and allowed to stir at room temperature for 3 h. Upon completion of the reaction, water was added and the compound was extracted with dichloromethane. The organic layer was concentrated under reduced pressure to afford crude mixture which was taken for further step without any purification.

To the above crude mixture in THF, 3.05 g (35.5 mmol) of LiBr was added and the contents were allowed to reflux overnight. After completion of the reaction, the reaction mixture was partitioned between water and dichloromethane. The aqueous layer was extracted twice with dichloromethane, dried over Na_2SO_4 and evaporated under reduced pressure. The crude product was purified by column chromatography using 30% dichloromethane in hexanes to afford the product (2.08 g, 87% yield). ^{1}H NMR ($CDCl_3$, ppm): δ 8.21-7.87 (m, 9H, a), 7.74-6.60 (m, 14H, b), 6.53 (s, 1H, c), 6.48 (s, 1H, d), 6.47 (s, 1H, e), 4.98 (s, 4H, f), 4.34 (s, 2H, g). ^{13}C NMR ($CDCl_3$, ppm): δ 160.2, 160.1, 149.2, 148.7, 140.9, 139.9, 138.1, 136.9, 131.5, 131.3, 129.9, 129.8, 129.5, 128.9, 128.5, 128.3, 128.0, 127.8, 127.5, 126.6, 126.5, 126.3, 125.5, 125.4, 125.1, 123.5, 122.6, 122.4, 121.5,

120.9, 120.9, 108.4, 108.3, 102.4, 70.3, 70.2, 33.8. MALDI-ToF MS: Found 672.70 (MH^+ calcd. 673.73).

Synthesis of compound 2-17

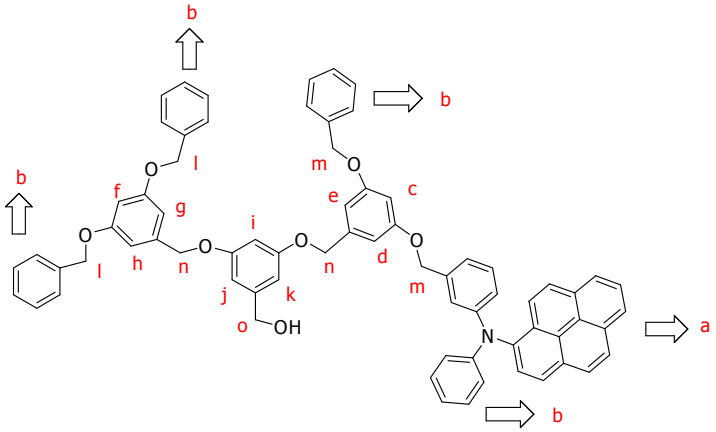

2-17

A mixture of 0.95 g (2.15 mmol) of monosubstituted G2-OH (**2-15**), 1.59 g (2.15 mmol) of dendron **2-12**, 1.76 g (12.9 mmol) of K_2CO_3 and 0.03 g (0.10 mmol) of 18-crown-6 was heated at reflux and stirred vigorously under argon for 12 h. The reaction mixture was allowed to cool to room temperature and solvent was evaporated to dryness. The residue was partitioned between water and dichloromethane. The organic layer was separated and aqueous layer was extracted with dichloromethane. The combined organic layer was dried over Na_2SO_4 and evaporated to dryness. The crude product was purified by column chromatography using 5% ethyl acetate in dichloromethane to afford the product (1.86 g, 76% yield). ^{1}H NMR ($CDCl_3$, ppm): δ 8.21-7.87 (m, 9H, a), 7.37-6.93 (m, 24H, b), 6.68 (s, 2H, c, f), 6.61-6.45 (m, 7H,d, e, g-k), 5.05 (s, 4H, m), 4.96 (s, 4H, l), 4.88 (s, 4H, n), 4.61 (s, 2H, o). ^{13}C NMR ($CDCl_3$, ppm): δ 160.4, 160.2, 160.1, 149.1, 148.7, 148.8, 140.9, 139.6, 139.4, 138.2, 137.0, 131.4, 131.2, 129.8, 129.7, 129.5, 128.8, 128.4, 128.3, 128.2, 127.9, 127.8, 127.4, 126.5, 126.5, 126.3, 125.5, 125.4, 125.0, 123.5,

122.5, 122.3, 121.5, 121.0, 120.9, 70.3, 70.2, 70.1, 70.0, 65.3. MALDI-ToF MS: Found 1035.12 (MH^+ calcd. 1034.08).

Synthesis of compound 2-18

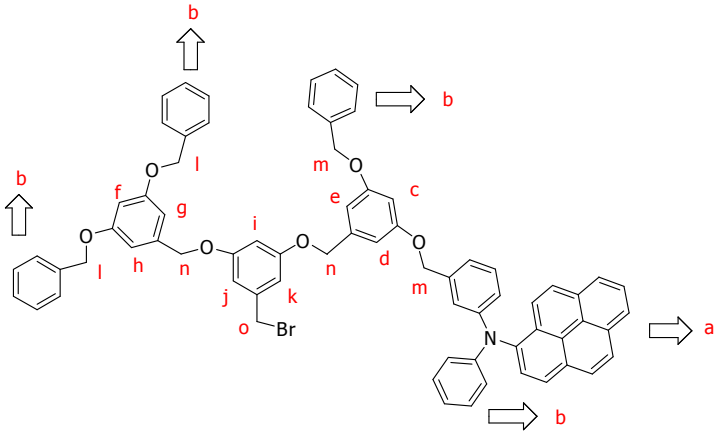

2-18

1.40 g (1.35 mmol) of compound **2-17** and 0.01 g (0.067 mmol) of DMAP were dissolved in THF and the solution was cooled to 0 ^oC under argon atmosphere. 0.47 mL (3.38 mmol) of triethylamine and 0.21 mL (2.71 mmol) of mesyl chloride were added dropwise, and allowed to stir at room temperature for 3 h. Upon completion of the reaction, water was added and the compound was extracted with dichloromethane. The organic layer was concentrated under reduced pressure to afford crude mixture which was taken for further step without any purification.

To the above crude mixture in THF, 0.72 g (8.10 mmol) of LiBr was added and the contents were allowed to reflux overnight. After completion of the reaction, the reaction mixture was partitioned between water and dichloromethane. The aqueous layer was extracted twice with dichloromethane, dried over Na_2SO_4 and evaporated under reduced pressure. The crude product was purified by column chromatography using 75% dichloromethane in hexanes to afford the product (1.48 g, 82% yield). ^1H NMR ($CDCl_3$,

ppm): δ 8.20-7.85 (m, 9H, a), 7.39-6.93 (m, 24H, b), 6.67-6.45 (m, 9H, c-k), 5.03 (s, 4H, m), 4.97 (s, 4H, l), 4.89 (s, 4H, n), 4.40 (s, 2H, o). ^{13}C NMR ($CDCl_3$, ppm): δ 160.2, 160.1, 148.4, 140.6, 139.7, 139.1, 138.9, 137.9, 136.8, 131.2, 129.6, 129.5, 129.3, 128.6, 128.2, 128.0, 127.7, 127.6, 127.2, 126.3 126.2, 126.0, 125.2, 125.1, 124.8, 123.3, 122.3, 122.0, 121.2, 120.7, 108.2, 106.4, 102.2, 101.7, 101.6, 70.1, 70.0, 69.9, 33.6. MALDI-ToF MS: Found 1099.51 (MH^+ calcd. 1096.38).

Synthesis of compound 2-21

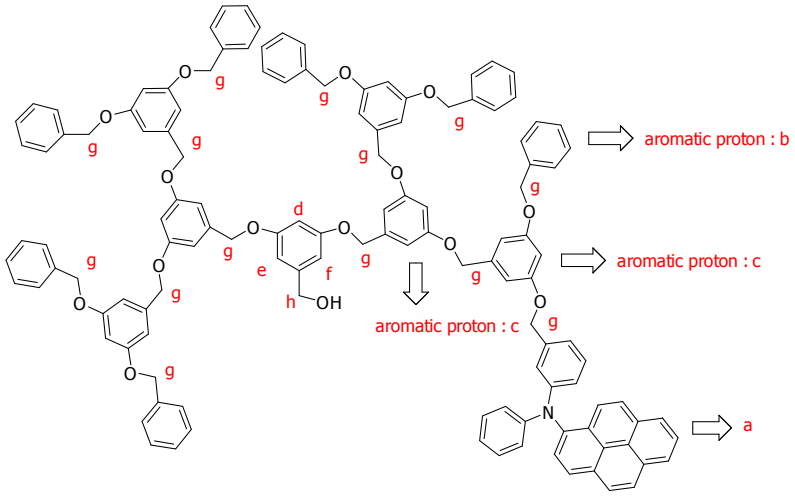

2-21

A mixture of 0.75 g (0.86 mmol) of monosubstituted G3-OH (**2-20**), 1.05 g (0.95 mmol) of compound **2-18**, 0.76 g (5.60 mmol) of K_2CO_3 and 0.03 g (0.17 mmol) of 18-crown-6 was heated at reflux and stirred vigorously under argon for 12 h. The reaction mixture was allowed to cool to room temperature and solvent was evaporated to dryness. The residue was partitioned between water and dichloromethane. The organic layer was separated and the aqueous layer was extracted with dichloromethane. The combined organic layer was dried over Na_2SO_4 and evaporated to dryness. The crude product was purified by column chromatography using 8% ethyl acetate in dichloromethane to afford the product (1.19 g, 66% yield). ^{1}H NMR ($CDCl_3$, ppm): δ 8.02-7.87 (m, 9H, a), 7.35-

6.94 (m, 44H, b), 6.73-6.52 (m, 19H, c, d), 6.45 (d, J = 4 Hz, 2H, e, f), 5.01-4.85 (s, 28H, g), 4.60 (s, 2H, h). ^{13}C NMR ($CDCl_3$, ppm): δ 160.2, 160.1, 159.9, 148.9, 148.4, 140.6, 139.3, 139.3, 139.1, 137.9, 136.8, 131.2, 131.0, 129.6, 129.5, 129.2, 128.6, 128.2, 128.0, 127.7, 127.6, 127.2, 126.3, 126.2, 126.0, 125.2, 125.1, 124.8, 123.2, 122.3, 122.0, 121.3, 120.7, 106.4, 105.8, 101.6, 70.1, 69.92, 65.8. MALDI-ToF MS: Found 1883.02 (MH^+ calcd. 1880.66).

Synthesis of compound 2-22

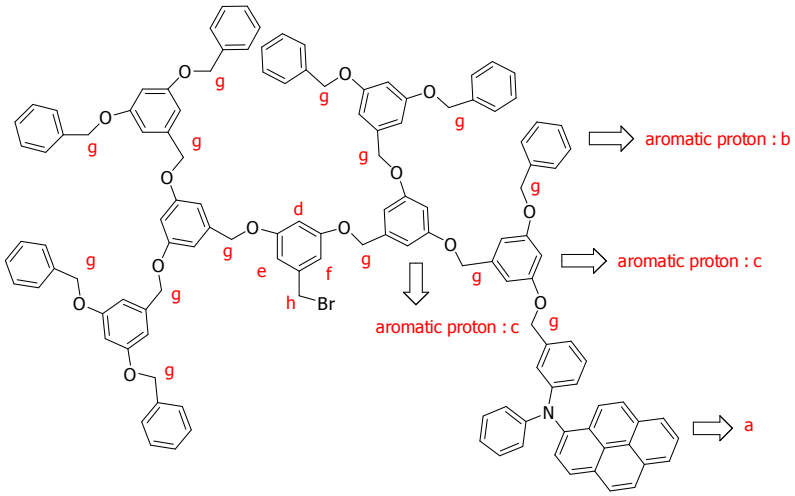

2-22

0.75 g (0.40 mmol) of compound **2-21** and 0.003 g (0.02 mmol) of DMAP were dissolved in THF and the solution was cooled to 0 ^{o}C under argon atmosphere. 0.14 mL (0.99 mmol) of triethylamine and 0.06 mL (0.79 mmol) of mesyl chloride were added dropwise, and allowed to stir at room temperature for 3 h. Upon completion of the reaction, water was added and the compound was extracted with dichloromethane. The organic layer was concentrated under reduced pressure to afford crude mixture which was taken for further step without any purification.

To the above crude mixture in THF, 0.21 g (2.39 mmol) of LiBr was added and the contents were allowed to reflux overnight. After completion of the reaction, the

reaction mixture was partitioned between water and dichloromethane. The aqueous layer was extracted twice with dichloromethane, dried over Na_2SO_4 and evaporated under reduced pressure. The crude product was purified by column chromatography using dichloromethane to afford the product (0.62 g, 80% yield). ^{1}H NMR ($CDCl_3$, ppm): δ 8.12-7.79 (m, 9H, a), 7.38-6.81 (m, 44H, b), 6.66-6.43 (m, 21H, c-f), 5.00-4.86 (m, 28H, g), 4.36 (s, 2H, h). ^{13}C NMR ($CDCl_3$, ppm): δ 160.5, 160.4, 149.2, 148.7, 141.0, 139.5, 139.4, 138.3, 137.1, 129.6, 128.9, 128.3, 128.0, 127.9, 127.5, 127.2, 126.6, 126.4, 125.5, 123.6, 122.6, 121.0, 106.7, 101.9, 70.4, 70.3, 70.2, 31.9. MALDI-ToF MS: Found 1946.79 (MH^+ calcd. 1943.66).

Synthesis of compound 2-1D

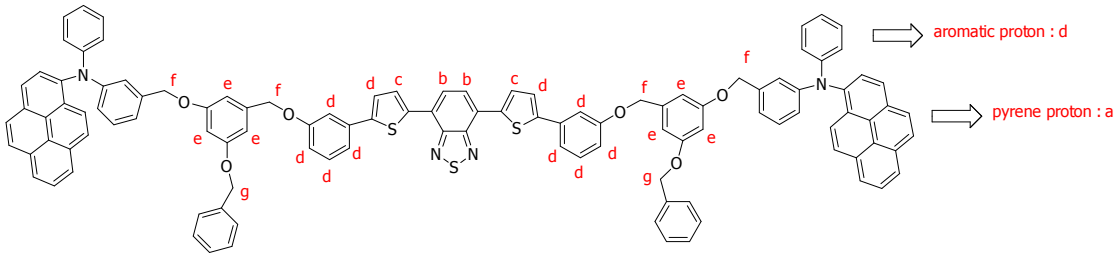

1D

A mixture of 0.12 g (0.25 mmol) of dihydroxyl benzthiadiazole core (**2-3**), 0.32 g (0.52 mmol) of compound **2-12**, 0.20 g (1.50 mmol) of K_2CO_3 and 0.33 g (0.12 mmol) of 18-crown-6 was heated at reflux and stirred vigorously under argon for 12 h. The reaction mixture was allowed to cool to room temperature and solvent was evaporated to dryness. The residue was partitioned between water and dichloromethane. The organic layer was separated and aqueous layer was extracted with dichloromethane. The combined organic layer was dried over Na_2SO_4 and evaporated to dryness. The crude product was purified by column chromatography using 40% dichloromethane in hexanes to afford compound

1D (0.18g, 74% yield). ^{1}H NMR ($CDCl_3$, ppm): δ 8.02-7.80 (m, 22H, a, b, c), 7.41-6.87 (m, 38H, d), 6.66-6.41 (m, 6H, e), 4.97 (s, 8H, f), 4.92 (s, 4H, g). ^{13}C NMR ($CDCl_3$, ppm) : δ 160.4, 160.3, 159.4, 152.6, 149.2, 148.7, 145.4, 140.9, 139.5, 138.9, 138.3, 137.1, 135.7, 131.5, 131.3, 130.3, 129.9, 129.8, 129.6, 128.9, 128.8, 128.5, 128.3, 128.0, 127.9, 127.5, 127.5, 126.6, 126.5, 126.4, 125.7, 125.5, 125.4, 125.8, 125.1, 124.5, 123.5, 122.6, 122.3, 121.6, 121.0, 121.0, 118.9, 114.3, 112.7, 106.8, 106.7, 101.9, 70.3, 70.2, 70.1. MALDI-ToF MS: Found 1671.41 (MH^+ calcd. 1672.04). Anal. Calc. for $C_{112}H_{78}N_4O_6S_3$: C, 80.45; H, 4.70; N, 3.35. Found C, 80.15; H, 4.53; N, 3.21.

Synthesis of compound 2-2D

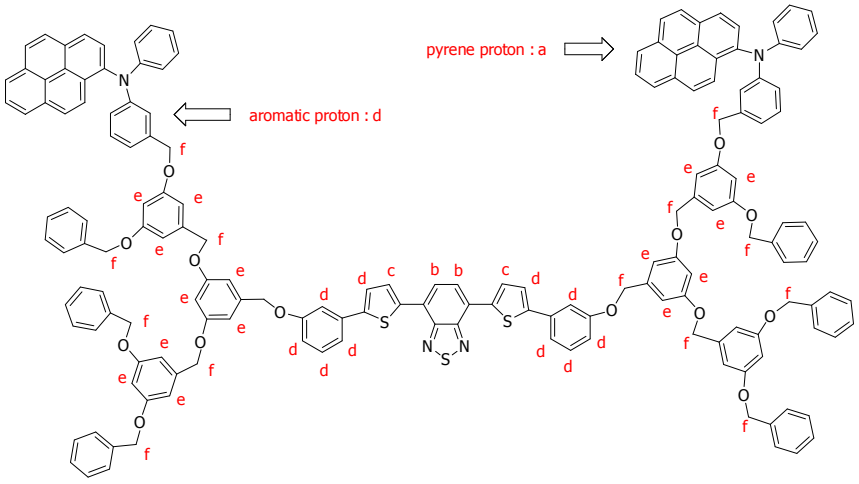

2-2D

A mixture of 0.08 g (0.17 mmol) of dihydroxyl benzthiadiazole core (**2-3**), 0.37 g (0.35 mmol) of compound **2-18**, 0.14 g (1.00 mmol) of K_2CO_3 and 0.023 g (0.09 mmol) of 18-crown-6 was heated at reflux and stirred vigorously under argon for 12 h. The reaction mixture was allowed to cool to room temperature and solvent was evaporated to dryness. The residue was partitioned between water and dichloromethane. The organic layer was separated and aqueous layer was extracted with dichloromethane. The combined organic layer was dried over Na_2SO_4 and evaporated to dryness. The crude

product was purified by column chromatography using 40% dichloromethane in hexanes to afford compound **2-2D** (0.11g, 71% yield). ^{1}H NMR ($CDCl_3$, ppm): δ 8.02-7.75 (m, 22H, a, b, c), 7.38-6.91 (m, 58H, d), 6.67-6.44 (m, 18H, e), 5.05-4.78 (m, 28H, f). ^{13}C NMR ($CDCl_3$, ppm): δ 160.5, 160.4, 160.3, 160.2, 159.4, 152.7, 149.2, 146.7, 145.5, 141.0, 139.6, 139.6, 139.4, 139.0, 138.3, 137.1, 135.7 131.5, 131.3, 130.4, 130.0, 129.8, 129.6, 129.4, 128.9, 128.6, 128.5, 128.3, 128.0, 127.9, 127.5, 126.6, 126.5, 126.4, 125.9, 125.6, 125.5, 125.5, 125.1, 124.6, 123.6, 122.6, 122.3, 121.6, 121.0, 119.0, 114.5, 112.8, 106.7, 105.7, 102.0, 101.9, 101.8, 70.4, 70.3, 70.2, 68.3. MALDI-ToF MS: Found 2521.02 (MH+ calcd. 2521.01). Anal. Calcd. for $C_{168}H_{126}N_4O_{14}S_3$: C, 80.04; H, 5.04; N, 2.22. Found C, 78.96; H, 4.81; N, 2.16.

Synthesis of compound 2-3D

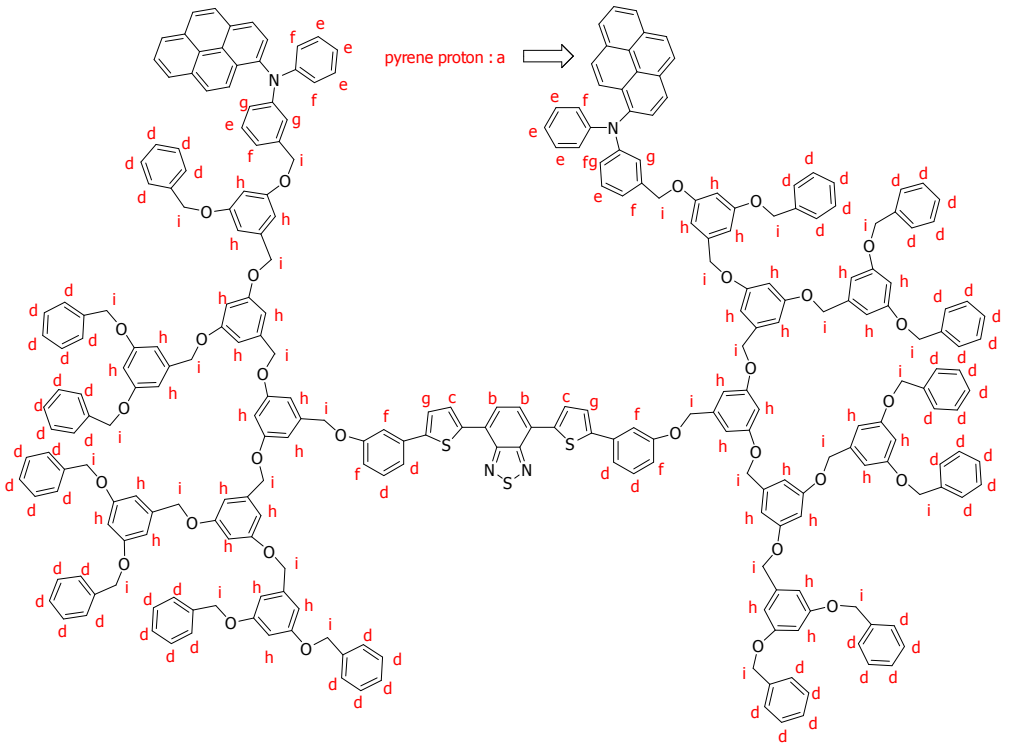

2-3D

A mixture of 0.05 g (0.11 mmol) of dihydroxyl benzthiadiazole core (**2-3**), 0.46 g (0.23 mmol) of compound **2-22**, 0.09 g (0.67 mmol) of K_2CO_3 and 0.01 g (0.05 mmol) of 18-crown-6 was heated at reflux and stirred vigorously under argon for 12 h. The reaction mixture was allowed to cool to room temperature and solvent was evaporated to dryness. The residue was partitioned between water and dichloromethane. The organic layer was separated and aqueous layer was extracted with dichloromethane. The combined organic layer was dried over Na_2SO_4 and evaporated to dryness. The crude product was purified by column chromatography using 5% ethyl acetate in dichloromethane to afford product (0.07g, 71% yield). ^{1}H NMR ($CDCl_3$, ppm): δ 8.18-7.67 (m, 22H, a, b, c), 7.38-7.21 (m, 74H, d), 7.17-7.14 (m, 8H, e), 7.08-7.03 (m, 8H, f), 6.98-6.87 (m, 8H, g), 6.71-6.42 (m, 42H, h), 5.02-4.84 (m, 60H, i). ^{13}C NMR ($CDCl_3$, ppm): δ 160.4, 160.3, 160.3, 160.2, 149.1, 143.7, 140.9, 139.5, 139.3, 138.3, 137.1, 131.5, 131.3, 129.9, 129.7, 129.5, 128.8, 128.4, 128.3, 127.9, 127.8, 127.5, 127.4, 126.3, 125.5, 125.4, 125.0, 123.5, 122.6, 121.5, 121.0, 120.9, 106.6, 101.9, 101.8, 70.3, 70.2, 70.1. MALDI-ToF MS: Found 4200.14 (MH^+ calcd. 4218.96). Anal. Calc. for $C_{280}H_{222}N_4O_{30}S_3$: C, 79.71; H, 5.30; N, 1.33. Found C, 79.92; H, 5.25; N, 1.35.

Synthesis of compound 2-24

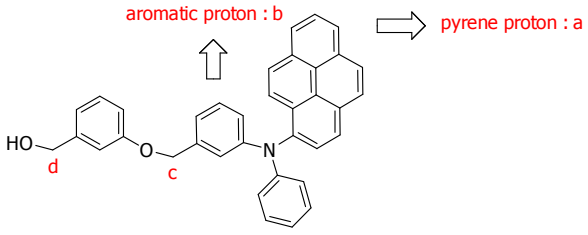

2-24

4.00 g (10.0 mmol) of hydroxy diarylaminopyrene (**2-23**), 1.10 g (9.00 mmol) of 3-hydroxy benzaldehyde and 3.93 g (13.5 mmol) of triphenylphosphine were taken in

THF solvent under N_2 atmosphere and cooled to 0 ^oC. To this cooled contents diethylazodicarboxylate (2.12 mL, 13.5 mmol) was added slowly *via* syringe and contents were allowed to stir at room temperature overnight. After completion of the reaction, water was added to quench the reaction and extracted using dichloromethane. The crude reaction mixture was purified by column chromatography using 50% dichloromethane in hexanes to afford the linear analog G1-CHO (2.98 g, 59% yield). ^{1}H-NMR: ($CDCl_3$, ppm) δ 9.93 (s, 1H), 8.16-7.83 (m, 9H), 7.22-6.73 (m, 13H), 4.93 (s, 2H).

To a stirring solution of 1.00 g (1.98 mmol) of G1-CHO in THF/methanol solvent mixture, 0.15 g (3.97 mmol) of sodium borohydride was added in portions with efficient stirring. After the addition was complete the mixture was allowed to stir overnight. The mixture was then poured into water and the compound was extracted with dichloromethane. The organic layer was concentrated under reduced pressure to afford the crude product, which was purified by column chromatography using 25% hexanes in dichloromethane as the eluent to afford the product (0.90 g, 90% yield). ^{1}H-NMR ($CDCl_3$, ppm): δ 8.17-7.80 (m, 9H, a), 7.21-6.72 (m, 13H, b), 4.90 (s, 2H, c), 4.56 (s, 2H, d). ^{13}C NMR ($CDCl_3$, ppm): δ 159.3, 149.1, 148.7, 142.8, 140.9, 138.6, 138.2, 131.4, 131.3, 129.8, 129.9, 129.6, 129.5, 128.5, 128.2, 127.9, 127.4, 127.4, 126.6, 126.5, 126.3, 125.5, 125.4, 125.1, 123.5, 122.5, 122.3, 121.5, 121.0, 120.8, 120.0, 119.3, 114.5, 114.3, 114.1, 113.4.

Synthesis of compound 2-25

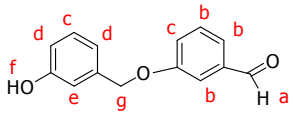

2-25

A 100 mL round bottom flask was charged with 4.08 g (24.25 mmol) of MOM-protected benzyl alcohol, 2.47 g (20.2 mmol) of 3-hydroxy benzaldehyde and 7.90 g (24.25 mmol) of triphenylphosphine under N_2 atmosphere and contents were cooled to 0^oC. To the stirred solution diethylazodicarboxylate (4.70 mL, 24.25 mmol) was added *via* syringe and allowed the contents to stir at room temperature overnight. Upon completion of the reaction, the reaction mixture was partitioned between water and ethyl acetate and organic layer was dried over Na_2SO_4 and solvent was evaporated under reduced pressure. The crude mixture was purified using silica-gel column chromatography using 10% ethyl acetate in hexanes to afford product (9.15 g, 51% yield). ^1H NMR ($CDCl_3$, ppm): δ 9.97 (s, 1H), 7.46 (t, *J* = 3.4 Hz, 3H), 7.34-7.24 (m, 2H), 7.13-7.00 (m, 3H), 5.18 (d, *J* = 3 Hz, 2H), 5.09 (s, 2H), 3.48 (d, *J* = 2.4 Hz, 3 H).

Above purified compound (1.71 g, 6.24 mmol) was taken in ethanol and 3.56 g (18.7 mmol) of *p*-toluene sulfonic acid was added and stirred for 3 h at room temperature. After the completion of the reaction, the reaction mixture was worked up using water and CH_2Cl_2. The crude reaction mixture was purified by column chromatography using 10 % ethyl acetate in hexanes to afford the product (1.15 g, 82 % yield). ^1H NMR ($CDCl_3$, ppm): δ 9.96 (s, 1H, a), 7.49- 7.43 (m, 3H, b), 7.29-7.23 (m, 2H, c), 6.97 (t, *J* = 20 Hz, 2H, d), 6.82 (d, J = 10.4 Hz, 1H, e), 5.68 (d, J = 10 Hz, 1H, f), 5.08 (s, 2H, g). ^{13}C NMR ($CDCl_3$, ppm): δ 159.3, 156.5, 142.6, 139.1, 130.3, 130.1, 120.1, 119.9, 115.5, 114.8, 114.8, 113.9, 70.1, 65.6.

Synthesis of compound 2-26

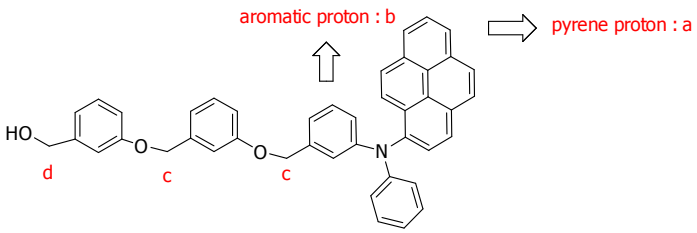

2-26

1.77 g (4.43 mmol) of hydroxyl diarylaminopyrene (**2-23**), 0.85 g (4.02 mmol) of compound **2-25** and 1.46 g (5.63 mmol) of triphenylphosphine were taken in THF under N_2 atmosphere and cooled to 0 ^oC. To the cooled contents, 0.88 mL (5.63 mmol) of diethylazodicarboxylate was added slowly *via* syringe and contents were allowed to stir at room temperature overnight. After completion of the reaction, water was added to quench the reaction and extracted using dichloromethane. The crude reaction mixture was purified by column chromatography using 20% dichloromethane in hexanes to afford the linear analog G2-CHO (1.54 g, 57% yield). ^1H NMR ($CDCl_3$, ppm): δ 9.91 (s, 1H), 8.26-7.97 (m, 9H) 7.32-6.81 (m, 17H), 5.01 (s, 2H), 5.00 (s, 2H).

To a stirring solution of 0.75 g (1.23 mmol) of G2-CHO in THF/methanol solvent mixture, 0.12 g (3.08 mmol) of sodium borohydride was added in portions with efficient stirring. After the addition was complete the mixture was allowed to stir overnight. The mixture was then poured into water and the compound was extracted with dichloromethane. The organic layer was concentrated under reduced pressure to afford the crude product, which was purified by column chromatography using 25% hexanes in dichloromethane as the eluent to afford the product (0.71 g, 94% yield). ^1H NMR ($CDCl_3$, ppm): δ 8.24-7.94 (m, 9H, a), 7.29-6.80 (m, 17H, b), 5.02 (s, 4H, c), 4.62 (s, 2H, d). ^{13}C NMR ($CDCl_3$, ppm): δ 159.2, 159.1, 149.2, 148.7, 142.9, 140.9, 138.8, 138.3,

131.5, 131.3, 129.9, 129.8, 129.8, 129.5, 128.5, 128.3, 128.0, 127.5, 127.5, 126.6, 126.5, 126.3, 125.5, 125.4, 125.1, 123.5, 122.6, 122.3, 121.6, 121.0, 121.0, 120.1, 119.6, 114.6, 114.3, 114.2, 113.5, 70.1, 69.9, 65.4. MALDI-ToF MS: Found 610.89 (MH^+ calcd. 611.73).

Synthesis of compound 2-27

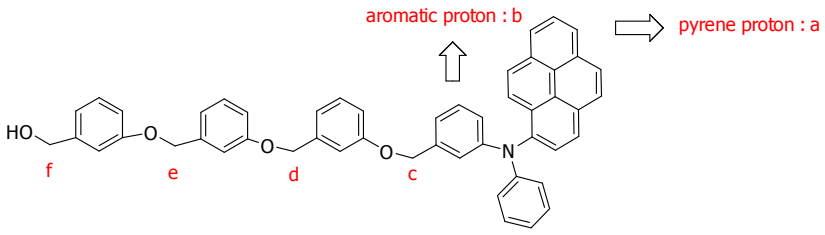

2-27

0.57 g (2.70 mmol) of compounds **2-24**, 1.49 g (2.97 mmol) of compound **2-25** and 0.98 g (2.97 mmol) of triphenylphosphine were taken in THF under N_2 atmosphere and cooled to 0 °C. To these cooled contents 0.59 mL (2.97 mmol) of diethylazodicarboxylate was added slowly *via* syringe and contents were allowed to stir at room temperature overnight. After completion of the reaction, water was added to quench the reaction and extracted using dichloromethane. The crude reaction mixture was purified by column chromatography using 40% dichloromethane in hexanes as the eluent to afford the product, linear analog G3-CHO (2.43 g, 52% yield). ^{1}H NMR ($CDCl_3$, ppm): δ 9.87 (s, 1H), 8.17-7.84 (m, 9H), 7.32-6.81 (m, 21H), 5.06 (s, 2H), 4.97 (s, 2H), 4.94 (s, 2H).

To a stirring solution of 0.74 g (1.03 mmol) of G3-CHO in THF/methanol solvent mixture, 0.10 g (2.57 mmol) of sodium borohydride was added in portions with efficient stirring. After the addition was complete the mixture was allowed to stir overnight. The mixture was then poured into water and the compound was extracted with

dichloromethane. The organic layer was concentrated under reduced pressure to afford the crude product, which was purified by column chromatography using 25% hexanes in dichloromethane as the eluent afforded product (0.69 g, 93% yield). ^{1}H NMR ($CDCl_3$, ppm): δ 8.15-7.82 (m, 9H, a), 7.30-6.80 (m, 21H, b), 5.04 (s, 2H, c), 4.95 (s, 2H, d), 4.92 (s, 2H, e), 4.66 (s, 2H, f). ^{13}C NMR ($CDCl_3$, ppm): δ 159.2, 159.0, 149.1, 148.7, 142.9, 140.9, 138.8, 138.9, 138.6, 138.3, 131.4, 131.3, 129.9, 129.9, 129.8, 129.8, 129.8, 129.5, 128.4, 128.3, 127.9, 127.5, 127.4, 126.6, 126.5, 126.3, 125.5, 125.4, 125.1, 123.5, 122.6, 122.3, 121.5, 121.0, 121.0, 120.1, 120.1, 119.6, 114.6, 114.3, 114.1, 113.4, 70.0, 69.9, 65.3. MALDI-ToF MS: Found 716.90 (MH^+ calcd. 717.85).

Synthesis of compound 2-1L

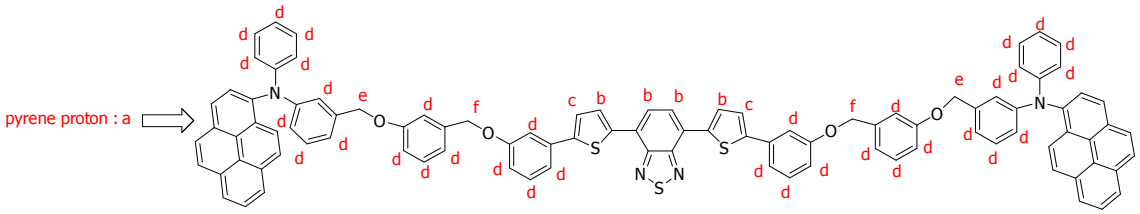

2-1L

0.44 g (0.86 mmol) of compound **2-24**, 0.20 g (0.41 mmol) of dihydroxy benzthiadiazole (**2-3**), 0.27 g (10.25 mmol) of tripheynylphosphine and THF (20 mL) were placed in a round bottom flask, and the reaction mixture was cooled to 0 ^{o}C. To the cold reaction mixture, 0.16 mL (10.25 mmol) of diethylazodicarboxylate was added *via* syringe and stirred at room temperature for 12 h. The crude reaction mixture was partitioned between water and dichloromethane and organic layer was dried over anhydrous Na_2SO_4 and the solvent was removed under reduced pressure. The product was purified by column chromatography using 40% dichloromethane in hexane as the eluent to afford the product (0.34 g, 71% yield). ^{1}H NMR ($CDCl_3$, ppm): δ 8.18-7.88 (m,

18H, a), 7.81-7.79 (m, 4H, b), 7.36 (d, *J* = *3.6* Hz, 2H, c), 7.35-6.81 (m, 34H, d), 5.00 (s, 4H, e), 4.94 (s, 4H, f). ^{13}C NMR ($CDCl_3$, ppm): δ 159.2, 158.9, 152.4, 148.9, 148.5, 145.3, 140.7, 138.7, 138.4, 138.1, 135.5, 131.2, 131.1, 130.0, 129.7, 129.6, 129.5, 129.3, 128.5, 128.2, 128.0, 127.7, 127.2, 127.2, 126.4, 126.2, 126.1, 125.6, 125.3, 125.2, 124.8, 124.3, 123.3, 122.4, 122.1, 121.3, 120.7, 119.9, 118.6, 114.5, 114.1, 114.0, 112.5, 69.9. MALDI-ToF MS: Found 1458.93 (MH^+ calcd. 1459.43). Anal. Calcd. for $C_{98}H_{66}N_4O_4S_3$: C, 80.63; H, 4.56, N, 3.84. Found C, 80.56; H, 4.64; N, 3.82.

Synthesis of compound 2-2L

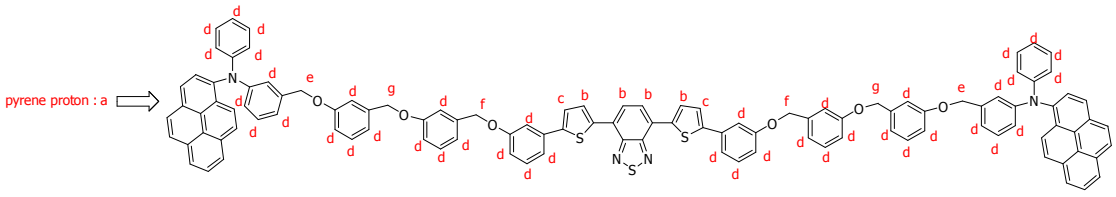

2-2L

0.53 g (0.86 mmol) of compound **2-26**, 0.20 g (0.41 mmol) of dihydroxy benzthiadiazole (**2-3**), 0.27 g (10.25 mmol) of tripheynylphosphine and THF (20 mL) were placed in a round bottom flask, and the reaction mixture was cooled to 0 ^{o}C. To the cold reaction mixture, 0.16 mL (1.03 mmol) of diethylazodicarboxylate was added *via* syringe and stirred at room temperature for 12 h. The crude reaction mixture was partitioned between water and dichloromethane and organic layer was dried over anhydrous Na_2SO_4 and solvent was removed under reduced pressure. The product was purified by column chromatography using 50% dichloromethane in hexanes as the eluent to afford the product (1.04 g, 72% yield). ^{1}H NMR ($CDCl_3$, ppm): δ 8.17-7.76 (m, 22H, a, b, c), 7.37-6.79 (m, 44H, d), 5.09 (s, 4H, e), 4.97 (s, 4H, f), 4.91 (s, 4H, g). ^{13}C NMR ($CDCl_3$, ppm): δ 159.5, 159.4, 159.1, 152.7, 149.2, 148.7, 145.6, 141.0, 139.0, 138.8,

138.7, 138.4, 135.8, 131.5, 131.3, 130.3, 130.0, 129.9, 129.8, 129.8, 129.5, 128.8, 128.5, 128.3, 128.0, 127.5, 127.5, 126.4, 126.6, 126.5, 126.3, 125.9, 125.5, 125.4, 125.1, 124.6, 124.6, 122.6, 122.3, 121.6, 121.0, 120.3, 120.1, 119.0, 114.8, 114.4, 114.2, 114.2, 112.8, 70.2, 70.1. MALDI-ToF MS: Found 1671.70 (MH^+ calcd. 1672.04). Anal. Calcd. for $C_{112}H_{78}N_4O_6S_3$: C, 80.45; H, 4.70; N, 3.35. Found C, 80.15, H, 4.81, N, 3.28.

Synthesis of compound 2-3L

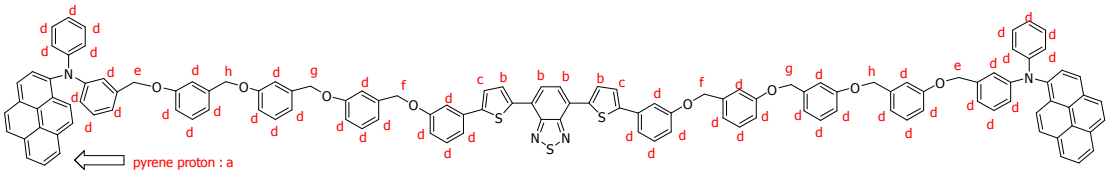

2-3L

0.50 g (0.69 mmol) of compound **2-27**, 0.16 g (0.33 mmol) of dihydroxy benzthiadiazole (**2-3**), 0.22 g (0.82 mmol) of tripheynylphosphine and THF (20 mL) were placed in a round bottom flask, and the reaction mixture was cooled to 0 ^oC. To the cold reaction mixture, 0.13 mL (0.82 mmol) of diethylazodicarboxylate was added *via* syringe and stirred at room temperature for 12 h. The crude reaction mixture was partitioned between water and dichloromethane and organic layer was dried over anhydrous Na_2SO_4 and solvent was removed under reduced pressure. The product was purified by column chromatography using 75% dichloromethane in hexane as the eluent to afford the product (0.96 g, 73% yield). ^1H NMR ($CDCl_3$, ppm): δ 8.18-7.77 (m, 22H, a, b, c), 7.36-6.77 (m, 52H, d), 5.09 (s, 4H, e), 5.05 (s, 4H, f), 4.93 (s, 4H, g), 4.89 (s, 4H, h). ^{13}C NMR ($CDCl_3$, ppm): δ 159.2, 159.1, 159.0, 158.8, 148.9, 148.4, 145.3, 140.6, 138.7, 138.5, 138.5, 138.4, 138.1, 135.4, 131.2, 131.0, 130.0, 129.7, 129.7, 129.6, 129.5, 129.2, 128.5, 128.2, 128.0, 127.7, 127.2, 126.3, 126.2, 126.0, 125.2, 125.1, 125.5, 124.8, 124.3, 123.2, 122.3, 122.0, 121.2, 120.7, 120.0, 119.8, 118.7, 114.5, 114.4, 114.1, 113.9, 113.8, 69.9, 69.8.

MALDI-ToF MS: Found 1883.89 (MH^+ calcd. 1884.28). Anal. Calcd. for $C_{126}H_{90}N_4O_8S_3$: C, 80.31; H, 4.81; N, 2.97. Found C, 80.12; H, 4.96; N, 2.84.

Synthesis of compound 3-16

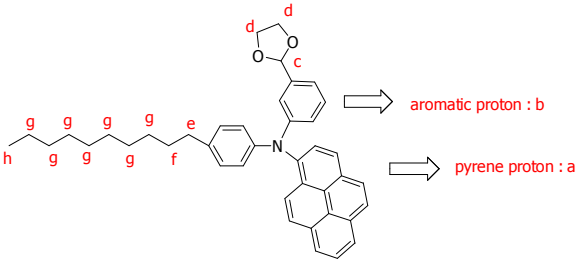

3-16

A mixture of N-phenylpyren-1-amine (5.00 g, 11.53 mmol), 2-(3-bromophenyl)-1,3-dioxolane (3.96 g, 17.30 mmol), $Pd(dba)_2$ (0.05 g, 0.06 mmol), $(t\text{-}Bu)_3P$ (0.06 g, 0.11 mmol), and toluene (100 mL) was heated at 80 ºC for 8 h. After cooling, the reaction mixture was poured into ice water and extracted with diethyl ether (3 × 30 mL) and the combined extract was dried over anhydrous $MgSO_4$. The solvent was evaporated to yield yellow syrup and further purified by column chromatography using 50% dichloromethane in hexane as the eluent to yield pale yellow solid as a product (5.50 g, 82% yield). ^{1}H NMR ($(CD_3)_2CO$), ppm): δ 8.46-7.67 (m, 9H, a), 7.66-6.90 (m, 8H, b), 5.62 (s, 1H, c), 4.00-3.81 (m, 4H, d), 2.62-2.50 (m, 2H, e), 1.60 (br, 2H, f), 1.29 (br, 14H, g), 0.85 (br, 3H, h). ^{13}C NMR ($CDCl_3$, ppm): δ 149.4, 146.4, 139.2, 137.4, 129.8, 129.5, 128.1, 128.0, 127.9, 126.6, 126.5, 125.4, 125.3, 125.3, 123.8, 119.3, 104.1, 65.4, 35.7, 32.2, 31.8, 30.0, 29.7, 23.0, 14.5.

Synthesis of compound 3-17

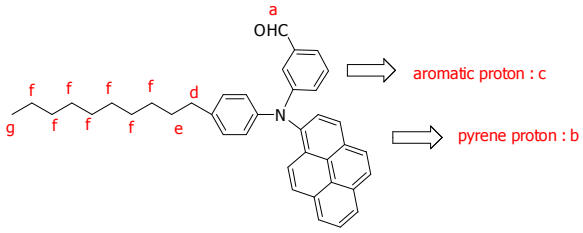

3-17

A suspension of compound **3-16** (2.21 g, 3.80 mmol) in glacial acetic acid (25 mL) was heated to 50 ºC. After a clear solution is formed 4 mL of water was added and maintained at 50 ºC for 3 h. The reaction mixture was then cooled and 50 mL ice water was added. The mixture was extracted with ethyl acetate and washed several times with water, $NaHCO_3$ solution and passed over Na_2SO_4. The organic layer was collected, combined and dried under reduced pressure and flushed through the column. The yellow solid was obtained as a product (1.59 g, 78% yield). ^{1}H NMR ($CDCl_3$, ppm) 9.79 (s, 1H, a), 8.30 – 7.67 (m, 9H, b), 7.59 – 6.93 (m, 8H, c), 2.59 – 2.47 (m, 2H, d), 1.53 (d, J = 1.0, 2H, e), 1.23 (s, 14H, f), 0.84 (d, J = 6.5, 3H, g). ^{13}C NMR, ($CDCl_3$, ppm): δ 192.8, 150.2, 145.6, 140.4, 138.5, 137.8, 131.6, 131.3, 130.2, 130.1, 129.8, 128.5, 127.8, 127.7, 127.5, 126.7, 126.6, 126.5, 126.2, 125.7, 125.6, 125.1, 123.8, 123.3, 122.2, 120.9, 35.7, 32.3, 31.8, 29.9, 23.0, 14.5.

Synthesis of compound 3-18

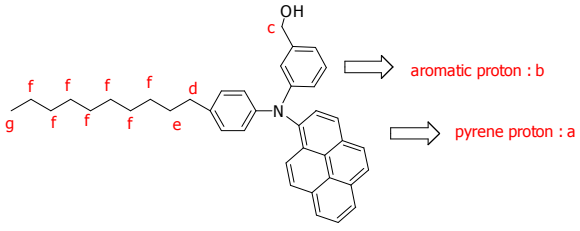

3-18

Compound **3-17** (1.99 g, 3.70 mmol) was dissolved in 20 mL tetrahydrofuran and diluted with 30 mL methanol. Sodium borohydride (0.17 g 4.44 mmol) was added in portions with efficient stirring. After the addition is complete the mixture was allowed to stir overnight. After completion of the reaction, the mixture was poured into water and the compound was extracted with diethyl ether. The organic extract was collected, dried over anhydrous $MgSO_4$ and evaporated to yield a yellow solid which was purified by column chromatography using 50% dichloromethane in hexane as the eluent to yield a yellow powder as a product (1.95 g, 98% yield). ^{1}H NMR ($CDCl_3$, ppm): δ 8.21-7.80 (br, 9H, a), 7.12-6.88 (m, 8H, b), 4.52 (s, 2H, c), 2.53 (br, 2H, d), 1.39 (br, 2H, e), 1.25 (br, 14H, f), 0.87 (br, 3H, g). ^{13}C NMR, ($CDCl_3$, ppm): δ 148.9, 148.5, 142.3, 141.3, 137.3, 131.5, 131.3, 129.8, 129.6, 129.5, 128.5, 128.1, 127.9, 127.5, 127.3, 126.6, 126.5, 126.3, 125.4, 125.3, 125.1, 123.7, 123.1, 120.7, 119.9, 119.8, 65.5, 35.6, 32.2, 31.8, 29.8, 23.0, 14.5.

Synthesis of compound 3-19

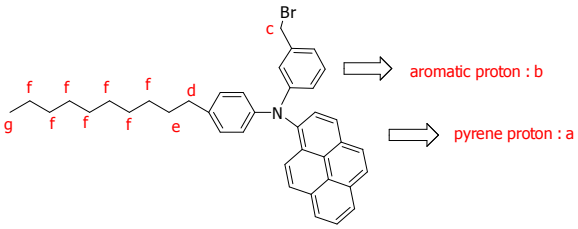

3-19

10.0 g (18.53 mmol) of compound **3-18** and catalytic amount of DMAP were dissolved in THF and the solution was cooled to 0 ^{o}C under argon atmosphere. 6.50 mL (37.05 mmol) of triethylamine and 2.87 mL (37.05 mmol) of mesyl chloride were added dropwise, and allowed to stir at room temperature for 3 h. Upon completion of the reaction, water was added and the compound was extracted with dichloromethane. The

organic layer was concentrated under reduced pressure to afford crude mixture which was taken for further step without any purification.

To the above crude mixture in THF, 7.96 g (92.46 mmol) of LiBr was added and the contents were allowed to reflux overnight. After completion of the reaction, the reaction mixture was partitioned between water and dichloromethane. The aqueous layer was extracted twice with dichloromethane. The combined organic layer was dried over Na_2SO_4 and evaporated under reduced pressure. The crude product was purified by column chromatography using 50% dichloromethane in hexane to afford the product. (11.20 g 97% yield) ^{1}H NMR ($CDCl_3$, ppm): δ 8.21-7.79 (m, 9H, a), 7.17-6.85 (m, 8H, b), 4.31 (s, 2H, c), 2.60 – 2.48 (br, 2H, d), 1.54 (br, 2H, e), 1.28 (br, 14H, f), 0.87 (t, *J* = 6.8, 3H, g). ^{13}C NMR ($CDCl_3$, ppm): δ 148.9, 148.0, 141.0, 139.0, 131.5, 131.4, 129.9, 129.8, 129.5, 128.5, 128.3, 127.9, 127.5, 127.4, 126.6, 125.5, 125.4, 125.1, 123.6, 123.4, 121.9, 121.2, 121.0, 35.6, 34.1, 32.2, 31.8, 29.9, 23.0, 14.5.

Synthesis of compound 3-20

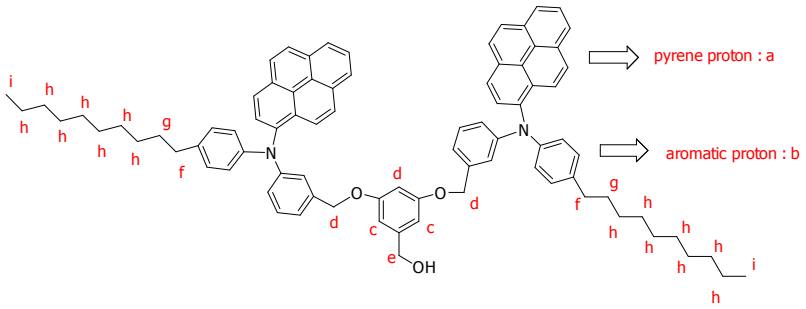

3-20

A mixture of 0.93 g (6.32 mmol) of 3,5-dihydroxybenzyl alcohol, 8.00 g (13.2 mmol) of compound **3-19**, 2.70 g (18.96 mmol) of K_2CO_3 and 0.17 g (0.63 mmol) of 18-crown-6 was heated at reflux and stirred vigorously under argon for 12 h. The reaction mixture was allowed to cool to room temperature and solvent was evaporated to dryness.

The residue was partitioned between water and dichloromethane. The organic layer was separated and aqueous layer was extracted with dichloromethane. The combined organic layer was dried over Na_2SO_4 and evaporated to dryness. The crude product was purified by column chromatography using 10% ethyl acetate in dichloromethane as the eluent to yield yellow solid as a product (4.55 g, 56% yield). ^{1}H NMR ($CDCl_3$, ppm): δ 8.18-7.76 (m, 18H, a), 7.21-6.86 (m, 16H, b), 6.30 (s, 2H, c), 6.23 (s, 1H, d), 4.77 (s, 4H, e), 4.38 (s, 2H, f), 2.52 (br, 4H, g), 1.46 (br, 4H, h) 1.24 (br, 28H, i), 0.86 (br, 6H, j). ^{13}C NMR ($CDCl_3$, ppm): δ 160.0, 149.5, 146.3, 143.4, 141.2, 138.2, 127.4, 131.5, 131.3, 129.7, 129.6, 129.5, 128.4, 128.1, 127.9, 127.5, 127.3, 126.6, 126.4, 126.3, 125.4, 124.3, 125.1, 123.7, 123.2, 120.7, 120.4, 120.2, 105.7, 101.2, 70.1, 65.3, 35.6, 32.2, 31.8, 29.9, 23.1, 14.5.

Synthesis of compound 3-6

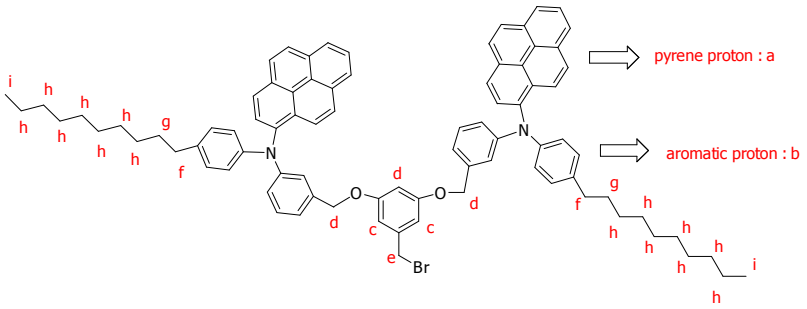

3-6

3.60 g (3.04 mmol) of compound **3-20** and catalytic amount of DMAP were dissolved in THF and the solution was cooled to 0 ^{o}C under argon atmosphere. 1.00 mL (7.60 mmol) of triethylamine and 0.50 mL (6.08 mmol) of mesyl chloride were added dropwise, and allowed to stir at room temperature for 3 h. Upon completion of the reaction, water was added and the compound was extracted with dichloromethane. The

organic layer was concentrated under reduced pressure to afford crude mixture which was taken for further step without any purification.

To the above crude mixture in THF, 1.31 g (15.20 mmol) of LiBr was added and the contents were allowed to reflux overnight. After completion of the reaction, the mixture was partitioned between water and dichloromethane. The aqueous layer was extracted twice with dichloromethane, dried over Na_2SO_4 and evaporated under reduced pressure. The crude product was purified by column chromatography using 50% hexane in dichloromethane as the eluent to afford the product. (3.69 g, quantitative yield) ^{1}H NMR ($CDCl_3$, ppm): δ 8.20-7.76 (m, 18H, a), 7.23-6.68 (m, 16H, b), 6.33 (s, 2H, c), 6.23 (s, 1H, d), 4.75 (s, 4H, e), 4.16 (s, 2H, f), 2.51 (br, 4H, g), 1.54 (br, 4H, h), 1.24 (br, 28H, i), 0.86 (m, 6H, j). ^{13}C NMR, ($CDCl_3$, ppm): δ 160.0, 149.5, 146.2, 141.2, 139.6, 138.0, 137.5, 131.5, 131.3, 129.8, 129.5, 128.4, 128.2, 127.9, 127.5, 127.3, 126.6, 126.5, 126.3, 125.4, 125.3, 125.1, 123.7, 123.3, 120.7, 120.3, 120.2, 108.2, 102.2, 70.2, 35.7, 33.8, 32.2, 21.8, 29.9, 23.0, 14.5.

Synthesis of compound 3-21

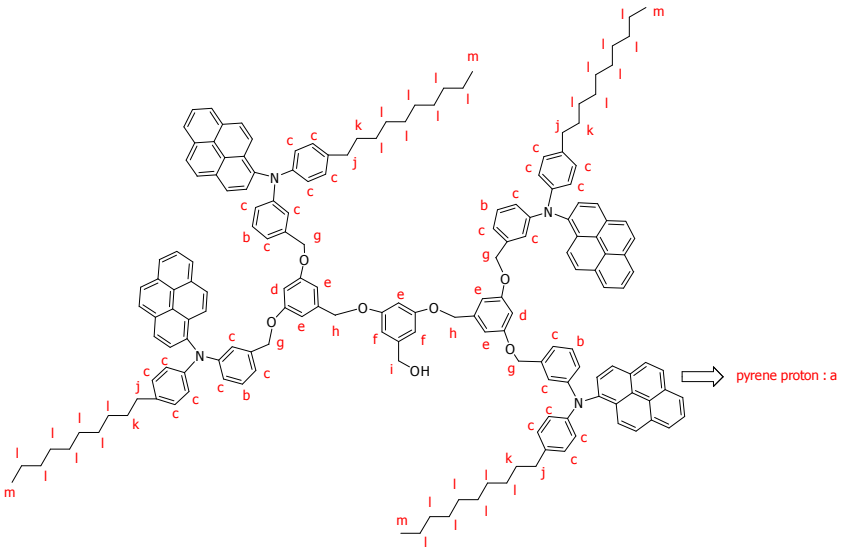

3-21

A mixture of 0.11 g (0.73 mmol) of 3,5-dihydroxybenzyl alcohol, 3.70 g (1.52 mmol) of compound **3-6**, 0.31 g (2.14 mmol) of K_2CO_3 and 0.04 g (0.07 mmol) of 18-crown-6 was heated at reflux and stirred vigorously under argon for 12 h. The reaction mixture was allowed to cool to room temperature and solvent was evaporated to dryness. The residue was partitioned between water and dichloromethane. The organic layer was separated and aqueous layer was extracted with dichloromethane. The combined organic layer was dried over Na_2SO_4 and evaporated to dryness. The crude product was purified by column chromatography using 50% dichloromethane in hexane as the eluent to afford the product. (1.47 g, 78% yield) ^{1}H NMR ($CDCl_3$, ppm): δ 8.15-7.72 (m, 36H, a), 7.19-7.08 (m, 4H, b), 7.05-6.85 (m, 28H, c), 6.48 (s, 2H, d), 6.38 (s, 5H, e), 6.25 (s, 2H, f), 4.74 (s, 8H, g), 4.69 (s, 4H, h), 4.53 (s, 2H, i), 2.49 (br, 8H, j), 1.54 (br, 8H, k), 1.22 (br, 56H, l), 0.85 (m, 12H, m). ^{13}C NMR, ($CDCl_3$, ppm): δ 160.3, 149.5, 146.3, 143.6, 141.2, 139.2, 138.2, 137.4, 131.5, 131.4, 129.8, 129.7, 129.5, 128.4, 128.2, 127.9, 127.5, 127.3, 126.6,126.5, 126.3, 125.4, 125.3, 125.1, 123.7, 123.2, 120.7, 120.3, 106.6, 105.9, 101.6, 70.2, 65.6, 35.7, 32.2, 31.8, 29.9, 23.0, 14.5.

Synthesis of compound 3-7

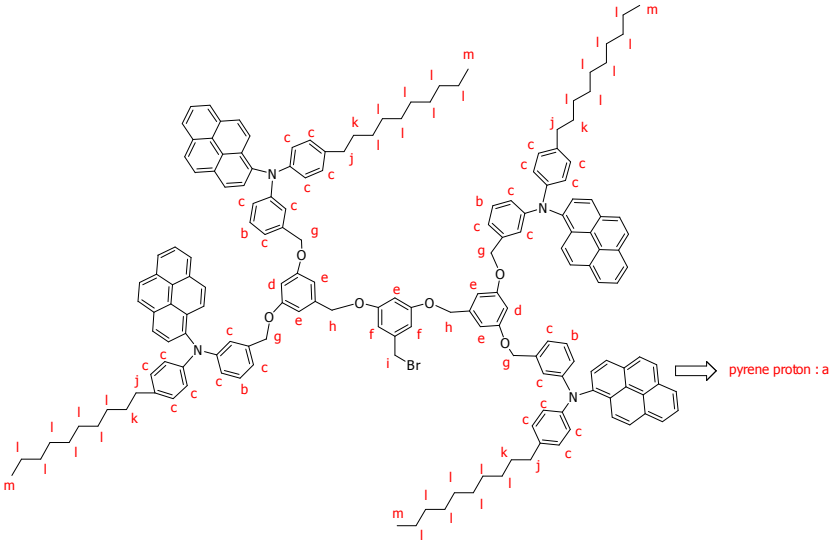

3-7

1.00 g (0.41 mmol) of compound **3-21** and catalytic amount of DMAP were dissolved in THF and the solution was cooled to 0 ^{o}C under argon atmosphere. 0.14 mL (1.02 mmol) of triethylamine and 0.06 mL (0.81 mmol) of mesyl chloride were added dropwise, and allowed to stir at room temperature for 3 h. Upon completion of the reaction, water was added and the compound was extracted with dichloromethane. The organic layer was concentrated under reduced pressure to afford crude mixture which was taken for further step without any purification.

To the above crude mixture in THF, 0.17 g (2.03 mmol) of LiBr was added and the contents were allowed to reflux overnight. After completion of the reaction, the reaction mixture was partitioned between water and dichloromethane. The aqueous layer was extracted twice with dichloromethane, dried over Na_2SO_4 and evaporated under reduced pressure. The crude product was purified by column chromatography using 50% dichloromethane in hexane to afford the product (1.03 g, quantitative yield) ^{1}H NMR ($CDCl_3$, ppm): δ 8.15-7.71 (m, 36H, a), 7.31-7.07 (m, 4H, b), 7.04-6.85 (m, 28H, c), 6.49 (s, 2H, d), 6.35 (s, 5H, e), 6.25 (s, 2H, f), 4.74 (s, 8H, g), 4.64 (s, 4H, h), 4.33 (s, 2H, i), 2.49 (br, 8H, j), 1.54 (br, 8H, k), 1.22 (br, 56H, l), 0.85 (m, 12H, m). ^{13}C NMR, ($CDCl_3$, ppm): δ 159.8, 149.11, 145.9, 140.8, 139.5, 138.5, 137.7, 137.0, 131.1, 130.9, 129.4, 129.3, 128.0, 127.7, 127.5, 127.1, 126.9, 126.2, 126.0, 125.9, 125.0, 124.9, 124.7, 123.3, 122.8, 120.3, 120.0, 119.8, 107.9, 106.2, 101.3, 69.7, 35.2, 33.5, 31.8, 29.5, 22.6, 14.1.

Synthesis of compound 3-22

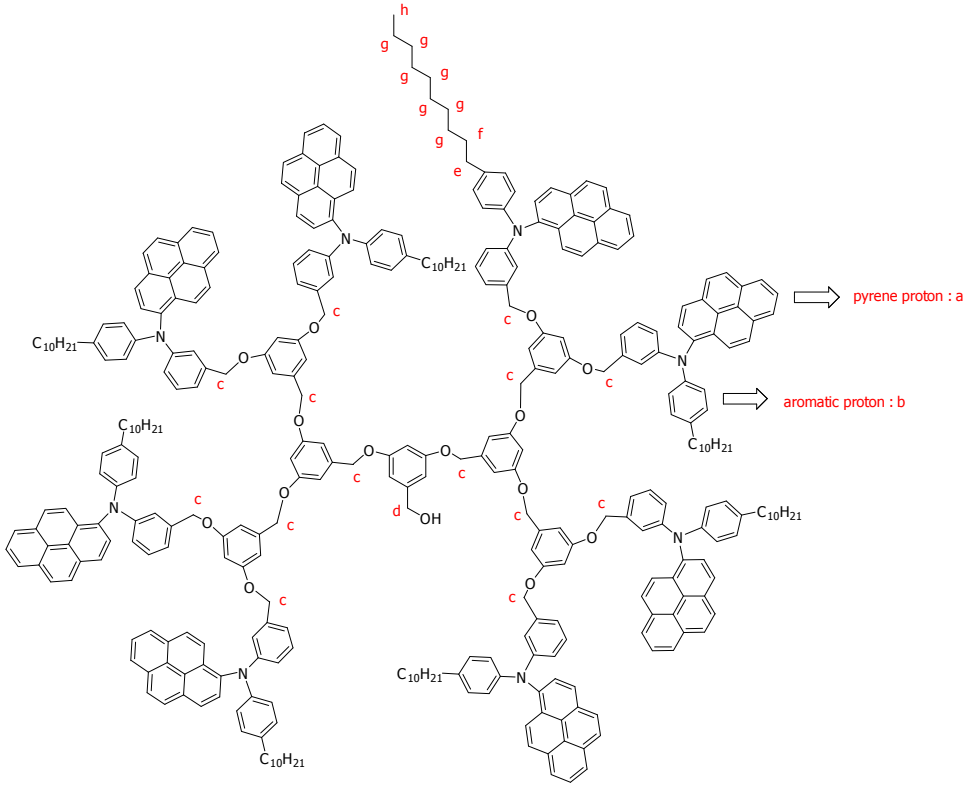

3-22

A mixture of 0.03 g (0.27 mmol) of 3,5-dihydroxybenzyl alcohol, 1.43 g (0.56 mmol) of compound **3-7**, 0.12 g (0.86 mmol) of K_2CO_3 and 0.07 g (0.03 mmol) of 18-crown-6 was heated at reflux and stirred vigorously under argon for 12 h. The reaction mixture was allowed to cool to room temperature and solvent was evaporated to dryness. The residue was partitioned between water and dichloromethane. The organic layer was separated and aqueous layer was extracted with dichloromethane. The combined organic layer was dried over Na_2SO_4 and evaporated to dryness. The crude product was purified by column chromatography using 50% dichloromethane in hexane to afford the product. (0.63 g, 53% yield) ^{1}H NMR ($CDCl_3$, ppm): δ 8.22-7.62 (m, 72H, a), 7.20-6.16 (m, 85H, b), 4.84-4.57 (m, 28H, c), 4.47 (s, 2H, d), 2.46 (br, 16H, e), 1.55 (br, 16H, j), 1.20 (br,

56H, g), 0.84 (br, 24H, h). ^{13}C NMR ($CDCl_3$, ppm): δ 160.4, 149.3, 145.9, 140.4, 138.2, 136.3, 130.9, 128.7, 127.5, 126.0, 124.8, 123.3, 120.3, 106.5, 106.1, 70.2, 35.0, 31.6, 29.3, 22.1, 14.0.

Synthesis of compound 3-8

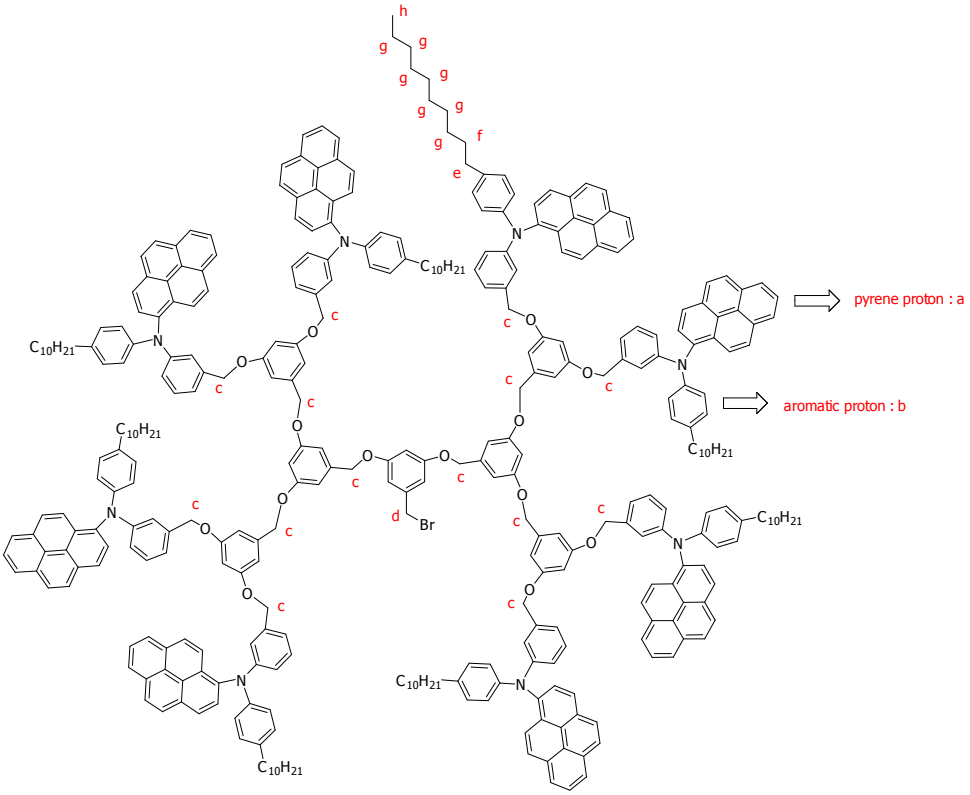

3-8

0.50 g (0.09 mmol) of compound **3-22** and catalytic amount of DMAP were dissolved in THF and the solution was cooled to 0 ^{o}C under argon atmosphere. 0.04 mL (0.25 mmol) of triethylamine and 0.02 mL (0.19 mmol) of mesyl chloride were added dropwise, and allowed to stir at room temperature for 3 h. Upon completion of the reaction, water was added and the compound was extracted with dichloromethane. The organic layer was concentrated under reduced pressure to afford crude mixture which was taken for further step without any purification.

To the above crude mixture in THF, 0.04 g (0.50 mmol) of LiBr was added and

the contents were allowed to reflux overnight. After completion of the reaction, the reaction mixture was partitioned between water and dichloromethane. The aqueous layer was extracted twice with dichloromethane, dried over Na_2SO_4 and evaporated under reduced pressure. The crude product was purified by column chromatography using dichloromethane to afford the product (0.21 g, 40% yield). ^{1}H NMR ($CDCl_3$, ppm): δ 8.22-7.65 (m, 72H, a), 7.15-6.79 (m, 63H, b), 6.51 (s, 8H, b), 6.32 (s, 10H, b), 6.21 (s, 4H, b), 4.81 (s, 4H, c), 4.53-4.74 (s, 24H, c), 4.25 (s, 2H, d), 2.46 (br, 16H, e), 1.54 (br, 16H, f), 1.20 (br, 56H, g), 0.84 (br, 24H, h). ^{13}C NMR, ($CDCl_3$, ppm): δ 159.6, 149.0, 145.9, 140.7, 139.0, 137.9, 136.5, 131.0, 129.3, 128.2, 127.9, 126.2, 124.8, 123.4, 122.7, 120.3, 119.6, 106.2, 69.7, 34.9, 31.8, 29.7, 22.5, 14.2.

Synthesis of compound 3-1

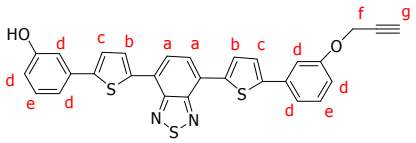

3-1

A mixture of 0.20 g (0.41 mmol) of dihydroxy benzthiadiazole unit (**2-3**), 0.03 g (0.38 mmol) of propargyl bromide, 0.15 g (1.13 mmol) of K_2CO_3 and 0.05 g (0.19 mmol) of 18-crown-6 was heated at reflux and stirred vigorously under argon overnight. The reaction mixture was allowed to cool to room temperature and solvent was evaporated to dryness. The residue was partitioned between water and dichloromethane. The organic layer was separated and aqueous layer was extracted with dichloromethane. The combined organic layer was dried over Na_2SO_4 and evaporated to dryness. The crude product was purified by column chromatography using 10% ethyl acetate in dichloromethane as the eluent to afford the product. (0.09g, 43% yield) ^{1}H NMR (DMSO-D6, ppm): δ δ 8.14 (br, 2H, a), 7.90 (br, 2H, b), 7.59-7.14 (m, 8H, c, d), 6.96-

6.79 (br, 2H, e), 4.80 (s, 2H, f), 2.59 (s, 1H, g) ^{13}C NMR, ($CDCl_3$, ppm): δ 157.4, 151.3, 145.5, 144.7, 137.9, 134.1, 129.2, 125.0, 118.4, 116.1, 114.6, 113.5, 111.9, 75.2, 55.4.

Synthesis of compound 3-9

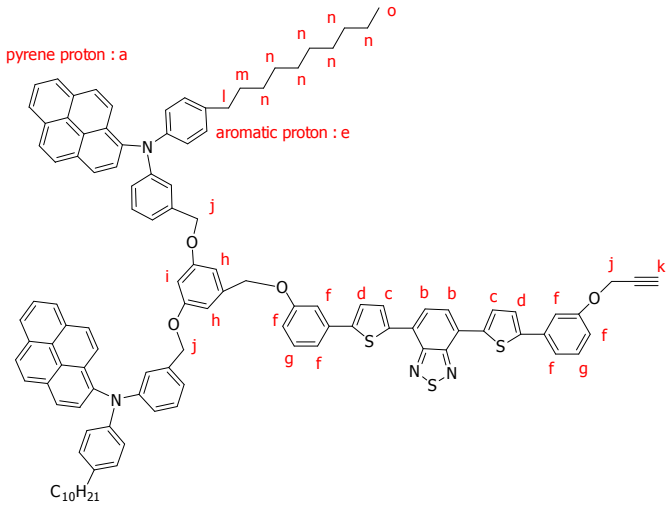

3-9

A mixture of 0.04 g (0.08 mmol) of **3-1**, 0.10 g (0.08 mmol) of compound **3-6**, 0.03 g (2.20 mmol) of K_2CO_3 and 2.00 mg (0.008 mmol) of 18-crown-6 was heated at reflux and stirred vigorously under argon for 12 h. The reaction mixture was allowed to cool to room temperature and solvent was evaporated to dryness. The residue was partitioned between water and dichloromethane. The organic layer was separated and aqueous layer was extracted with dichloromethane. The combined organic layer was dried over Na_2SO_4 and evaporated to dryness. The crude product was purified by column chromatography using 30% ethyl acetate in hexane to afford the product. (0.05 g, 48% yield) ^{1}H NMR ($CDCl_3$, ppm): δ 8.20-7.74 (m, 22H, a, b, c), 7.46-6.82 (br, 26H, d, e, f, g), 6.47 (s, 2H, h), 6.30 (s, 1H, i), 4.71-4.92 (m, 8H, j), 2.57 (s, 1H, k), 2.51 (br, 4H, l), 1.56 (br, 4H, m), 1.26 (br, 28H, n), 0.87 (t, *J* = 6.8, 6H, o). ^{13}C NMR ($CDCl_3$, ppm): δ: 159.8, 159.0, 158.0, 152.4, 149.2, 145.9, 145.3, 145.1, 140.8, 138.9, 138.6, 137.8, 137.1,

135.5, 135.3, 131.1, 129.9, 129.4, 129.1, 128.5, 128.1, 127.8, 127.6, 127.2, 126.9, 126.3, 125.9, 125.7, 125.3, 124.7, 124.4, 123.3, 122.8, 120.5, 119.9, 119.2, 118.6, 113.9, 112.5,106.2, 101.5, 69.7, 55.6, 35.2, 31.8, 29.4, 22.1, 13.8.

Synthesis of compound 3-10

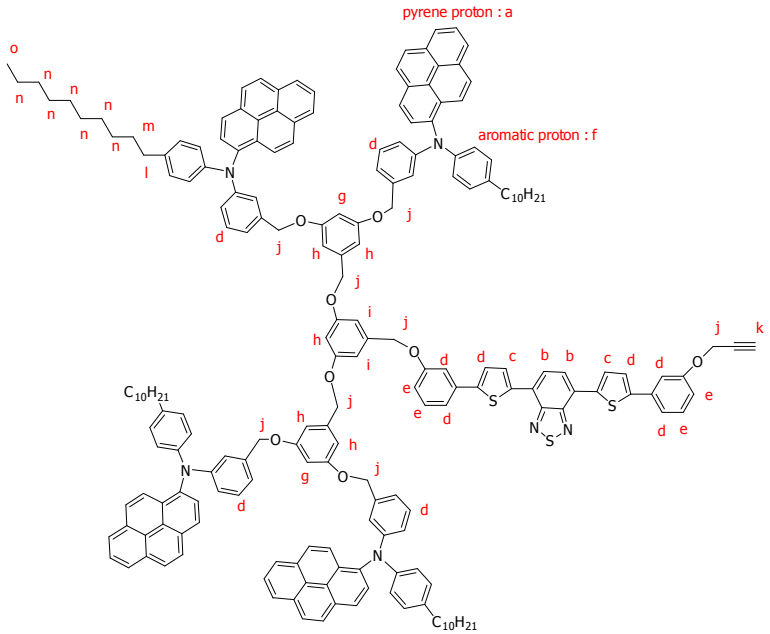

3-10

A mixture of 0.02 g (0.04 mmol) of **3-1**, 0.10 g (0.04 mmol) of compound **3-7**, 0.02 g (0.11 mmol) of K_2CO_3 and 1.00 mg (0.004 mmol) of 18-crown-6 was heated at reflux and stirred vigorously under argon for 12 h. The reaction mixture was allowed to cool to room temperature and solvent was evaporated to dryness. The residue was partitioned between water and dichloromethane. The organic layer was separated and aqueous layer was extracted with dichloromethane. The combined organic layer was dried over Na_2SO_4 and evaporated to dryness. The crude product was purified by column chromatography using 30% ethyl acetate in hexane to afford the product. (0.17g, 75% yield). ^{1}H NMR ($CDCl_3$, ppm): δ 8.31-7.52 (m, 40H, a, b, c), 7.47-7.27 (m, 10H, d), 7.21-7.06 (m, 4H, e), 7.08-6.79 (m, 28H, f), 6.62 (s, 2H, g), 6.37 (s, 5H, h), 6.25 (s, 2H,

i), 4.63-5.07 (s, 16H, j), 2.57 (br, 1H, k), 2.47 (br, 8H, l), 1.56 (br, 8H, m), 1.11-1.39 (br, 28H, n), 0.84 (m, 12H, o). ^{13}C NMR ($CDCl_3$, ppm): δ 160.1, 159.7, 159.1, 157.9, 152.4, 149.1, 145.9, 145.3, 145.0, 140.9, 139.2, 138.8, 137.9, 137.0, 135.6, 131.2, 131.0, 129.9, 129.5, 129.3, 129.1, 128.6, 128.1, 127.9, 127.5, 127.3, 127.1, 126.3, 126.0, 125.7, 125.3, 125.1, 124.8, 124.3, 123.4, 122.9, 120.4, 120.1, 119.7, 119.2, 118.5, 114.1 112.5, 106.2, 101.2, 70.1, 55.9, 35.2, 31.4, 29.4, 22.5, 13.8.

Synthesis of compound 3-11

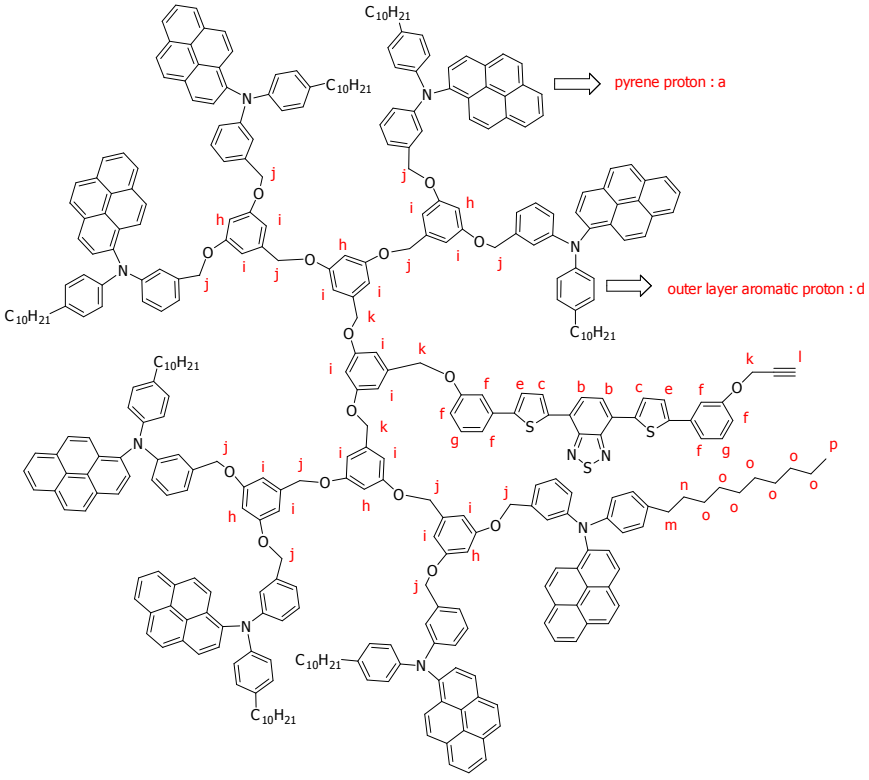

3-11

A mixture of 0.01 g (0.03 mmol) of **3-1**, 0.15 g (0.03 mmol) of compound **3-8**, 0.01 g (0.08 mmol) of K_2CO_3 and 3.00 mg (0.01 mmol) of 18-crown-6 was heated at reflux and stirred vigorously under argon for 12 h. The reaction mixture was allowed to cool to room temperature and solvent was evaporated to dryness. The residue was partitioned between water and dichloromethane. The organic layer was separated and

aqueous layer was extracted with dichloromethane. The combined organic layer was dried over Na_2SO_4 and evaporated to dryness. The crude product was purified by column chromatography using 50% dichloromethane in hexane to afford the product. (0.03 g, 19% yield) ^{1}H NMR ($CDCl_3$, ppm): δ 8.11-7.67 (m, 76H, a, b, c), 7.14-6.80 (m, 72H, d, e, f), 6.63-6.51 (br, 8H, g, h), 6.30-6.19 (m, 15H, i), 4.98-4.81 (br, 8H, k), 4.71-4.53 (m, 24H, j), 2.54 (s, 1H, l), 2.44 (br, 16H, m), 1.55 (br, 16H, n), 1.20 (br, 56H, o), 0.83 (br, 24H, p). ^{13}C NMR, ($CDCl_3$, ppm): δ 160.0, 149.3, 145.9, 141.0, 137.9, 136.9, 131.4, 129.3, 128.2, 127.2, 125.8, 125.1, 122.7, 119.6, 35.2, 31.4, 29.1, 22.5, 13.8.

Synthesis of compound 3-3

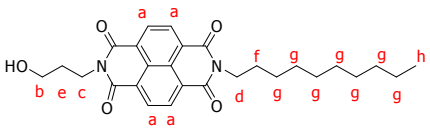

3-3

Naphthalene dianhydride (15.0 g, 0.55 mol) was taken into a three-necked flask with freshly distilled DMF. The slurry was heated to about 140 ^{o}C under N_2 atmosphere. To this, decylamine (11.1 mL, 0.55 mol) was added dropwise for about 10 minutes and the reaction mixture was refluxed overnight. After the complete consumption of naphthalene dianhydride, 3-amino-1-propanol (4.20 mL, 0.55 mol) was added and the mixture was left at reflux for overnight. After completion of the reaction, the mixture was cooled down and DMF was evaporated under low pressure. The residue was partitioned between dichloromethane and water and dried over $MgSO_4$. The organic layer was collected and concentrated under low pressure. The crude product was purified by column chromatography using 30% dichlomethane in hexane to afford the product (13.25 g, 51% yield). ^{1}H NMR ($CDCl_3$, ppm): δ 8.72 (s, 4H, a), 4.45(br, 2H, b), 4.20 (br, 2H, c), 3.68 (br, 2H, d), 1.98 (br, 2H, e), 1.75(2H, f), 1.30 (br, 14H, g), 0.98 (br, 3H, h)

^{13}C-NMR ($CDCl_3$, ppm): δ 163.5, 131.2, 120.6, 59.2, 40.4, 36.4, 31.8, 29.5, 29.3, 28.1, 27.1, 22.7, 14.1.

Synthesis of compound 3-4

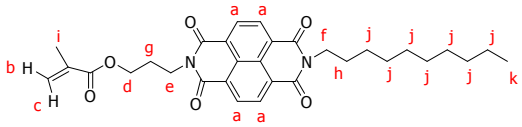

3-4

Compound **3-3** (1.32 g, 2.84 mmol) and a catalytic amount of DMAP were placed into a round bottom flask and THF was added as a solvent. The solution was cooled to 0 ^{o}C and triethylamine (0.79 mL, 5.67 mmol) was added followed by mathacryloyl chloride (0.55 mL, 5.67 mmol). The mixture was left at room temperature overnight. After the completion of the reaction, the mixture was extracted using water and dichloromethane. Organic layer was collected and evaporated under reduced pressure. The crude product was purified by column chromatography using dichloromethane to afford pale yellow solid as a product (0.79g, 49% yield). ^{1}H NMR ($CDCl_3$, ppm): δ 8.78 (s, 4H, a), 6.12 (m, 1H, b), 5.54 (m, 1H, c), 4.30 (m, 6H, d, e, f), 2.20 (m, 2H, g), 1.76 (m, 2H, h), 1.45 (s, 3H, i), 1.28 (m, 14H, j), 0.89 (s, 3H, k) ^{13}C NMR ($CDCl_3$, ppm): δ 167.2, 163.1, 136.3, 131. 3, 131.1, 126.8, 126.3, 125.4, 63.7, 41.0, 38.2, 31.9, 29.5, 29.1, 28.0, 27.4, 26.9, 22.5, 18.3, 14.1.

Synthesis of compound 3-23

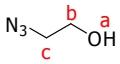

3-23

To a round bottom flask, 0.25 g (3.08 mmol) chloroethanol and 0.30 g (4.61 mmol) sodium azide were taken and 5 mL DMSO was added as a solvent. The mixture was heated at 100 ^{o}C for overnight. After completion of the reaction, water was added

and the mixture was extracted with dichloromethane (3x25 mL). The organic layer was combined and the solvent was evaporated. The product was obtained without any purifificaiton. ^{1}H NMR ($CDCl_3$, ppm): δ 5.24 (s, 1H, a), 3.68 (m, 2H, b), 3.31 (m, 2H, c) ^{13}C-NMR ($CDCl_3$, ppm): δ 60.7, 53.3.

Synthesis of compound 3-2

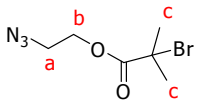

3-2

. 0.25 g (0.99 mmol) of compound **3-23** and 0.96 g (1.99 mmol) 2-bromoisobutylic acid were dissolved in 30 mL dichloromethane. The reaction mixture was cooled down in ice-water bath and a solution of 1.18 g (1.99 mmol) dicylclohexyl carbodiimide in 10 mL dichloromethane was slowly added while stirring. A solution of 0.17 g (0.49 mmol) 4-dimethylaminopyridine in 5 mL dichloromethane was subsequenly added. The mixture was stirred at 0 ^{o}C for 1 h and then at room temperature for 24 h. The precipitated dicyclohexyl urea was filltered on cotton twice and washed with dichloromethane. The solution was extraced with a solution of $NaHCO_3$ (5%) followed by dichloromethane (3x25 mL) and dried over $MgSO_4$. The volatiles were removed by reduced pressure and the crude product was purified by column chromatography using 10% ethylacetate in hexane. The product was obtained as a colorless liquid with a quantitative yield. ^{1}H NMR ($CDCl_3$, ppm): δ 4.34 (br, 2H, a), 3.53 (br, 2H, b), 1.96 (s, 6H, c) ^{13}C NMR ($CDCl_3$, ppm): δ 171.4, 64.6, 55.2, 49.6, 30.6.

Synthesis of compound 3-5

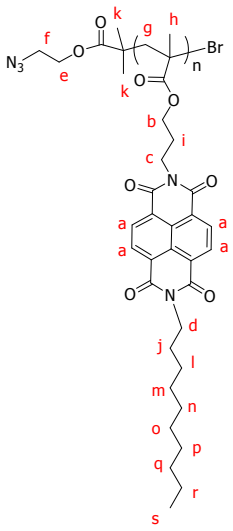

3-5

4.00 mg (0.03 mmol) of Cu(I)Br was taken in a 5 mL round bottom flask equipped with a septum and gas inlet/outlet. The flask was degassed with argon for 5 min. Then, 12.0 µL (0.06 mmol) of *N,N,N',N'',N''*-pentamethyl diethylenetriamine (PMDETA) was added and stirred for 5 more minutes. To this reaction mixture, the solution of the monomer **3-4** (800 mg, 1.50 mmol) in 400 µL degassed anisole was added and it was stirred for another 5 minutes. To this mixture, 5.00 µL (0.03 mmol) of the initiator **3-2** was added and the flask was transferred to a preheated oil bath at 65 °C. The polymerization was carried out at the same temperature under argon atmosphere for 6 h. After that, the reaction was stopped and the polymer was dissolved in THF. The polymer solution was filtered though silica to remove copper salt and then precipitated from diethylether and dried over vacuum for 6 h. The polymer was obtained as a yellow-brown solid with 58% yield. ^{1}H NMR ($CDCl_3$, ppm): δ 8.94-7.95 (br, 4H, a), 4.35-3.83 (br, 8H, b, c, d, e), 3.72 (br, 2H, f), 2.21-1.89 (br, 7H, g, h, i), 1.89-1.54 (br, 2H, j), 1.49-0.93 (br, 20H, k, l-r), 0.93-0.79 (br, 3H, s). Mn= 9326; PDI= 1.14; Degree of polymerization = 17.

Synthesis of G1 dendron-rod coil

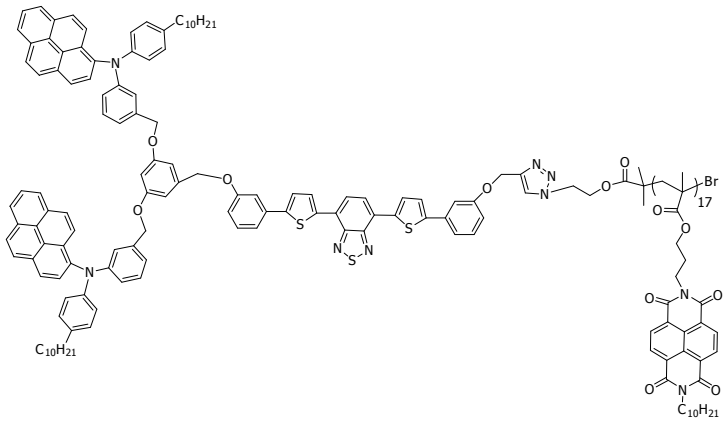

G1 dendron-rod coil

Compound **3-9** (19.0 mg, 11.0 µmole), compound **3-5** (75.0 mg, 9.20 µmole), CuBr (5.30 mg, 37.0 µmole) and PMDETA (8.00 µL, 37.0 µmole) were added into a Schlenk flask and 1 mL anhydrous THF was added as a solvent. The mixture was stirred for 10 min and degassed by three freeze-thaw cycles. The Schlenk flask was placed in a constant temperature oil bath at 25 ^{0}C for 24 h. After completion of the reaction, the THF in the mixture was removed by evaporation and the dry crude product was purified by column chromatography using 5% THF in dichloromethane to afford the product. (46.0 mg, 48% yield), SEC, Mn= 10800, PDI= 1.07.

Synthesis of compound G2 dendron-rod-coil

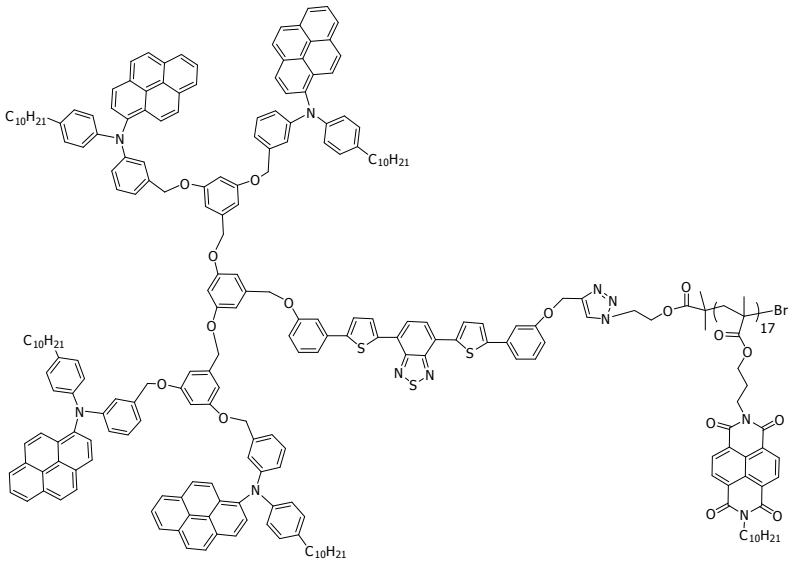

G2 dendron-rod-coil

Compound **3-10** (33.0 mg, 11.0 µmole), compound **3-5** (75.0 mg, 9.20 µmole), CuBr (5.30 mg, 37.0 µmole) and PMDETA (8.00 µL, 37.0 µmole) were added into a Schlenk flask and 1 mL anhydrous THF was added as a solvent. The mixture was stirred for 10 min and degassed by three freeze-thaw cycles. The Schlenk flask was placed in a constant temperature oil bath at 25 ^{0}C for 24 h. After completion of the reaction, the THF in the mixture was removed by evaporation and the dry crude product was purified by column chromatography using 5% THF in dichloromethane to afford the product. (80.0 mg, 76% yield), SEC, Mn= 12900, PDI= 1.05.

Synthesis of compound G3 dendron-rod-coil

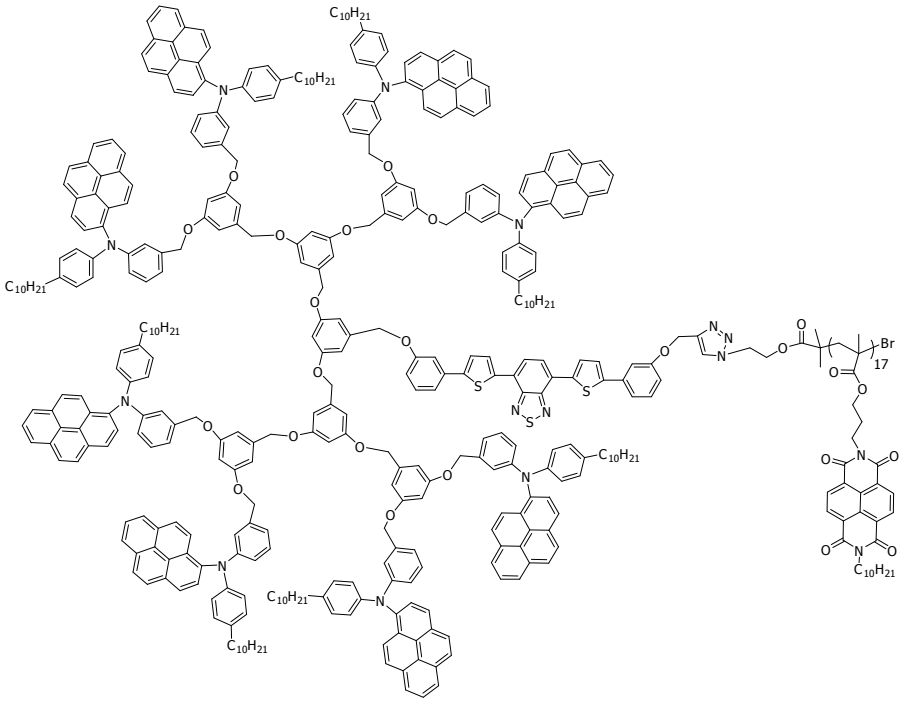

G3 dendron-rod-coil

Compound **3-11** (76.0 mg, 11.0 µmole), compound **3-5** (75.0 mg, 9.20 µmole), CuBr (5.30 mg, 37.0 µmole) and PMDETA (8.00 µL, 37.0 µmole) were added into a Schlenk flask and 1 mL anhydrous THF was added as a solvent. The mixture was stirred for 10 min and degassed by three freeze-thaw cycles. The Schlenk flask was placed in a constant temperature oil bath at 25 °C for 24 h. After completion of the reaction, the THF in the mixture as removed by evaporation and the dry crude product was purified by column chromatography using 5% THF in dichloromethane to afford the product. (62.0 mg, 41% yield), SEC, Mn= 13200, PDI= 1.09.

Synthesis of compound 3-24

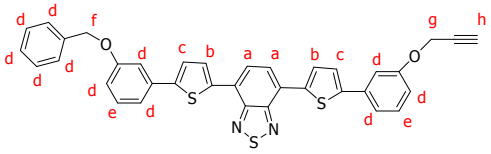

3-24

A mixture of 0.05 g (0.10 mmol) of **3-1**, 0.02 g (0.30 mmol) of benzyl bromide, 0.04 g (0.29 mmol) of K_2CO_3 and 13.00 mg (0.05 mmol) of 18-crown-6 was heated at reflux and stirred vigorously under argon for 12 h. The reaction mixture was allowed to cool to room temperature and solvent was evaporated to dryness. The residue was partitioned between water and dichloromethane. The organic layer was separated and aqueous layer was extracted with dichloromethane. The combined organic layer was dried over Na_2SO_4 and evaporated to dryness. The crude product was purified by column chromatography using 50% ethyl acetate in hexane as the eluent to afford the product (0.04 g, 67% yield). ^{1}H NMR ($CDCl_3$, ppm): δ 8.13 (s, 2H, a), 7.91 (s, 2H, b), 7.38 (m, 13H, c, d), 7.02 – 6.91 (m, 2H, e), 5.15 (s, 2H, f), 4.78 (s, 2H, g), 2.57 (s, 1H, h).^{13}C ($CDCl_3$, ppm): δ 159.2, 157.9, 145.6, 138.7, 136.8, 135.3, 130.1, 129.0, 127.5, 125.6, 123.9, 119.6, 118.7, 114.4, 112.3, 69.9, 55.9.

Synthesis of compound 3-12

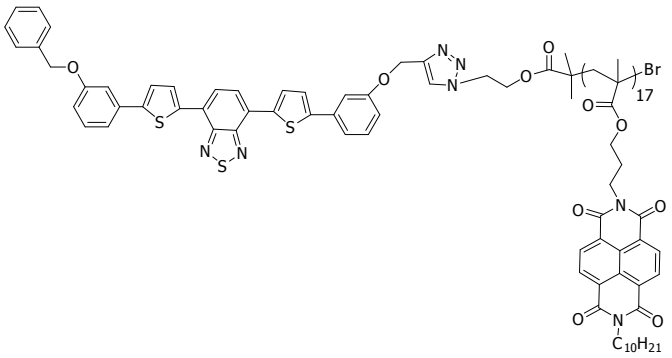

3-12

Compound **3-24** (7.0 mg, 11.0 µmole), compound **3-5** (75.0 mg, 9.20 µmole), CuBr (5.30 mg, 37.0 µmole) and PMDETA (8.00 µL, 37.0 µmole) were added into a Schlenk flask and 1 mL anhydrous THF was added as a solvent. The mixture was stirred for 10 min and degassed by three freeze-pump-thaw cycles. The Schlenk flask was placed in a constant temperature oil bath at 25 °C for 24 h. After completion of the reaction, the THF in the mixture as removed by evaporation and the dry crude product was purified by column chromatography using 5% THF in dichloromethane to afford the product. (34.0 mg, 40% yield), SEC, Mn= 9980 PDI= 1.08.

Synthesis of compound 3-25

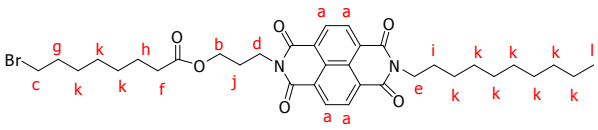

3-25

1.00 g (4.78 mmol) of 8-bromooctanoic acid was placed in a round bottom flask and 20 mL of dichloromethane was added as a solvent. To this solution, 0.83 mL (9.57 mmol) of oxalyl chloride was slowly added. The reaction mixture was stirred at room temperature for 6 h. Then, the solvent was removed by a rotary evaporator to yield the corresponding acid chloride which was further used for the next step without purification.

To the round bottom flask, 1.09 g (4.78 mmol) of acid chloride, 1.11 g (2.38 mmol) of compound **3-3,** 0.45 mL (4.78 mmol) of triethylamine, and catalytic amount of DMAP were added and THF was used as a solvent. The mixture was stirred at room temperature overnight. After completion of the reaction, water was added and the mixture was partitioned between dichloromethane and water. The organic layer was collected and concentrated using a rotary evaporator. The crude product is purified by

column chromatography using 50% dichloromethane in hexane to obtain the product. (0.37 g, 23% yield) ^{1}H NMR ($CDCl_3$, ppm): δ 8.79 (s, 4H, a), 4.35 (t, *J* = 7.1, 2H, b), 4.27 – 4.15 (m, 4H, c, d), 3.43 (m, 4H, e, f), 1.94 – 1.86 (m, 4H, g, h), 1.66 (m, 4H, i, j), 1.36 (m, 20H, k), 0.89 (t, *J* = 6.7, 3H, l). ^{13}C NMR ($CDCl_3$, ppm): δ 173.0, 162.3, 130.9, 126.4, 61.8, 45.1, 41.0, 38.1, 34.2, 32.6, 31.9, 29.6, 29.3, 28.9, 28.5, 28.1, 27.4, 27.0, 26.6, 24.8, 22.5, 14.2.

Synthesis of compound 3-15

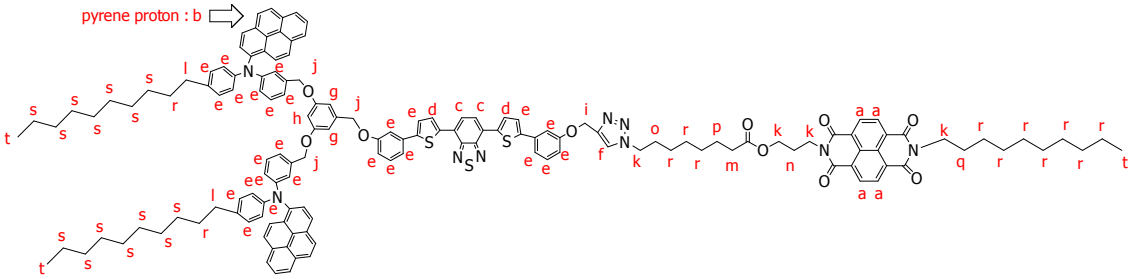

3-15

0.046 g (0.07 mmol) of compound **3-25** and 0.007 g (0.11 mmol) of sodium azide were added into a round bottom flask and acetonitrile was added as a solvent. The mixture was left at reflux overnight. After completion of the reaction, water was added and the mixture was partitioned between dichloromethane and water. The organic layer was collected and evaporated to obtain an azide functionalized naphthalene bisimide derivative (**3-14**). This product was further used in the next step without purification. ^{1}H NMR ($CDCl_3$, ppm): δ 8.79 (s, 4H), 4.35 (t, *J* = 7.2, 2H), 4.29 – 4.17 (m, 4H), 3.28 (t, *J* = 6.9, 2H), 2.31 (t, *J* = 7.5, 2H), 2.23 – 2.10 (m, 2H), 1.77 (s, 2H), 1.68 – 1.52 (m, 4H), 1.31 (d, *J* = 22.1, 20H), 0.89 (t, *J* = 6.8, 3H).

Above prepared compound (**3-14**) (8.00 mg, 9.20 µmole), compound **3-9** (19.0 mg, 11.0 µmole), CuBr (5.30 mg, 37.0 µmole) and PMDETA (8.00 µL, 37.0 µmole)

were added into a Schlenk flask and 1 mL anhydrous THF was added as a solvent. The mixture was stirred for 10 min and degassed by three freeze-pump-thaw cycles. The Schlenk flask was placed in a constant temperature oil bath at 25 °C for 24 h. After completion of the reaction, the THF in the mixture as removed by evaporation and the dry crude product was purified by column chromatography using 5% THF in dichloromethane to afford the product (22.0 mg, 78% yield). ^{1}H NMR ($CDCl_3$, ppm): δ 8.62 (s, 4H, a), 8.16 – 7.55 (m, 22H, b, c, d), 7.39 – 6.87 (m, 26H, e), 6.88 – 6.74 (m, 1H, f), 6.46 (s, 2H, g), 6.30 (s, 1H, h), 5.29 (s, 2H, i), 4.81 (s, 6H, j), 4.01-4.38 (m, 8H, k), 2.57 – 2.43 (m, 4H, l), 2.26 (m, 2H, m), 2.07 (m, 2H, n), 1.93 (m, 2H, o), 1.59 (m, 28H, p, q, r), 1.24 (br, 28H, s), 0.85 (br, 9H, t) ^{13}C NMR ($CDCl_3$, ppm): δ 174.2, 162.7, 159.7, 158.5, 152.4, 149.3, 145.5, 143.5, 140.9, 138.8, 137.9, 137.1, 135.4, 131.3, 131.0, 130.0, 129.2, 128.6, 127.9, 127.8, 127.4, 127.2, 126.9, 126.6, 126.3, 126.1, 126.9, 125.6, 125.3, 125.0, 124.8, 124.2, 123.4, 122.9, 122.6, 120.4, 120.1, 119.9, 118.9, 111.9, 106.9, 101.5, 69.4, 62.5, 50.7, 35.3, 34.0, 31.9, 31.4, 29.7, 28.8, 27.5, 27.0, 26.1, 24.7, 22.7, 14.1 SEC, Mn= 2700, PDI= 1.03.

Synthesis of compound 4-5

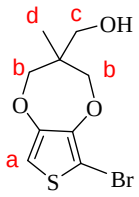

4-5

In a two-necked 250 mL round-bottom flask filled with 20 mL chloroform, 1.00 g (5.00 mmol) of ProDOT was added and the solution was bubbled under argon for 20 min. Then, 0.88 g (5.00 mmol) of N-bromosuccinimide (NBS) was added and the solution was stirred for 20 h. After completion, the solvent was removed under vaccuo and the

resulting residue was purified by column chromatography using 10% ethyl acetate in CH_2Cl_2 to get a white solid was as a product (0.49 g, 32 %yield). ^{1}H NMR ($(CD_3)_2CO$, ppm): δ 6.72 (s, 1H, a), 4.00 (m, 2H, b), 3.61 (m, 2H, b), 3.61 (s, 2H, c), 0.96 (s, 3H, d) ^{13}C NMR ($(CD_3)_2CO$, ppm): δ 147.8, 90.8, 76.9, 63.7, 43.7, 16.1.

Synthesis of compound 4-2

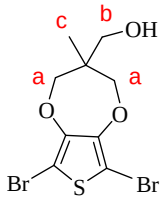

4-2

In a two-necked 250 mL round-bottom flask filled with 20 mL chloroform, 0.66 g (3.00 mmol) of ProDOT was added and the solution was bubbled under argon for 20 minutes. Then, 1.11 g (9.00 mmol) of N-bromosuccinimide (NBS) was added and the solution was stirred for 20 h. After completion, the solvent was removed under vaccuo and the resulting residue was purified by column chromatography using 100% CH_2Cl_2. The white solid was obtained as a product (1.17 g, quantitative yield). ^{1}H NMR ($(CD_3)_2CO$, ppm): δ 4.00 (d, 2H, *J* = 12.0, a), 3.73 (d, 2H, *J* = 12, a), 3.60 (s, 2H, b), 0.97 (s, 3H, d) ^{13}C NMR ($(CD_3)_2CO$, ppm): δ 147.8, 90.8, 76.9, 63.7, 43.7, 16.1.

Synthesis of compound 4-3

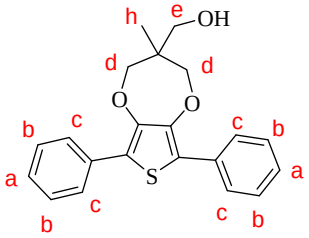

4-3

1.00 g, (2.80 mmol) of compound **4-2**, 0.75 g (6.15 mmol) of phenyl boronic acid and 1 M aqueous solution of Na_2CO_3 (30 mL) were deaerated several times and placed

under argon followed by the addition of 0.10 g (0.08 mmol) of $Pd(PPh_3)_4$. The mixture was stirred under reflux for 10 h. After this period, another portion of catalysts (0.01 g, 0.008 mmol) was added after which the reaction mixture was stirred for another 4 hours under reflex. The reaction mixture was then poured into CH_2Cl_2/ H_2O and extracted with CH_2Cl_2 several times, and the combined organic fractions were washed with water, dried and then concentrated. The resulting solid was purified by column chromatography using 40% ethyl acetate in hexane to obtain a white solid as a product (0.60 g, 61% yield). ^1H NMR ($CDCl_3$, ppm): δ 7.72 (d, J = 8.2, 4H, c), 7.46 – 7.33 (m, 4H, b), 7.31 – 7.20 (m, 2H, a), 4.25 (m, 2H, d), 3.90 (m, 2H, d), 3.84 (m, 2H, e), 1.03 (br, 3H, h). ^{13}C NMR ($CDCl_3$, ppm): δ 146.2, 132.4, 128.6, 126.5, 120.3, 65.6, 43.5, 17.0.

Synthesis of compound 4-6

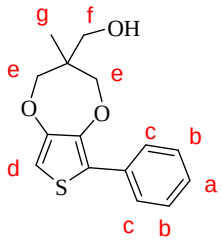

4-6

1.00 g, (3.48 mmol) of compound **4-5**, 0.52 g (4.30 mmol) of phenyl boronic acid and 1 M aqueous solution of Na_2CO_3 (30 mL) were deaerated several times and placed under argon followed by the addition of 0.12 g (0.11 mmol) of $Pd(PPh_3)_4$. The mixture was stirred under reflux for 10 h. After this period, another portion of catalysts (0.01 g, 0.01 mmol) was added after which the reaction mixture was stirred for another 4 hours under reflex. The reaction mixture was then poured into CH_2Cl_2/ H_2O and extracted with CH_2Cl_2 several times, and the combined organic fractions were washed with water, dried and then concentrated. The resulting solid was purified by column chromatography using

50% ethyl acetate in hexane to get a white solid as a product (0.70 g, 70% yield). ^{1}H NMR ($CDCl_3$, ppm): δ 7.67 (d, *J* = 8.1, 2H, c), 7.36 (t, *J* = 7.7, 2H, b), 7.30 – 7.21 (m, 1H, a), 6.46 (s, 1H, d), 4.17 (dd, *J* = 12.1, 26.3, 2H, e,), 3.90 – 3.75 (m, 4H, e, f), 0.99 (s, 3H, g). ^{13}C NMR ($CDCl_3$, ppm): δ 150.4, 145.2, 133.1, 128.2, 126.5, 122.7, 103.1, 65.9, 43.8, 16.6.

Synthesis of compound 4-18

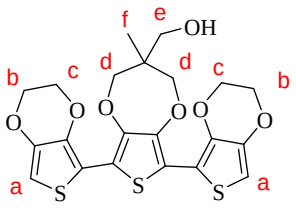

4-18

To a two-necked 50 mL round bottom flask, 0.50 g (1.40 mmol) of compound **4-2**, 1.32 g (3.07 mmol) of 2-tributyltin EDOT (**4-13**) in DMF were deaerated several times and then handled under argon. 0.07 g (0.10 mmol) of $Pd(PPh_3)_2Cl_2$ was added and the mixture was stirred at 80 ^{o}C for 2 h. After completion of the reaction, water was added and the mixture was extracted using CH_2Cl_2 (3x20 mL). The organic layer was collected and dried over anhydrous $MgSO_4$. The resulting residue was purified by column chromatography using 50% ethylacetate in dichloromethane. The yellow solid was obtained as a product (0.36 g, 53% yield). ^{1}H NMR ($CDCl_3$, ppm): δ 6.24 (s, 2H, a), 4.33 (s, 4H, b), 4.21 (br, 6H, c, d), 3.85 (br, 2H, d), 3.75 (br, 2H, e), 0.96 (s, 3H, f) ^{13}C NMR ($CDCl_3$, ppm): δ 145.2, 141.0, 137.2, 112.8, 109.7, 97.6, 76.9, 65.5, 64.2, 63.5, 43.5, 15.6.

Synthesis of compound 4-11

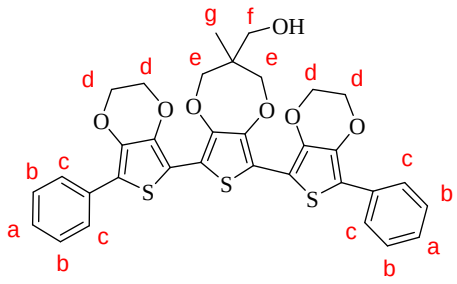

4-11

To a two-necked 50 mL round bottom flask, 0.50 g (1.36 mmol) of compound **4-2**, 1.52 g (2.99 mmol) of 2-phenyl-5-tributyl tin EDOT (**4-8**) in DMF were deaerated several times and then handled under argon. 0.07 g (0.10 mmol) of $Pd(PPh_3)_2Cl_2$ was added and the mixture was stirred at 80 ^oC for 2 h. After completion of the reaction, water was added and the mixture was extracted using CH_2Cl_2 (3x20 mL). The organic layer was collected and dried over anhydrous $MgSO_4$. The resulting residue was purified by column chromatography using 10% ethyl acetate in dichloromethane. The yellow solid was obtained as a product (0.46 g, 17 %yield). ^1H NMR ($(CD_3)_2CO$, ppm): δ 7.74 (br, 4H, c), 7.39 (t, *J* = 7.7, 4H, b), 7.22 (br, 2H, a), 4.45 (s, 8H, d), 4.25 (d, *J* = 11.9, 2H, e), 3.91 (d, *J* = 11.9, 2H, e), 3.78 (d, *J* = 6.0, 2H, f), 1.07 (s, 3H, g). ^{13}C-NMR ($(CD_3)_2CO$, ppm): δ 144.1, 128.6, 126.2, 125.5, 76.3, 64.9, 63.0, 43.5, 15.9.

Synthesis of compound 4-7

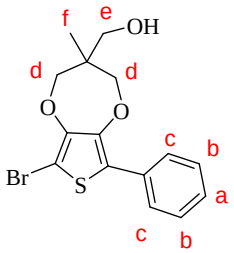

4-7

In a two-necked 250 mL round-bottom flask filled with 20 mL chloroform, 0.30 g (1.09 mmol) of compound **4-6** was added and the solution was bubbled under argon for 20 min. Then, 0.39 g (2.17 mmol) of N-bromosuccinimide (NBS) was added and the solution was stirred for 20 h. After completion, the solvent was removed under vaccuo and the resulting residue was purified by column chromatography using 10% ethyl acetate in hexane to obtain a white solid as a product (0.25 g, 39% yield). ^{1}H NMR ($CDCl_3$, ppm): δ 7.62 (d, *J* = 7.3, 2H, c), 7.38 (t, *J* = 7.6, 2H, b), 7.30 (m, 1H, a), 4.22 (dd, *J* = 7.1, 12.1, 2H, d), 3.95 – 3.76 (m, 4H, d e), 1.03 (s, 3H,f). ^{13}C-NMR ($CDCl_3$, ppm): δ149.0, 145.2, 132.7, 131.4, 128.6, 127.6, 125.5, 90.7, 76.3, 64.2, 43.5, 15.9.

Synthesis of compound 4-9

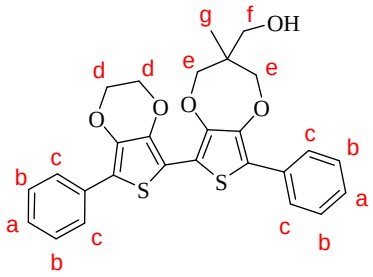

4-9

To a two-necked 50 mL round bottom flask, 1.00 g (3.01 mmol) of compound **4-7**, 1.83 g (3.62 mmol) of 2-phenyl-5-tributyl tin EDOT (**4-8**) in DMF were deaerated several times and then handled under argon. 0.15 g (0.21 mmol) of $Pd(PPh_3)_2Cl_2$ was added and the mixture was stirred at 80 ^{o}C for 2 h. After completion of the reaction, water was added and the mixture was extracted using CH_2Cl_2 (3x20 mL). The organic layer was collected and dried over anhydrous $MgSO_4$. The resulting residue was purified by column chromatography using dichloromethane to obtain a white solid as a product (0.42 g, 29% yield).^{1}H NMR ($CDCl_3$, ppm): δ 7.82 – 7.66 (m, 4H, c), 7.38 (t, *J* = 7.4, 4H, b), 7.27 – 7.18 (m, 2H, a), 4.36 (m, 6H, d, e), 4.01 – 3.79 (m, 4H, e, f), 1.04 (s, 3H, g).

^{13}C NMR ($CDCl_3$, ppm): δ 146.2, 145.2, 138.2, 137.4, 133.1, 128.6, 126.7, 125.7, 120.0, 115.5, 113.3, 108.3, 65.6, 64.7, 43.7, 17.0.

Synthesis of compound 4-14

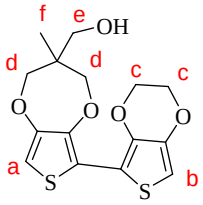

4-14

To a two-necked 50 mL round bottom flask, 1.00 g (3.60 mmol) of compound **4-5**, 1.86 g (4.32 mmol) of 2-tributyltin EDOT (**4-13**) in DMF were deaerated several times and then handled under argon. 0.18 g (0.25 mmol) of $Pd(PPh_3)_2Cl_2$ was added and the mixture was stirred at 80 ^{o}C for 2 h. After completion of the reaction, water was added and the mixture was extracted using CH_2Cl_2 (3x20 mL). The organic layer was collected and dried over anhydrous $MgSO_4$. The resulting residue was purified by column chromatography using 30% ethyl acetate in hexane to obtain a yellow solid as a product (1.04 g, 85% yield). ^{1}H NMR ($(CD_3)_2CO$, ppm): δ 6.54 (s, 1H, a), 6.34 (s, 1H, b) , 4.34 (m, 2H, c), 4.26 (m, 2H, c), 4.10 (d, J = 16.0 Hz, 1H, d), 4.00 (d, J = 16.0 Hz, 1H, d), 3.79 (d, J = 25.2 Hz, 1H, d), 3.72 (d, J = 25.2 Hz, 1H, d), 3.67 (m, 2H, e), 0.99 (s, 3H, f) ^{13}C NMR ($(CD_3)_2CO$, ppm): δ 149.9, 141.4, 102.8, 97.6, 78.4, 78.1, 77.8, 76.8, 76.5, 65.1, 64.5, 64.0, 43.8, 17.5.

Synthesis of compound 4-15

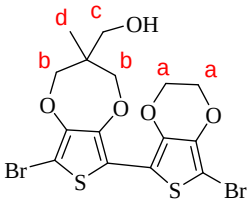

4-15

A round bottom flask with a stirring bar was charged with 0.11 g (0.33 mmol) of compound **4-14** in dry dichloromethane. 0.12 g (0.69 mmol) of N-bromosuccinimide was added and the reaction was allowed to stir at 0 ^{o}C for 2 h. The slightly blue mixture was dissolved in 500 mL of dichloromethane and washed by $NH_3.H_2O$ (10%, 150 mL), H_2O (3x50 mL) and brine (2x50 mL) and dried over $MgSO_4$. The CH_2Cl_2 was evaporated to give a yellowish solid that was further used in the next step without purification. ^{1}H NMR ($CDCl_3$, ppm): δ 4.34 (s, 4H, a), 4.22 (t, *J* = 12.5, 2H, b), 3.89 – 3.75 (m, 4H, b, c), 1.02 (s, 3H, d).^{13}C-NMR is not taken due to its instability.

Synthesis of compound 4-16

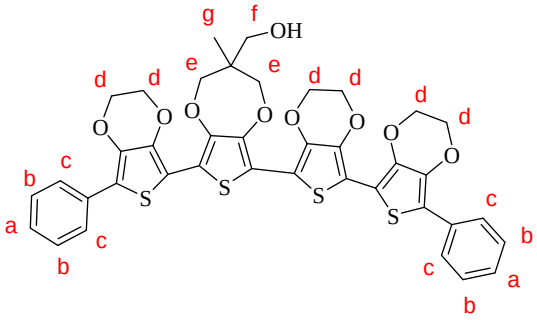

4-16

To a two-necked 50 mL round bottom flask, 0.12 g (0.24 mmol) of compound **4-15**, 0.26 g (0.51 mmol) of 2-phenyl-5-tributyl tin EDOT (**4-8**) in DMF were deaerated several times and then handled under argon. 0.01 g (0.17 mmol) of $Pd(PPh_3)_2Cl_2$ was added and the mixture was stirred at 80 ^{o}C for 2 h. After completion of the reaction, water was added and the mixture was extracted using CH_2Cl_2 (3x20 mL). The organic layer was collected and dried over anhydrous $MgSO_4$. The resulting residue was purified by column chromatography using 30% ethylacetate in hexane to obtain an orange solid as a product (0.02 g, 11% yield). ^{1}H NMR (DMSO-D6, ppm): δ 7.73 – 7.60 (m, 4H, c), 7.40 (t, *J* = 7.8, 4H, b), 7.24 (br, 2H, a), 4.43 (d, *J* = 13.0, 12H, d), 4.09 (br, 2H, e), 3.84

(br, 2H, e), 3.57 (br, 2H, f), 0.96 (s, 3H, g). ^{13}C NMR (DMSO-D6, ppm): δ 144.7, 138.7, 137.1, 133.2, 129.5, 125.3, 114.1, 64.9, 33.5, 16.3.

Synthesis of compound 4-4

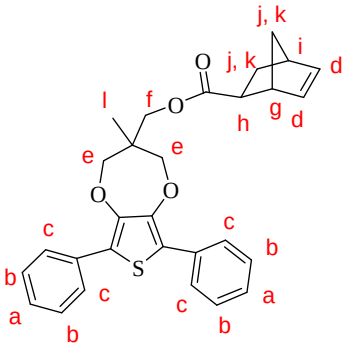

4-4

0.25 g (0.77 mmol) of compound **4-3** and 0.22 g (1.54 mmol) of 5-exo-norbornene-2-acetic acid were dissolved in dry THF or dichloromethane and the mixture was cooled down to 0 ^{o}C. 0.32 g (1.54 mmol) of dicyclohexyl carbodiimide followed by 0.19 g (1.54 mmol) of 4-dimethyl aminopyridine were added portionwise. The mixture was stirred at 0 ^{o}C for 2 h. After completion of the reaction, the precipitated dicyclohexyl urea was filtered. Then, water was added and the mixture was extracted using CH_2Cl_2 (3x20 mL). The organic layer was collected and dried over anhydrous $MgSO_4$. The resulting residue was purified by column chromatography using hexane to obtain a yellow solid as a product (0.36 g, quantitative yield). ^{1}H NMR ($CDCl_3$, ppm): δ 7.74 (d, *J* = 7.5, 4H, c), 7.40 (t, *J* = 7.6, 4H, b), 7.29 (br, 2H, a), 6.16 (d, *J* = 9.8, 2H, d), 4.29 (s, 2H, e), 4.23 (d, *J* = 12.2, 2H, e), 3.98 (d, *J* = 11.9, 2H, f), 3.10 (s, 1H, g), 2.96 (s, 1H, h), 2.31 (s, 1H, i), 1.96 (s, 2H, j, k), 1.42 (s, 2H, j, k), 1.11 (s, 3H, l). ^{13}C NMR ($CDCl_3$, ppm): δ 174.1, 145.9, 138.3, 135.2, 132.7, 128.6, 126.9, 120.3, 100.4, 76.2, 46.2, 42.8, 41.7, 29.7, 16.2.

Synthesis of compound 4-10

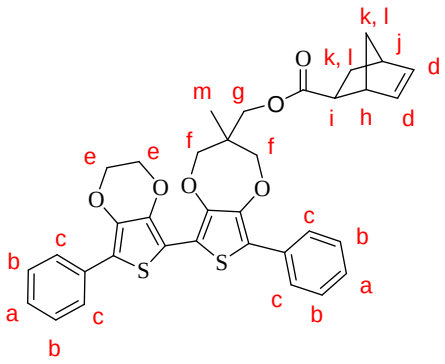

4-10

0.30 g (0.61 mmol) of compound **4-9** and 0.17 g (1.22 mmol) of 5-exo-norbornene-2-acetic acid were dissolved in dry THF or dichloromethane and the mixture was cooled down to 0 ^{o}C. 0.25 g (1.22 mmol) of dicyclohexyl carbodiimide followed by 0.15 g (1.22 mmol) of 4-dimethyl aminopyridine were added portionwise. The mixture was stirred at 0 ^{o}C for 2 h. After completion of the reaction, the precipitated dicyclohexyl urea was filtered. Then, water was added and the mixture was extracted using CH_2Cl_2 (3x20 mL). The organic layer was collected and dried over anhydrous $MgSO_4$. The resulting residue was purified by column chromatography using hexane to obtain a yellow solid as a product (0.28 g, 76% yield). ^{1}H NMR ($CDCl_3$, ppm) δ 7.74 (m, 4H, c), 7.36 (t, *J* = 7.6, 4H, b), 7.29 – 7.16 (m, 2H, a), 6.21 – 6.08 (m, 2H, d), 4.47 – 4.13 (m, 8H, e, f), 3.94 (m, 2H, g), 3.09 (s, 1H, h), 2.94 (s, 1H, i), 2.30 (s, 1H, j), 1.97 (d, *J* = 11.9, 2H, k, l), 1.41 (t, *J* = 9.5, 2H, k, l), 1.09 (s, 3H, m). ^{13}C NMR ($CDCl_3$, ppm): δ 176.1, 145.1, 137.9, 135.6, 132.9, 128.3, 126.0, 66.0, 64.9, 53.4, 46.2, 43.4, 41.5, 30.0, 16.7.

Synthesis of compound 4-12

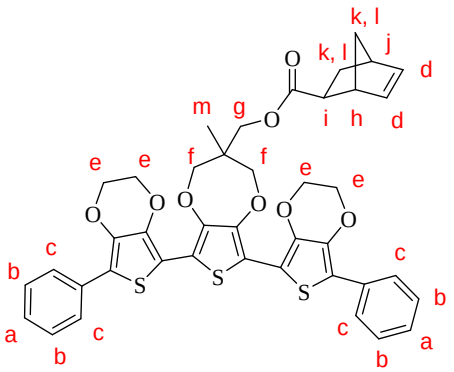

4-12

0.10 g (0.16 mmol) of compound **4-11** and 0.04 g (0.32 mmol) of 5-exo-norbornene-2-acetic acid were dissolved in dry THF or dichloromethane and the mixture was cooled down to 0 ^{o}C. 0.05 g (1.32 mmol) of dicyclohexyl carbodiimide followed by 0.04 g (0.32 mmol) of 4-dimethyl aminopyridine were added portionwise. The mixture was stirred at 0 ^{o}C for 2 h. After the completion of the reaction, the precipitated dicyclohexyl urea was filtered. Then, water was added and the mixture was extracted using CH_2Cl_2 (3x20 mL). The organic layer was collected and dried over anhydrous $MgSO_4$. The resulting residue was purified by column chromatography using 30% ethylacetate in hexane to obtain a yellow solid as a product (0.03 g, 69% yield). ^{1}H NMR ($CDCl_3$, ppm): δ 7.72 (br, 4H, c), 7.44 (br, 4H, b), 7.29 (br, 2H, a), 6.22 (br, 2H, d), 4.47 (d, *J* = 12.9, 8H, e), 4.36 – 4.22 (m, 4H, f), 3.96 (d, *J* = 9.6, 2H, g), 3.13 (br, 1H, h), 2.96 (br, 1H, i), 2.37 (br, 1H, j), 1.96 – 1.89 (m, 2H, k, l), 1.28 (br, 2H, k, l), 1.05 (s, 3H, m). ^{13}C-NMR ($CDCl_3$, ppm): δ 176.5, 135.8, 128.6, 126.3, 124.8, 69.7, 66.6, 64.5, 46.2, 43.1, 41.1, 30.4, 16.6.

Synthesis of compound 4-19

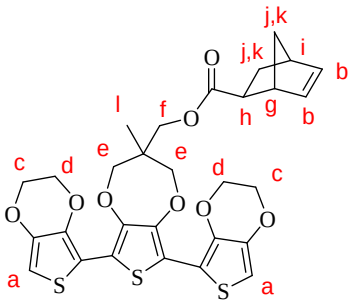

4-19

0.10 g (0.16 mmol) of compound **4-18** and 0.06 g (0.43 mmol) of 5-exo-norbornene-2-acetic acid were dissolved in dry THF or dichloromethane and the mixture was cooled down to 0 ^{o}C. 0.09 g (0.43 mmol) of dicyclohexyl carbodiimide followed by 0.05 g (0.43 mmol) of 4-dimethyl aminopyridine were added portionwise. The mixture was stirred at 0^{o}C for 2 h. After completion of the reaction, the precipitated dicyclohexyl urea was filtered. Then, water was added and the mixture was extracted using CH_2Cl_2 (3x20 mL). The organic layer was collected and dried over anhydrous $MgSO_4$. The resulting residue was purified by column chromatography using 30% ethyl acetate in hexane to obtain a yellow solid as a product (008 g, 65% yield). ^{1}H NMR ($CDCl_3$, ppm): δ 6.29 (s, 2H, a), 6.16 (br, 2H, b), 4.37-4.19 (m, 12H, c-e), 3.87 (br, 2H, f), 3.10 (br, 1H, g), 2.96 (br, 1H, h), 2.33 – 2.28 (br, 1H, i), 1.96 (br, 2H, j, k), 1.43 (br, 2H, j, k), 1.07 (s, 3H, l). ^{13}C-NMR ($CDCl_3$, ppm): δ 176.2, 143.8, 141.0, 137.9, 137.2, 135.2, 113.1, 97.6, 66.3, 64.9, 64.2, 46.6, 43.1, 41.4, 33.9, 30.4, 16.6.

Synthesis of compound 4-17

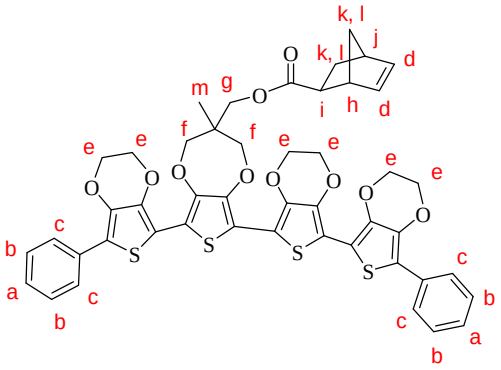

4-17

0.16 g (0.21 mmol) of compound **4-16** and 0.06 g (0.42 mmol) of 5-exo-norbornene-2-acetic acid were dissolved in dry THF or dichloromethane and the mixture was cooled down to 0 ^{o}C. 0.09 g (0.43 mmol) of dicyclohexyl carbodiimide followed by 0.05 g (0.43 mmol) of 4-dimethyl aminopyridine were added portionwise. The mixture was stirred at 0 ^{o}C for 2 h. After completion of the reaction, the precipitated dicyclohexyl urea was filtered. Then, water was added and the mixture was extracted using CH_2Cl_2 (3x20 mL). The organic layer was collected and dried over anhydrous $MgSO_4$. The resulting residue was purified by column chromatography using 30% ethyl acetate in hexane to obtain an orange solid as a product (0.15 g, 79 % yield). ^{1}H NMR (DMSO-D6, ppm): δ 7.70-7.72 (m , 4H, a), 7.42-7.46, (m, 4H, b), 7.29 (br, 2H, c), 6.22 (br, 2H, d), 4.48 (12H, m, e), 4.20-4.37 (4H, m, f), 3.92 (m, 2H, g), 3.11 (s, 1H, h), 2.96 (s, 1H, i), 2.36 (s, 1H, j), 1.96 (2H, k, l), 1.29 (2H, k, l), 1.05 (s, 3H, m) ^{13}C NMR (DMSO-D6, ppm): δ 176.2, 138.1, 135.5, 132.9, 128.8, 126.5, 126.1, 66.9, 64.7, 53.3, 46.8, 43.6, 41.7, 30.7, 17.4

Synthesis of polymer of diphenyl monoEDOT

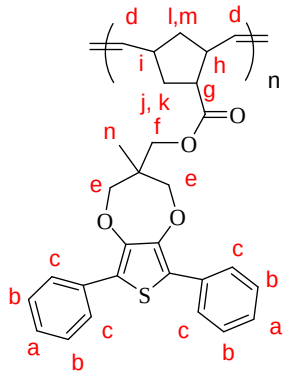

polymer of diphenyl monoEDOT

Dry THF was taken into a round bottom flask and was freezed-pumped-thawn 3 times before used. 0.10 g (0.17 mmol) of monomer **4-4** and 0.04 g (0.04 mmol) of 3rd generation Grubbs catalyst were put under vacuum into two separated round bottom flasks for 30 minutes before THF was added. Then, the solution of monomers in THF was injected into a stirred solution of catalyst. The mixture was allowed to stir for 3 minutes at room temperature followed by irreversible termination via the addition of 2 mL of ethyl vinyl ether. The solution was then concentrated under vacuum. The polymers were obtained by precipitation twice in methanol to yield a yellow solid as a product (0.07 g, 67% yield). ^{1}H NMR ($CDCl_3$, ppm) δ 7.66 (br, 4H, c), 7.48 – 7.04 (br, 6H, a, b), 5.49 – 4.90 (br, 2H, d), 4.13 (br, 4H, e), 3.75 (br, 2H, f), 3.22 – 2.77 (br, 2H, g, h), 2.77 – 2.25 (br, 1H, i), 2.01 (br, 4H, j-m), 0.94 (br, 3H, o). Mn= 16862, PDI= 1.05.

Synthesis of polymer of diphenyl diEDOT

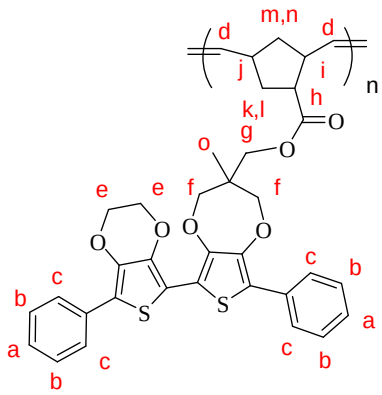

polymer of diphenyl diEDOT

Dry THF was taken into a round bottom flask and was freezed-pumped-thawn 3 times before used. 0.10 g (0.17 mmol) of monomer **4-10** and 0.04 g (0.04 mmol) of 3rd generation Grubbs catalyst were put under vacuum into two separated round bottom flasks for 30 minutes before THF was added. Then, the solution of monomers in THF was injected into a stirred solution of catalyst. The mixture was allowed to stir for 3 minutes at room temperature followed by irreversible termination via the addition of 2 mL of ethyl vinyl ether. The solution was then concentrated under vacuum. The polymers were obtained by precipitation twice in methanol to yield a yellow solid as a product (0.06 g, 59% yield). ^{1}H NMR ($CDCl_3$, ppm): δ 7.68 (br, 4H, c), 7.26 (br, 4H, b), 7.14 (br, 2H, a), 5.44 – 4.87 (br, 2H, d), 4.24 (br, 8H, e, f), 3.90 – 3.51 (br, 2H, g), 3.33 – 2.76 (br, 2H, h, i), 2.76 – 2.28 (br, 1H, j), 2.27 – 1.70 (br, 4H, k-m), 0.88 (br, 3H, o). Mn= 17679, PDI= 1.36.

Synthesis of polymer of diphenyl triEDOT

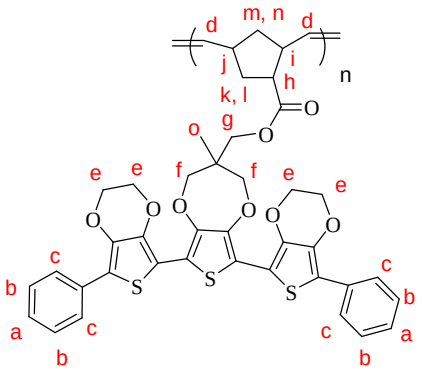

polymer of diphenyl triEDOT

Dry THF was taken into a round bottom flask and was freezed-pumped-thawn 3 times before used. 0.15 g (0.20 mmol) of monomer **4-12** and 0.04 g (0.04 mmol) of 3rd generation Grubbs catalyst were put under vacuum into two separated round bottom flasks for 30 minutes before THF was added. Then, the solution of monomers in THF was injected into a stirred solution of catalyst. The mixture was allowed to stir for 3 minutes at room temperature followed by irreversible termination via the addition of 2 mL of ethyl vinyl ether. The solution was then concentrated under vacuum. The polymers were obtained by precipitation twice in methanol to yield a yellow solid as a product (0.09 g, 60% yield). ^{1}H NMR ($CDCl_3$, ppm): δ 7.84 – 7.53 (br, 4H, c), 7.26 (br, 4H, b), 7.18 – 6.91 (br, 2H, a), 5.46 – 4.79 (br, 2H, d), 4.25 (br, 10H, e, f), 3.94 – 3.49 (br, 4H, f, g), 3.23 – 2.73 (br, 2H, h, i), 2.73 – 2.17 (br, 1H, j), 2.13-1.71 (br, 4H, k-m), 1.10 – 0.65 (br, 3H, o). Mn= 9975, PDI= 1.09.

Synthesis of polymer of triEDOT

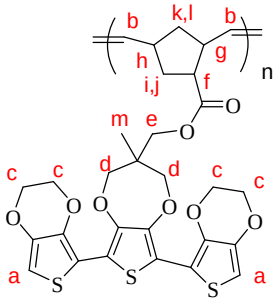

polymer of triEDOT

Dry THF was taken into a round bottom flask and was freezed-pumped-thawn 3 times before used. 0.10 g (0.14 mmol) of monomer **4-19** and 0.06 g (0.004 mmol) of 3rd generation Grubbs catalyst (1 equiv) were put under vacuum into two separated round bottom flasks for 30 minutes before THF was added. Then, the solution of monomers in THF was injected into a stirred solution of catalyst. The mixture was allowed to stir for 3 minutes at room temperature followed by irreversible termination via the addition of 2 mL of ethyl vinyl ether. The solution was then concentrated under vacuum. The polymers were obtained by precipitation twice in either methanol or ether to yield a product as a yellow solid (0.09 g, 60% yield). ^{1}H NMR ($CDCl_3$, ppm): δ 6.23 (br, 2H, a), 5.51 – 4.93 (br, 2H, b), 4.24 (br, 12H, c, d), 3.75 (br, 2H, e), 3.30 – 2.81 (m, 2H, f, g), 2.81 – 2.32 (m, 1H, h), 2.17 (s, 4H, i-l), 0.94 (s, 3H, m). Mn= 12775, PDI= 1.09.

Synthesis of polymer of diphenyl tetraEDOT

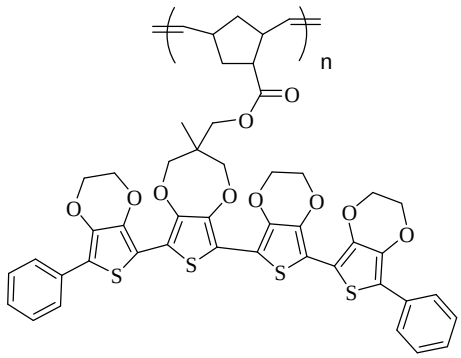

polymer of diphenyl tetraEDOT

Dry THF was taken into a round bottom flask and was freezed-pumped-thawn 3 times before used. 0.08 g (0.10 mmol) of monomer **4-17** and 0.01 g (0.01 mmol) of 3rd generation Grubbs catalyst were put under vacuum into two separated round bottom flasks for 30 minutes before THF was added. Then, the solution of monomers in THF was injected into a stirred solution of catalyst. The mixture was allowed to stir for 3 minutes at room temperature followed by irreversible termination via the addition of 2 mL of ethyl vinyl ether. The solution was then concentrated under vacuum. The polymers were obtained by precipitation twice in methanol to yield a product as a yellow solid (0.05 g, 63% yield). Due to the insolubility of the polymer in deuterated solvents, NMR is not taken. Mn= 16802, PDI = 1.12.

Synthesis of copolymer

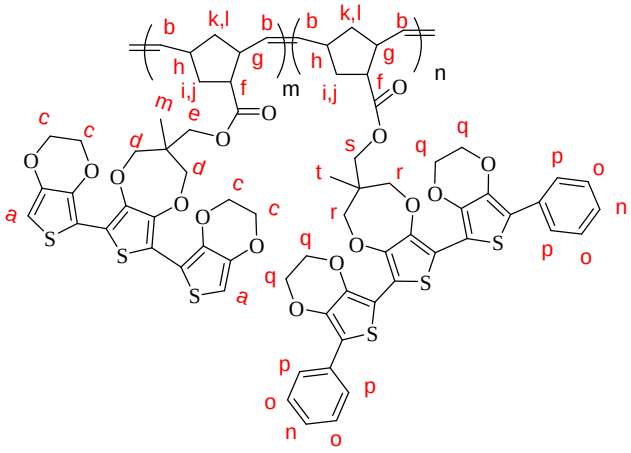

copolymer

Dry THF was taken into a round bottom flask and was freezed-pumped-thawn 3 times before used. The mixture of 1:3, 1:1 and 3:1 ratio of monomer **4-12**: monomer **4-19** and 100 equiv of 3rd generation Grubbs catalyst were put under vacuum into two separated round bottom flasks for 30 minutes before THF was added. Then, the solution of monomers in THF was injected into a stirred solution of catalyst. The mixture was allowed to stir for 3 minutes at room temperature followed by irreversible termination via the addition of 2 mL of ethyl vinyl ether. The solution was then concentrated under vacuum. The polymers were obtained by precipitation twice in either methanol or ether to yield a product as a yellow solid. ^{1}H NMR ($CDCl_3$, ppm) δ 7.81 – 7.61 (br, 4H, p), 7.26 (br, 6H, n, o), 6.30 – 6.05 (br, 2H, a), 5.50 – 4.88 (br, 4H, b), 4.27 (br, 24H, c, d, q, r), 3.92 – 3.54 (br, 4H, s, e), 3.19 – 2.79 (br, 4H, j, g), 2.79 – 2.28 (br, 2H, h), 2.28 – 1.67 (br, 8H, i-l), 1.33 – 0.69 (br, 6H, m, t).

6.1 References

1. Nantalaksakul, A.; Dasari, R. R.; Ahn, T. S.; Al-Kaysi, R.; Bardeen, C. J.; Thayumanavan, S., "Dendrimer Analogues of Linear Molecules to Evaluate Energy and Charge-transfer Properties" *Org. Lett.* **2006,** 8, (14), 2981-2984.

2. Thomas, K. R. J.; Thompson, A. L.; Sivakumar, A. V.; Bardeen, C. J.; Thayumanavan, S., "Energy and Electron Transfer in Bifunctional Non-conjugated Dendrimers" *J. Am. Chem. Soc.* **2005,** 127, (1), 373-383.

3. Ganesh, R. N.; Shraberg, J.; Sheridan, P. G.; Thayumanavan, S., "Synthesis of Difunctionalized Dendrimers: an Approach to Main-chain Poly(dendrimers)" *Tet. Lett.* **2002,** 43, (40), 7217-7220.

4. Hawker, C. J.; Frechet, J. M. J., "Preparation of Polymers with Controlled Molecular Architecture - A New Convergent Approach to Dendritic Macromolecules" *J. Am. Chem. Soc.* **1990,** 112, (21), 7638-7647.

5. Kawa, M.; Frechet, J. M. J., "Self-assembled Lanthanide-cored Dendrimer Complexes: Enhancement of the Luminescence Properties of Lanthanide Ions through Site-isolation and Antenna Effects" *Chem. Matter.* **1998,** 10, (1), 286-296.

6. Effenberger, F.; Jager, J., "Enzyme-catalyzed Reactions :Synthesis of the Adrenergic Bronchodilators (R)-terbutaline and (R)-salbutamol from (R)-cyanohydrins" *J. Org. Chem.* **1997,** 62, (12), 3867-3873.

7. Kaiser, F.; Schwink, L.; Velder, J.; Schmalz, H. G., "Studies towards the Total Synthesis of Mumbaistatin: Synthesis of Highly Substituted Benzophenone and Anthraquinone Building Blocks" *Tetrahedron* **2003,** 59, (18), 3201-3217.

8. Love, J. A.; Morgan, J. P.; Trnka, T. M.; Grubbs, R. H., "A Practical and Highly Active Ruthenium-based Catalyst that Effects the Cross Metathesis of Acrylonitrile" *Angew. Chem. Int. Ed.* **2002,** 41, (21), 4035-4037.

9. Shallcross, R. C.; D'Ambruoso, G. D.; Korth, B. D.; Hall, H. K.; Zheng, Z. P.; Pyun, J.; Armstrong, N. R., "Poly(3,4-ethylenedioxythiophene)-Semiconductor Nanoparticle Composite Thin Films Tethered to Indium Tin Oxide Substrates via Electropolymerization" *J. Am. Chem. Soc.* **2007,** 129, (37), 11310-11311.

10. Durmus, A.; Gunbas, G. E.; Toppare, L., "New, Highly Stable Electrochromic Polymers from 3,4-Ethylenedioxythiophene-bis-substituted Qinoxalines toward Green Polymeric Materials" *Chem. Matter.* **2007,** 19, (25), 6247-6251.

11. Ko, H. C.; Kim, S.; Lee, H.; Moon, B., "Multicolored Electrochromism of a Poly{1,4-bis[2-(3,4-ethylenedioxy)thienyl]benzene} Derivative Bearing Viologen Functional Groups" *Adv. Funct. Mater.* **2005,** 15, (6), 905-909.

12. Turbiez, M.; Frere, P.; Allain, M.; Videlot, C.; Ackermann, J.; Roncali, J., "Design of Organic Semiconductors: Tuning the Electronic Properties of pi-Conjugated Oligothiophenes with the 3,4-Ethylenedioxythiophene (EDOT) Building Block" *Chem. Eur. J.* **2005,** 11, (12), 3742-3752.

13. Apperloo, J. J.; Groenendaal, L.; Verheyen, H.; Jayakannan, M.; Janssen, R. A. J.; Dkhissi, A.; Beljonne, D.; Lazzaroni, R.; Bredas, J. L., "Optical and Redox Properties of a Series of 3,4-Ethylenedioxythiophene Oligomers" *Chem. Eur. J.* **2002,** 8, (10), 2384-2396.

BIBLIOGRAPHY

Adronov, A.; Frechet, J. M. J. "Light-harvesting Dendrimers" *Chem. Commun.* **2000**, 1701-1710.

Adronov, A.; Gilat, S. L.; Frechet, J. M. J.; Ohta, K.; Neuwahl, F. V. R.; Fleming, G. R. "Light Harvesting and Energy Transfer in Laser-dye-labeled Poly(aryl ether) Dendrimers" *J. Am. Chem. Soc.* **2000**, *122*, 1175-1185.

Ahn, T. S.; Nantalaksakul, A.; Dasari, R. R.; Al-Kaysi, R. O.; Muller, A. M.; Thayumanavan, S.; Bardeen, C. J. "Energy and Charge Transfer Dynamics in Fully Decorated Benzyl Ether Dendrimers and Their Disubstituted Analogues" *J. Chem. Phys. B* **2006**, *110*, 24331-24339.

Aida, T.; Jiang, D. L.; Yashima, E.; Okamoto, Y. "A New Approach to Light-harvesting with Dendritic Antenna" *Thin Solid Films* **1998**, *331*, 254-258.

Apperloo, J. J.; Groenendaal, L.; Verheyen, H.; Jayakannan, M.; Janssen, R. A. J.; Dkhissi, A.; Beljonne, D.; Lazzaroni, R.; Bredas, J. L. "Optical and Redox Properties of a Series of 3,4-Ethylenedioxythiophene Oligomers" *Chem. Eur. J.* **2002**, *8*, 2384-2396.

Arunachalam, V. S.; Fleischer, E. L. "Harnessing Materials for Energy - Preface" *Mrs Bulletin* **2008**, *33*, 261-263.

Baffreau, J.; Leroy-Lhez, S.; Van Anh, N.; Williams, R. M.; Hudhomme, P. "Fullerene C-60-Perylene-3,4: 9,10-Bis(dicarboximide) Light-harvesting Dyads: Spacer-length and Bay-substituent Effects on Intramolecular Singlet and Triplet Energy Transfer" *Chem. Eur. J.* **2008**, *14*, 4974-4992.

Balashov, S. P.; Imasheva, E. S.; Boichenko, V. A.; Anton, J.; Wang, J. M.; Lanyi, J. K. "Xanthorhodopsin: A Proton Pump with a Light-harvesting Carotenoid Antenna" *Science* **2005**, *309*, 2061-2064.

Balzani, V.; Ceroni, P.; Giansante, C.; Vicinelli, V.; Klarner, F. G.; Verhaelen, C.; Vogtle, F.; Hahn, U. "Tweezering the Core of a Dendrimer: A Photophysical and Electrochemical Study" *Angew. Chem. Int. Ed.* **2005**, *44*, 4574-4578.

Balzani, V.; Ceroni, P.; Maestri, M.; Vicinelli, V. "Light-harvesting Dendrimers" *Curr. Opin. Chem. Biol.* **2003**, *7*, 657-665.

Bar-Haim, A.; Klafter, J. "Geometric versus Energetic Competition in Light Harvesting by Dendrimers" *J. Chem. Phys. B* **1998**, *102*, 1662-1664.

Baranoff, E.; Collin, J. P.; Flamigni, L.; Sauvage, J. P. "From Ruthenium(II) to Iridium(III): 15 Years of Triads Based on Bis-terpyridine Complexes" *Chem. Soc. Rev.* **2004**, *33*, 147-155.

Barber, J.; Andersson, B. "Reveling the Blueprint of Photosynthesis" *Nature* **1994**, *370*, 31-34.

BarHaim, A.; Klafter, J.; Kopelman, R. "Dendrimers as Controlled Artificial Energy Antennae" *J. Am. Chem. Soc.* **1997**, *119*, 6197-6198.

Baumann, J.; Fayer, M. D. "Excitation Transfer in Disordered Two-dimensional and Anisotropic 3-Dimensional Systems -Effect of Spatial Geometry on Time-resolved Observables" *J. Chem. Phys.* **1986**, *85*, 4087-4107.

Benanti, T. L.; Saejueng, P.; Venkataraman, D. "Segregated Assemblies in Bridged Electron-rich and Electron-poor Pi-conjugated Moieties" *Chem. Commun.* **2007**, 692-694.

Benites, M. D.; Johnson, T. E.; Weghorn, S.; Yu, L. H.; Rao, P. D.; Diers, J. R.; Yang, S. I.; Kirmaier, C.; Bocian, D. F.; Holten, D.; Lindsey, J. S. "Synthesis and Properties of Weakly Coupled Dendrimeric Multiporphyrin Light-harvesting Arrays and Hole-storage Reservoirs" *J. Mater. Chem.* **2002**, *12*, 65-80.

Berson, S.; De Bettignies, R.; Bailly, S.; Guillerez, S. "Poly (3-hexylthiophene) Fibers for Photovoltaic Applications" *Adv. Funct. Mater.* **2007**, *17*, 1377-1384.

Bielawski, C. W.; Grubbs, R. H. "Living Ring-opening Metathesis Polymerization" *Prog. Polym. Sci.* **2007**, *32*, 1-29.

Biemans, H. A. M.; Rowan, A. E.; Verhoeven, A.; Vanoppen, P.; Latterini, L.; Foekema, J.; Schenning, A.; Meijer, E. W.; de Schryver, F. C.; Nolte, R. J. M. "Hexakis Porphyrinato Benzenes. A New Class of Porphyrin Arrays" *J. Am. Chem. Soc.* **1998**, *120*, 11054-11060.

Bolognesi, A.; DiGianvincenzo, P.; Giovanella, U.; Mendichi, R.; Schieroni, A. G. "Polystyrene Functionalized with EDOT Oligomers" *Eur. Polym. J.* **2008**, *44*, 793-800.

Bosman, A. W.; Janssen, H. M.; Meijer, E. W. "About Dendrimers: Structure, Physical Properties, and Applications" *Chem. Rev.* **1999**, *99*, 1665-1688.

Brabec, C. J.; Durrant, J. R. "Solution-processed Organic Solar Cells" *MRS Bull.* **2008**, *33*, 670-675.

Braun, M.; Atalick, S.; Guldi, D. M.; Lanig, H.; Brettreich, M.; Burghardt, S.; Hatzimarinaki, M.; Ravanelli, E.; Prato, M.; van Eldik, R.; Hirsch, A. "Electrostatic Complexation and Photoinduced Electron Transfer between Zn-cytochrome c and Polyanionic Fullerene Dendrimers" *Chem. Eur. J.* **2003**, *9*, 3867-3875.

Browne, W. R.; O'Boyle, N. M.; McGarvey, J. J.; Vos, J. G. "Elucidating Excited State Electronic Structure and Intercomponent Interactions in Multicomponent and Supramolecular Systems" *Chem. Soc. Rev.* **2005**, *34*, 641-663.

Bundgaard, E.; Krebs, F. C. "Low Band Gap Polymers for Organic Photovoltaics" *Sol. Energy Mater. Sol. Cells* **2007**, *91*, 954-985.

Caldeira, K.; Jain, A. K.; Hoffert, M. I. "Climate Sensitivity Uncertainty and the Need for Energy without CO2 Emission" *Science* **2003**, *299*, 2052-2054.

Capitosti, G. J.; Cramer, S. J.; Rajesh, C. S.; Modarelli, D. A. "Photoinduced Electron Transfer within Porphyrin-containing Poly(amide) Dendrimers" *Org. Lett.* **2001**, *3*, 1645-1648.

Chang, M. C. Y. "Harnessing Energy from Plant Biomass" *Curr. Opin. Chem. Biol.* **2007**, *11*, 677-684.

Cho, B. K.; Jain, A.; Gruner, S. M.; Wiesner, U. "Mesophase Structure-mechanical and Ionic Transport Correlations in Extended Amphiphilic Dendrons" *Science* **2004**, *305*, 1598-1601.

Choi, M. S.; Aida, T.; Yamazaki, T.; Yamazaki, I. "Dendritic Multiporphyrin Arrays as Light-harvesting Antennae: Effects of Generation Number and Morphology on Intramolecular Energy Transfer" *Chem. Eur. J.* **2002**, *8*, 2668-2678.

Choi, M. S.; Yamazaki, T.; Yamazaki, I.; Aida, T. "Bioinspired Molecular Design of Light-harvesting Multiporphyrin Arrays" *Angew. Chem. Int. Ed.* **2004**, *43*, 150-158.

Chow, J.; Kopp, R. J.; Portney, P. R. "Energy Resources and Global Development" *Science* **2003**, *302*, 1528-1531.

Coakley, K. M.; McGehee, M. D. "Conjugated Polymer Photovoltaic Cells" *Chem. Mater.* **2004**, *16*, 4533-4542.

Coessens, V.; Pintauer, T.; Matyjaszewski, K. "Functional Polymers by Atom Transfer Radical Polymerization" *Prog. Polym. Sci.* **2001**, *26*, 337-377.

Colladet, K.; Fourier, S.; Cleij, T. J.; Lutsen, L.; Gelan, J.; Vanderzande, D.; Nguyen, L. H.; Neugebauer, H.; Sariciftci, S.; Aguirre, A.; Janssen, G.; Goovaerts, E. "Low Band Gap Donor-acceptor Conjugated Polymers toward Organic Solar Cells Applications" *Macromolecules* **2007**, *40*, 65-72.

Cotlet, M.; Vosch, T.; Habuchi, S.; Weil, T.; Mullen, K.; Hofkens, J.; De Schryver, F. "Probing Intramolecular Forster Resonance Energy Transfer in a Naphthaleneimide-peryleneimide-terrylenediimide-based Dendrimer by Ensemble and Single-molecule Fluorescence Spectroscopy" *J. Am. Chem. Soc.* **2005**, *127*, 9760-9768.

Cravino, A. "Conjugated Polymers Electron-accepting with Tethered Moieties as Ambipolar Materials for Photovoltaics" *Polym. Int.* **2007**, *56*, 943-956.

Cravino, A. "Origin of The Open Circuit Voltage of Donor-acceptor Solar Cells: Do Polaronic Energy Levels Play a Role?" *Appl. Phys. Lett.* **2007**, *91*, 243502-3.

Cravino, A.; Sariciftci, N. S. "Double-cable Polymers for Fullerene Based Organic Optoelectronic Applications" *J. Mater. Chem.* **2002**, *12*, 1931-1943.

Cravino, A.; Zerza, G.; Maggini, M.; Bucella, S.; Svensson, M.; Andersson, M. R.; Neugebauer, H.; Brabec, C. J.; Sariciftci, N. S. "A Soluble Donor-acceptor Double-cable Polymer: Polythiophene with Pendant Fullerenes" *Mon. Fur. Chem.* **2003**, *134*, 519-527.

Cravino, A.; Zerza, G.; Neugebauer, H.; Maggini, M.; Bucella, S.; Menna, E.; Svensson, M.; Andersson, M. R.; Brabec, C. J.; Sariciftci, N. S. "Electrochemical and Photophysical Properties of a Novel Polythiophene with Pendant Fulleropyrrolidine Moieties: Toward "Double Cable" Polymers for Optoelectronic Devices" *J. Chem. Phys. B* **2002**, *106*, 70-76.

Cremer, J.; Bauerle, P.; Wienk, M. M.; Janssen, R. A. J. "High Open-circuit Voltage Poly(ethynylene bithienylene): Fullerene Solar Cells" *Chem. Mater.* **2006**, *18*, 5832-5834.

Currie, M. J.; Mapel, J. K.; Heidel, T. D.; Goffri, S.; Baldo, M. A. "High-efficiency Organic Solar Concentrators for Photovoltaics" *Science* **2008**, *321*, 226-228.

D'Souza, F.; Ito, O. "Photoinduced Electron Transfer in Supramolecular Systems of Fullerenes Functionalized with Ligands Capable of Binding to Zinc Porphyrins and Zinc Phthalocyanines" *Coord. Chem. Rev.* **2005**, *249*, 1410-1422.

D'Souza, F.; Smith, P. M.; Zandler, M. E.; McCarty, A. L.; Itou, M.; Araki, Y.; Ito, O. "Energy Transfer Followed by Electron Transfer in a Supramolecular Triad Composed of Boron Dipyrrin, Zinc Porphyrin, and Fullerene: A Model for the Photosynthetic Antenna-reaction Center Complex" *J. Am. Chem. Soc.* **2004**, *126*, 7898-7907.

de Boer, B.; Stalmach, U.; van Hutten, P. F.; Melzer, C.; Krasnikov, V. V.; Hadziioannou, G. "Supramolecular Self-assembly and Opto-electronic Properties of Semiconducting Block Copolymers" *Polymer* **2001**, *42*, 9097-9109.

Deisenhofer, J.; Epp, O.; Miki, K.; Huber, R.; Michel, H. "Structure of the Protein Subunits in the Photosynthetic Reaction Center of Rhodopseudomonas-viridis at 3A Resolution" *Nature* **1985**, *318*, 618-624.

Deisenhofer, J.; Michel, H. "The Photosynthetic Reaction Center from the Bacterium Rhodopseudomonas-Viridis" *Science* **1989**, *245*, 1463-1473.

Devadoss, C.; Bharathi, P.; Moore, J. S. "Energy Transfer in Dendritic Macromolecules: Molecular Size Effects and the Role of an Energy Gradient" *J. Am. Chem. Soc.* **1996**, *118*, 9635-9644.

Di Valentin, M.; Bisol, A.; Agostini, G.; Liddell, P. A.; Kodis, G.; Moore, A. L.; Moore, T. A.; Gust, D.; Carbonera, D. "Photoinduced Long-lived Charge Separation in a Tetrathiafulvalene-porphyrin-fullerene Triad Detected by Time-resolved Electron Paramagnetic Resonance" *J. Chem. Phys. B* **2005**, *109*, 14401-14409.

Dichtel, W. R.; Hecht, S.; Frechet, J. M. J. "Functionally Layered Dendrimers: A New Building Block and Its Application to the Synthesis of Multichromophoric Light-harvesting Systems" *Org. Lett.* **2005**, *7*, 4451-4454.

Durmus, A.; Gunbas, G. E.; Toppare, L. "New, Highly Stable Electrochromic Polymers from 3,4-Ethylenedioxythiophene-bis-substituted Qinoxalines toward Green Polymeric Materials" *Chem. Matter.* **2007**, *19*, 6247-6251.

Dykes, G. M. "Dendrimers: A Review of Their Appeal and Applications" *J. Chem. Technol. Biotechnol.* **2001**, *76*, 903-918.

Effenberger, F.; Jager, J. "Enzyme-catalyzed Reactions :Synthesis of the Adrenergic Bronchodilators (R)-terbutaline and (R)-salbutamol from (R)-cyanohydrins" *J. Org. Chem.* **1997**, *62*, 3867-3873.

Elim, H. I.; Jeon, S. H.; Verma, S.; Ji, W.; Tan, L. S.; Urbas, A.; Chiang, L. Y. "Nonlinear Optical Transmission Properties of C-60 Dyads Consisting of a Light-harvesting Diphenylaminofluorene Antenna" *J. Chem. Phys. B* **2008**, *112*, 9561-9564.

Feast, W. J. "Applications of Romp in the Synthesis of New Materials" *Makromol. Chemie* **1992**, *53*, 317-326.

Ferraris, J. P.; Yassar, A.; Loveday, D. C.; Hmyene, M. "Grafting of Buckminsterfullerene onto Polythiophene: Novel Intramolecular Donor-acceptor Polymers" *Opt. Mater.* **1998**, *9*, 34-42.

Forrest, S. R. "The Path to Ubiquitous and Low-cost Organic Electronic Appliances on Plastic" *Nature* **2004**, *428*, 911-918.

Fox, H. H.; Fox, M. A. "Fluorescence and Singlet Energy Migration in Conformationally Restrained Acrylate Polymers Bearing Pendant Chromophores" *Macromolecules* **1995**, *28*, 4570-4576.

Fox, M. A. "Polymeric and Supramolecular Arrays for Directional Energy and Electron Transport over Macroscopic Distances" *Acc. Chem. Res.* **1992**, *25*, 569-574.

Furuta, P. T.; Deng, L.; Garon, S.; Thompson, M. E.; Frechet, J. M. J. "Platinum-functionalized Random Copolymers for Use in Solution-processible, Efficient, Near-white Organic Light-emitting Diodes" *J. Am. Chem. Soc.* **2004**, *126*, 15388-15389.

Gaab, K. M.; Thompson, A. L.; Xu, J. J.; Martinez, T. J.; Bardeen, C. J. "Meta-conjugation and Excited-state Coupling in Phenylacetylene Dendrimers" *J. Am. Chem. Soc.* **2003**, *125*, 9288-9289.

Gadisa, A.; Svensson, M.; Andersson, M. R.; Inganas, O. "Correlation between Oxidation Potential and Open-circuit Voltage of Composite Solar Cells Based on Blends of Polythiophenes/fullerene Derivative" *Appl. Phys. Lett.* **2004**, *84*, 1609-1611.

Ganesh, R. N.; Shraberg, J.; Sheridan, P. G.; Thayumanavan, S. "Synthesis of Difunctionalized Dendrimers: an Approach to Main-chain Poly(dendrimers)" *Tet. Lett.* **2002**, *43*, 7217-7220.

Ghaddar, T. H.; Wishart, J. F.; Thompson, D. W.; Whitesell, J. K.; Fox, M. A. "A Dendrimer-based Electron Antenna: Paired Electron-transfer Reactions in Dendrimers with a 4,4 '-Bipyridine Core and Naphthalene Peripheral Groups" *J. Am. Chem. Soc.* **2002**, *124*, 8285-8289.

Giacalone, F.; Martin, N. "Fullerene Polymers: Synthesis and Properties" *Chem. Rev.* **2006**, *106*, 5136-5190.

Gilat, S. L.; Adronov, A.; Frechet, J. M. J. "Light Harvesting and Energy Transfer in Novel Convergently Constructed Dendrimers" *Angew. Chem. Int. Ed.* **1999**, *38*, 1422-1427.

Gittins, P. J.; Twyman, L. J. "Dendrimers and Supramolecular Chemistry" *Supramol Chem.* **2003**, *15*, 5-23.

Goh, C.; Scully, S. R.; McGehee, M. D. "Effects of Molecular Interface Modification in Hybrid Organic-inorganic Photovoltaic Cells" *J. Appl. Phys.* **2007**, *101*, 5-23.

Grayson, S. M.; Frechet, J. M. J. "Convergent Dendrons and Dendrimers: from Synthesis to Applications" *Chem. Rev.* **2001**, *101*, 3819-3867.

Gregg, B. A. "Excitonic Solar Cells" *J. Phys. Chem. B* **2003**, *107*, 4688-4698.

Gronheid, R.; Hofkens, J.; Kohn, F.; Weil, T.; Reuther, E.; Mullen, K.; De Schryver, F. C. "Intramolecular Forster Energy Transfer in a Dendritic System at the Single Molecule Level" *J. Am. Chem. Soc.* **2002**, *124*, 2418-2419.

Guldi, D. M.; Marcaccio, M.; Paolucci, F.; Paolucci, D.; Ramey, J.; Taylor, R.; Burley, G. A. "Fluorinated Fullerenes: Sources of Donor-acceptor Dyads with [18]Trannulene Acceptors for Energy- and Electron-transfer Reactions" *J. Phys. Chem. A* **2005**, *109*, 9723-9730.

Guldi, D. M.; Swartz, A.; Luo, C. P.; Gomez, R.; Segura, J. L.; Martin, N. "Rigid Dendritic Donor-acceptor Ensembles: Control over Energy and Electron Transduction" *J. Am. Chem. Soc.* **2002**, *124*, 10875-10886.

Gunes, S.; Neugebauer, H.; Sariciftci, N. S. "Conjugated Polymer-based Organic Solar Cells" *Chem. Rev.* **2007**, *107*, 1324-1338.

Gust, D.; Moore, T. A.; Moore, A. L. "Mimicking Photosynthetic Solar Energy Transduction" *Acc. Chem. Res.* **2001**, *34*, 40-48.

Gust, D.; Moore, T. A.; Moore, A. L. "Molecular Mimicry of Photosynthetic Energy and Electron Transfer" *Acc. Chem. Res.* **1993**, *26*, 198-205.

Gutierrez-Nava, M.; Accorsi, G.; Masson, P.; Armaroli, N.; Nierengarten, J. F. "Polarity Effects on the Photophysics of Dendrimers with an Oligophenylenevinylene Core and Peripheral Fullerene Units" *Chem. Eur. J.* **2004**, *10*, 5076-5086.

Ha, Y. H.; Nikolov, N.; Pollack, S. K.; Mastrangelo, J.; Martin, B. D.; Shashidhar, R. "Towards a Transparent, Highly Conductive Poly(3,4-ethylenedioxythiophene)" *Adv. Funct. Mater.* **2004**, *14*, 615-622.

Haerter, J. O.; Chasteen, S. V.; Carter, S. A.; Scott, J. C. "Numerical Simulations of Layered and Blended Organic Photovoltaic Cells" *Appl. Phys. Lett.* **2005**, *86*, 164101-3.

Hagfeldt, A.; Gratzel, M. "Molecular Photovoltaics" *Acc. Chem. Res.* **2000**, *33*, 269-277.

Hahn, U.; Gorka, M.; Vogtle, F.; Vicinelli, V.; Ceroni, P.; Maestri, M.; Balzani, V. "Light-harvesting Dendrimers: Efficient Intra- and Intermolecular Energy-transfer Processes in a Species Containing 65 Chromophoric Groups of Four Different Types" *Angew. Chem. Int. Ed.* **2002**, *41*, 3595-3598.

Harth, E. M.; Hecht, S.; Helms, B.; Malmstrom, E. E.; Frechet, J. M. J.; Hawker, C. J. "The Effect of Macromolecular Architecture in Nanomaterials: A Comparison of Site Isolation in Porphyrin Core Dendrimers and Their Isomeric Linear Analogues" *J. Am. Chem. Soc.* **2002**, *124*, 3926-3938.

Hartwig, J. F. "Transition Metal Catalyzed Synthesis of Arylamines and Aryl Ethers from Aryl Halides and Triflates: Scope and Mechanism" *Angew. Chem. Int. Ed.* **1998**, *37*, 2047-2067.

Hawker, C. J.; Frechet, J. M. J. "Preparation of Polymers with Controlled Molecular Architecture - A New Convergent Approach to Dendritic Macromolecules" *J. Am. Chem. Soc.* **1990**, *112*, 7638-7647.

Hawker, C. J.; Malmstrom, E. E.; Frank, C. W.; Kampf, J. P. "Exact Linear Analogs of Dendritic Polyether Macromolecules: Design, Synthesis, and Unique Properties" *J. Am. Chem. Soc.* **1997**, *119*, 9903-9904.

Hayakawa, T.; Horiuchi, S. "From Angstroms to Micrometers: Self-organized Hierarchical Structure within a Polymer Film" *Angew. Chem. Int. Ed.* **2003**, *42*, 2285-2289.

Haycock, R. A.; Yartsev, A.; Michelsen, U.; Sundstrom, V.; Hunter, C. A. "Self-assembly of Pentameric Porphyrin Light-harvesting Antennae Complexes" *Angew. Chem. Int. Ed.* **2000**, *39*, 3616-3619.

Heiser, T.; Adamopoulos, G.; Brinkmann, M.; Giovanella, U.; Ould-Saad, S.; Brochon, C.; van de Wetering, K.; Hadziioannou, G. "Nanostructure of Self-assembled Rod-coil Block Copolymer Films for Photovoltaic Applications" *Thin Solid Films* **2006**, *511*, 219-223.

Hepbasli, A. "A Key Review on Exergetic Analysis and Assessment of Renewable Energy Resources for a Sustainable Future" *Renew. Sust. Energy Rev.* **2008**, *12*, 593-661.

Hindin, E.; Kirmaier, C.; Diers, J. R.; Tomizaki, K. Y.; Taniguchi, M.; Lindsey, J. S.; Bocian, D. F.; Holten, D. "Photophysical Properties of Phenylethyne-linked Porphyrin and Oxochlorin Dyads" *J. Phys. Chem. B* **2004**, *108*, 8190-8200.

Hoffert, M. I.; Caldeira, K.; Jain, A. K.; Haites, E. F.; Harvey, L. D. D.; Potter, S. D.; Schlesinger, M. E.; Schneider, S. H.; Watts, R. G.; Wigley, T. M. L.; Wuebbles, D. J. "Energy Implications of Future Stabilization of Atmospheric CO2 Content" *Nature* **1998**, *395*, 881-884.

Hu, X. C.; Damjanovic, A.; Ritz, T.; Schulten, K. "Architecture and Mechanism of the Light-harvesting Apparatus of Purple Bacteria" *Proc. Natl. Acad. Sci. U.S.A.* **1998**, *95*, 5935-5941.

Huijser, A.; Suijkerbuijk, B.; Gebbink, R.; Savenije, T. J.; Siebbeles, L. D. A. "Efficient Exciton Transport in Layers of Self-assembled Porphyrin Derivatives" *J. Am. Chem. Soc.* **2008**, *130*, 2485-2492.

Irwin, M. D.; Buchholz, B.; Hains, A. W.; Chang, R. P. H.; Marks, T. J. "p-Type Semiconducting Nickel Oxide as an Efficiency-enhancing Anode Interfacial Layer in Polymer Bulk-heterojunction Solar Cells" *Proc. Natl. Acad. Sci. U.S.A.* **2008**, *105*, 2783-2787.

Ishi-i, T.; Murakami, K.; Imai, Y.; Mataka, S. "Light-harvesting and Energy-transfer System Based on Self-assembling Perylene Diimide-appended Hexaazatriphenylene" *Org. Lett.* **2005**, *7*, 3175-3178.

Ishwara, T.; Bradley, D. D. C.; Nelson, J.; Ravirajan, P.; Vanseveren, I.; Cleij, T.; Vanderzande, D.; Lutsen, L.; Tierney, S.; Heeney, M.; McCulloch, I. "Influence of Polymer Ionization Potential on the Open-circuit Voltage of Hybrid Polymer/TiO2 Solar Cells" *Appl. Phys. Lett.* **2008**, *92*, 053308-3.

Jang, S. Y.; Sotzing, G. A.; Marquez, M. "Intrinsically Conducting Polymer Networks of Poly(thiophene) via Solid-state Oxidative Cross-linking of a Poly(norbornylene) Containing Terthiophene Moieties" *Macromolecules* **2002**, *35*, 7293-7300.

Jang, W. D.; Kataoka, K. "Bioinspired Applications of Functional Dendrimers" *J. Drug Deliv. Sci. Technol.* **2005**, *15*, 19-30.

Jester, T. L. "Crystalline Silicon Manufacturing Progress" *Prog. Photovoltaics* **2002**, *10*, 99-106.

Jiang, D. L.; Aida, T. "Bioinspired Molecular Design of Functional Dendrimers" *Prog. Polym. Sci.* **2005**, *30*, 403-422.

Jiang, D. L.; Aida, T. "Morphology-dependent Photochemical Events in Aryl Ether Dendrimer Porphyrins: Cooperation of Dendron Subunits for Singlet Energy Transduction" *J. Am. Chem. Soc.* **1998**, *120*, 10895-10901.

Kaiser, F.; Schwink, L.; Velder, J.; Schmalz, H. G. "Studies towards the Total Synthesis of Mumbaistatin: Synthesis of Highly Substituted Benzophenone and Anthraquinone Building Blocks" *Tetrahedron* **2003**, *59*, 3201-3217.

Kawa, M.; Frechet, J. M. J. "Self-assembled Lanthanide-cored Dendrimer Complexes: Enhancement of the Luminescence Properties of Lanthanide Ions through Site-isolation and Antenna Effects" *Chem. Mat.* **1998**, *10*, 286-296.

Khudyakov, I. V.; Serebrennikov, Y. A.; Turro, N. J. "Spin-orbit-coupling in Free-radical Reactions -On the Way to Heavy-elements" *Chem. Rev.* **1993**, *93*, 537-570.

Klajnert, B.; Bryszewska, M. "Dendrimers: Properties and Applications" *Acta Biochim. Pol.* **2001**, *48*, 199-208.

Ko, H. C.; Kim, S.; Lee, H.; Moon, B. "Multicolored Electrochromism of a Poly{1,4-bis[2-(3,4-ethylenedioxy)thienyl]benzene} Derivative Bearing Viologen Functional Groups" *Adv. Funct. Mater.* **2005**, *15*, 905-909.

Kobori, Y.; Yamauchi, S.; Akiyama, K.; Tero-Kubota, S.; Imahori, H.; Fukuzumi, S.; Norris, J. R. "Primary Charge-recombination in an Artificial Photosynthetic Reaction Center" *Proc. Natl. Acad. Sci. U.S.A.* **2005**, *102*, 10017-10022.

Kohl, C.; Weil, T.; Qu, J. Q.; Mullen, K. "Towards Highly Fluorescent and Water-soluble Perylene Dyes" *Chem. Eur. J.* **2004**, *10*, 5297-5310.

Kuciauskas, D.; Liddell, P. A.; Lin, S.; Johnson, T. E.; Weghorn, S. J.; Lindsey, J. S.; Moore, A. L.; Moore, T. A.; Gust, D. "An Artificial Photosynthetic Antenna-Reaction Center Complex" *J. Am. Chem. Soc.* **1999**, *121*, 8604-8614.

Kuramochi, Y.; Satake, A.; Itou, M.; Ogawa, K.; Araki, Y.; Ito, O.; Kobuke, Y. "Light-harvesting Supramolecular Porphyrin Macrocycle Accommodating a Fullerene-Tripodal Ligand" *Chem. Eur. J.* **2008**, *14*, 2827-2841.

Kurreck, H.; Huber, M. "Model Reactions for Photosynthesis-photoinduced Charge and Energy-transfer between Covalently-linked Porphyrin and Quinone Units" *Angew. Chem. Int. Ed.* **1995**, *34*, 849-866.

Lecommandoux, S.; Klok, H. A.; Sayar, M.; Stupp, S. I. "Synthesis and Self-organization of Rod-dendron and Dendron-rod-dendron Molecules" *J. Polym. Sci. Pol. Chem.* **2003**, *41*, 3501-3518.

Lee, K. C. B.; Siegel, J.; Webb, S. E. D.; Leveque-Fort, S.; Cole, M. J.; Jones, R.; Dowling, K.; Lever, M. J.; French, P. M. W. "Application of the Stretched Exponential Function to Fluorescence Lifetime Imaging" *Biophys. J.* **2001**, *81*, 1265-1274.

Lewis, N. S.; Nocera, D. G. "Powering the planet: Chemical Challenges in Solar Energy Utilization" *Proc. Nat. Acad. Sci. U. S. A.* **2006**, *103*, 15729-15735.

Li, W.-S.; Yamamoto, Y.; Fukushima, T.; Saeki, A.; Seki, S.; Tagawa, S.; Masunaga, H.; Sasaki, S.; Takata, M.; Aida, T. "Amphiphilic Molecular Design as a Rational Strategy for Tailoring Bicontinuous Electron Donor and Acceptor Arrays: Photoconductive Liquid Crystalline Oligothiophene-C60 Dyads" *J. Am. Chem. Soc.* **2008**, *130*, 8886-8887.

Li, X. Y.; Sinks, L. E.; Rybtchinski, B.; Wasielewski, M. R. "Ultrafast Aggregate-to-aggregate Energy Transfer within Self-assembled Light-harvesting Columns of Zinc Phthalocyanine Tetrakis(perylenediimide)" *J. Am. Chem. Soc.* **2004**, *126*, 10810-10811.

Liu, D. J.; De Feyter, S.; Cotlet, M.; Stefan, A.; Wiesler, U. M.; Herrmann, A.; Grebel-Koehler, D.; Qu, J. Q.; Mullen, K.; De Schryver, F. C. "Fluorescence and Intramolecular Energy Transfer in Polyphenylene Dendrimers" *Macromolecules* **2003**, *36*, 5918-5925.

Liu, D. J.; De Feyter, S.; Cotlet, M.; Wiesler, U. M.; Weil, T.; Herrmann, A.; Mullen, K.; De Schryver, F. C. "Fluorescent Self-assembled Polyphenylene Dendrimer Nanofibers" *Macromolecules* **2003**, *36*, 8489-8498.

Lor, M.; Thielemans, J.; Viaene, L.; Cotlet, M.; Hofkens, J.; Weil, T.; Hampel, C.; Mullen, K.; Verhoeven, J. W.; Van der Auweraer, M.; De Schryver, F. C. "Photoinduced Electron Transfer in a Rigid First Generation Triphenylamine Core Dendrimer Substituted with a Peryleneimide Acceptor" *J. Am. Chem. Soc.* **2002**, *124*, 9918-9925.

Love, J. A.; Morgan, J. P.; Trnka, T. M.; Grubbs, R. H. "A Practical and Highly Active Ruthenium-based Catalyst that Effects the Cross Metathesis of Acrylonitrile" *Angew. Chem. Int. Ed.* **2002**, *41*, 4035-4037.

Lungenschmied, C.; Dennler, G.; Neugebauer, H.; Sariciftci, S. N.; Glatthaar, M.; Meyer, T.; Meyer, A. "Flexible, Long-lived, Large-area, Organic Solar Cells" *Sol. Energy Mater. Sol. Cells* **2007**, *91*, 379-384.

Mammo, W.; Admassie, S.; Gadisa, A.; Zhang, F. L.; Inganas, O.; Andersson, M. R. "New Low Band Gap Alternating Polyfluorene Copolymer-based Photovoltaic Cells" *Sol. Energy Mater. Sol. Cells* **2007**, *91*, 1010-1018.

Martinez-Junza, V.; Rizzi, A.; Jolliffe, K. A.; Head, N. J.; Paddon-Row, M. N.; Braslavsky, S. E. "Conformational and Photophysical Studies on Porphyrin-containing Donor-bridge-acceptor Compounds. Charge Separation in Micellar Nanoreactors" *Phys. Chem. Chem. Phys.* **2005**, *7*, 4114-4125.

Maus, M.; Mitra, S.; Lor, M.; Hofkens, J.; Weil, T.; Herrmann, A.; Mullen, K.; De Schryver, F. C. "Intramolecular Energy Hopping in Polyphenylene Dendrimers with an Increasing Number of Peryleneimide Chromophores" *J. Phys. Chem. A* **2001**, *105*, 3961-3966.

Mayer, A. C.; Scully, S. R.; Hardin, B. E.; Rowell, M. W.; McGehee, M. D. "Polymer-Based Solar Cells" *Mater. Today* **2007**, *10*, 28-33.

McDermott, G.; Prince, S. M.; Freer, A. A.; Hawthornthwaitelawless, A. M.; Papiz, M. Z.; Cogdell, R. J.; Isaacs, N. W. "Crystal-structure of an Integral Membrane Light-Harvesting Complex from Photosynthetic Bacteria" *Nature* **1995**, *374*, 517-521.

Melinger, J. S.; Pan, Y. C.; Kleiman, V. D.; Peng, Z. H.; Davis, B. L.; McMorrow, D.; Lu, M. "Optical and Photophysical Properties of Light-harvesting Phenylacetylene Monodendrons Based on Unsymmetrical Branching" *J. Am. Chem. Soc.* **2002**, *124*, 12002-12012.

Messmore, B. W.; Hulvat, J. F.; Sone, E. D.; Stupp, S. I. "Synthesis, Self-assembly, and Characterization of Supramolecular Polymers from Electroactive Dendron Rodcoil Molecules" *J. Am. Chem. Soc.* **2004**, *126*, 14452-14458.

Mihailetchi, V. D.; Blom, P. W. M.; Hummelen, J. C.; Rispens, M. T. "Cathode Dependence of the Open-circuit Voltage of Polymer : Fullerene Bulk Heterojunction Solar Cells" *J. Appl. Phys.* **2003**, *94*, 6849-6854.

Milliron, D. J.; Gur, I.; Alivisatos, A. P. "Hybrid Organic - Nanocrystal Solar Cells" *Mrs Bull.* **2005**, *30*, 41-44.

Moet, D. J. D.; Koster, L. J. A.; de Boer, B.; Blom, P. W. M. "Hybrid Polymer Solar Cells from Highly Reactive Diethylzinc: MDMO-PPV versus P3HT" *Chem. Mat.* **2007**, *19*, 5856-5861.

Murata, Y.; Suzuki, M.; Komatsu, K. "Synthesis and Electropolymerization of Fullerene-terthiophene Dyads" *Org. Biomol. Chem.* **2003**, *1*, 2624-2625.

Mutolo, K. L.; Mayo, E. I.; Rand, B. P.; Forrest, S. R.; Thompson, M. E. "Enhanced Open-circuit Voltage in Subphthalocyanine/C-60 Organic Photovoltaic Cells" *J. Am. Chem. Soc.* **2006**, *128*, 8108-8109.

Nantalaksakul, A.; Dasari, R. R.; Ahn, T. S.; Al-Kaysi, R.; Bardeen, C. J.; Thayumanavan, S. "Dendrimer Analogues of Linear Molecules to Evaluate energy and Charge-transfer Properties" *Org. Lett.* **2006**, *8*, 2981-2984.

Nantalaksakul, A.; Reddy, D. R.; Bardeen, C. J.; Thayumanavan, S. "Light Harvesting Dendrimers" *Photosynth. Res.* **2006**, *87*, 133-150.

Nelson, J. "Organic Photovoltaic Films" *Curr. Opin. Solid State Mat. Sci.* **2002**, *6*, 87-95.

Neuwahl, F. V. R.; Righini, R.; Adronov, A.; Malenfant, P. R. L.; Frechet, J. M. J. "Femtosecond Transient Absorption Studies of Energy Transfer within Chromophore-labeled Dendrimers" *J. Phys. Chem. B* **2001**, *105*, 1307-1312.

Nunzi, J. M. "Organic Photovoltaic Materials and Devices" *C. R. Phys.* **2002**, *3*, 523-542.

Oekermann, T.; Schlettwein, D.; Wohrle, D. "Characterization of N,N'-Dimethyl-3,4,9,10-perylenetetracarboxylic Acid Diimide and Phthalocyaninatozinc(II) in Electrochemical Photovoltaic Cells" *J. Appl. Electrochem.* **1997**, *27*, 1172-1178.

Offermans, T.; Meskers, S. C. J.; Janssen, R. A. J. "Photoinduced Absorption Spectroscopy on MDMO-PPV:PCBM Solar Cells under Operation" *Org. Electron.* **2007**, *8*, 325-335.

Peet, J.; Kim, J. Y.; Coates, N. E.; Ma, W. L.; Moses, D.; Heeger, A. J.; Bazan, G. C. "Efficiency Enhancement in Low-bandgap Polymer Solar Cells by Processing with Alkane Dithiols" *Nat. Mater.* **2007**, *6*, 497-500.

Peng, Q.; Park, K.; Lin, T.; Durstock, M.; Dai, L. M. "Donor-pi-acceptor Conjugated Copolymers for Photovoltaic Applications: Tuning the Open-circuit Voltage by Adjusting the Donor/acceptor Ratio" *J. Phys. Chem. B* **2008**, *112*, 2801-2808.

Perzon, E.; Zhang, F. L.; Andersson, M.; Mammo, W.; Inganas, O.; Andersson, M. R. "A Conjugated Polymer for near Infrared Optoelectronic Applications" *Adv. Mater.* **2007**, *19*, 3308-3311.

Phillips, J. C. "Stretched Exponential Relaxation in Molecular and Electronic Glasses" *Rep. Prog. Phys.* **1996**, *59*, 1133-1207.

Pintauer, T.; Matyjaszewski, K. "Atom Transfer Radical Addition and Polymerization Reactions Catalyzed by ppm Amounts of Copper Complexes" *Chem. Soc. Rev.* **2008**, *37*, 1087-1097.

Plummer, B. F.; Steffen, L. K.; Braley, T. L.; Reese, W. G.; Zych, K.; Vandyke, G.; Tulley, B. "Study of Geometry-effects of Heavy Atom Perturbation of the Electronic-properties of Derivatives of the Nonalternant Polycyclic Aromatic-hydrocarbons Fluoranthene and Acenaphtho[1,2-K]Fluoranthene" *J. Am. Chem. Soc.* **1993**, *115*, 11542-11551.

Qu, J. Q.; Pschirer, N. G.; Liu, D. J.; Stefan, A.; De Schryver, F. C.; Mullen, K. "Dendronized Perylenetetracarboxdiimides with Peripheral Triphenylamines for Intramolecular Energy and Electron Transfer" *Chem. Eur. J.* **2004**, *10*, 528-537.

Qu, J. Q.; Zhang, J. Y.; Grimsdale, A. C.; Mullen, K.; Jaiser, F.; Yang, X. H.; Neher, D. "Dendronized Perylene Diimide Emitters: Synthesis, Luminescence, and Electron and Energy Transfer Studies" *Macromolecules* **2004**, *37*, 8297-8306.

Ramos, A. M.; Rispens, M. T.; van Duren, J. K. J.; Hummelen, J. C.; Janssen, R. A. J. "Photoinduced Electron Transfer and Photovoltaic Devices of a Conjugated Polymer with Pendant Fullerenes" *J. Am. Chem. Soc.* **2001**, *123*, 6714-6715.

Ranasinghe, M. I.; Varnavski, O. P.; Pawlas, J.; Hauck, S. I.; Louie, J.; Hartwig, J. F.; Goodson, T. "Femtosecond Excitation Energy Transport in Triarylamine Dendrimers" *J. Am. Chem. Soc.* **2002**, *124*, 6520-6521.

Robel, I.; Bunker, B. A.; Kamat, P. V. "Single-walled Carbon Nanotube-CdS Nanocomposites as Light-harvesting Assemblies: Photoinduced Charge-transfer Interactions" *Adv. Mater.* **2005**, *17*, 2458-2463.

Roncali, J. "Linear Pi-conjugated Systems Derivatized with C-60-fullerene as Molecular Heterojunctions for Organic Photovoltaics" *Chem. Soc. Rev.* **2005**, *34*, 483-495.

Roncali, J. "Molecular Engineering of the Band Gap of Pi-conjugated Systems: Facing Technological Applications" *Macromol. Rapid Commun.* **2007**, *28*, 1761-1775.

Roncali, J.; Blanchard, P.; Frere, P. "3,4-Ethylenedioxythiophene (EDOT) as a Versatile Building Block for Advanced Functional p-Conjugated Systems" *J. Mater. Chem.* **2005**, *15*, 1589-1610.

Roquet, S.; Cravino, A.; Leriche, P.; Aleveque, O.; Frere, P.; Roncali, J. "Triphenylamine-thienylenevinylene Hybrid Systems with Internal Charge Transfer as Donor Materials for Heterojunction Solar Cells" *J. Am. Chem. Soc.* **2006**, *128*, 3459-3466.

Rybtchinski, B.; Sinks, L. E.; Wasielewski, M. R. "Combining Light-harvesting and Charge Separation in a Self-assembled Artificial Photosynthetic System Based on Perylenediimide Chromophores" *J. Am. Chem. Soc.* **2004**, *126*, 12268-12269.

Sadamoto, R.; Tomioka, N.; Aida, T. "Photoinduced Electron Transfer Reactions through Dendrimer Architecture" *J. Am. Chem. Soc.* **1996**, *118*, 3978-3979.

Scerf, U.; Gutacker, A.; Koenen, N. "All-Conjugated Block Copolymers" *Acc. Chem.. Res.* **2008**, *ASAP article*.

Scharber, M. C.; Wuhlbacher, D.; Koppe, M.; Denk, P.; Waldauf, C.; Heeger, A. J.; Brabec, C. L. "Design Rules for Donors in Bulk-heterojunction Solar Cells - Towards 10 % Energy-conversion Efficiency" *Adv. Mater.* **2006**, *18*, 789-794.

Senft, D. C. "Progress in Crystalline Multijunction and Thin-film Photovoltaics" *J. Electron. Mater.* **2005**, *34*, 571-574.

Serin, J. M.; Brousmiche, D. W.; Frechet, J. M. J. "Cascade Energy Transfer in a Conformationally Mobile Multichromophoric Dendrimer" *Chem. Commun.* **2002**, 2605-2607.

Shaheen, S. E.; Brabec, C. J.; Sariciftci, N. S.; Padinger, F.; Fromherz, T.; Hummelen, J. C. "2.5% Efficient Organic Plastic Solar Cells" *Appl. Phys. Lett.* **2001**, *78*, 841-843.

Shallcross, R. C.; D'Ambruoso, G. D.; Korth, B. D.; Hall, H. K.; Zheng, Z. P.; Pyun, J.; Armstrong, N. R. "Poly(3,4-ethylenedioxythiophene)-Semiconductor Nanoparticle Composite Thin Films Tethered to Indium Tin Oxide Substrates via Electropolymerization" *J. Am. Chem. Soc.* **2007**, *129*, 11310-11311.

Shen, P.; Sang, G. Y.; Lu, J. J.; Zhao, B.; Wan, M. X.; Zou, Y. P.; Li, Y. F.; Tan, S. T. "Effect of 3D pi-pi Stacking on Photovoltaic and Electroluminescent Properties in Triphenylamine-containing Poly(p-phenylenevinylene) Derivatives" *Macromolecules* **2008**, *41*, 5716-5722.

Shin, W. S.; Kim, S. C.; Lee, S. J.; Jeon, H. S.; Kim, M. K.; Naidu, B. V. K.; Jin, S. H.; Lee, J. K.; Lee, J. W.; Gal, Y. S. "Synthesis and Photovoltaic Properties of a Low-band-gap Polymer Consisting of Alternating Thiophene and Benzothiadiazole Derivatives for Bulk-heterojunction and Dye-sensitized Solar Cells" *J. Polym. Sci. Pol. Chem.* **2007**, *45*, 1394-1402.

Shortreed, M. R.; Swallen, S. F.; Shi, Z. Y.; Tan, W. H.; Xu, Z. F.; Devadoss, C.; Moore, J. S.; Kopelman, R. "Directed Energy Transfer Funnels in Dendrimeric Antenna Supermolecules" *J. Phys. Chem. B* **1997**, *101*, 6318-6322.

Sista, S.; Yao, Y.; Yang, Y.; Tang, M. L.; Bao, Z. A. "Enhancement in Open Circuit Voltage through a Cascade-type Energy Band Structure" *Appl. Phys. Lett.* **2007**, *91*, 223508-3.

Soci, C.; Hwang, I. W.; Moses, D.; Zhu, Z.; Waller, D.; Gaudiana, R.; Brabec, C. J.; Heeger, A. J. "Photoconductivity of a Low-bandgap Conjugated Polymer" *Adv. Funct. Mater.* **2007**, *17*, 632-636.

Spanggaard, H.; Krebs, F. C. "A Brief History of the Development of Organic and Polymeric Photovoltaics" *Sol. Energy Mat. & Sol. Cells* **2004**, *83*, 125-146.

Stalmach, U.; de Boer, B.; Videlot, C.; van Hutten, P. F.; Hadziioannou, G. "Semiconducting Diblock Copolymers Synthesized by Means of Controlled Radical Polymerization Techniques" *J. Am. Chem. Soc.* **2000**, *122*, 5464-5472.

Stewart, G. M.; Fox, M. A. "Chromophore-labeled Dendrons as Light Harvesting Antennae" *J. Am. Chem. Soc.* **1996**, *118*, 4354-4360.

Straight, S. D.; Andreasson, J.; Kodis, G.; Bandyopadhyay, S.; Mitchell, R. H.; Moore, T. A.; Moore, A. L.; Gust, D. "Molecular AND and INHIBIT Gates Based on Control of Porphyrin Fluorescence by Photochromes" *J. Am. Chem. Soc.* **2005**, *127*, 9403-9409.

Sugou, K.; Sasaki, K.; Kitajima, K.; Iwaki, T.; Kuroda, Y. "Light-harvesting heptadecameric porphyrin assemblies" *J. Am. Chem. Soc.* **2002**, *124*, 1182-1183.

Sun, S.; Fan, Z.; Wang, Y.; Haliburton, J. "Organic Solar Cell Optimizations" *J. Mater. Sci.* **2005**, *40*, 1429-1443.

Sun, S.; Fan, Z.; Wang, Y.; Haliburton, J.; Taft, C.; Maaref, S.; Seo, K.; Bonner, C. E. "Conjugated Block Copolymers for Opto-electronic Functions" *Synth. Met.* **2003**, *137*, 883-884.

Sun, S. S. "Design of a Block Copolymer Solar Cell" *Sol. Energy Mater. Sol. Cells* **2003**, *79*, 257-264.

Sun, S. S. "Polymer Photovoltaic Optimizations from Exciton Level" *J. Mater. Sci. Mater. Electron.* **2007**, *18*, 1143-1146.

Sun, S. S.; Fan, Z.; Wang, Y. Q.; Winston, K.; Bonner, C. E. "Morphological Effects to Carrier Mobility in a RO-PPV/SF-PPV Donor/acceptor Binary Thin Film Opto-electronic Device" *Mater. Sci. Eng. B Solid State Mater. Adv. Technol.* **2005**, *116*, 279-282.

Sun, S. S.; Zhang, C.; Ledbetter, A.; Choi, S.; Seo, K.; Bonner, C. E.; Drees, M.; Sariciftci, N. S. "Photovoltaic Enhancement of Organic Solar Cells by a Bridged Donor-acceptor Block Copolymer Approach" *Appl. Phys. Lett.* **2007**, *90*, 043117-3.

Thomas, K. G.; George, M. V.; Kamat, P. V. "Photoinduced Electron-transfer Processes in Fullerene-based Donor - Acceptor Systems" *Helv. Chim. Acta* **2005**, *88*, 1291-1308.

Thomas, K. R. J.; Thompson, A. L.; Sivakumar, A. V.; Bardeen, C. J.; Thayumanavan, S. "Energy and Electron Transfer in Bifunctional Non-conjugated Dendrimers" *J. Am. Chem. Soc.* **2005**, *127*, 373-383.

Thompson, A. L.; Gaab, K. M.; Xu, J. J.; Bardeen, C. J.; Martinez, T. J. "Variable Electronic Coupling in Phenylacetylene Dendrimers: The Role of Forster, Dexter, and Charge-transfer Interactions" *J. Phys. Chem. A* **2004**, *108*, 671-682.

Tian, L.; Hammond, P. T. "Comb-dendritic Block Copolymers as Tree-shaped Macromolecular Amphiphiles for Nanoparticle Self-assembly" *Chem. Mat.* **2006**, *18*, 3976-3984.

Turbiez, M.; Frere, P.; Allain, M.; Videlot, C.; Ackermann, J.; Roncali, J. "Design of Organic Semiconductors: Tuning the Electronic Properties of pi-Conjugated Oligothiophenes with the 3,4-Ethylenedioxythiophene (EDOT) Building Block" *Chem. Eur. J.* **2005**, *11*, 3742-3752.

Turbiez, M.; Frere, P.; Roncali, J. "Stable and Soluble Oligo(3,4-ethylenedioxythiophene)s End-capped with Alkyl Chains" *J. Org. Chem.* **2003**, *68*, 5357-5360.

Waldauff, C.; Schilinsky, P.; Hauch, J.; Brabec, C. J. "Material and Device Concepts for Organic Photovoltaics: Towards Competitive Efficiencies" *Thin Solid Films* **2004**, *451-52*, 503-507.

Walker, T. W. "Harnessing Natural Energy" *Chem. Eng. Prog.* **2008**, *104*, S23-S28.

Wasielewski, M. R. "Photoinduced Electron Transfer in Supramolecular Systems for Artificial Photosynthesis " *Chem. Rev.* **1992**, *92*, 435-461.

Watkins, D. M.; Fox, M. A. "Rigid, Well-defined Block-copolymers for Efficient Light-harvesting" *J. Am. Chem. Soc.* **1994**, *116*, 6441-6442.

Webber, S. E. "Photon-harvesting Polymers" *Chem. Rev.* **1990**, *90*, 1469-1482.

Weiss, E. A.; Chernick, E. T.; Wasielewski, M. R. "Modulation of Radical Ion Pair Lifetimes by the Presence of a Third Spin in Rodlike Donor-acceptor Triads" *J. Am. Chem. Soc.* **2004**, *126*, 2326-2327.

Winder, C.; Sariciftci, N. S. "Low Bandgap Polymers for Photon Harvesting in Bulk Heterojunction Solar Cells" *J. Mater. Chem.* **2004**, *14*, 1077-1086.

Wolfe, J. P.; Wagaw, S.; Marcoux, J. F.; Buchwald, S. L. "Rational Development of Practical Catalysts for Aromatic Carbon-nitrogen Bond Formation" *Acc. Chem. Res.* **1998**, *31*, 805-818.

Wurthner, F.; Ahmed, S.; Thalacker, C.; Debaerdemaeker, T. "Core-substituted Naphthalene Bisimides: New Fluorophors with Tunable Emission Wavelength for FRET Studies" *Chem. Eur. J.* **2002**, *8*, 4742-4750.

Xiao, S. X.; Wang, S.; Fang, H. J.; Li, Y. L.; Shi, Z. Q.; Du, C. M.; Zhu, D. B. "Synthesis and Characterization of a Novel Class of PPV Derivatives Covalently Linked to C-60" *Macromol. Rapid Commun.* **2001**, *22*, 1313-1318.

Xu, Q. H.; Wang, S.; Korystov, D.; Mikhailovsky, A.; Bazan, G. C.; Moses, D.; Heeger, A. J. "The Fluorescence Resonance Energy Transfer (FRET) Gate: A Time-resolved Study" *Proc. Natl. Acad. Sci. U.S.A.* **2005**, *102*, 530-535.

Xu, Z. F.; Moore, J. S. "Design and Synthesis of a Convergent and Directional Molecular Antenna" *Acta Polym* **1994**, *45*, 83-87.

Yamada, T.; Iida, K.; Yamago, S. "Living radical polymerization - Current status and future perspective" *Kobunshi Ronbunshu* **2007**, *64*, 329-342.

Yamamoto, Y.; Fukushima, T.; Saeki, A.; Seki, S.; Tagawa, S.; Ishii, N.; Aida, T. "Molecular Engineering of Coaxial Donor-acceptor Heterojunction by Coassembly of Two Different Hexabenzocoronenes: Graphitic Nanotubes with Enhanced Photoconducting Properties" *J. Am. Chem. Soc.* **2007**, *129*, 9276-9277.

Yamamoto, Y.; Fukushima, T.; Suna, Y.; Ishii, N.; Saeki, A.; Seki, S.; Tagawa, S.; Taniguchi, M.; Kawai, T.; Aida, T. "Photoconductive Coaxial Nanotubes of Molecularly Connected Electron Donor and Acceptor Layers" *Science* **2006**, *314*, 1761-1764.

Yassar, A.; Hmyene, M.; Loveday, D. C.; Ferraris, J. P. "Synthesis and Characterization of Polythiophenes Functionalized by Buckminsterfullerene" *Synth. Met.* **1997**, *84*, 231-232.

Yourre, T. A.; Rudaya, L. I.; Klimova, N. V.; Shamanin, V. V. "Organic Materials for Photovoltaic and Light-emitting Devices" *Semiconductors* **2003**, *37*, 807-815.

Zahedi, A. "Solar Photovoltaic (PV) Energy; Latest Developments in the Building Integrated and Hybrid PV Systems" *Renew. Energy* **2006**, *31*, 711-718.

Zhang, C.; Choi, S.; Haliburton, J.; Cleveland, T.; Li, R.; Sun, S. S.; Ledbetter, A.; Bonner, C. E. "Design, Synthesis, and Characterization of a Donor-Bridge-Acceptor-Bridge-Type Block Copolymer Via Alkoxy- and Sulfone-Derivatized Poly(phenylenevinylenes)" *Macromolecules* **2006**, *39*, 4317-4326.

Zhang, F. L.; Svensson, M.; Andersson, M. R.; Maggini, M.; Bucella, S.; Menna, E.; Inganas, O. "Soluble Polythiophenes with Pendant Fullerene Groups as Double Cable Materials for Photodiodes" *Adv. Mater.* **2001**, *13*, 1871-1874.

Zhang, T.; Ceder, M.; Inganas, O. "Enhancing the Photovoltage of Polymer Solar Cells by using a Modified Cathode" *Adv. Mater.* **2007**, *19*, 1835-1838.

Zubarev, E. R.; Sone, E. D.; Stupp, S. I. "The Molecular Basis of Self-assembly of Dendron-rod-coils into One-dimensional Nanostructures" *Chem. Eur. J.* **2006**, *12*, 7313-7327.